

INTERIM REPORT

NRC Research and Technical Assistance Report

Accession No. _____

Contract Program or Project Title: Thermal Hydraulic LMFBR Safety Experiments

Subject of this Document: "Heat Removal Characteristics of Volume-Heated Boiling Pools With Inclined Boundaries"

Type of Document: Informal Report

Author(s): G. A. Greene, O. C. Jones, Jr., C. E. Schwarz, and N. Abuaf

Date of Document: June 1979

Responsible NRC Individual and NRC Office or Division: M. Silberberg
Division of Reactor Safety Research
U.S. Nuclear Regulatory Commission
Washington, D.C. 20555

This document was prepared primarily for preliminary or internal use. It has not received full review and approval. Since there may be substantive changes, this document should not be considered final.

Brookhaven National Laboratory

Upton, NY 11973

Associated Universities, Inc.

for the

U.S. Department of Energy

Prepared for

U.S. Nuclear Regulatory Commission

Washington, D. C. 20555

Under Interagency Agreement EY-76-C-02-0016

NRC FIN No. A- 3024

INTERIM REPORT 494 035

7908010 545

HEAT REMOVAL CHARACTERISTICS OF VOLUME HEATED BOILING POOLS
WITH INCLINED BOUNDARIES

By

G. A. Greene, O. C. Jones, Jr., C. E. Schwarz and N. Abuaf

Brookhaven National Laboratory
Thermal Hydraulic Development Division
Department of Nuclear Energy
Upton, New York 11973

MAY 1979

DEPARTMENT OF NUCLEAR ENERGY BROOKHAVEN NATIONAL LABORATORY
UPTON, NEW YORK 11973

494 036



Prepared for the U.S. Nuclear Regulatory Commission
Office of Nuclear Regulatory Research
Contract No. EY-76-C-02-0016

ASD

NOTICE

This report was prepared as an account of work sponsored by the United States Government. Neither the United States nor the United States Nuclear Regulatory Commission, nor any of their employees, nor any of their contractors, subcontractors, or their employees, makes any warranty, express or implied, or assumes any legal liability or responsibility for the accuracy, completeness or usefulness of any information, apparatus, product or process disclosed, or represents that its use would not infringe privately owned rights.

494 037

HEAT REMOVAL CHARACTERISTICS OF VOLUME HEATED BOILING POOLS
WITH INCLINED BOUNDARIES

By

G. A. Greene, O. C. Jones, Jr., C. E. Schwarz and N. Abuaf

Brookhaven National Laboratory
Thermal Hydraulic Development Division
Department of Nuclear Energy
Upton, New York 11973

MAY 1979

Prepared for the U.S. Nuclear Regulatory Commission
Office of Nuclear Regulatory Research
Contract No. EY-76-C-02-0016
FIN NO. A-3024

NOTICE: This document contains preliminary information and was prepared primarily for interim use. Since it may be subject to revision or correction and does not represent a final report, it should not be cited as reference without the expressed consent of the author(s).

494 037

TABLE OF CONTENTS

ABSTRACT iii

LIST OF FIGURES v

LIST OF TABLES vi

NOMENCLATURE vii

1. INTRODUCTION 1

2. HISTORICAL REVIEW 1

3. ANALYTICAL MODELING 9

 3.1 Heat Transfer 9

 3.2 Void Dynamics 12

4. EXPERIMENTAL 16

 4.1 Pool Description 16

 4.2 Test Plate 16

 4.3 Test Plate Instrumentation 20

 4.4 Data Acquisition 25

5. EXPERIMENTAL RESULTS 26

 5.1 Range of Experiments 26

 5.2 Nonboiling Regime 29

 5.3 Incipient Boiling Regime 30

 5.4 Bubbly Flow Regime 32

 5.5 Bubbly-Churn Turbulent Transition 35

 5.6 Churn-Turbulent Flow Regime 38

6. DATA ANALYSIS AND DISCUSSIONS 42

 6.1 Comparison of Calculated and Measured Pool
 Void Fraction 42

 6.2 Natural Convection Analysis of Previous Data^{12,11}
 for Heat Transfer from a Volume Boiling Pool to a
 Vertical Boundary 47

 6.3 Correlation of Present Data 55

Table of Contents (Cont'd)

7. SUMMARY AND CONCLUSIONS	59
7.1 Bubbly Flow Regime	59
7.1.1 <u>Hydrodynamics</u>	59
7.1.2 <u>Heat Transfer</u>	62
7.2 Churn-Turbulent Flow Regime	64
7.2.1 <u>Hydrodynamics</u>	64
7.2.2 <u>Heat Transfer</u>	65
8. ACKNOWLEDGEMENTS	66
9. REFERENCES	67
APPENDIX A: ERROR ANALYSIS	69
APPENDIX B: SAMPLE CALCULATION (RUN 9001)	
APPENDIX C: TABULATION OF EXPERIMENTAL DATA	
APPENDIX D: ALGEBRAIC DERIVATION OF EQUATIONS 28 AND 29	

494 039

ABSTRACT

The state-of-the-art of heat transfer from boiling liquids having internal heat generation is reviewed. Considerable scatter is found in the existing data. Attempts to correlate these data have relied on both natural and forced convection concepts. This report describes a new series of experiments wherein the data scatter appears to have been improved by a factor of four to six from previous experiments when compared on the basis of standard deviation in correlation coefficients.

Local heat transfer data to both vertical and inclined surfaces (up to 30° from vertical) are reported having maximum to minimum heat transfer ratios of up to 5:1. It is shown that with surface vapor fluxes up to twice the free bubble rise velocities given by Harmathy²² there are two distinct flow regimes: bubbly and churn-turbulent.

In bubbly flows, the pool is generally quiescent and surface temperature fluctuations negligible. Two heat transfer regimes were identified: laminar-where $\overline{Nu} = 1.54 Ra^* (L, \bar{\alpha}, \theta)^{0.25}$ for $Ra^* \leq 1.865 \times 10^{11}$, and turbulent-where $\overline{Nu} = 0.0314 Ra^* (L, \bar{\alpha}, \theta)^{0.40}$ for $Ra^* > 1.865 \times 10^{11}$. Standard deviations in the correlation coefficients were 0.08 and 0.0016 respectively.

In churn-turbulent flows, the pool is generally chaotic and three dimensional. The surface temperatures showed large fluctuations up to the maximum pool-to-wall difference indicating intermittent destruction and renewal of boundary layer. Heat transfer coefficients were more uniform, and the maximum was observed to be in the range .25-.30 cal/cm² s °C.

The data reported herein are in general agreement with the data reported by Gabor, et al.¹¹, but with significantly less scatter. On the other hand, the more recent data of Gustavson, et al.¹² are lower than those reported herein by approximately a factor of two.

494 041

LIST OF FIGURES

- Figure 1 Proposed Correlation Scheme for Matching Forced and Free Convection Components of Boundary Heat Transfer Relation. (BNL Neg. No. 9-591-76).
- Figure 2 Schematic of Boundary Layer Flow and Heat Transfer From Volume Boiling Pool. (BNL Neg. No. 9-369-76).
- Figure 3 Modified Laminar Natural Convection Correlation of Boundary Heat Transfer from Volumetric-Boiling Pools (Based on Data from Ref. 12). (BNL Neg. No. 1-1295-79).
- Figure 4 Schematic View of Inclined-Wall Volumetric Boiling Pool Apparatus. (BNL Neg. No. 1-1385-79).
- Figure 5 Schematic View of Inclined Wall Test Plate. (BNL Neg. No. 1-1384-79).
- Figure 6 Photograph of Assembled Test Pool. (BNL Neg. No. 3-1418-77).
- Figure 7 Schematic View of Gold Plated Microthermocouple. (BNL Neg. No. 2-376-77).
- Figure 8 End View of Unplated Thermocouple Cross Section. (BNL Neg. No. 3-1422-77).
- Figure 9 Photograph of Assembled Test Pool Facility. (BNL Neg. No. CN2-798-78).
- Figure 10 Profile of Local Boundary Heat Transfer Coefficient From Volume Boiling Pool - Run No. 9001 - Incipient Boiling. (BNL Neg. No. 4-844-79).
- Figure 11 Profile of Local Boundary Heat Transfer Coefficient From Volume Boiling Pool - Run No. 9013 - Bubbly Flow. (BNL Neg. No. 3-1891-79).
- Figure 12 Profile of Local Boundary Heat Transfer Coefficient From Volume Boiling Pool - Run No. 6009 - Transition. (BNL Neg. No. 4-845-79).
- Figure 13 Profile of Local Boundary Heat Transfer Coefficient From Volume Boiling Pool - Run No. 7516 - Churn-Turbulent. (BNL Neg. No. 4-846-79).
- Figure 14 Pool Average Void Fraction, $\bar{\alpha}$, vs Dimensionless Superficial Vapor Velocity Based on Total Vaporization Power. (BNL Neg. No. 4-993-79).

494 042

LIST OF FIGURES (Cont'd)

- Figure 15 Comparison of Measured Average Void Fraction to Calculated Average Void Fraction Based on Net Boiling Power. (BNL Neg. No. 4-992-79).
- Figure 16 Natural Convection Correlation of Average Heat Transfer Data of Gustavson, et al.¹² (BNL Neg. No. 4-1304-79).
- Figure 17 Natural Convection Correlation of Average Heat Transfer Data of Gabor, et al.¹¹ (BNL Neg. No. 4-1306-79).
- Figure 18 Natural Convection Correlation of Average Heat Transfer Data Based On Current Data. (BNL Neg. No. 4-1305-79).

LIST OF TABLES

- Table 1 Review of Natural Convection Heat Transfer. (BNL Neg. #4-849-79)
- Table 2 Thermocouple Locations in Test Plate (No Negative No.)
- Table 3 List of Measuring Devices Used and Their Uncertainty (No Negative No.)
- Table 4 Average Heat Transfer and Void Fraction Data of Gustavson, et al.¹² and Comparison to Existing Models (BNL Neg. #4-848-79)
- Table 5 Average Heat Transfer and Void Fraction Data of Gabor, et al.¹¹ and Comparison to Existing Models (BNL-Neg. #4-847-79)
- Table 6 Comparison of Measured and Calculated Average Void Fraction and Heat Transfer Coefficient from Volumetric Boiling Pool (BNL-Neg. #6-175-79)
- Table 7 Summary of Local and Average Correlations for Heat Transfer From Volume Boiling Pools (No Negative No.)
- Table A-1 Summary of Experimental Uncertainties (No Negative No.)
- Table D-1 Summary of Local-to-Average Heat Transfer Correlation Conversion Upon Free Stream Void Distribution (No Negative No.)

494 043

NOMENCLATURE

a	Test plate thickness
C	Constant
C_o	Distribution parameter
g	Gravitational acceleration
Gr	Grashof number
h	Heat transfer coefficient
\bar{h}	Average heat transfer coefficient
H	Height
h_{fg}	Heat of vaporization
j	Superficial velocity
$j_{g\infty}$	Superficial vapor velocity at pool surface
k	Thermal conductivity
K_i	Correlation coefficient
L	Length
n	Defined in Eq. 10
Nu	Nusselt number
\bar{Nu}	Average Nusselt number ($\equiv \bar{h}L/k$)
P	Pressure
Pr	Prandtl number ($\equiv \mu C_p/k$)
Q	Heat Flux
Q'''	Volumetric power density
Ra	Rayleigh number
Re	Reynolds number
T	Temperature
U_∞	Terminal rise velocity of bubble

494 044

NOMENCLATURE (Cont'd)

V	Velocity
V_{gj}	Drift velocity
x	Coordinate (along wall)
Y	Defined in Eq. 8
Z	Defined in Eq. 9
α	Void fraction
$\bar{\alpha}$	Average void fraction
β	Coefficient of thermal expansion
ϵ	Fractional uncertainty
μ	Dynamic viscosity
ν	Kinematic viscosity
ρ	Density
σ	Standard deviation
θ	Wall angle from vertical
Γ_v	Volumetric vapor source
ξ	Normalized coordinate

Subscripts

ave	Average
B	Boiling
BN	Boron nitride
C	Forced convective
eff	Effective
f	Film
g	Gas

494 045

NOMENCLATURE (Cont'd)

ℓ	Liquid
L	Laminar
N	Natural convective
o	Initial
T	Turbulent
TC	Thermal convective
v	Vapor
w	Wall
∞	Infinity
*	Modified

494 046

1. INTRODUCTION







The heat transfer characteristics of volume-heated boiling pools are of importance in the safety analysis of hypothetical core disruptive accidents (HCDA) in liquid metal fast breeder reactors (LMFBR). In general, these pools would be composed of molten fuel and steel and would generate heat as a result of fission product decay. The fluid dynamic characteristics, as well as the containability of such boiling systems, would depend intimately on the heat loads applied to the surrounding boundaries. In addition, the thermodynamic and hydrodynamic states of the boiling mixture might determine the initial or boundary conditions for separate but related phenomena, such as nuclear recriticality, structural integrity, flow and freezing of multi-phase fluids, etc. Confidence in the conceptualization, as well as computation of such hypothetical events depends to a great deal upon the ability to predict the vapor generation rate, void fraction, and local boundary heat flux from such volume-boiling pools. It is the purpose of this report to present new experimental data for local boundary heat transfer coefficients and average void fraction in volume-boiling pools and compare these results to previous experimental data, as well as to existing empirical models.

2. HISTORICAL REVIEW

Numerous studies exist in the literature concerning heat transfer from liquid pools with an internal heat source. A brief review of this literature is indicated in Table 1.^{1-7,13} However, investigations into the heat

TABLE 1

REVIEW OF NATURAL CONVECTION HEAT TRANSFER

GEOMETRY	CORRELATION	REFERENCE
 Vertical Cylinder Volume Heating Natural Convection	Numerical Finite Difference	(1) Essam (2) Murgatroyd, Watson
 Horizontal Plates Volume Heating Natural Convection	$Nu = KRa^n$	(3) Kulacki, et al (4) Nagle, et al (5) Suo-Antilla, Catton
 Vertical Plates Volume Heating Natural Convection	$T(\cdot), q_w(t)$	(6) Novotny, Eckert
 Lenticular Pool Volume Heating Natural Convection	$Nu(\theta) = K[Gr \cdot Da \cdot Pr]^n$	(7) Jahn, Reineke
 Inclined Plate Natural Convection	$Nu(x) = KRa(x, \theta)^n$	(13) Fujii, Imura
 Volume Boiling Pool Mixed Convection	\bar{Nu} $Nu(x)$	(8-9) Hesson, Gunther, Stein (10-11) Gabor, et al (12) Gustafson, Kazimi, Chen

transfer and hydrodynamic behavior of volume-heated boiling pools have been few and none are known to exist prior to this decade.^{8-12,15,18}

The earliest known attempt to consider the heat transfer from volume-heated boiling pools is the work performed at Argonne National Laboratory by Stein, et al.⁹ In this work, a solution of NaCl and water was boiled in an open container by joule heating. The average downward and horizontal heat fluxes were measured by thermocouples soldered in small dead-end holes in the plates making up the electrodes and base, and in the coolant system.

A model was presented which separated the boundary heat transfer into a natural convection and forced convection regime. The natural convection regime was shown to agree with the correlation below,

$$\overline{Nu}_N = .677 [Pr/(.952 + Pr)]^{1/4} Ra^{1/4} \quad (1)$$

where $\overline{Nu}_N = \dot{Q}_N L / (k\Delta T)$, $Ra = PrGr$, and $Gr = g\beta\Delta TL^3/\nu^2$. The forced convection regime was shown to be correlated by the relation,

$$\overline{Nu}_C = .644 Pr^{1/3} Re^{1/2} \quad (2)$$

where $\overline{Nu}_C = \dot{Q}_C L / (k\Delta T)$ and $Re = V_B L / \nu$. Both relations were valid only for laminar flow conditions. For convenience, a thermal convection reference velocity,

V_{TC} , was defined as

$$V_{TC} = (g\beta\Delta TL)^{1/2} = [g(\rho_w - \rho_\infty)L/\rho_f]^{1/2} \quad (3)$$

and an equivalent free stream velocity, V_B , was defined as below;

$$V_B = 40 \dot{Q}_B^{0.72} \quad (4)$$

494 049

it was reported that for $V_B/V_{TC} \leq 0.2$, forced convection heat transfer was negligible and Eq. 1 was applied. For $V_B/V_{TC} > 3.0$, thermal convection was negligible and Eq. 2 applied. For values of V_B/V_{TC} intermediate to these values, mixed convection existed. The results of this investigation indicated that downward heat fluxes were found to be significantly larger than predictions from conduction theory would indicate; in addition, at the higher boiling heat fluxes, horizontal heat transfer was found to be significantly larger than values calculated by thermal convection alone, and could be correlated empirically by the laminar forced convection model.

The next attempt to experimentally characterize boundary heat transfer from volume-boiling pools was the work of Gabor, et al.¹¹ from Argonne National Laboratory. In their work, they used simulant solutions of $ZnSO_4$ in water. Base plates of two lengths (191 and 381 mm) and three electrode heights (64, 114, 230 mm) were used. The volumetric boiling power was supplied by joule heating as in the previous work. The electrodes and base plate were used as the heat transfer surfaces; thermocouples were buried halfway into the copper plates for temperature measurements, seven into the base plate, and two in each of the electrodes. Boundary heat losses were measured by calculating the enthalpy increase of the water coolant flowing in coils of copper tubing brazed to the backs of the electrodes. In these tests, the heat transfer rate to the vertical electrode was measured in two segments; for the 114 mm pool depth, the electrode was split into separately cooled segments of 25 mm at the top and 89 mm at the bottom. For the 230 mm pool depth, the electrode was split into a 25 mm upper segment and a 205 mm

lower segment. The opposite electrode was unsegmented and of the same overall length.

The ratios of the boundary heat fluxes, $\dot{Q}_{\text{upper}}/\dot{Q}_{\text{lower}}$, were investigated as a function of the boiling heat flux, \dot{Q}_B . It was found that for low boiling heat flux (\dot{Q}_B less than 3.5 cal/cm² s for the 230 mm pool; \dot{Q}_B less than 6 cal/cm² s for the 114 mm pool), the ratio $\dot{Q}_{\text{upper}}/\dot{Q}_{\text{lower}}$ was in the range of 1.5 to 2, in agreement with the prediction from thermal convection theory. For high boiling heat flux (\dot{Q}_B greater than 4.5 cal/cm² s for the 230 mm pool; \dot{Q}_B greater than 9 cal/cm² s for the 114 mm pool), the heat flux ratio was more nearly equal unity and equal to the heat flux to the unsplit electrode. The data was correlated in terms of a Nusselt number and Reynolds number based on the superficial vapor velocity. The Prandtl number was assigned separate exponential weight of 0, 1/3, and 1/2 powers. As a result, a new model was presented for horizontal heat flux based on bubble-induced laminar forced convection of the form

$$\overline{\text{Nu}} = C \text{Re}^{1/2} \quad (5)$$

where the constant C included the effect of the Prandtl number and the superficial vapor velocity was defined as in Eq. 4.

While the studies reported so far have contributed to the understanding of some hydrodynamic and heat transfer processes occurring in internally heated boiling pools, they do not provide a mechanistic model for predicting local boundary heat transfer or void fraction in such pools. Recognizing this shortcoming, Gustavson, et al.¹² undertook an investigation into the local distribution of boundary heat transfer and void fraction in internally

heated boiling pools. In their work, they also considered a rectangular pool of $ZnSO_4$ and water, joule heated by passing a-c current through the pool between two electrodes. Instead of using the electrode as the heat transfer surface, an instrumented test plate was installed, designed to allow measurement of local heat transfer to thermally isolated segments. Each segment was cooled by flowing water through separate cooling channels, and each flow rate was separately controlled to insure an isothermal pool-side surface temperature. The heat flux to each segment was measured by measuring the temperature rise and the flow rate of the coolant for each segment. The surface temperature of each segment was determined by extrapolating the interior thermocouple reading at the segment centerline to the test wall surface across 0.38 mm of aluminum and 0.76 mm Teflon sheet, which was cemented to the aluminum test wall surface for electrical insulation from the pool. A constant level weir was connected to an inlet at the pool bottom, which fed a steady flow of fluid to the pool to identically replace the losses due to vaporization. In this fashion, the net power for vaporization could be determined. The accuracy of the measured heat transfer coefficient in these tests was reported to be ± 40 percent.

The authors proposed that boundary heat transfer from volume-heated boiling pools was a mixed convection-type heat transfer phenomenon in which the effects were superimposable. They proposed, for laminar flow, that the thermal convective component be modeled as

$$Nu_N(x) = 0.42[Gr(x) \cdot Pr]^{0.25} \quad (6)^*$$

* In Ref. 12, the coefficient in Eq. 6 appeared as 0.41 instead of 0.42 suggested by Sparrow, et al.²³ for $Pr \approx 1.86$, average Pr for all the present experiments.

where $Gr(x)$ was the local Grashof number based on the average pool film density difference, and $Nu_N(x)$ now represented the local natural heat transfer correlation where x was measured along the heat transfer surface downward from the free surface. The forced convective component was represented by

$$Nu_C(x) = 0.332 Re(x)^{1/2} \cdot Pr^{1/3} \quad (7) **$$

where $Re(x)$ was the local Reynolds number based on the superficial vapor velocity at the pool surface. The method of modeling the combined natural/forced convection from a volume-boiling pool consisted of correlating the ratio

$$Y = \frac{Nu}{Nu_N} \quad (8)$$

to the group

$$Z = \frac{Nu_C}{Nu_i} \quad (9)$$

where Nu was the effective Nusselt number, either local or average, for the combined heat transfer process. Following a general correlation procedure,¹⁴ it was suggested that the functional form of the correlation should be

$$Y = [1 + Z^n]^{1/n} \quad (10)$$

where n was determined by a best fit evaluation of the data (see Fig. 1). Alternate forms of Eqs. 6 and 7 were proposed for the case of turbulent heat

** In Ref. 12, the exponent of the Prandtl number appeared as 1/2 instead of 1/3 as suggested by Kays²⁴

494
054

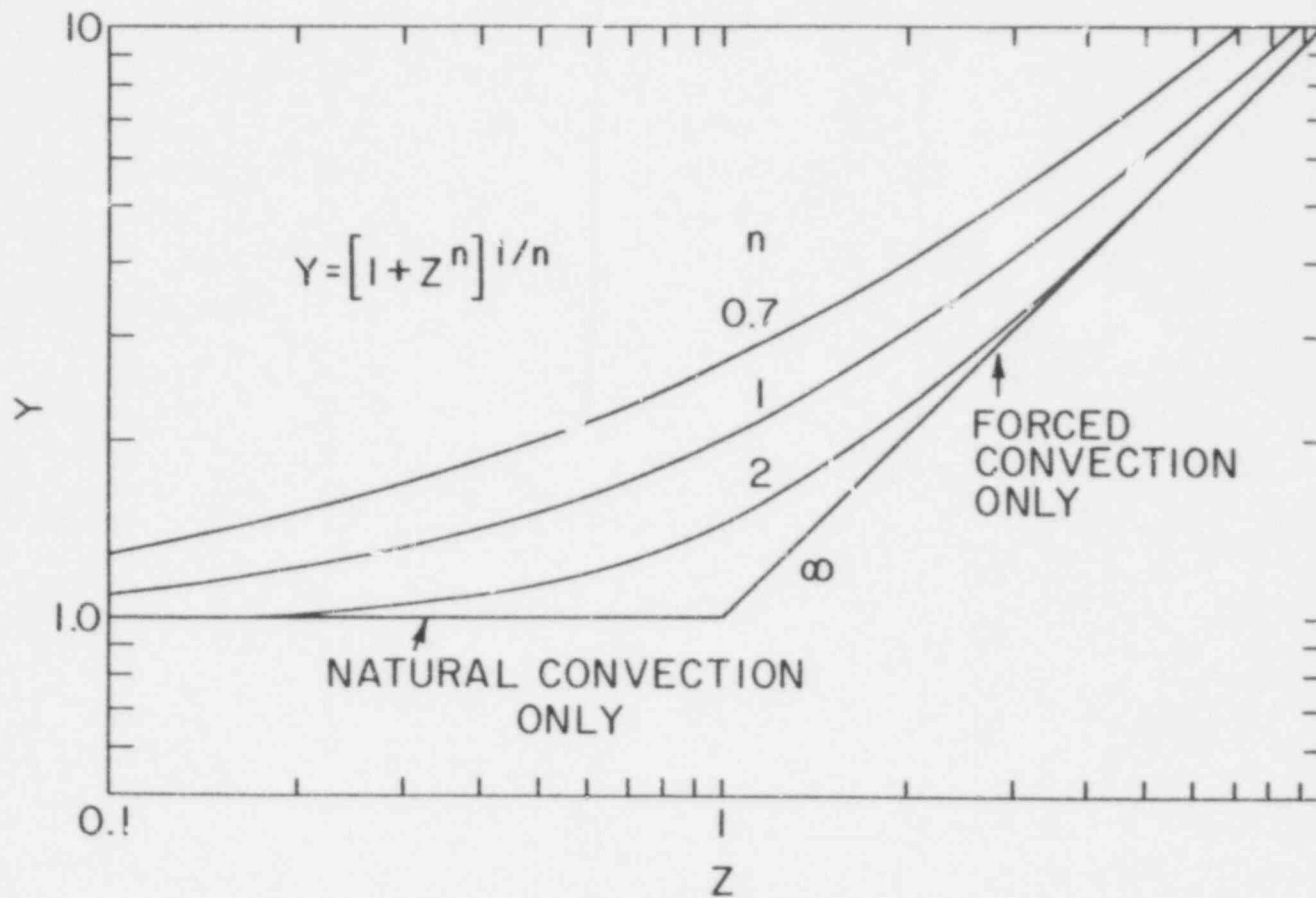


Figure 1 Proposed Correlation Scheme for Matching Forced and Free Convection Components of Boundary Heat Transfer Relation. (BNL Neg. No. 9-591-76).

transfer. The correlation was tested against the measured average heat transfer data from their tests. The best agreement was obtained using the laminar relations and a value of $n = 1.12$

3. ANALYTICAL MODELING

3.1 Heat Transfer

The data of Gustavson, et al. represent the first data available for local convective heat transfer coefficient from volume-heated boiling pools. The present authors conceived from the available data that the mode of heat transfer, instead of resembling mixed convection in which the effects were approximately superimposed, more closely approximated an enhanced mode of natural convection boundary layer flow and heat transfer. The phenomenon of boundary layer flow and heat transfer is depicted in Fig. 2. It is assumed that the vapor rising through the pool causes a net liquid drift upward, which encounters the free surface and is forced to return downward along the cold boundary. In this case, the net buoyancy effect is due to the liquid-to-two-phase density difference. The heat transfer distribution from the volumetrically boiling pool to the boundary exhibits behavior not unlike a single-phase natural convection boundary layer, enhanced by the flow of net liquid recirculation due to upward vapor drag through the central liquid and downward along the walls. With this point of view in mind, single-phase natural convection boundary layer theory coupled with the buoyancy effect of the two-phase flow in the bulk liquid was used to attempt to correlate the Nusselt number to a modified Rayleigh number.

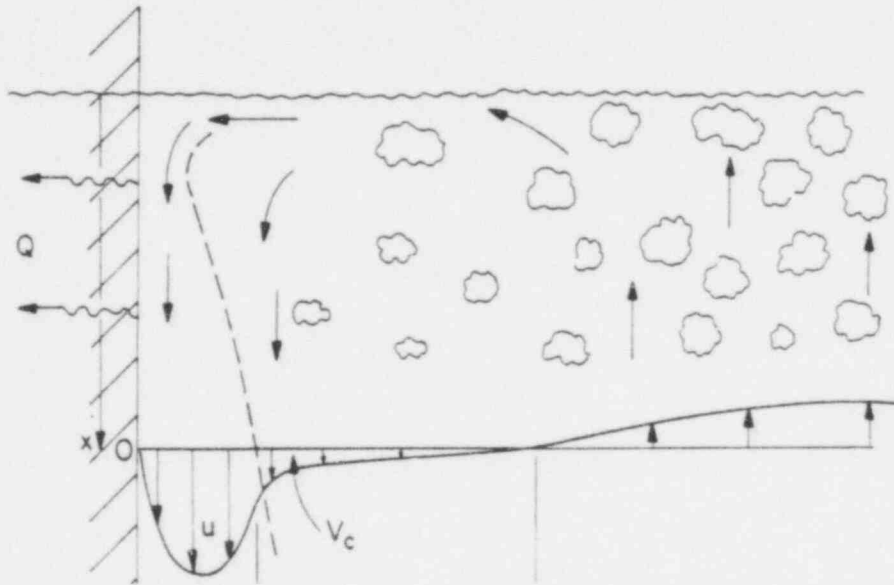


Figure 2 Schematic of Boundary Layer Flow and Heat Transfer From Volume Boiling Pool. (BNL Neg. No. 9-369-76).

Assuming that $\alpha\rho_{v\infty} \ll (1 - \alpha)\rho_{l\infty}$, it has been shown that a modified Grashof number based on the void fraction may be defined as,¹⁵

$$Gr^*(x, \alpha) = g_{eff} [\rho_w - (1 - \alpha)\rho_{l\infty}] \rho_f x^3 / \mu_f^2 \quad (11)$$

Furthermore, if the boundary is inclined from the vertical by an angle θ in such a manner that the boundary layer remains attached to the wall, the angle of inclination may be used to define the effective gravitational component in the direction of flow and Eq. 11 becomes

$$Gr^*(x, \alpha, \theta) = g \cos\theta [\rho_w - (1 - \alpha)\rho_{l\infty}] \rho_f x^3 / \mu_f^2 \quad (12a)$$

If $\alpha\rho_{l\infty} \gg \rho_w - \rho_{l\infty}$, this may be reduced to the simple form below

$$Gr^*(x, \alpha, \theta) = \frac{g \cos\theta \alpha x^3}{\nu_f^2} \quad (12b)$$

The experimental data of Gustavson, et al. were correlated on the bases of modified single-phase natural convection theory of the forms below;

a: Using average pool void fraction,

$$Nu(x, \bar{\alpha}) = K_1 [Gr^*(x, \bar{\alpha}) \cdot Pr]^{0.25} \quad (13a)$$

and

b: Using locally measured void fraction,

$$Nu(x, \alpha) = K_2 [Gr^*(x, \alpha) \cdot Pr]^{0.25} \quad (13b)$$

in which the properties used were the measured properties for the zinc sulfate solution at the appropriate film temperature. The value K_1 was determined from a log-log-linear least-squares fit to the data, and the

forms of the correlations are

$$a - \text{Nu}(x, \bar{\alpha}) = 0.78[\text{Gr}^*(x, \bar{\alpha}) \cdot \text{Pr}]^{0.25} \quad (14a)$$

with a standard deviation in the correlation coefficient of $\pm .35$,
and

$$b - \text{Nu}(x, \alpha) = 0.76[\text{Gr}^*(x, \alpha) \cdot \text{Pr}]^{0.25} \quad (14b)$$

with a standard deviation in the correlation coefficient of $\pm .56$.

The data was visually interpreted to be in the laminar regime and for the most part, fell in the range $\text{Ra}(x) < 10^{11}$. The experimental data, as well as the log-log-linear least squares fit to the data for Eq. 14a are shown in Fig. 3. The scatter in the correlation is basically the experimental scatter, and no finer structure was observed. The form of the correlation was insensitive to whether the average or local void fraction was used probably because the effects of the 1/4 root of the void fraction over the measured range of α was lost in the scatter of the data. The use of the average void fraction is attractive since then the computation of local heat flux will not require knowledge of the local void distribution which is more difficult to measure and compute.

In order to use either correlation method to predict the effects of boundary heat transfer from volume-heated boiling pools, knowledge of the local or pool-average void fraction, as seen in Eqs. 13a,b is required.

3.2 Void Dynamics

The void distribution may be calculated based on a one-dimensional

494 059

-13-

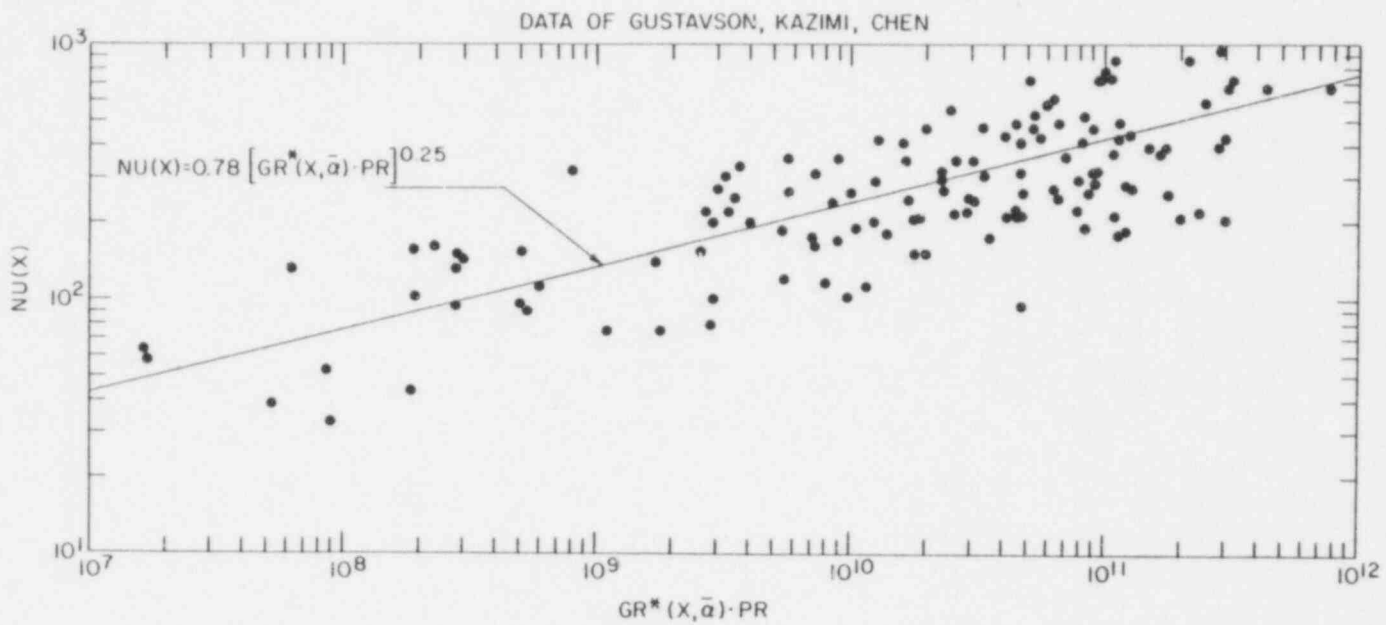


Figure 3 Modified Laminar Natural Convection Correlation of Boundary Heat Transfer from Volumetric-Boiling Pools (Based on Data from Ref. 12). (BNL Neg. No. 1-1295-79).

two-phase drift flux model.¹⁵ Consider a volume-heated boiling pool in which the volumetric vapor source may be written as

$$\Gamma_v = \frac{\dot{Q}_B (1 - \alpha)}{h_{fg}} \quad (15)$$

where the term $(1 - \alpha)$ signifies that the local heat generation occurs only in the liquid and Γ_v is the vapor source ($\text{gm}/\text{cm}^3 \text{ s}$). For most low power boiling pools in which the evaporated liquid is "made-up," the liquid volume flux will be negligible in comparison to the vapor volume flux. The steady state vapor mass conservation equation may be written as

$$\frac{dj_g}{dx} = \frac{\dot{Q}_B (1 - \alpha)}{\rho_v h_{fg}} \quad (16)$$

The relation between the superficial vapor velocity, j_g , and the drift velocity, V_{gj} , may be written as,¹⁶

$$\frac{\langle j_g \rangle}{\langle \alpha \rangle} = C_o \langle j \rangle + V_{gj} \quad (17)$$

where the notation $\langle \rangle$ indicates a cross-sectional area average quantity. If we assume $\langle j \rangle \sim \langle j_g \rangle$ and the distribution parameter $C_o = 1.2$, this reduces to

$$\langle j_g \rangle = \frac{\langle \alpha \rangle V_{gj}}{1 - C_o \langle \alpha \rangle} \quad (18)$$

Assuming that the drift velocity, V_{gj} , can be represented as

$$V_{gj} = U_\infty (1 - \alpha)^{1/4} \quad (19)$$

where $n = 0$ for churn-turbulent flow, and $n = 2$ for bubbly flow and dropping the bracket notation, Eq. 16 becomes

$$\frac{d}{d\xi} \left[\frac{\alpha(1 - \alpha)^n}{1 - C_o \alpha} \right] = K(1 - \alpha) \quad (20)$$

subject to the initial condition

$$\alpha = 0 \quad \text{at} \quad \xi = 0 \quad (21)$$

where $\xi = x/H_o$ and $K = \frac{Q_B H_o}{\rho_v h f_g U_\infty} = j_{g\infty}/U_\infty$. Equation 20 has been numerically integrated by two algorithms, an Euler predictor-corrector method and a fourth order Runge-Kutta method, with good agreement. The average void fraction, $\bar{\alpha}$, is defined as

$$\bar{\alpha} = \frac{\xi_{\max} - 1}{\xi_{\max}} \quad (22)$$

The results of the local void fraction calculation were compared to the local void fraction data of Gustavson, et al.,¹² for four selected experimental runs for a value of $K = 1.75$. Although agreement between calculation and experiment was poor on a local basis, the average void fraction for the four runs, $\bar{\alpha}_{\text{meas}} \sim .40$, agreed quite well with the calculated average void fraction, $\bar{\alpha}_{\text{calc}} \sim .41$.

The data of Gustavson, et al.¹² tend to support the concepts of boundary layer heat transfer and one-dimensional two-phase drift flux vapor distribution modeling for pools in the bubbly flow regime. However, the uncertainty in the measurements performed make it difficult to differentiate the degree of agreement with the various models proposed, as well as to

identify the various flow regime transition criteria for hydrodynamic and heat transfer behavior. In particular, the conditions for transition from bubbly flow to churn-turbulent flow are not clear, nor are the changes in the associated hydrodynamic and heat transfer behavior. As a result, it is difficult to extrapolate these results to other heat transfer systems of interest, in particular the behavior of internally-heated boiling pools of nuclear fuel in an HCDA, which may exist at power levels beyond the range of the previous work. For these reasons, the experiment described herein was undertaken.

4. EXPERIMENTAL

4.1 Pool Description

A schematic view of the overall pool construction is seen in Fig. 4. The pool was rectangular in cross-section, 18 cm wide x 33.5 cm long. The electrodes were recessed into lexan walls and polished to eliminate surface nucleation. The electrodes, as well as the walls and base, could be supplied with cooling water flow to eliminate preferential surface nucleation if necessary. Evaporative and boiling vapor losses were recovered through a make-up water flow port connected to a constant level weir adjusted to H_0 . The net make-up water flow rate was measured and converted to gross vaporization power. The make-up flow was introduced from the pool bottom into a baffled space to pre-heat the water to T_{sat} and prevent inlet subcooling effects. No boiling occurred in this space. The entire pool was

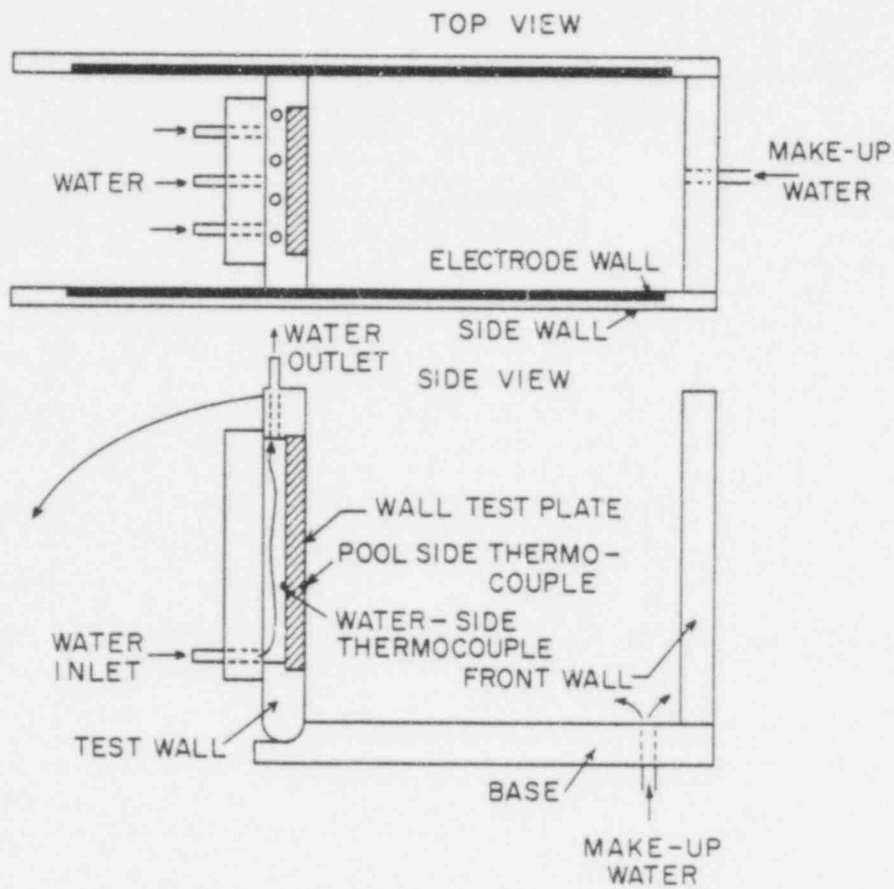


Figure 4 Schematic View of Inclined-Wall Volumetric Boiling Pool Apparatus. (BNL Neg. No. 1-1385-79).

constructed of lexan with the exception of the copper electrodes and boron nitride test plate.

The boiling and nonboiling depths of the pool were measured with a voltage probe connected to a precision traversing mechanism. The conductor was lowered by the traversing mechanism until continuity was achieved and the voltmeter indicated the pool voltage. The pool was powered to the operating power and the probe was once again lowered until the operating voltage was again indicated. In this fashion, visual observations of pool depth were eliminated and more objective measurement of H_o and H_B was possible. The uncertainty in this measurement technique was essentially the fluctuations in pool height while boiling.

4.2 Test Plate

The test wall was constructed of lexan and was machined in such a fashion that the base of the test wall was continuously inclinable from the vertical position to any inclined position. A schematic of the test wall is shown in Fig. 5. The test surface was composed of boron nitride sheet (1.27 cm x 30.5 cm x 12.7 cm), machined and recessed into the lexan wall with the pool-side surface flush with the lexan and in direct contact with the boiling pool. The material has heat transfer characteristics of an excellent thermal conductor, but is electrically insulating at the same time. These properties, along with low water absorption and thermal expansion and ease of machining, made BN an ideal material for these tests. In addition, no electrically insulating covering was necessary, eliminating contact heat transfer resistance and temperature extrapolation. The back

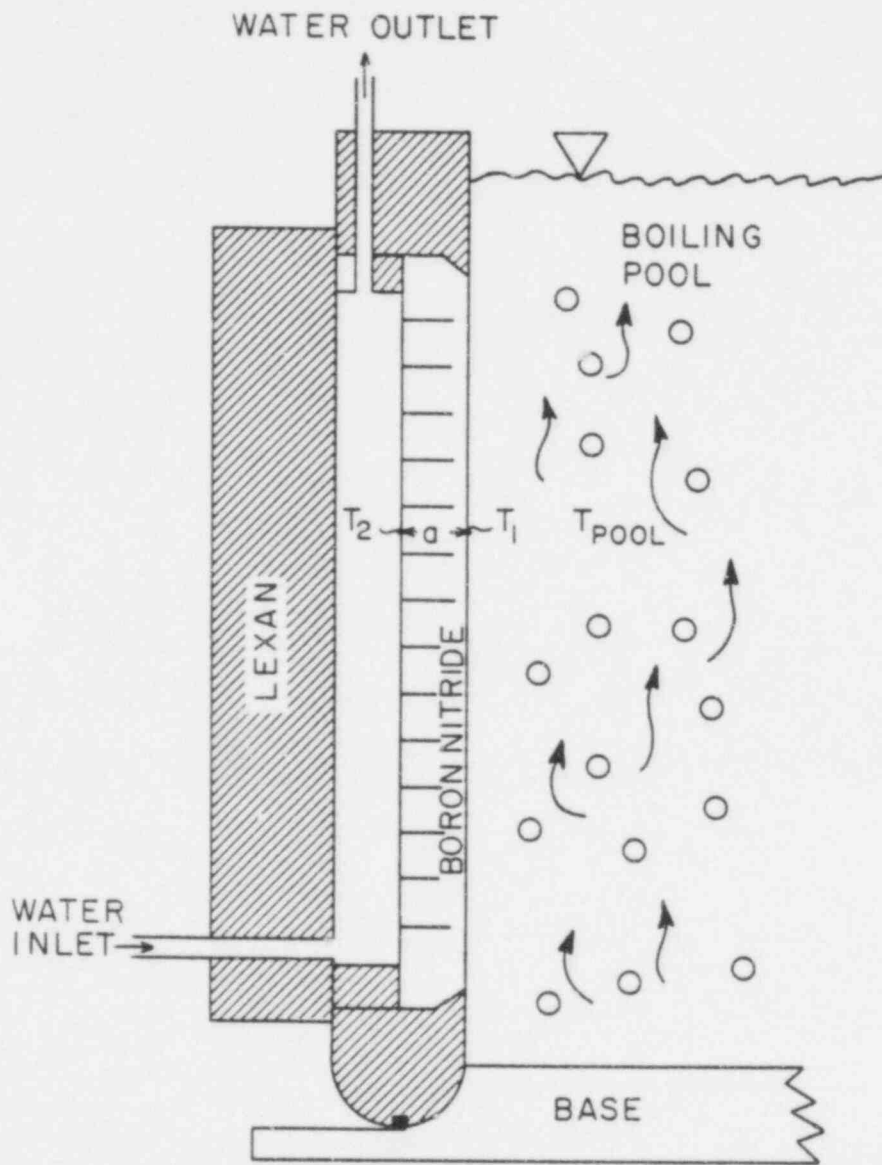


Figure 5 Schematic View of Inclined Wall Test Plate. (BNL Neg. No. 1-1384-79).

surface of the BN test plate was cooled by flowing water. A separate flow loop was designed to supply a continuous flow of water, 15-20 lpm, to remove the heat transferred to the wall. The flow rate was designed to be high enough that the convective resistance to heat transfer in the coolant loop was negligible. The entire back surface of the BN was exposed to the coolant flow. This eliminated channel coolant effects, as well as hot and cold spots from coil cooling techniques previously employed (see Fig. 5.). A picture of the assembled test pool may be seen in Fig. 6.

4.3 Test Plate Instrumentation

The BN was instrumented with chromel-alumel thermocouples for local heat transfer measurements. The thermocouples were 0.025 cm diameter stainless steel-clad microthermocouples, which were machined flat at the junction and electro-gold-plated with ~ 0.003 cm of gold forming the hot junction across the isolated chromel and alumel leads. A schematic of the cross-sectionally polished and gold-plated microthermocouples is shown in Fig. 7. A photograph of the polished but unplated thermocouple tip may be seen in Fig. 8. The thermocouples were individually calibrated at the ice point and steam point taking local barometric pressure into account, and the average calibration data for each was compared to NBS type K data. It was found that all the gold-plated thermocouples calibrated to within $\pm .07$ °C from the steam to the ice point. The gold-plated microthermocouples were then cemented into 26 locations in the BN wall, 19 on the front at 1.27 cm intervals, and 7 on the back at 3.81 cm intervals at locations listed in Table 2. They were installed in such a manner that the measuring junction

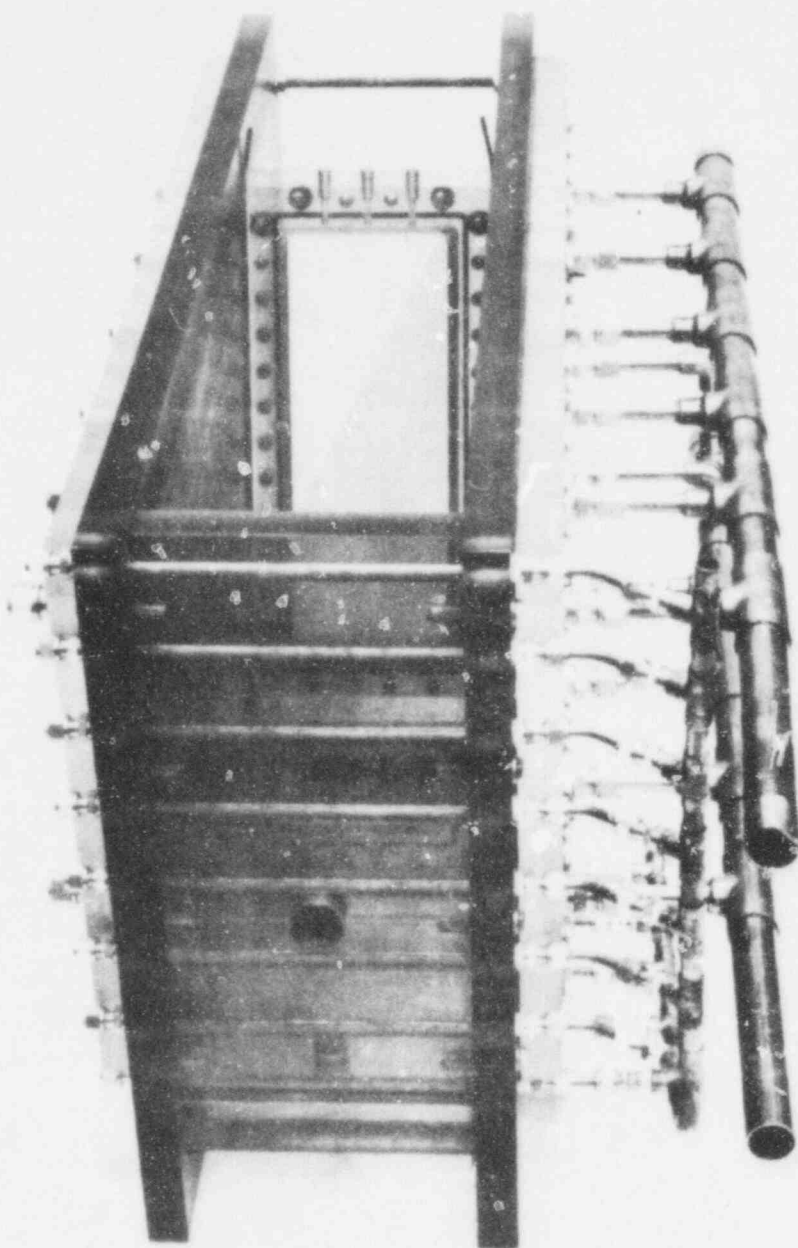


Figure 6 Photograph of Assembled Test Pool. (BNL Neg. No. 3-1418-77).

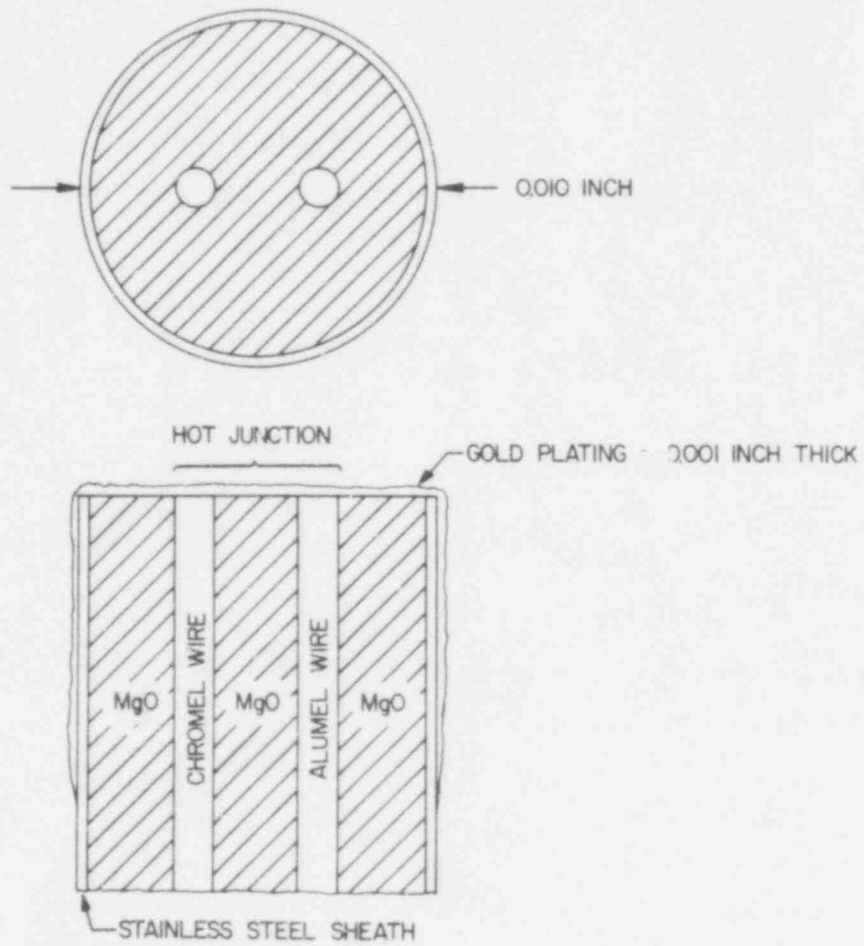


Figure 7 Schematic View of Gold Plated Microthermocouple.
 (BNL Neg. No. 2-376-77).

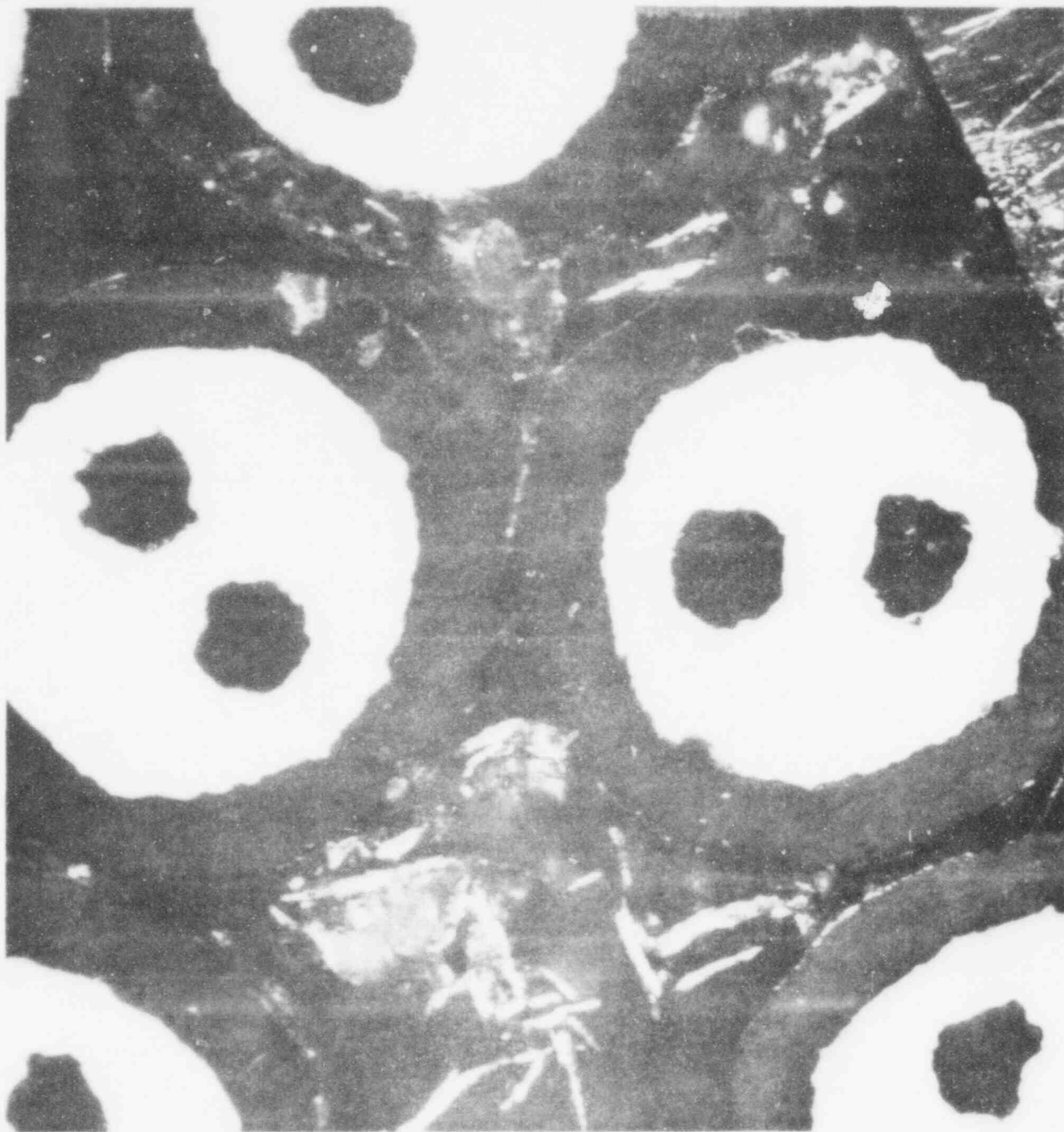


Figure 8 End View of Unplated Thermocouple Cross Section.
(BNL Neg. No. 3-1422-77).

494 069

TABLE 2

THERMOCOUPLE LOCATIONS IN TEST PLATE

Pool Side		Coolant Side	
Thermocouple No.	Elevation Above Base(cm)	Thermocouple No.	Elevation Above Base(cm)
1	31.40	20	8.54
2	30.13	21	12.35
3	28.86	22	16.16
4	27.59	23	19.97
5	26.32	24	23.78
6	25.05	25	27.59
7	23.78	26	31.40
8	22.51		
9	21.24		
10	19.97		
11	18.70		
12	17.43		
13	16.16		
14	14.89		
15	13.62		
16	12.35		
17	11.08		
18	9.81		
19	8.54		

was flush with the wall surface within an estimated $\pm .003$ cm tolerance and cemented in place under a microscope. The gold-plated junction thus comprised part of the test wall surface. Heat losses along the thermocouple sheath were negligible since the leads were immersed in the plate at least 50 diameters.

4.4 Data Acquisition

The thermocouples were connected to a $150^{\circ}\text{F} \pm .2^{\circ}\text{F}$ oven-type reference junction along with a thermocouple in the bulk pool, and the data was then routed to the automated data acquisition system. The centralized data acquisition and analysis system was constructed around an HP 9640 system, consisting of a 21 MX minicomputer with 112 kilowords of central memory, 7.5 megaword cartridge disk, and 9 track magnetic tape transport. Control of the system was accomplished by interactive software, which received transfer parameters from the experimenter and proceeded to scan the data channels upon command. The thermocouples were scanned by a 300 channel guarded crossbar scanner, which transferred data to an integrating digital voltmeter with microvolt resolution. Each thermocouple was sequentially sampled until the standard deviation of the output converged to a preset criterion or the maximum sample limit was exceeded. At this point, the scanner proceeded to the next thermocouple and repeated the same procedure until all 27 thermocouples had been integrated. The raw data was transferred to magnetic tape and preliminary engineering calculations were performed to convert the thermocouple output and system properties into local convective heat transfer coefficient and average pool void fraction.

A photograph of the entire inclined wall boiling pool test apparatus may be seen in Fig. 9.

All the measuring devices and their uncertainties are listed in Table 3.

5. EXPERIMENTAL RESULTS

5.1 Range of Experiments

The experiments described have been performed over a range of dimensionless vaporization power, $j_{g\infty}/U_{\infty}$, up to 1.8. Local heat fluxes along the inclined boundary were measured as indicated in Eq. 23.

$$h(x) = \frac{k_{BN}(T_{front}(x) - T_{back}(x))}{a \cdot (T_{pool} - T_{front}(x))} \quad (23)$$

Accuracy of these measurements was estimated to be within ± 5 percent. The tests reported herein do not have local void fraction measurements included, but rather have been correlated only on an overall average basis. The pool-average void fraction was measured as indicated in Eq. 24 with an estimated accuracy of ± 3 percent.

$$\bar{\alpha} = (H_B - H_O)/H_B \quad (24)$$

A complete error analysis is presented in Appendix A. Sample calculation of the heat transfer data is presented in Appendix B. For the boiling experiments presented here, the wall angles investigated were 90° , 75° , and 60° from horizontal with an accuracy of $\pm .5^\circ$. The flow regimes that were investigated are listed below and will be discussed in this order:

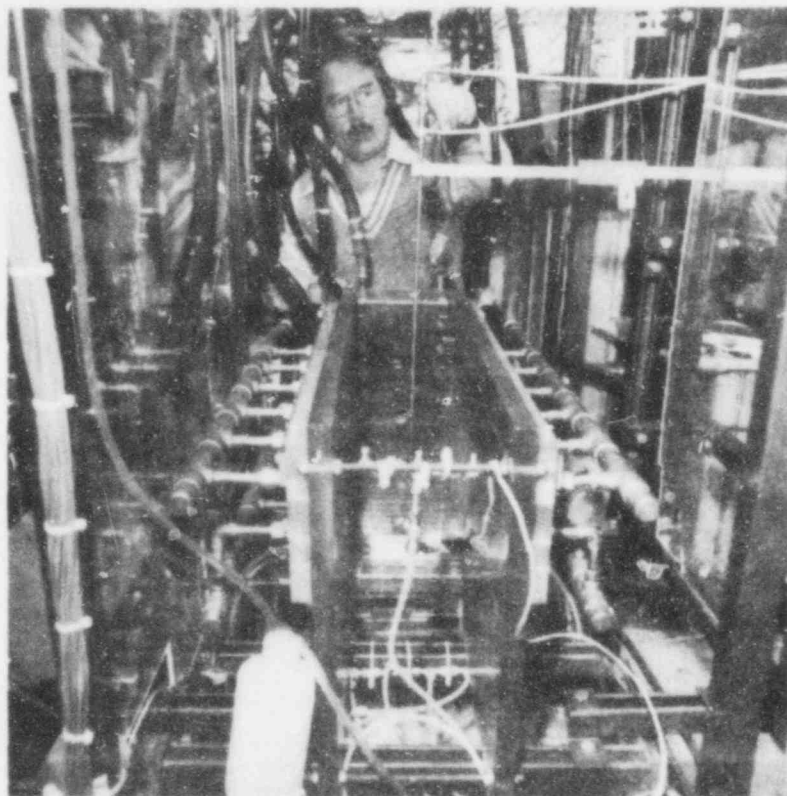


Figure 9 Photograph of Assembled Test Pool Facility.
(BNL Neg. No. CN2-798-78).

494 073

TABLE 3

LIST OF MEASURING DEVICES USED
AND THEIR UNCERTAINTY

INSTRUMENT	UNCERTAINTY
Thermocouple, Gold-Plated, Type K	$\pm .07$ °C
Digital Voltmeter, HP 3455A	± 1 μ v
Reference Junction, REF-CEL 200	$\pm .10$ °C
Traversing Mechanism	$\pm .001$ m
Make-Up Flow Meter System	$\pm .2$ ml/s
Power Stats	± 1 percent
Cross-Bar Scanner, HP 2911A,B,	
Hewlett-Packard Minicomputer, 21MX Series	
Printer-Plotter, Statos 42	

494 074

1. Nonboiling, single-phase
2. Boiling
 - a. Incipient boiling
 - b. Bubbly flow regime
 - c. Transition
 - d. Churn-turbulent flow regime

Tests were performed to determine if there were any measurable effects of the test wall coolant flow rate and make-up water temperature upon the boundary heat transfer distribution. The coolant flow rate was varied from 15-20 lpm with no measurable effect upon the magnitude of the measured heat transfer coefficients. The make-up water temperature was observed to have no effect as long as it entered the pool from the baffled preheating space at or close to T_{sat} .

5.2 Nonboiling Regime

Initial experiments were performed in nonboiling pools in order to perform operational checkout of the equipment and instrumentation. In addition, the nonboiling heat transfer to vertical and inclined boundaries was of interest in order to examine the nature of the boundary layer heat transfer. For these experiments, the total power applied to the pool was in the range of 1.0 to 2.5 kw. Boiling was not allowed to occur and heat transfer was single phase only. The profile of local boundary heat transfer behaved similar to single-phase laminar natural convection. The greatest magnitude of the local heat transfer coefficient was measured at or near the top of the test plate (i.e., the leading edge of boundary layer) and was in

the range 0.015-0.020 cal/cm²s °C. Correlation of this data indicated that the behavior agreed very well with established single phase laminar natural convection as expected and verified the ability of the equipment to measure local boundary heat flux from volume-heated pools accurately. Also the use of the effective gravitational component,

$$g_{\text{eff}} = g \cos\theta \quad (25)$$

was verified for natural convection, and the effect of the internal heat source on the boundary layer thickness was found to be negligible as calculated by the correction method of Randall and Sesonske.¹⁷

5.3 Incipient Boiling Regime

As the power that was applied to the pool was increased, the regime changed as volumetric bubble nucleation in the bulk liquid began to appear. The onset of nucleation was determined solely by visual observation of the pool. This regime was called the incipient boiling regime. The behavior was characterized by bubble formation and rise with little measurable increase in average pool height. The pool average void fraction was in the approximate range 0.00 to 0.03. The behavior of the boundary heat transfer was once again observed to resemble laminar natural convection as in the nonboiling tests. However, it was observed as in Fig. 10 that the maximum local heat transfer coefficient increased to approximately 0.08 cal/cm² s °C. This was an increase over the nonboiling case of approximately a factor of 4-5. This indicated that although boundary layer-type heat transfer behavior was persisting, the superficial vapor velocity of the rising steam was causing a net recirculation of liquid which was rising through the

VOLUMETRIC BOILING POOL DATA

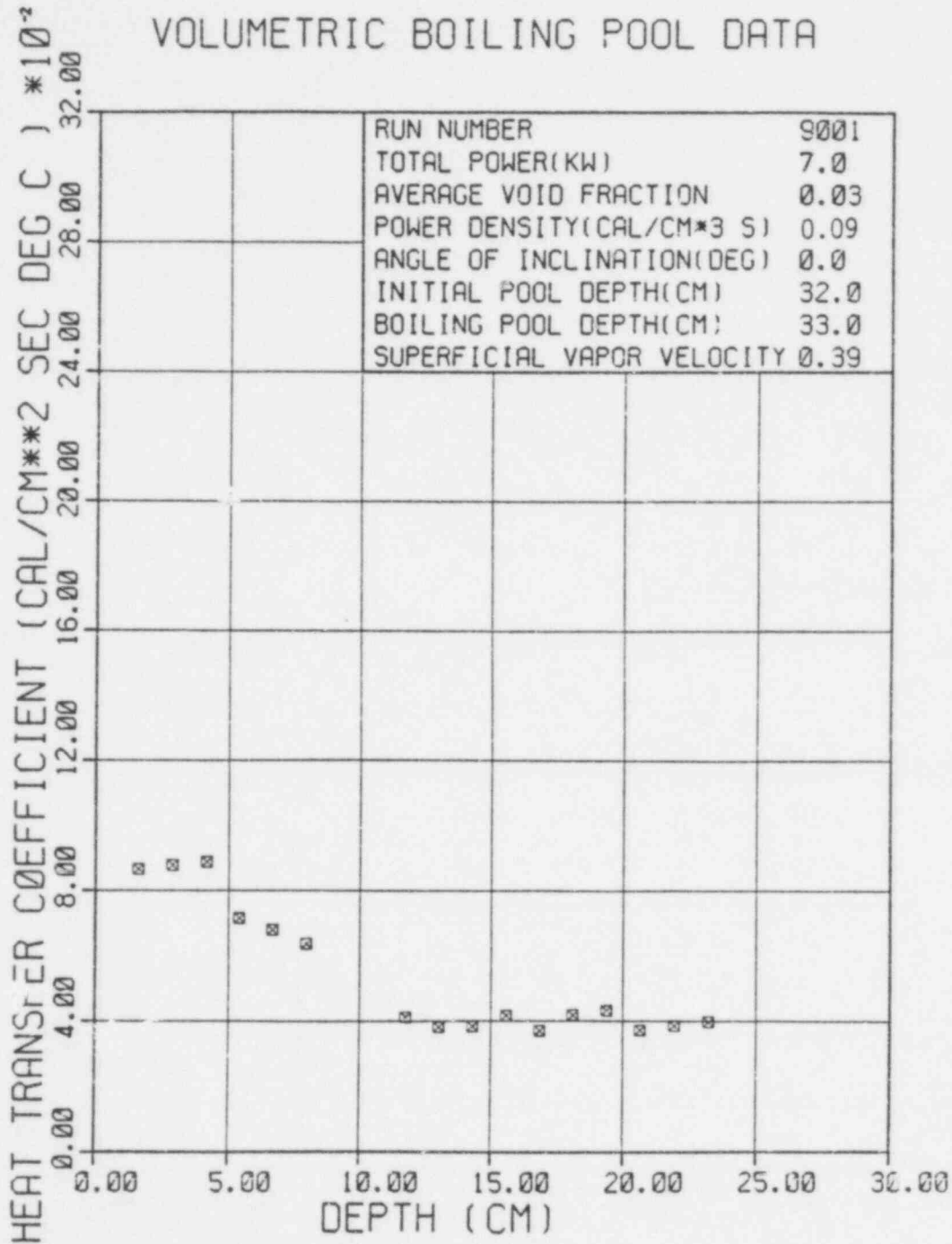


Figure 10 Profile of Local Boundary Heat Transfer Coefficient From Volume Boiling Pool - Run No. 9001 - Incipient Boiling. (BNL Neg. No. 4-844-79).

saturated pool. This liquid drift would encounter the free surface and turn towards the cold boundaries and flow downwards along the wall, enhancing the boundary layer heat transfer as evidenced in the magnitude of the convective coefficient. Boiling inception appeared to begin at a threshold value of $j_{g\infty}/U_{\infty}$ approximately equal to 0.2. Below this value, the pool was volume-heated single phase and above this value, two-phase effects and volumetric boiling became evident. This value of dimensionless superficial vapor velocity indicated the magnitude of the evaporative power losses from the pool. Reducing the total vaporization power, $j_{g\infty}/U_{\infty}$, by the evaporative losses, $(j_{g\infty}/U_{\infty})_0$, yields the net boiling power presented in dimensionless form below:

$$(j_{g\infty}/U_{\infty})^* = j_{g\infty}/U_{\infty} - (j_{g\infty}/U_{\infty})_0 \quad (26)$$

It is recognized that this evaporative loss term, $(j_{g\infty}/U_{\infty})_0$, will be system dependent and will diminish as the pool free surface area to volume ratio decreases. Analysis of the void distribution was performed on the basis of $(j_{g\infty}/U_{\infty})^*$ as will be seen.

5.4 Bubbly Flow Regime

A further increase in power applied to the pool resulted in net production of vapor and a finite void fraction. This flow regime was characterized by a stable array of densely packed bubbles which formed initially in the upper region of the pool above an essentially quiescent single-phase region below. As boiling power was increased further, the thickness of the bubbly boiling region increased, penetrating downward through the nonboiling region. The bubbly flow regime is a liquid-continuous flow regime in which

VOLUMETRIC BOILING POOL DATA

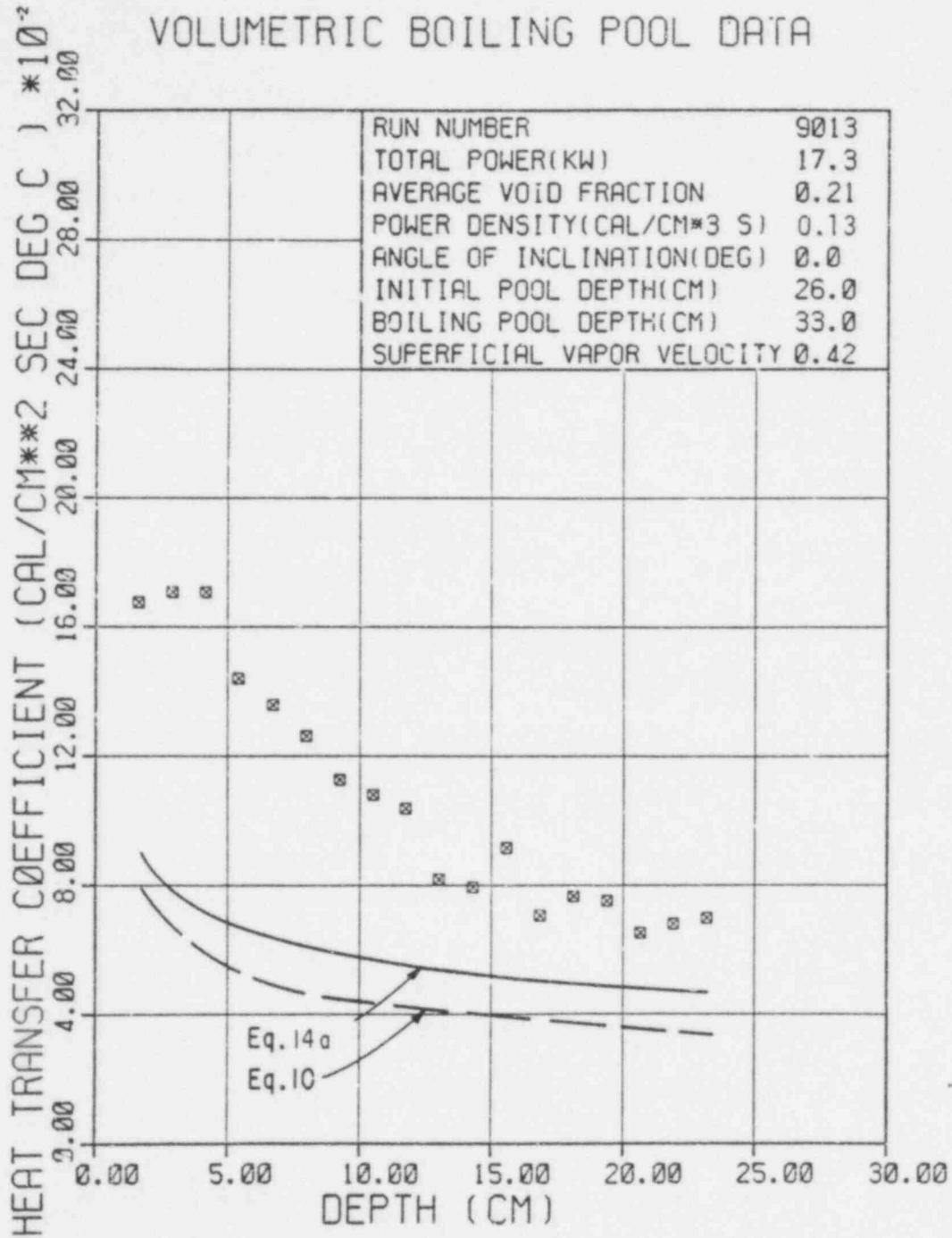


Figure 11 Profile of Local Boundary Heat Transfer Coefficient From Volume Boiling Pool - Run No. 9013 - Bubbly Flow. (BNL Neg. No. 3-1891-79).

the dispersed phase is the vapor. As verification of this assumption, the time trace of power vs time was examined to determine the effect of bubbly motion upon electrical coupling of the liquid. Any decoupling of the liquid from the applied electric field would be recognized by a transient fluctuation of the power trace. None was evidenced, indicating that the pool power was evenly applied and distributed through the continuous liquid phase creating a constant volumetric power density. The pool average void fraction was observed to be very sensitive to the vaporization power in the bubbly flow regime. A small increase in $j_{g\infty}/U_{\infty}$ resulted in a rather large increase in $\bar{\alpha}$, as shown later in Fig. 14.

The maximum average void fraction achieved in these tests occurred for the bubbly flow regime just prior to flow regime transition and was approximately 0.55-0.60. While in the bubbly flow regime, the pool was observed to swell periodically. This is believed to be caused by local subcooling effects due to reentry into the pool of cold liquid from recirculating boundary layer flow which would cool the pool temporarily below the saturation temperature and induce partial void collapse.

The spatial profile of local boundary heat transfer coefficient maintained its boundary layer nature as before. An example of this is shown in Fig. 11. The maximum local heat transfer coefficient was observed, in all cases, to be at or near the pool surface, and its magnitude was measured at approximately $0.20 \text{ cal/cm}^2 \text{ s } ^\circ\text{C}$. The coefficient was observed to decrease as depth along the heat transfer surface increased and it was observed to vary in magnitude along the test plate surface by approximately a factor of 3-5. The average heat transfer coefficient for all the runs in the bubbly

flow regime was calculated to be approximately 0.10; this was greater than the single-phase tests by about a factor of 5. The local heat transfer coefficient data was compared to the predictions of the models previously described in Eqs. 10¹² and 14a¹⁵, and the comparison is shown graphically, for Run 9013, in Fig. 11; the comparison on a local basis is available for all the runs in Appendix C and will be presented later on an average basis in Table 6. It is clear in Fig. 11 that the local convective heat transfer coefficients for these experiments exceeded the calculations of both local heat transfer models available^{12,15} (derived from the local boundary heat transfer data from volume boiling pools reported in Ref. 12) by as much as a factor of 2 or more. This will be supported by Table 6 which will present a comparison of the average convective coefficients for all the experiments reported to the models referenced^{12,15} on an average basis.

5.5 Bubbly-Churn Turbulent Transition

As the pool power was increased further, a flow regime transition was observed to begin in the vicinity of $j_{g\infty}/U_{\infty} \sim 0.8-1.0$. This flow regime was characterized by an increasing instability in bubble array order and the onset of bubble agglomeration; densely packed bubbles in a liquid continuous flow began to break down into large regions of liquid and large regions of vapor. The onset of this transition region appeared for the most part to coincide with full penetration of the boiling region to the pool bottom. The runs that characterize this region are runs 6009-6011 and 6014-6015 (hydrodynamic only). These runs demonstrated a partial pool collapse due to

the bubble agglomeration mechanism previously mentioned. Such behavior is observed in adiabatic bubble columns as previously shown.^{19,20,21} The previously observed good agreement between measured and calculated average void fraction based on $(j_{g\infty}/U_{\infty})^*$ for the bubbly flow regime was no longer observed; instead the measured void fraction fell between the calculated values based on both the bubbly and the churn turbulent drift flux. This will be seen in Table 6 where the calculated average void fraction is that based on the bubbly flow drift flux model, and the number in parentheses is that for the churn-turbulent drift flux model. In addition, the previously observed periodic pool swelling behavior diminished.

The spatial profile of local boundary heat transfer coefficient continued to maintain a strong boundary layer behavior as before. However, as seen in Fig. 12, a great deal of scatter appeared, and the variation along the test wall became less. As has been noted previously¹¹, the magnitude of the heat flux became more nearly constant, and for this case, the ratio $\bar{h}_{\text{upper}}/\bar{h}_{\text{lower}}$ was approximately 4/3. The average boundary heat transfer coefficient was measured for transition runs 6009-6011 only, and was found to be approximately 0.125. This was greater by 25 percent over the average heat transfer coefficient in the bubbly flow regime and indicated that the hydrodynamic instability causing bubble agglomeration and flow regime transition was responsible for a corresponding increase in the boundary heat transfer coefficient. In spite of this apparent increase in the average boundary heat transfer, the measured heat transfer coefficients were in the range of those for the highest power bubbly flow regime runs. Correlation of the transition region data was close to the bubbly flow data, as we will

VOLUMETRIC BOILING POOL DATA

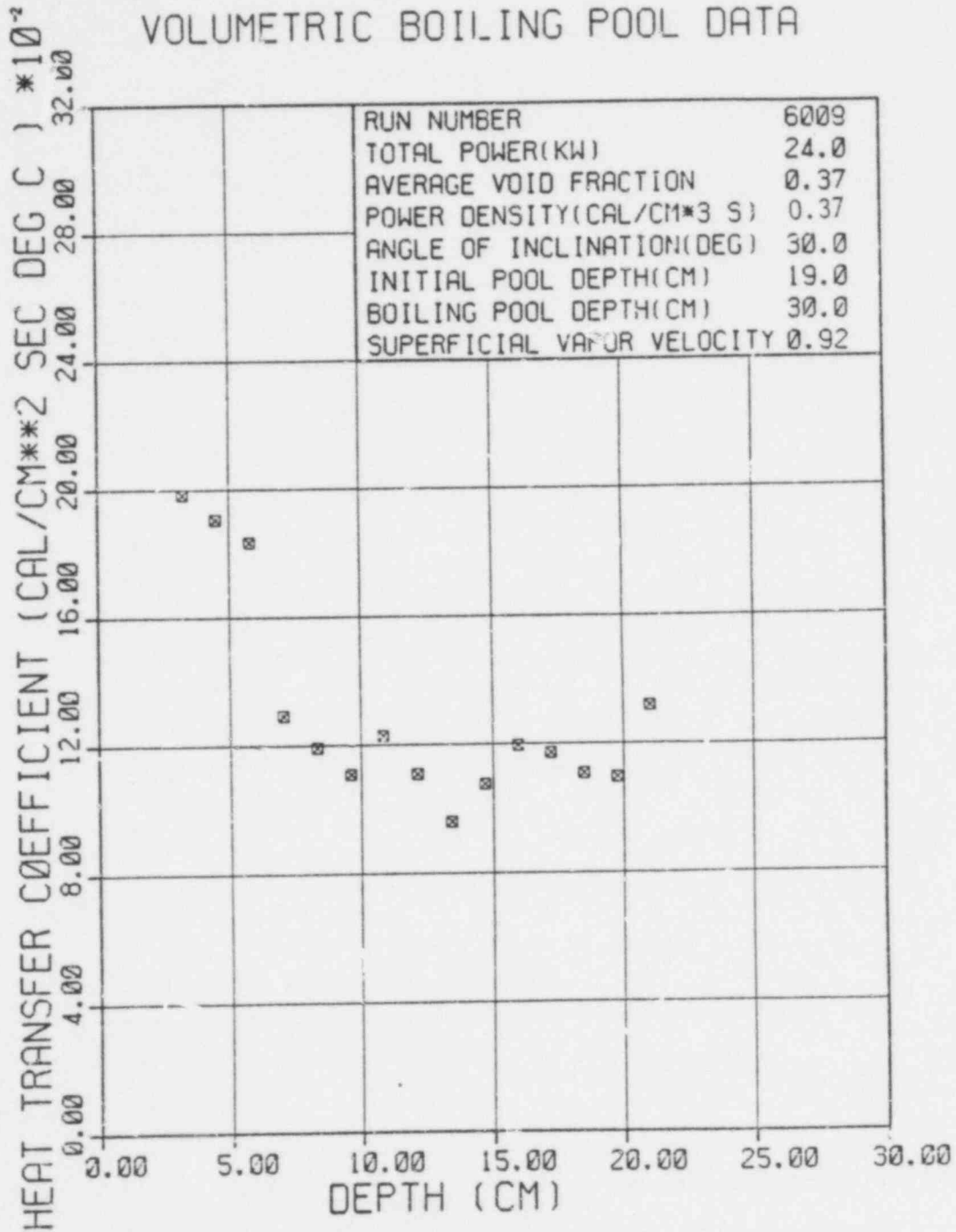


Figure 12 Profile of Local Boundary Heat Transfer Coefficient From Volume Boiling Pool - Run No. 6009 - Transition. (BNL Neg. No. 4-845-79).

see in the next section, however, the scatter in the measurements was greater, indicative of the instability in void dynamics observed.

5.6 Churn-Turbulent Flow Regime

The churn-turbulent flow regime appeared to dominate for $j_{g\infty}/U_{\infty} \geq 1.0$. This flow regime was characterized by a total breakdown in the well-ordered close packed bubble array observed for the bubbly flow regime. Instead, the hydrodynamic behavior appeared chaotic and highly "turbulent." Well-ordered flow patterns caused by upward vapor drift and downward boundary layer flow were no longer evident. In addition, the liquid-continuous flow hydrodynamics was destroyed by massive bubble agglomeration. This phenomenon appeared to be responsible for the creation of large regions locally which were entirely liquid or vapor. Large vapor flow paths appeared in the flow, allowing the escape of greater vapor mass flux than in the bubbly flow regime with considerably less liquid hold up. The result was a considerably lower average void fraction, as defined previously.

The flow regime transition from bubbly to churn turbulent flow occurred suddenly and completely at a value of $j_{g\infty}/U_{\infty}$ approximately equal to one. At this point, the average void fraction suddenly collapsed from a value of 0.55-0.60 to approximately 0.40. Simultaneously, the apparently reasonable assumption (born out at this time by visual observations only) of one-dimensional flow for the bubbly flow regime and corresponding good agreement in average void fraction between experiments and one-dimensional drift flux void calculations appeared to no longer be valid for churn-turbulent flow. On the contrary, the flow appeared to become more three-dimensional in

behavior, and the applicability of one-dimensional drift flux modeling under these conditions is questionable. Nevertheless, comparison between experimentally measured average void fraction data and calculated values based on the one-dimensional drift flux model for churn-turbulent flow was good. The average void fraction measured for the cases of transition and churn-turbulent flow was in the range of 0.40 and relatively insensitive to an increase in power for $j_{g\infty}/U_{\infty}$ up to 2.0.

During some of the bubbly flow runs, a thin but stable foaming layer was observed to form on the pool surface. The $ZnSO_4$ electrolyte solution was frequently replaced to avoid the addition of unwanted contaminants, but no surface active chemicals were added to destroy this thin foam. The reasons for its formation are not well known, although its presence has been observed before.^{12,18} Regardless of its cause, the foam layer was invariably observed to completely and immediately disappear upon transition to the churn-turbulent flow regime, indicating that foams may not be an effective flow regime in such dynamic flow systems at dimensionless superficial vapor velocities in excess of unity, corresponding to vapor velocities greater than the bubble terminal rise velocity.

The heat transfer behavior also changed dramatically, and a sample of the local distribution of boundary heat transfer coefficient is demonstrated in Fig. 13. The apparent boundary layer nature of the heat transfer distribution seemed to disappear, replaced by a more uniform heat transfer coefficient along the boundary. The maximum local heat transfer coefficient was observed to be in the range $0.25-0.30 \text{ cal/cm}^2 \text{ s } ^\circ\text{C}$. The coefficient was observed to fluctuate temporally and spatially as well.

VOLUMETRIC BOILING POOL DATA

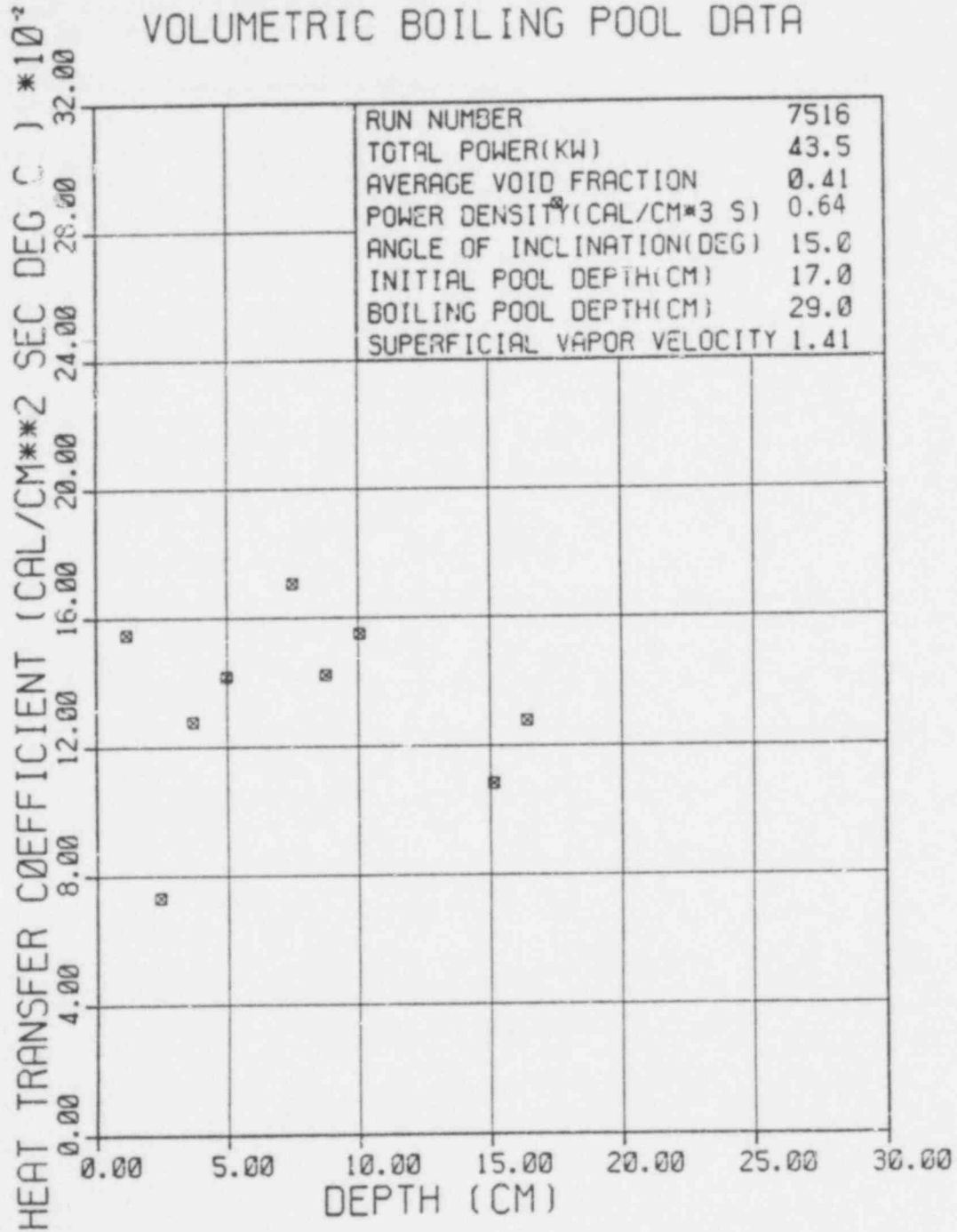


Figure 13 Profile of Local Boundary Heat Transfer Coefficient From Volume Boiling Pool - Run No. 7516 - Churn-Turbulent. (BNL Neg. No. 4-846-79).

The temporal fluctuations are evident in the standard deviation data of the local boundary temperature history. Whereas for the bubbly flow regime, the standard deviation of the discretely sampled instantaneous wall temperature distribution was found to be in the range 0.2-0.6 °C, and for the transition flow regime, the standard deviation of the wall temperature was found to be in the range of 1.0 °C, a dramatic increase was observed for the churn-turbulent flow regime. The standard deviation of the local wall temperature averaging technique was found to be in the range 2.0-7.0 °C, an order of magnitude greater than previously observed for the well-ordered bubbly flow regime. Interpretation of this data concerning the standard deviation of the local wall temperature in churn-turbulent flow indicated that the standard deviation was nearly equal in most cases to the difference between the saturated pool temperature and the average wall temperature, i.e.,

$$\sigma_w \approx T_{\text{pool}} - \bar{T}_w \quad (27)$$

This was interpreted to mean that, intermittently, free stream conditions were present at the boundary of the pool. This indicated that the wall boundary layer was periodically being destroyed by the highly chaotic three-dimensional hydrodynamic behavior of the churn-turbulent flow and subsequently being reestablished. This type of intermittent renewal of the boundary layer may account for the enhanced heat transfer observed.

Investigation of the time trace of power applied to the pool was used to evaluate the effective overall electrical coupling of the liquid to the applied electric field as before. The power trace was observed to experience high frequency fluctuations in contrast to the steady nature of the

bubbly flow regime. This was interpreted to mean that due to hydrodynamic fluctuations in the pool, the electrical resistance was fluctuating and perhaps portions of the liquid were becoming electrically isolated from the electric field; under such conditions the pool could no longer be characterized by liquid-continuous concepts. It is not clear at what dimensionless superficial vapor velocity (power) joule heating becomes ineffective in supplying uniform power density per unit liquid volume due to the observed electrical uncoupling mechanism in churn-turbulent flow. In the churn-turbulent flow regime for the heat transfer runs presented, the average boundary heat transfer coefficient was measured to be approximately $0.15 \text{ cal/cm}^2 \text{ s } ^\circ\text{C}$. This represented an increase of 50 percent over the average heat transfer coefficient measured for the bubbly flow regime.

6. DATA ANALYSIS AND DISCUSSIONS

6.1 Comparison of Calculated and Measured Pool Void Fraction

For the experiments presented so far, the average void fraction, $\bar{\alpha}$, was measured and compared to the dimensionless superficial vapor velocity based upon total vaporization power, $j_{g\infty}/U_\infty$. It was demonstrated that there existed a threshold velocity, $(j_{g\infty}/U_\infty)_0$, below which the pool would not boil. Subsequently, a net boiling superficial vapor velocity was defined, $(j_{g\infty}/U_\infty)^*$, as seen in Eq. 26. It has been determined that the quantity $(j_{g\infty}/U_\infty)_0$ was a system parameter and approximately equal to 0.2 for these tests.

A composite diagram of all the average void fraction data is plotted in

Fig. 14 as a function of the dimensionless superficial vapor velocity for the incipient boiling, bubbly flow, transition and churn-turbulent flow regimes.

The incipient boiling bubbly flow data and the churn-turbulent data were compared to the predictions of the one-dimensional drift flux model based upon net vaporization power and the appropriate drift flux model. In addition, the transition data were compared to both bubbly and churn-turbulent flow models. The comparisons are shown in graphical form in Fig. 15. The model was in fair agreement with the bubbly flow and incipient boiling data for small values of $j_{g\infty}/U_{\infty}$ and improved considerably as this value increased. This behavior was not unexpected in view of the strong sensitivity of the void fraction in the bubbly flow regime to small changes in boiling power as demonstrated in Fig. 14.

The transition data, due to the nature of the onset of flow instability, demonstrated poor agreement with both the bubbly and churn-turbulent flow models. As expected, however, the measured values did all fall intermediate to the two model predictions.

For the churn-turbulent flow data, good overall agreement between experiment and analysis was achieved. As pointed out previously, the sensitivity of the void fraction in the churn-turbulent flow regime to the vaporization power was considerably less than in the bubbly flow regime. This means that fluctuations in the power are not strongly reflected in the measured or calculated void fraction. This behavior is evident in Fig. 14 where the churn-turbulent data demonstrated a flat profile.

These data indicated the following behavior:

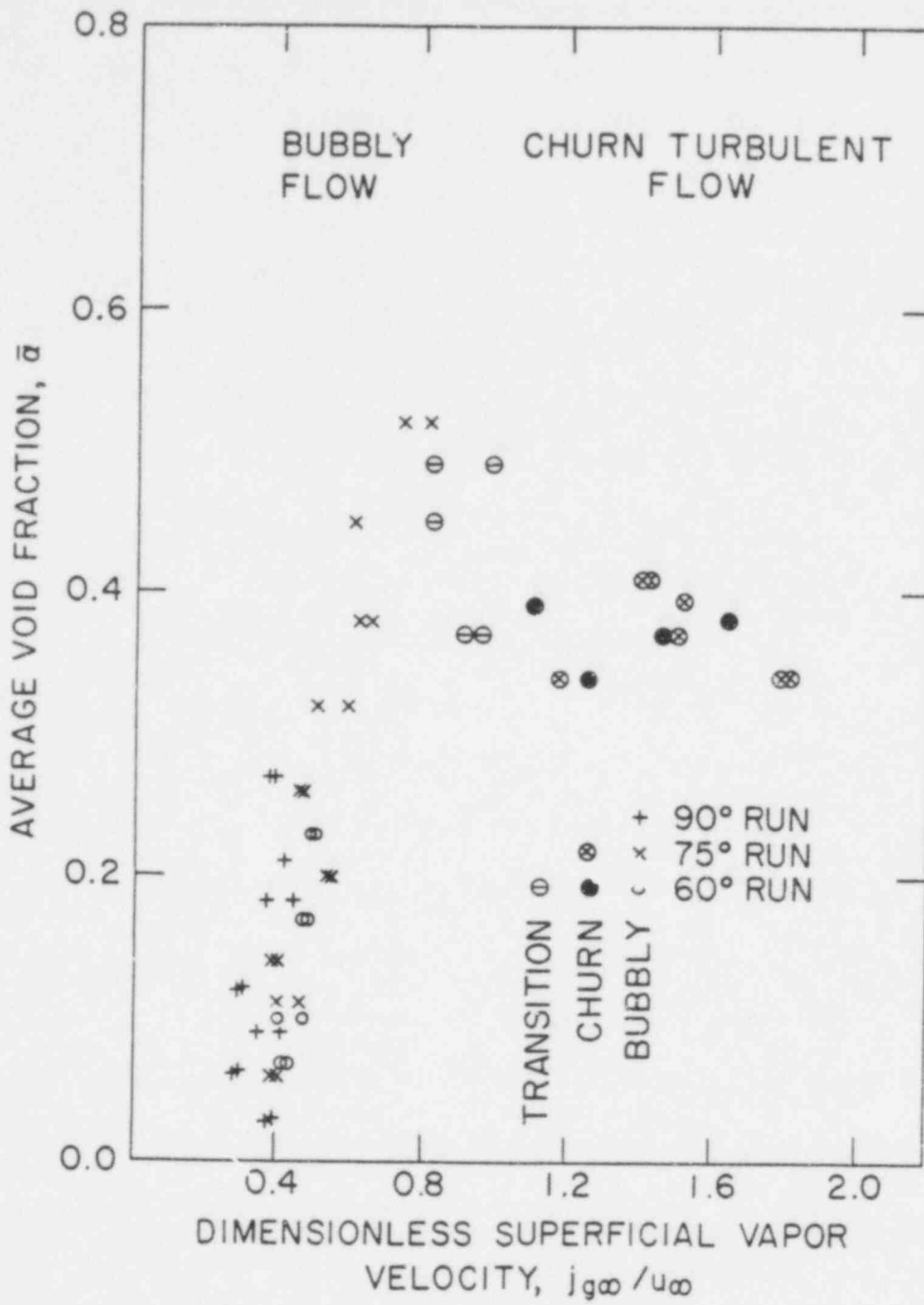


Figure 14 Pool Average Void Fraction, $\bar{\alpha}$, vs Dimensionless Superficial Vapor Velocity Based on Total Vaporization Power. (BNL Neg. No. 4-993-79).

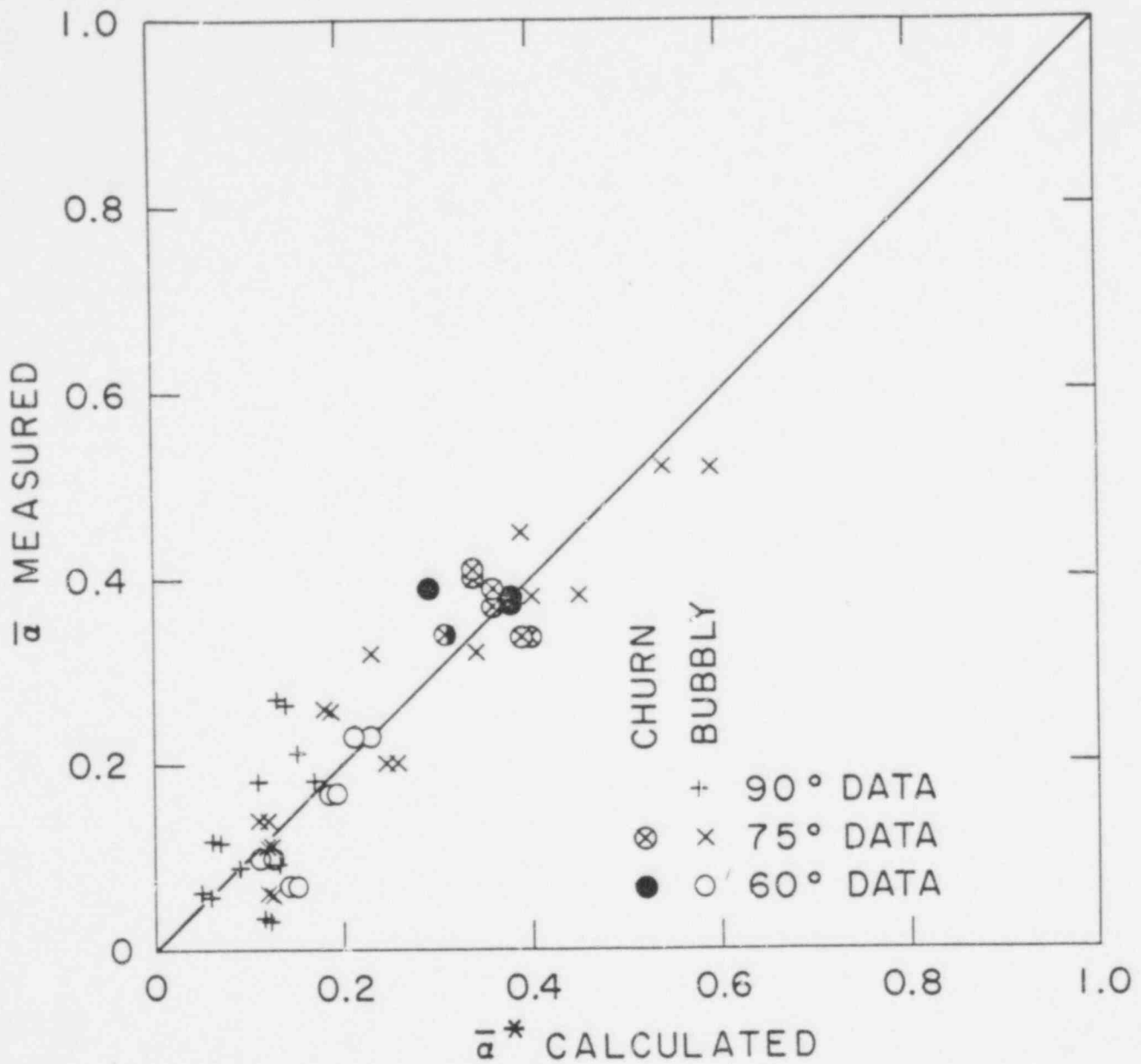


Figure 15 Comparison of Measured Average Void Fraction to Calculated Average Void Fraction Based on Net Boiling Power. (BNL Neg. No. 4-992-79).

1. Evaporative losses were substantial in the bubbly flow regime for this pool with a large surface to volume ratio. For pools with smaller surface to volume ratio, this dependence is expected to diminish. In the churn-turbulent regime, the void fraction was less sensitive to the power and uncertainty in the boiling power and boundary heat losses contributed smaller uncertainty in the measured and calculated void fraction as demonstrated.
2. The nonboiling portion of the pool in the bubbly flow regime was not taken into account by the drift flux model. In addition, the effect of wall angle on the superficial vapor velocity is not presently incorporated into the analysis presented.
3. For the experiments reported to date, the pool-average void fraction never exceeded 0.60.
4. Transition from bubbly flow to churn-turbulent flow occurred for the total dimensionless superficial vapor velocity, $j_{g\infty}/U_{\infty}$, in the range 0.8 to 1.0. This transition was accompanied by an immediate and sudden collapse in pool average void fraction from approximately 0.55-0.60 to 0.40.
5. The thin foaming layer which existed for some of the bubbly flow runs invariably was destroyed during transition to churn-turbulent flow. This was interpreted to mean that foaming flows were unstable for $j_{g\infty}/U_{\infty}$ greater than unity.

6.2 Natural Convection Analysis of Previous Data^{12,11} For Heat Transfer From A Volume Boiling Pool to a Vertical Boundary

The correlation techniques described by Eqs. 13a,b were applied to local convective boundary heat transfer data of Gustavson, et al.¹² The assumption inherent in these equations is that the boundary layer is laminar, resulting in the assumed 1/4 exponent on the Rayleigh number. The local heat transfer correlations derived from the local heat transfer data and the (a) averaged void fraction data, (b) local void fraction data were found to be

$$a - \text{Nu}(x, \bar{\alpha}) \approx 0.78 [\text{Gr}^*(x, \bar{\alpha}) \cdot \text{Pr}]^{0.25} \quad (14a)$$

and

$$b - \text{Nu}(x, \alpha) \approx 0.76 [\text{Gr}^*(x, \alpha) \cdot \text{Pr}]^{0.25} \quad (14b)$$

The standard deviations were found to be ± 0.35 and ± 0.56 , respectively. It was observed that the convenience of utilizing the average void fraction, $\bar{\alpha}$, instead of the local void fraction, α , resulted in little change in the correlation for heat transfer. The ratio of the correlation coefficients for the local heat transfer based on average vs. local void fraction was 1.03.

The same correlation technique was employed to test the existing data from 11 and 12 on an overall average basis. In this method, the average heat transfer coefficient and average void fraction were used. In conventional natural convection, it is assumed that the free stream density based on an equation of state is a constant since all properties outside the

boundary layer are evaluated at free stream temperature and pressure. This would be the case of using the average void fraction in the heat transfer correlation. For this case, it can be shown for laminar flow that direct integration of the local heat transfer correlation yields the average heat transfer correlation with h replaced by \bar{h} and x replaced by L . The coefficient for the average correlation, K_L' , is related to the coefficient for the local correlation from Eq. 13a as

$$K_L' = 1.33 K_L \quad \text{for } \alpha(x) = \bar{\alpha} \quad (28)$$

For the turbulent natural convection case, it can be shown similarly that the average turbulent correlation coefficient, K_T' , is related to the local correlation coefficient, K_T , by

$$K_T' = .83 K_T \quad \text{for } \alpha(x) = \bar{\alpha} \quad (29)$$

(See Appendix D for the derivation of Eqs. 28 and 29).

The average heat transfer data of Gustavson, et al.¹² were analyzed using the reported values for the superficial vapor velocity, average heat transfer coefficient, and average void fraction, as well as measured properties for $ZnSO_4$ electrolytic solution.

The average heat transfer coefficients for the data of Gabor, et al.¹¹ were not reported. They were calculated from the reported values of electrode heat flux, wall temperature, and pool temperature as

$$\bar{h} = \frac{q_{\text{electrode}}}{(T_{\text{pool}} - \bar{T}_w)} \quad (30)$$

The superficial vapor velocity, $j_{g\infty}$, was calculated from the reported value for the boiling heat flux as

$$j_{g\infty} = \frac{q_{BOIL}}{\rho_v h_{fg}} \quad (31)$$

The average void fraction data was reported. Only runs with an average void fraction greater than or equal to 0.05 were analyzed.

The results of the analysis of the data from Ref. 12 and Ref. 11 are presented in tabular form in Tables 4 and 5, and in graphical form in Figs. 16 and 17. It was found that the average natural convection correlation of the data of Gustavson, et al.¹² was

$$\overline{Nu} = \frac{\overline{hL}}{k} = 1.07 \left[\frac{g\alpha L^3 Pr}{v_f^2} \right]^{0.25} \quad (32)$$

with a standard deviation of $\pm .30$. The exponent was assigned from inspection of the data. The standard deviation of the correlation coefficient was found to be 0.30 or 28 percent, indicative of the scatter in the data. The majority of the data fell in the range of $Ra^* < 10^{12}$. As indicated in Fig. 16, there was no noticeably different trend observed for the foam or dense data. Examination of the magnitude of the average heat transfer coefficient and superficial vapor velocity indicated that most of the data fell in the bubbly flow region previously identified. The ratio of the correlation coefficients, K'/K , was 1.37, tending to reinforce the use of the average void fraction in correlating the local heat transfer data as well, as indicated in Fig. 3.

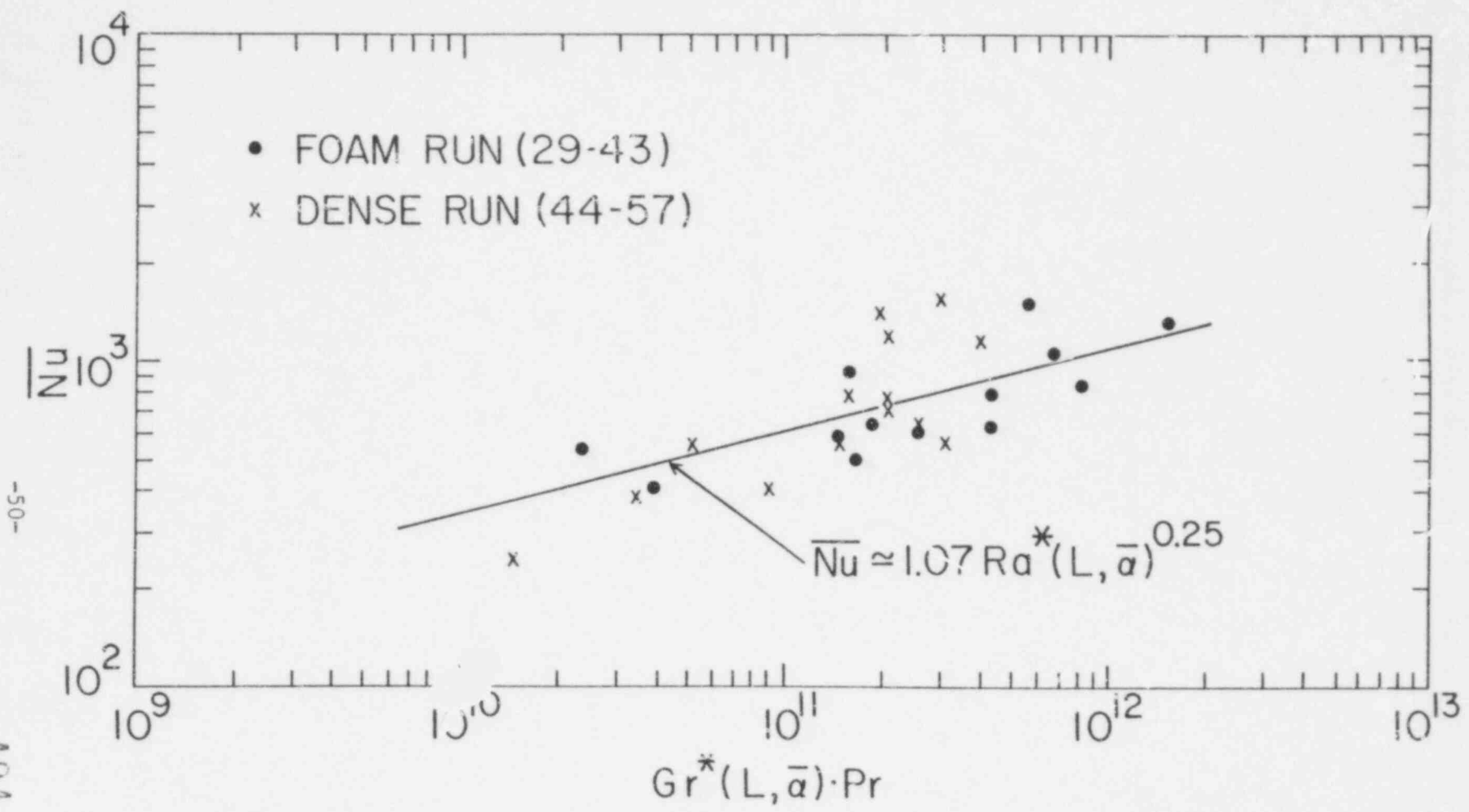


Figure 16 Natural Convection Correlation of Average Heat Transfer Data of Gustavson, et al.¹² (BNL Neg. No. 4-1304-79).

494 096

-50-

TABLE 4

AVERAGE HEAT TRANSFER AND VOID FRACTION DATA OF GUSTAVSON, ET AL.¹² AND COMPARISON TO EXISTING MODELS

RUN	WALL TEMP DEG C	VOID FRACTION EXP	AVERAGE HEAT TRANS COEFF			SV	DEPTH CM	NUX	RAX	
			EXP	EQ 14a	EQ 10 N=1.0					EQ 10 N=0.7
29	86.8	.44	.075	.079	.057	.071	.19	17.10	788.6	.4363E+12
30	86.8	.61	.077	.092	.067	.084	.22	12.80	606.1	.2530E+12
31	89.0	.67	.095	.082	.063	.079	.43	27.50	1314.	.1529E+13
32	90.8	.41	.132	.076	.054	.067	.17	18.90	1532.	.5609E+12
34	90.2	.62	.098	.086	.060	.074	.17	17.60	1060.	.6782E+12
35	88.6	.62	.073	.084	.078	.100	1.75	18.89	843.6	.8214E+12
36	87.0	.64	.068	.090	.083	.106	1.03	15.00	627.0	.4301E+12
37	89.2	.40	.078	.085	.068	.087	.35	12.20	584.6	.1465E+12
38	88.3	.24	.072	.080	.069	.088	.35	9.30	411.4	.3887E+11
39	88.7	.33	.075	.078	.063	.079	.34	14.10	649.9	.1854E+12
40	83.0	.05	.066	.049	.039	.049	.11	13.40	544.2	.2353E+11
42	88.6	.41	.122	.084	.067	.084	.31	12.40	929.9	.1559E+12
43	89.2	.63	.074	.097	.073	.092	.27	11.00	590.4	.1673E+12
44	92.5	.36	.084	.080	.088	.112	1.54	14.10	727.4	.2050E+12
45	87.7	.37	.088	.080	.087	.112	1.62	14.10	762.9	.2060E+12
46	87	.43	.113	.079	.078	.101	1.24	16.70	1161.	.3959E+12
47	87.0	.36	.074	.081	.085	.109	1.28	12.80	582.6	.1487E+12
48	84.9	.43	.059	.081	.087	.111	1.71	15.40	559.0	.3079E+12
49	90.2	.46	.072	.084	.073	.094	.62	14.10	623.8	.2593E+12
50	91.9	.42	.084	.097	.111	.141	1.47	7.40	381.9	.3426E+11
51	87.0	.31	.064	.093	.097	.124	.78	6.20	244.1	.1456E+11
52	66.1	.11	.087	.051	.039	.052	.16	21.90	1179.	.2042E+12
53	87.3	.12	.110	.053	.040	.051	.9	23.30	1577.	.2983E+12
54	89.4	.20	.137	.065	.053	.067	.29	17.00	1432.	.1949E+12
55	81.9	.10	.066	.057	.043	.054	.12	13.80	561.1	.5032E+11
56	86.2	.23	.084	.069	.062	.080	.55	15.20	785.7	.1579E+12
57	81.8	.28	.056	.077	.071	.090	.59	11.90	410.5	.9056E+11

↑ Foaming Runs
↓ Dense Runs

* SVV indicates the dimensionless superficial vapor velocity.

It was found that the average natural convection correlation of the data of Gabor, et al.¹¹ was

$$\overline{Nu} = \frac{\overline{hL}}{k} = 1.58 \left[\frac{g\alpha L^3 Pr}{v_f^2} \right]^{0.25} \quad (33)$$

with a standard deviation of ± 0.33 . There were no local void fraction or heat flux measurements available for this work to perform a similar comparison of the local and average heat transfer correlation coefficients as performed for the data in Ref. 12. Once again, the exponent was assigned after examining the data. The majority of the data fell in the range $Ra^* < 10^{12}$ as did Gustavson's data¹². If the data were divided into two groups at $Ra^* = 10^{11}$, the correlation of the data on the basis of laminar and turbulent behavior would result in the set of correlations below,

$$a - \quad \overline{Nu} = (1.42)Ra^{*.25} \quad Ra^* < 10^{11} \quad (34a)$$

with a standard deviation of ± 0.25 for the laminar data and

$$b - \quad \overline{Nu} = (.0309)Ra^{*.40} \quad Ra^* > 10^{11} \quad (34b)$$

with a standard deviation of $\pm .0058$ for the turbulent data. Although scatter in the data makes the determination of laminar vs. turbulent boundary layer behavior tenuous, both sets of correlations for Gabor's data are plotted in Fig. 17. This will be discussed in greater depth in the next section. Examination of the magnitudes of the average heat transfer coefficients and dimensionless superficial vapor velocities indicated that the majority of this data was also expected to fall in the bubbly flow regime.

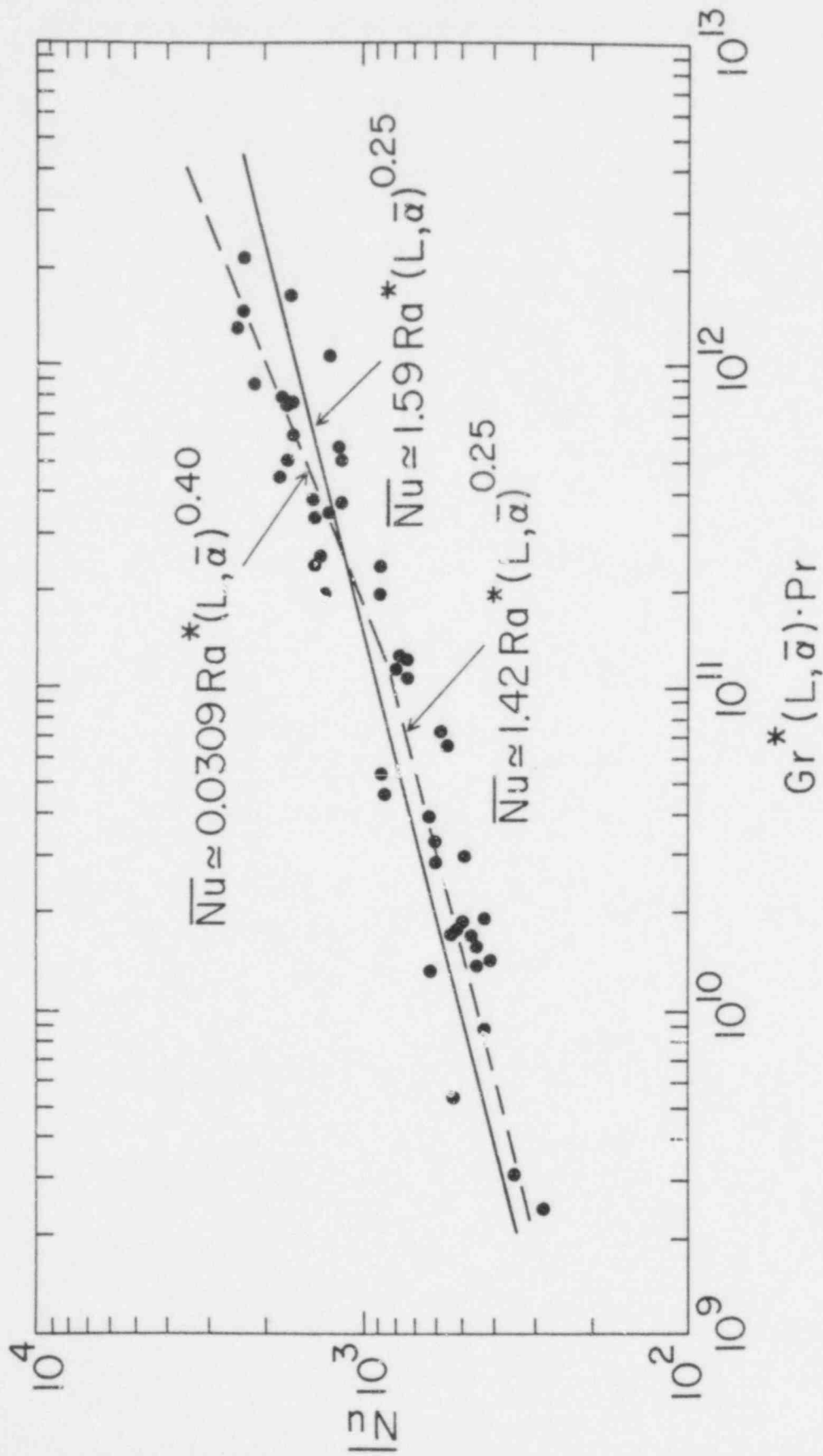


Figure 17 Natural Convection Correlation of Average Heat Transfer Data of Gabor, et al. 11 (BNL Neg. No. 4-1306-79).

RUN	WALL TEMP DEG C	VOID FRACTION EXP	AVERAGE HEAT TRANS COEFF				SVV*	DEPTH CM	NUX	RAX
			EXP	EQ 14a	EQ 10	EQ 10				
1	59.7	.41	.098	.072	.073	.093	1.34	19.30	1174.	.5034E+12
2	60.3	.42	.097	.072	.072	.091	1.28	19.70	1186.	.5502E+12
3	55.6	.31	.085	.069	.065	.082	.74	16.50	872.0	.2326E+12
4	55.9	.51	.088	.072	.061	.077	.67	23.30	1275.	.1079E+13
5	49.7	.16	.065	.061	.056	.070	.41	13.60	551.0	.6502E+11
6	50.3	.17	.068	.062	.056	.070	.40	13.70	580.6	.7086E+11
13	67.0	.06	.057	.051	.046	.059	.25	12.10	426.7	.1887E+11
15	69.1	.20	.083	.066	.064	.081	.67	14.30	733.9	.1050E+12
16	72.1	.21	.089	.067	.062	.079	.56	14.40	791.7	.1143E+12
17	76.1	.36	.130	.073	.065	.082	.66	17.80	1428.	.3777E+12
18	74.7	.35	.116	.073	.070	.089	.96	17.50	1253.	.3465E+12
19	77.0	.42	.136	.074	.077	.099	1.61	19.70	1653.	.6001E+12
20	77.4	.58	.137	.074	.069	.089	1.35	27.10	2290.	.2162E+13
21	76.0	.45	.133	.074	.072	.092	1.20	20.70	1699.	.7422E+12
23	70.2	.05	.061	.049	.044	.056	.22	12.00	452.5	.1560E+11
24	76.9	.27	.092	.070	.063	.081	.58	15.60	885.3	.1915E+12
25	81.3	.45	.130	.075	.067	.086	.85	20.70	1658.	.7619E+12
26	83.2	.53	.156	.075	.076	.098	1.80	24.30	2334.	.1465E+13
27	82.8	.05	.064	.050	.042	.053	.15	12.00	473.0	.1661E+11
28	83.1	.10	.080	.058	.052	.066	.31	12.70	625.7	.3945E+11
29	88.0	.45	.137	.076	.061	.077	.46	20.70	1744.	.7868E+12
30	88.1	.39	.148	.075	.072	.092	1.07	18.70	1702.	.5030E+12
37	53.0	.06	.070	.049	.050	.063	.38	12.10	527.2	.1750E+11
38	52.3	.09	.063	.051	.051	.065	.36	12.50	490.3	.2882E+11
39	58.3	.23	.084	.066	.064	.081	.69	14.80	772.1	.1264E+12
40	57.1	.23	.081	.066	.064	.081	.68	14.80	744.8	.1256E+12
46	50.4	.09	.077	.054	.061	.076	.74	17.50	599.8	.2851E+11
52	44.5	.05	.060	.047	.049	.061	.40	12.00	450.0	.1355E+11
55	50.8	.10	.076	.055	.062	.078	.77	12.70	601.4	.3330E+11
56	58.1	.56	.103	.072	.067	.084	1.14	25.90	1657.	.1647E+13
57	48.4	.06	.072	.049	.059	.073	.75	12.10	543.4	.1705E+11
58	57.7	.37	.105	.071	.073	.093	1.30	18.10	1181.	.3707E+12
92	58.7	.09	.123	.063	.069	.087	.50	7.00	534.6	.5244E+10
95	59.2	.17	.130	.073	.073	.092	.51	7.70	621.4	.1322E+11
96	61.2	.32	.146	.081	.083	.105	.86	9.40	851.4	.4576E+11
97	60.4	.34	.146	.082	.083	.105	.87	9.70	878.8	.5320E+11
102	65.3	.11	.087	.049	.043	.055	.43	25.80	1390.	.3325E+12
103	70.8	.20	.121	.056	.053	.068	.91	28.80	2154.	.8652E+12
105	64.9	.09	.085	.047	.042	.054	.44	25.30	1332.	.2560E+12
106	71.2	.25	.129	.058	.053	.067	.83	30.70	2447.	.1313E+13
109	63.8	.14	.106	.055	.049	.063	.45	19.90	1307.	.1926E+12
112	64.2	.16	.113	.057	.050	.063	.43	20.40	1429.	.2377E+12
113	66.3	.23	.132	.061	.060	.076	.96	22.20	1814.	.4452E+12
117	52.4	.06	.082	.057	.064	.080	.43	6.80	347.1	.3095E+10
118	53.8	.13	.094	.068	.072	.091	.54	7.40	432.8	.8710E+10
121	56.3	.21	.099	.075	.075	.094	.55	8.10	498.4	.1871E+11
122	53.0	.18	.084	.073	.070	.089	.44	7.80	407.8	.1406E+11
123	49.2	.05	.068	.054	.056	.070	.27	6.70	284.1	.2423E+10

* SVV indicates the dimensionless superficial vapor velocity.

-54-
494 100

6.3 Correlation of Present Data

In a similar fashion to the natural convection correlation procedure employed to analyze the data from Refs. 11 and 12, the average heat transfer data for the present tests were likewise analyzed. The local distribution of boundary heat transfer coefficient, $h(x)$, was integrated to determine the average heat transfer coefficient. The average void fraction was determined as described in Eq. 24. The superficial vapor velocity, $j_{g\infty}$, was determined by converting the flow rate of make-up water into an average vapor flux as

$$j_{g\infty} = \frac{G \rho_l H_o}{\text{Vol. } \rho_v} \quad (35)$$

where G is the make-up flow rate (cm^3/sec), H_o is the nonboiling pool depth (cm), and Vol. is the total pool volume (cm^3).

In a straight-forward fashion, the average heat transfer correlation was determined as indicated below for laminar bubbly flow,

$$\overline{\text{Nu}} = (1.54) \text{Ra}^*(L, \bar{\alpha}, \theta)^{0.25} \quad \text{Ra}^* \leq 1.865 \times 10^{11} \quad (36a)$$

with a standard deviation of ± 0.08 , and for turbulent bubbly flow

$$\overline{\text{Nu}} = (0.0314) \text{Ra}^*(L, \bar{\alpha}, \theta)^{0.40} \quad \text{Ra}^* > 1.865 \times 10^{11} \quad (36b)$$

with a standard deviation of ± 0.0016 . These data are available in Table 6, and the two correlations are plotted in Fig. 18. The scatter in the data is seen to be less by a factor of 4-6 than previously observed as can be seen in the standard deviation in the correlation coefficients and the transition from laminar to turbulent behavior is more evident. It was on

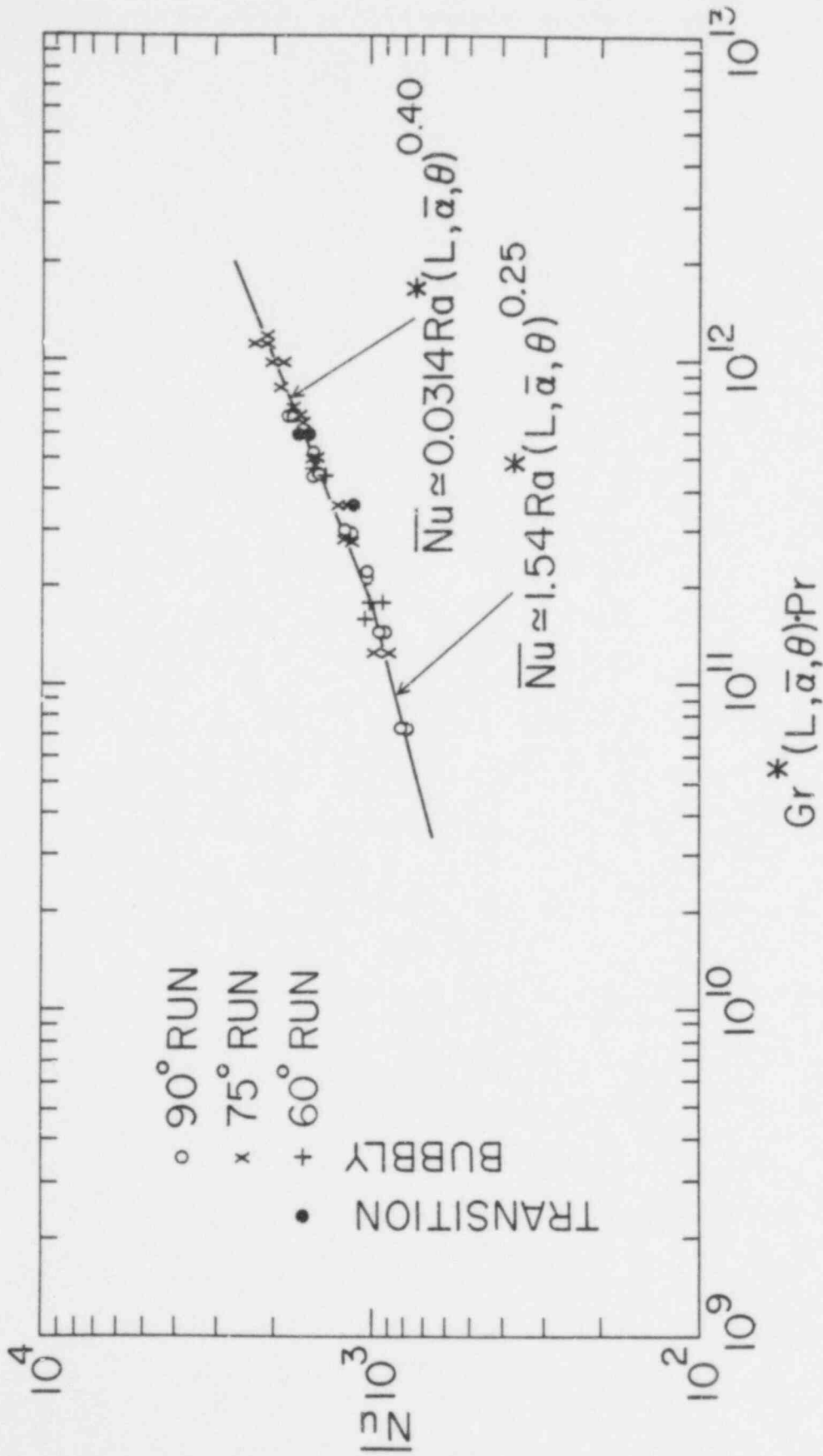


Figure 18 Natural Convection Correlation of Average Heat Transfer Data Based On Current Data. (BNL Neg. No. 4-1305-79).

TABLE 6
COMPARISON OF MEASURED AND CALCULATED AVERAGE VOID FRACTION
AND HEAT TRANSFER COEFFICIENT FROM VOLUMETRIC BOILING POOL

RUN	WALL TEMP DEG C	VOID FRACTION		AVERAGE HEAT TRANS COEFF				SVV*	DEPTH CM	NUX	RAX	
		EXP	CALC	EXP	EQ 14a	EQ 10	EQ 10					
						N=1.0	N=0.7					
9001	82.3	.03	.12	.054	.037	.037	.047	.39	23.2	771.5	.7225E+11	
9002	83.1	.03	.12	.056	.037	.037	.047	.39	23.2	779.9	.7253E+11	
9003	83.5	.06	.05	.063	.044	.038	.049	.28	23.2	899.7	.1453E+12	
9004	83.8	.06	.05	.064	.044	.038	.049	.28	23.2	914.0	.1455E+12	
9005	84.3	.09	.13	.072	.049	.044	.056	.41	23.2	1028.	.2190E+12	
9006	84.2	.09	.09	.072	.049	.043	.054	.35	23.2	1028.	.2184E+12	
9007	85.9	.12	.06	.081	.053	.044	.055	.30	73.2	1156.	.2940E+12	
9008	86.9	.12	.06	.080	.053	.044	.056	.30	23.2	1142.	.2952E+12	
9009	88.3	.18	.11	.104	.059	.048	.062	.37	23.2	1484.	.4453E+12	
9010	88.3	.18	.17	.109	.059	.050	.064	.45	23.2	1555.	.4453E+12	
9011	89.8	.27	.13	.121	.065	.052	.066	.38	23.2	1725.	.6728E+12	
9012	89.8	.27	.13	.128	.065	.052	.066	.38	23.2	1825.	.6722E+12	
9013	89.1	.21	.15	.105	.061	.051	.065	.42	23.2	1498.	.5212E+12	
7501	84.7	.11	.12	.079	.051	.046	.059	.46	23.8	1157.	.2796E+12	Bubbly
7502	85.0	.11	.12	.079	.051	.045	.057	.40	23.8	1157.	.2800E+12	
7503	85.7	.14	.12	.086	.055	.046	.059	.39	23.8	1259.	.3574E+12	
7504	85.5	.14	.11	.081	.055	.046	.059	.38	23.8	1186.	.3571E+12	
7505	88.5	.20	.25	.106	.060	.052	.066	.54	23.8	1551.	.5167E+12	
7506	88.4	.20	.25	.104	.060	.052	.066	.54	23.8	1522.	.5160E+12	
7507	89.8	.26	.18	.115	.064	.053	.067	.46	23.8	1682.	.6760E+12	
7508	89.4	.26	.18	.112	.064	.053	.067	.46	23.8	1639.	.6748E+12	
7509	90.8	.32	.34	.121	.068	.057	.073	.59	23.8	1770.	.8357E+12	
7510	91.1	.32	.23	.131	.068	.056	.071	.51	23.8	1916.	.8369E+12	
7511	91.7	.38	.40	.136	.071	.059	.076	.62	23.8	1989.	.9965E+12	
7512	91.5	.38	.45	.131	.071	.060	.076	.65	23.8	1916.	.9956E+12	
7513	92.3	.45	.39	.148	.074	.061	.077	.61	23.8	2164.	.1183E+13	
7514	93.2	.52	.54	.168	.078	.066	.084	.74	22.3	2301.	.1129E+13	
7515	92.7	.52	.59	.159	.078	.067	.085	.81	22.3	2178.	.1127E+13	
7516	93.4	.41	.34	.162	.078	.079	.101	1.41	17.7	1761.	.4442E+12	
7517	93.1	.41	.34	.141	.078	.079	.101	1.43	17.7	1533.	.4436E+12	
7518	94.5	.34	.40	.143	.074	.081	.104	1.79	17.7	1554.	.3705E+12	Churn-Turbulent
7519	94.7	.34	.40	.136	.074	.082	.105	1.82	17.7	1478.	.3699E+12	
7520	82.9	.06	.12	.064	.045	.042	.053	.40	23.2	878.7	.1243E+12	Bubbly
7521	82.3	.06	.12	.072	.045	.042	.053	.40	23.2	988.7	.1239E+12	
7522**		.34	.31					1.18				Churn-Turbulent
7523**		.39	.36					1.52				
7524**		.37	.36					1.50				
6001	83.4	.07	.15	.067	.045	.041	.052	.43	24.8	1023.	.1787E+12	
6002	88.4	.17	.19	.103	.057	.048	.061	.48	24.8	1571.	.4445E+12	
6003	83.4	.07	.15	.060	.045	.041	.052	.43	24.8	916.1	.1788E+12	
6004	87.5	.17	.19	.094	.057	.048	.061	.48	24.8	1434.	.4423E+12	Bubbly
6005	86.2	.10	.12	.086	.051	.044	.056	.40	22.3	1180.	.1180E+12	
6006	87.0	.10	.11	.083	.052	.045	.058	.40	21.0	1072.	.1577E+12	
6007	90.5	.23	.21	.123	.064	.054	.069	.50	21.0	1588.	.3678E+12	
6008	90.7	.23	.23	.130	.064	.054	.069	.51	21.0	1678.	.3681E+12	
6009	91.4	.37	.25(.65)	.130	.072	.065	.084	.92	21.0	1678.	.5946E+12	
6010	91.9	.37	.26(.66)	.122	.072	.066	.084	.96	21.0	1574.	.5944E+12	Transition
6011	90.7	.45	.22(.60)	.115	.080	.071	.091	.83	16.6	1173.	.3599E+12	
6012	92.2	.38	.38	.153	.079	.084	.108	1.64	15.1	1420.	.2278E+12	
6013**		.37	.38					1.46				Churn-Turbulent
6014**		.49	.22(.59)					.82				
6015**		.49	.26(.67)					.99				Transition
6016**		.39	.29					1.11				
6017**		.34	.31					1.26				Churn-Turbulent

* SVV indicates the dimensionless superficial vapor velocity.

** No heat transfer data were recorded for these runs.

the basis of these observations that the laminar-turbulent correlation of the data in Fig. 17 was analyzed. Although there have been no boundary layer measurements to substantiate the claim of turbulent boundary layer transition, the assignment of the laminar exponent (i.e., 0.25) and the turbulent exponent (i.e., 0.40) to the data correlation, similar to a single-phase natural convection, was done on the justification of observation of the marked change in the behavior of the data in the vicinity of $Ra^* \sim 1-2 \times 10^{11}$. This observation was made possible due to the elimination of the majority of the scatter in the data which was present in previous work. This is demonstrated by the relative scatter in the correlation coefficient which is 5 percent for both the laminar and turbulent cases. This is in sharp contrast to the 28 percent and 21 percent standard deviation in the correlations of the data of Gustavson¹² and Gabor¹¹ presented here, respectively.

The data in the transition region between bubbly and churn-turbulent flow exhibited more scatter than the bubbly flow data. However, correlation of this data behaved similar to the turbulent bubbly flow data as indicated in Fig. 18.

The churn-turbulent regime data, however, deviated sharply from the above observed behavior. For the same Rayleigh number, the churn-turbulent data was observed to lie significantly above the correlation for bubbly flow. There is insufficient data at this point to make any quantitative statements to correlate the data to particular model assumptions. However, the magnitude of the temporal fluctuations in the wall temperature, as well as the significantly higher boundary heat transfer coefficient were interpreted to indicate that the multi-dimensional hydrodynamic nature of the

boiling pool was interfering with the formation of the wall boundary layer, if not destroying it.

The correlations derived from the data of Gustavson, et al.¹² and Gabor, et al.¹¹, as well as the present data, are summarized in Table 7. The local correlations of the data of Gustavson, et al.¹² indicated little sensitivity to the use of either the average or local void fraction. The ratio of the local and average correlation coefficients supported the use of the average void fraction in the correlation of the local heat transfer data. The correlations of the data of Gabor, et al.¹¹ and of the present work have been performed on an average basis only. Examination of the correlations derived revealed that the data agreed within the standard deviation of Gabor's data.¹¹ However, both exceeded the correlation of Gustavson's data¹² by a factor of approximately 1.5. This is in agreement with observations that the local heat transfer data exceeded the calculations of the previous existing models^{12,15} derived from the data of Ref. 12 by a wide margin. The local heat transfer data of this work will be analyzed on a local basis in the future.

7. SUMMARY AND CONCLUSIONS

7.1 Bubbly Flow Regime

For volume-heated boiling pools characteristic of the kind investigated here and in the bubbly flow regime, the following conclusions can be made:

7.1.1 Hydrodynamics

- (1) The bubbly flow regime persisted for a value of $j_{g\infty}/U_\infty$

TABLE 7

SUMMARY OF LOCAL AND AVERAGE CORRELATIONS FOR
HEAT TRANSFER FROM VOLUME BOILING POOLS

AUTHOR	WALL ANGLE	LOCAL OR AVERAGE HEAT TRANSFER	LAMINAR OR TURBULENT	CORRELATION	STANDARD DEVIATION	RANGE OF RAYLEIGH NUMBER
Gustavson, et al. ¹²	Vertical	Local	Laminar	$Nu(x) = .78 Ra^*(x, \alpha)^{0.25}$	$\pm .35$	$Ra^* < 10^{12}$
		Local	Laminar	$Nu(x) = .76 Ra^*(x, \alpha)^{0.25}$	$\pm .56$	$Ra^* < 10^{12}$
		Average	Laminar	$\bar{Nu} = 1.07 Ra^*(L, \alpha)^{0.25}$	$\pm .30$	$Ra^* < 2 \times 10^{12}$
Gabor, et al. ¹¹	Vertical	Average	Laminar	$\bar{Nu} = 1.58 Ra^*(L, \alpha)^{0.25}$	$\pm .33$	$Ra^* < 2 \times 10^{12}$
		Average	Laminar	$\bar{Nu} = 1.42 Ra^*(L, \alpha)^{0.25}$	$\pm .25$	$Ra^* < 10^{11}$
		Average	Turbulent	$\bar{Nu} = .0309 Ra^*(L, \alpha)^{0.4}$	$\pm .0058$	$Ra^* > 10^{11}$
Present Work	90°, 75° 60°	Average	Laminar	$\bar{Nu} = 1.54 Ra^*(L, \alpha, \theta)^{0.25}$	$\pm .08$	$Ra^* < 1.865 \times 10^{11}$
		Average	Turbulent	$\bar{Nu} = .0314 Ra^*(L, \alpha, \theta)^{0.40}$	$\pm .0016$	$Ra^* > 1.865 \times 10^{11}$

-60-

494
106

up to unity. In this flow regime, the pool underwent periodic swelling possibly due to subcooling from the returning cold boundary layer fluid into the pool bottom. The pool exhibited a stratified state with a boiling region over an essentially nonboiling single phase region below. The depth of the nonboiling region decreased as the volumetric vaporization source increased such that the nonboiling region was confined to the conditions where $j_{g\infty}/U_{\infty} < 0.2$.

- (2) The maximum average void fraction observed in the bubbly flow regime was in the range 0.55 to 0.60 at $j_{g\infty}/U_{\infty}$ approximately unity. In this range of power, transition to a churn-turbulent flow regime was observed in which boiling penetrated to the pool bottom, and a sudden collapse in average pool void fraction was observed from approximately 0.55-0.60 to 0.40. While it might be coincidental, the upper limit in bubbly flow corresponds approximately with the packing density of spheres at $j_{g\infty}/U_{\infty} \sim 1$.
- (3) In the bubbly flow regime, it was observed that surface evaporative losses were non-negligible for pool geometry utilized herein having a large surface-to-volume ratio, and that a significant fraction of the volumetric power density went into these losses. The net boiling power was defined as the total vaporization power minus the evaporative losses. It was found

that calculation of the pool-average void fraction by means of a one-dimensional drift flux model based on the net boiling power agreed well with the experimental data independent of the wall angle. Agreement between calculated and measured average void fraction improved for increasing power.

- (4) The average void fraction in the bubbly flow regime was found to be very sensitive to the volumetric boiling power. Small changes in $j_{g\infty}/U_{\infty}$ were observed to cause large variations in the pool-average void fraction.

7.1.2 Heat Transfer

- (1) Boundary heat transfer from volume-boiling pools in the bubbly flow regime behaved similar to natural convection-type boundary layer heat transfer. The spatial variation in the local heat transfer coefficient was as great as a factor of 3-5 along the wall, with the greatest heat transfer at or near the pool surface. The data reported here for local convective heat transfer coefficient exceeded those previously reported by Gustavson, et al.¹² by a factor of 2 or more but agreed with the earlier average pool data of Gabor, et al.¹¹ within the scatter in their data.
- (2) For boundary layer-type heat transfer from volume-boiling pools in the bubbly flow regime, the effect of small angle

of inclination of the boundary from vertical was modeled by defining an effective gravitational component along the wall as indicated below;

$$g_{\text{eff}} = g \cos\theta \quad (37)$$

where θ is the angle of inclination from the vertical.

For the data described herein with inclinations up to 30° , this correlation proved adequate.

- (3) Correlation of average heat transfer based on the average void fraction indicates laminar flow behavior up to Rayleigh number of 1.865×10^{11} . The correlation is of the approximate form

$$\overline{\text{Nu}} = 1.54 \overline{\text{Ra}}^* (L, \overline{\alpha}, \theta)^{0.25} \text{ for } \text{Ra}^* < 1.865 \times 10^{11} \quad (38a)$$

For higher Rayleigh number, the data behaves similar to turbulent natural convection and the correlation for the range $\text{Ra} > 1.865 \times 10^{11}$ is

$$\overline{\text{Nu}} = 0.0314 \overline{\text{Ra}}^* (L, \overline{\alpha}, \theta)^{0.40} \text{ for } \text{Ra}^* > 1.865 \times 10^{11} \quad (38b)$$

The consistency of the data presented herein represents a significant improvement over previously reported data of Gabor, et al.¹¹ and Gustavson, et al.¹². The standard deviation in both cases was found to be 5 percent in marked contrast to the previous data having standard deviations of 21 to 28 percent.

7.2 Churn-Turbulent Flow Regime

For volume-heated boiling pools characteristic of the kind investigated here and in the churn-turbulent flow regime, the following conclusions can be made:

7.2.1 Hydrodynamics

- (1) Flow regime transition from bubbly flow to churn-turbulent flow was observed to occur in the vicinity of $j_{g\infty}/U_\infty$ equal to one. Flow regime transition was accompanied by a marked collapse in the pool average void fraction from 0.55-0.60 to 0.40, similar to the bubble column observations in adiabatic flow as observed by Zuber and Hench and others.^{19,21}
- (2) The pool hydrodynamics appeared not to behave in a one-dimensional fashion any longer. Three-dimensional circulations appeared to dominate and caused large-scale bubble agglomeration, responsible for the lower void fraction even at higher vapor generation rates than in bubbly flow. Periodic swelling behavior of the pool ended.
- (3) The liquid-continuous nature of the bubbly flow regime began to break down due to the three-dimensional nature of the flow and appearance of large vapor pockets in the flow. This behavior was indicated by fluctuations recorded in the power trace of the pool.

- (4) Surface evaporative losses were found to be less significant for this regime than for bubbly flow. The void fraction appeared to be somewhat insensitive to increases in pool power in the range $1.0 < j_{g\infty}/U_{\infty} < 2.0$. The average void fraction in this range was measured to be approximately 0.40. The measured and calculated average void fraction data agreed well for the range of superficial velocity investigated.

7.2.2 Heat Transfer

- (1) The average heat transfer coefficient was approximately $0.15 \text{ cal/cm}^2 \text{ s}^{\circ}\text{C}$. Large fluctuations were observed in the standard deviation of the local wall temperature fluctuations. In some instances, the fluctuations were of the same magnitude as the difference between the pool temperature and the time-averaged wall temperature, indicating partial or complete local destruction and renewal of the wall boundary layer. It is this mechanism that is believed responsible for the increased boundary heat transfer coefficient.
- (2) The profile of local heat transfer coefficient was more uniformly distributed along the wall, exhibiting large fluctuations spatially. The maximum local heat transfer coefficient was observed to be in the range $0.25\text{-}0.30 \text{ cal/cm}^2 \text{ s}^{\circ}\text{C}$.

8. ACKNOWLEDGEMENTS

The authors wish to express their appreciation to Dr. John D. Gabor of Argonne National Laboratory, Professor Mujid S. Kazimi of Massachusetts Institute of Technology, and Professor John C. Chen of Lehigh University for their valuable discussions and insights into the work presented.

The technical assistance of George A. Zimmer, James H. Klein, and Laurie Sweeney, and the skillful preparation of the manuscript by Nancy Schneider are acknowledged and greatly appreciated.

494 112

9. REFERENCES

1. Essam, P., "Free Convection of Heat Generating Fluids in Cylindrical Tanks," Nuclear Engineering and Design, 11, 57-68 (1969).
2. Murgatroyd, W. and Watson, A., "An Experimental Investigation of Natural Convection of a Heat Generating Fluid Within a Closed Vertical Cylinder," J. Mech. Engr. Sci., 12 (5), 345-363 (1970).
3. Kulacki, F. A. and Goldstein, R. J., "Thermal Convection in a Horizontal Fluid Layer With Uniform Volumetric Energy Sources," J. Fluid Mechanics, 55, Part 2, 271-287 (1972).
4. Kulacki, F. A. and Nagle, M. E., "Natural Convection in a Horizontal Layer with Volumetric Energy Sources," J. Heat Transfer, 204-211 (May 1975).
5. Suo-Antilla, A. J. and Catton, I., "An Experimental Study of a Horizontal Layer of Fluid With Volumetric Heating and Unequal Surface Temperatures," Paper No. AIChE 6, 10th National Heat Transfer Conference, St. Louis (August 1976).
6. Novotny, J. L. and Eckert, E.R.G., "Experimental Study of Laminar Convection in the Channel Between Parallel Plates With Uniform Heat Sources in the Fluid," Int. J. Heat Mass Transfer, 7, 955-968 (1964).
7. Jahn, M. and Reineke, H. M., "Free Convection Heat Transfer With Internal Heat Source Calculations and Measurements," 5th International Heat Transfer Conference, Tokyo (1974).
8. Hesson, J. C. and Gunther, W. H., "Heat Transfer from Boiling Pools With Internal Heat Generation," Trans. Amer. Nucl. Soc., 15, 864-865 (1972).
9. Stein, R. P., Hesson, J. C., and Gunther, W. H., "Studies of Heat Removal From Heat Generating Boiling Pools," ANS Fast Reactor Safety Conference, CONF-740401, pp 865-880 (April 1974).
10. Gabor, J. D., et al., "Heat Removal from Heat Generating Pools," Trans. Amer. Nucl. Soc., 19, 257 (1974).
11. Gabor, J. D., Baker, L., Jr., Cassulo, J. C., and Mansoori, G. A., "Heat Transfer from Heat Generating Boiling Pools," ASME-AIChE National Heat Transfer Conference, St. Louis, MO, pp 78-80 (1976).
12. Gustavson, W. R., Chen, J. C., and Kazimi, M. S., "Heat Transfer and Fluid Dynamic Characteristics of Internally Heated Boiling Pools," BNL-NUREG-50759 (September 1977).

REFERENCES (Cont'd)

13. Fujii, T. and Imura, H., "Natural Convection Heat Transfer From a Plate With Arbitrary Inclination," *Int. J. Heat Mass Transfer*, 15, 755-767 (1972).
14. Churchill, S. W. and Usagi, R., "A General Expression for the Correlation of Rates of Transfer and Other Phenomena," *AIChE*, 18(6), pp. 1121-1128 (1972).
15. Greene, G. A., Jones, O. C., Jr., and Schwarz, C. E., "Thermo-Fluid Mechanics of Volume-Heated Boiling Pools," Third PAHR Information Exchange, Argonne National Laboratory, ANL-78-10, BNL-NUREG-50759, (November 1977).
16. Zuber, N. and Findlay, J. A., "Average Volumetric Concentration in Two-Phase Flow Systems," *J. Heat Transfer*, pp. 453-468 (November 1965).
17. Randall, I. E. and Sesonske, A., "Effect of a Volume-Heat Source on Free Convection Heat Transfer," *AIChE*, 5(2), pp. 150-154 (June 1959).
18. Ginsberg, T., Jones, O. C., Jr., Schwarz, C. E., and Chen, J. C., "Observations of Flow Characteristics of Volume Heated Boiling Pools," BNL-NUREG-24270 (December 1977).
19. Zuber, N. and Hench, J., "Steady-State and Transient Void Fraction of Bubbling Systems and Their Operating Limits," Part I: Steady-State Operation, General Electric Report 62GL100 (July 1962).
20. Wallis, G. B., One-Dimensional Two-Phase Flow, McGraw Hill Book Co., Inc., New York (1969).
21. Jones, O. C., Jr., "Statistical Considerations in Heterogeneous, Two-Phase Flowing Systems," Ph.D. Thesis, Rensselaer Polytechnic Institute, Troy, New York (1973).
22. Harmathy, T. Z., "Velocity of Large Drops and Bubbles in Media of Infinite or Restricted Extent," *AIChE*, 6, 281-288 (1960).
23. Sparrow, E. M. and Gregg, J. L., "Similar Solutions for Free Convection from a Nonisothermal Vertical Plate," *Trans. ASME*, 80, p. 379 (1958).
24. Kays, W. M., Convective Heat and Mass Transfer, McGraw-Hill Book Co., p. 207 (1966).
25. Rich, B. R., "An Investigation of Heat Transfer From an Inclined Flat Plate in Free Convection," *Trans. ASME*, 75, 489-499 (May 1953).
26. Eckert, E.R.G. and Jackson, T. W., "Analysis of Turbulent Free-Convection Boundary Layer on Flat Plate," Lewis Flight Propulsion Laboratory, Report 1015 (1950).

APPENDIX A

Error Analysis:

1) Uncertainty in Heat Transfer Coefficient, $h(x)$:

It was shown that the heat transfer coefficient is represented by the relation

$$h(x) = \frac{k_{BN}(T_{front}(x) - T_{back}(x))}{a \cdot (T_{pool} - T_{front}(x))} \quad (23)$$

The total uncertainty in $h(x)$ may be computed by taking the total differential of Eq. 23 as follows:

$$dh = \frac{\partial h}{\partial k_{BN}} dk_{BN} + \frac{\partial h}{\partial \Delta T_{fb}} d\Delta T_{fb} + \frac{\partial h}{\partial a} da + \frac{\partial h}{\partial \Delta T_{pf}} d\Delta T_{pf} \quad (A-1)$$

where

$$\Delta T_{fb} \equiv T_{front}(x) - T_{back}(x) \quad (A-2)$$

and

$$\Delta T_{pf} \equiv T_{pool} - T_{front}(x) \quad (A-3)$$

The most probable mean square error, ϵ_h^2 , is written as

$$\epsilon_h^2 = \left(\frac{dh}{h} \right)^2 \quad (A-4)$$

and this reduces to

$$\epsilon_h = \left[\epsilon_{k_{BN}}^2 + \epsilon_{\Delta T_{fb}}^2 + \epsilon_a^2 + \epsilon_{\Delta T_{pf}}^2 \right]^{1/2} \quad (A-5)$$

The magnitude of each quantity in Eq. A-5 and its uncertainty are listed below:

QUANTITY	MAGNITUDE	UNCERTAINTY
k_{BN}	0.041 cal/cm s °C	0.001
T_{fb}	20 °C *	0.2
T_{pf}	20 °C *	0.2
a	1.27 cm	0.002

* Nominal Value

The result is that the most probable uncertainty in $h(x)$ is approximately ± 3 percent.

3) Uncertainty in Average Void Fraction, $\bar{\alpha}$:

The average void fraction may be written as

$$\bar{\alpha} = (H_B - H_O) / H_B \quad (24)$$

This may be written in differential form as shown before to represent the mean square error in the average void fraction as

$$\frac{\epsilon}{\bar{\alpha}} = \left[\left(\frac{H_O}{H_B(H_B - H_O)} dH_B \right)^2 + \left(\frac{1}{H_B - H_O} dH_O \right)^2 \right]^{1/2} \quad (A-6)$$

where $dH_B \sim 0.5$ and $dH_O \sim 0.1$ cm. One can readily see that for small $\bar{\alpha}$ (i.e., $(H_B - H_O)$ small), the fractional error will be large and approaching ∞ as $(H_B - H_O) \rightarrow 0$.

For $H_o = 20$. cm and $H_B = 30$. cm, the result is the most probable error in $\bar{\alpha}$ was approximately 3 percent. For $H_o = 25$. cm and $H_B = 30$. cm, the error was found to be approximately 8 percent. The value 3 percent is being used for the remaining calculations.

3) Uncertainty in Boundary Layer Coordinate, x

The coordinate from the free surface along the boundary layer, x, may be shown to be represented by

$$x_i = HBOIL/\cos \theta - HONE + (i - 1)EPSI \quad (A-7)$$

in centimeters where HBOIL is the boiling depth measured from the pool bottom to the boiling free surface, HONE is the distance along the test wall from the base to the first thermocouple, and EPSI is the spacing along the test plate between thermocouples. The errors are independent and the incremental part, $(i - 1) (EPSI)$, does not accumulate as may be expected. The reason for this is that each thermocouple location was sited with respect to the same reference point and not with respect to the previous thermocouple along the plate. In this fashion, the positional uncertainty was not accumulative.

In a similar fashion to A-2, the linearly independent uncertainties in x may be shown to be

$$\epsilon_x = [\epsilon_{HBOIL}^2 + \epsilon_{HONE}^2 + \epsilon_{EPSI}^2]^{1/2} \quad (A-8)$$

The magnitude of each quantity in Eq. A-7 and its uncertainty are listed below:

QUANTITY	MAGNITUDE(cm)	UNCERTAINTY
HBOIL	30.0 *	.5
HONE	31.4	.2
EPSI	1.27	.05

* Nominal Value

The result is that the most probable uncertainty in x is approximately 5 percent.

4) Uncertainty in $Nu(x)$:

The Nusselt number is written as

$$Nu(x) = \frac{h(x)x}{k_f} \quad (A-9)$$

where the uncertainty in k_f is negligible. Similar to A-1 and A-2, it may be shown that the most probable error in $Nu(x)$ is

$$\epsilon_{Nu} = [\epsilon_h^2 + \epsilon_x^2]^{1/2} \quad (A-10)$$

From the previous sections, it is clear that the most probable error in $Nu(x)$ is 6 percent.

5) Uncertainty in $Ra^*(x)$:

The Rayleigh number may be shown to be represented as

$$Ra^*(x) = \frac{\bar{g} \bar{\alpha} x^3 \cos \theta Pr}{v_f^2} \quad (A-11)$$

The uncertainty in $\bar{\alpha}$ has been shown previously to be approximately 3 percent. The uncertainties in \bar{g} , $\cos \theta$, Pr , and v_f are negligible. This then reduces to

$$\epsilon_{Ra^*} = \left[\epsilon_{\bar{\alpha}}^2 + 9 \epsilon_x^2 \right]^{1/2} \quad (A-12)$$

From previously computed results, the most probable error in $Ra(x)$ is shown to be 15 percent.

6) Uncertainty in Laminar Correlation Coefficient, K :

For laminar bubbly flow, the correlation coefficient may be shown to be

$$K = Nu/Ra^{*1/4} \quad (A-13)$$

It is readily shown that the most probable error in K is

$$\epsilon_K = \left[\epsilon_{Nu}^2 + \frac{1}{16} \epsilon_{Ra^*}^2 \right]^{1/2} \quad (A-14)$$

The result is that for laminar bubbly flow, the most probable error in the correlation coefficient is expected to be 7 percent. Recall that the standard deviation in the correlation coefficient was computed to be 5 percent, further substantiating this result.

7) Uncertainty in Turbulent Correlation Coefficient, K :

For turbulent bubbly flow, the correlation coefficient may be shown to be

$$K = Nu/Ra^{*0.4} \quad (A-15)$$

It may be readily shown that the most probable error in K is

$$\epsilon_K = \left[\epsilon_{Nu}^2 + (.4)^2 \epsilon_{Ra^*}^2 \right]^{1/2} \quad (A-16)$$

The result is that for turbulent bubbly flow, the most probable error in the correlation coefficient is expected to be 8 percent. Recall that the standard deviation in the correlation coefficient was computed to be 5 percent, further substantiating this result.

All the quantities and their calculated probable errors are tabulated in Table A-1.

TABLE A-1

SUMMARY OF EXPERIMENTAL UNCERTAINTIES

QUANTITY	FRACTIONAL UNCERTAINTY
Heat Transfer Coefficient	3 %
Boundary-Layer Coordinate	5 %
Average Void Fraction	3-8 %
Nusselt Number	6 %
Rayleigh Number	15 %
Laminar Correlation Coefficient	7 %
Turbulent Correlation Coefficient	8 %

APPENDIX B

Sample Calculation (Run 9001)

For each experimental run, 27 thermocouple readings are shown in Appendix A corresponding to the 27 local heat transfer measurements. The locations of all the test plate thermocouples are listed in Table 2. Let TC_i , TF_i , TB_i and T_{POOL} represent the actual thermocouple output, test plate front surface temperature, test plate coolant-side surface temperature, and pool temperature, respectively. Then the values TC_i ($i = 1-27$) are mapped as follows:

$$TF_i = TC_i \quad i = 1, 19 \text{ on } 1.27 \text{ cm centers} \quad (B-1)$$

$$TB_i = TC_{i+19} \quad i = 1, 7 \text{ on } 3.81 \text{ cm centers} \quad (B-2)$$

$$T_{POOL} = TC_{27} \quad (B-3)$$

The test plate coolant-side has only seven thermocouples; the temperature distribution is filled out to 19 values by linearly interpolating two values between each pair of back-side thermocouples as follows.

An array TBFUL is defined and equivalent to TB by the assignment indicated below:

$$TBFUL_i = TB_j \quad (B-4)$$

for $i = 1, 4, 7, 10, 13, 16, 19$ $j = 7, 6, 5, 4, 3, 2, 1$. Next, TBFUL (2, 3, ..., 17, 18) are linearly interpolated between the measured values TBFUL (1, 4, 7, 10, 13, 16, 19). This fills out the front and coolant side temperature distributions to 19 points each. For $i = 1$, the data point is at the test plate top nearest to the free surface; for $i = 19$, the data point is at the test plate bottom furthest from the free surface.

The following quantities are required for the actual calculation of the heat transfer data:

HBOIL is the boiling pool depth (cm) measured from the pool bottom.

θ is the wall angle inclination from vertical.

k_{wall} is the boron nitride (BN) test plate thermal conductivity (= 0.041 cal/cm s °C).

a is the BN thickness (= 1.27 cm).

T_f is the average film temperature for calculating boundary layer

properties ($= (\bar{T}_{front} + T_{pool})/2$) where $\bar{T}_{front} = \frac{\sum_{i=1}^{19} TF_i}{19}$.

$\bar{\alpha}$ is the average void fraction ($= (H_B - H_O)/H_B$).

Pr is the Prandtl number evaluated at T_f (= 1.94 for Run 9001).

k_f is the film thermal conductivity evaluated at T_f (= .00162 cal/cm s °C) for Run 9001.

ν_f is the film kinematic viscosity evaluated at T_f (= .3124 cs for Run 9001).

$T_{film} = 91.7$ °C for Run 9001.

The local coordinate, x_i , local heat transfer coefficient, h_i , local Nusselt number, Nu_i , and the local Rayleigh number, Ra_i are calculated according to the following formulae:

$$x_i = HBOIL/\cos \theta - 31.4 + (i - 1) 1.27 \quad (B-5)$$

$$h_i = \frac{(TF_i - T_{BFUL_i}) k_{wall}}{a \cdot (T_{pool} - TF_i)} \quad (B-6)$$

$$Nu_i = h_i x_i / k_f \quad (B-7)$$

$$Ra_1 = \bar{g} x_1^3 \cos \theta \text{ Pr} / \nu_f^2 \quad (\text{B-8})$$

for $i = 1, 19$ where g is the gravitational acceleration coefficient.

The procedure is identical for all the runs; \bar{a} , HBOIL, and T_f may be different for each run.

EXAMPLE: RUN 9001, $i = 1$ (top most heat transfer channel, nearest pool surface).

$$\text{HBOIL} = 33.0 \text{ cm}$$

$$\cos \theta = 1.0$$

$$x_1 = 33.0 - 31.4 = 1.60 \text{ cm}$$

$$h_1 = \frac{(89.8 - 59.5) \cdot 0.041}{1.27(101.1 - 89.8)} = .0866 \text{ cal/cm s}^\circ\text{C}$$

$$\text{Nu}_1 = (.0866)(1.60) / (.00162) = 85.4$$

$$Ra_1 = (980.) (.03) (1.60)^3 (1.94) / (.003124)^2 = .2394 \times 10^8$$

494 124

APPENDIX C

In this appendix are listed the local heat transfer data for all the experiments performed. They are compiled in numerical order with the vertical wall (90°) data first, the 75° data second, and the 60° data last. The flow regime for each run is listed in Table 6. The detailed thermocouple readings are indicated in the figures, and their locations on the test plate are tabulated in Table 2.

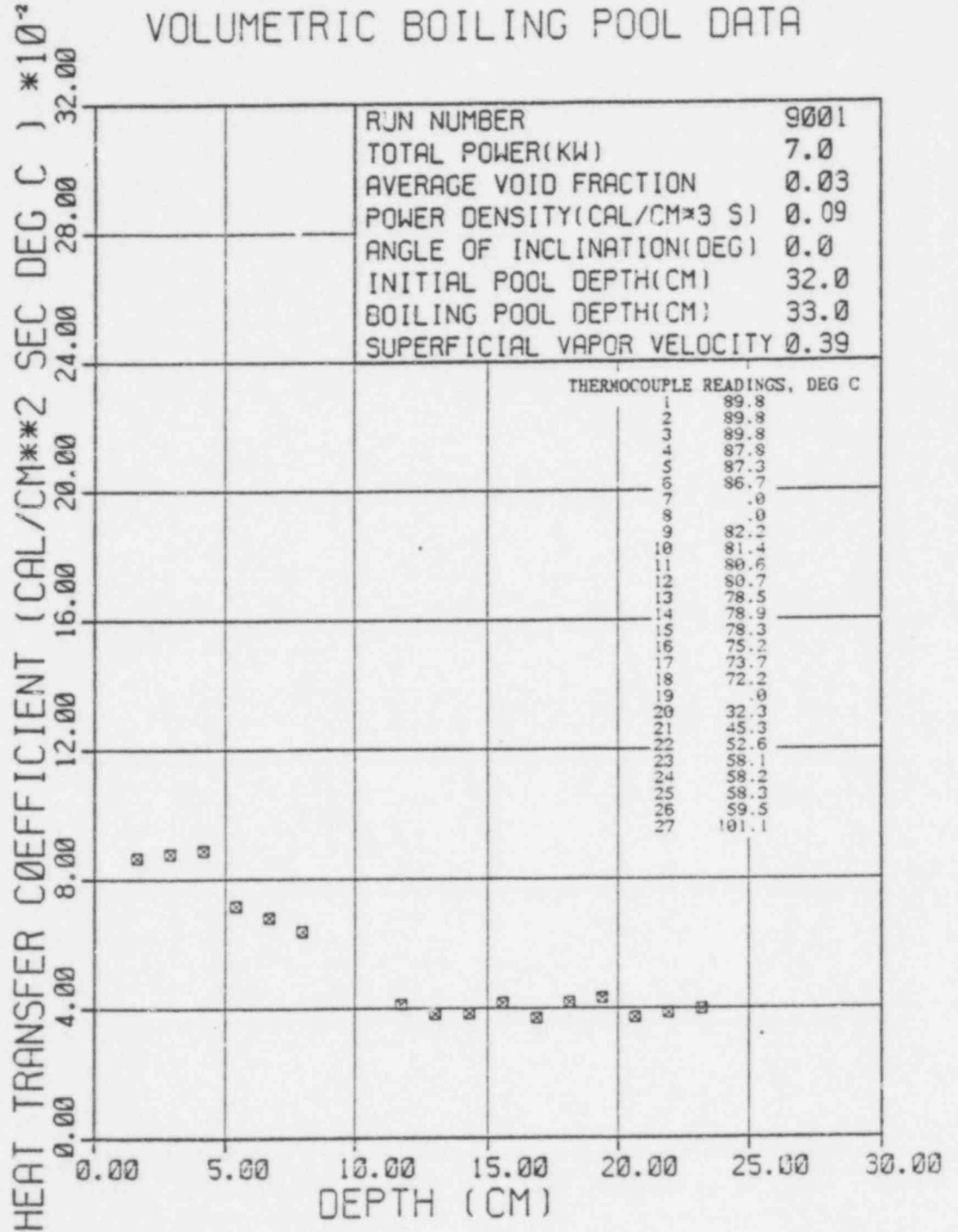
494 125

RUN NUMBER... 9001

AVERAGE VOID FRACTION..... .03
 INITIAL POOL DEPTH(CM)..... 32.0
 BOILING POOL DEPTH(CM)..... 33.0
 VOL. POWER DENS. (CAL/CM3 SEC). .09
 SUPERFICIAL VAPOR VELOCITY..... .39
 ANGLE OF INCLINATION(DEGREES). .06
 POOL VOLUME(CM*3)..... 19238.
 PRANDTL NUMBER..... 1.94
 TOTAL POWER(KW)..... 7.0
 AVERAGE SURFACE TEMP(DEG C) ... 82.3

DEPTH (CM)	LOCAL HEAT TRANSFER COEFF (CAL/CM2 SEC DEG C) EXPT EQ 14a EQ 10 EQ 10 N=1.0 N=0.7	RUSSELLT NUMBER	MODIFIED RAYLEIGH NUMBER
1.600	.0866	85.3	.2394E+08
2.870	.0877	155.0	.1382E+09
4.140	.0889	226.5	.4147E+09
5.410	.0716	238.5	.9254E+09
6.680	.0679	279.4	.1742E+10
7.950	.0638	312.4	.2936E+10
9.220	.0352		
10.49	.0341		
11.76	.0331		
13.03	.0323		
14.30	.0383		
15.57	.0416		
16.84	.0370		
18.11	.0418		
19.38	.0433		
20.65	.0373		
21.92	.0386		
23.19	.0397		
24.46	.0276		
	.0296		
	.0286		
	.0277		
	.0356		
	.0346		
	.0337		
	.0328		
	.0247		
	.0293		
	.0288		
	.0232		
	.0307		
	.0301		
	.0228		
	.0276		
	.0296		
	.0286		
	.0368		
	.0356		
	.0346		
	.0337		
	.0328		
	.0247		
	.0293		
	.0288		
	.0232		
	.0307		
	.0301		
	.0228		
	.0276		
	.0296		
	.0286		
	.0368		
	.0356		
	.0346		
	.0337		
	.0328		
	.0247		
	.0293		
	.0288		
	.0232		
	.0307		
	.0301		
	.0228		
	.0276		
	.0296		
	.0286		
	.0368		
	.0356		
	.0346		
	.0337		
	.0328		
	.0247		
	.0293		
	.0288		
	.0232		
	.0307		
	.0301		
	.0228		
	.0276		
	.0296		
	.0286		
	.0368		
	.0356		
	.0346		
	.0337		
	.0328		
	.0247		
	.0293		
	.0288		
	.0232		
	.0307		
	.0301		
	.0228		
	.0276		
	.0296		
	.0286		
	.0368		
	.0356		
	.0346		
	.0337		
	.0328		
	.0247		
	.0293		
	.0288		
	.0232		
	.0307		
	.0301		
	.0228		
	.0276		
	.0296		
	.0286		
	.0368		
	.0356		
	.0346		
	.0337		
	.0328		
	.0247		
	.0293		
	.0288		
	.0232		
	.0307		
	.0301		
	.0228		
	.0276		
	.0296		
	.0286		
	.0368		
	.0356		
	.0346		
	.0337		
	.0328		
	.0247		
	.0293		
	.0288		
	.0232		
	.0307		
	.0301		
	.0228		
	.0276		
	.0296		
	.0286		
	.0368		
	.0356		
	.0346		
	.0337		
	.0328		
	.0247		
	.0293		
	.0288		
	.0232		
	.0307		
	.0301		
	.0228		
	.0276		
	.0296		
	.0286		
	.0368		
	.0356		
	.0346		
	.0337		
	.0328		
	.0247		
	.0293		
	.0288		
	.0232		
	.0307		
	.0301		
	.0228		
	.0276		
	.0296		
	.0286		
	.0368		
	.0356		
	.0346		
	.0337		
	.0328		
	.0247		
	.0293		
	.0288		
	.0232		
	.0307		
	.0301		
	.0228		
	.0276		
	.0296		
	.0286		
	.0368		
	.0356		
	.0346		
	.0337		
	.0328		
	.0247		
	.0293		
	.0288		
	.0232		
	.0307		
	.0301		
	.0228		
	.0276		
	.0296		
	.0286		
	.0368		
	.0356		
	.0346		
	.0337		
	.0328		
	.0247		
	.0293		
	.0288		
	.0232		
	.0307		
	.0301		
	.0228		
	.0276		
	.0296		
	.0286		
	.0368		
	.0356		
	.0346		
	.0337		
	.0328		
	.0247		
	.0293		
	.0288		
	.0232		
	.0307		
	.0301		
	.0228		
	.0276		
	.0296		
	.0286		
	.0368		
	.0356		
	.0346		
	.0337		
	.0328		
	.0247		
	.0293		
	.0288		
	.0232		
	.0307		
	.0301		
	.0228		
	.0276		
	.0296		
	.0286		
	.0368		
	.0356		
	.0346		
	.0337		
	.0328		
	.0247		
	.0293		
	.0288		
	.0232		
	.0307		
	.0301		
	.0228		
	.0276		
	.0296		
	.0286		
	.0368		
	.0356		
	.0346		
	.0337		
	.0328		
	.0247		
	.0293		
	.0288		
	.0232		
	.0307		
	.0301		
	.0228		
	.0276		
	.0296		
	.0286		
	.0368		
	.0356		
	.0346		
	.0337		
	.0328		
	.0247		
	.0293		
	.0288		
	.0232		
	.0307		
	.0301		
	.0228		
	.0276		
	.0296		
	.0286		
	.0368		
	.0356		
	.0346		
	.0337		
	.0328		
	.0247		
	.0293		
	.0288		
	.0232		
	.0307		
	.0301		
	.0228		
	.0276		
	.0296		
	.0286		
	.0368		
	.0356		
	.0346		
	.0337		
	.0328		
	.0247		
	.0293		
	.0288		
	.0232		
	.0307		
	.0301		
	.0228		
	.0276		
	.0296		
	.0286		
	.0368		
	.0356		
	.0346		
	.0337		
	.0328		
	.0247		
	.0293		
	.0288		
	.0232		
	.0307		
	.0301		
	.0228		
	.0276		
	.0296		
	.0286		
	.0368		
	.0356		
	.0346		
	.0337		
	.0328		
	.0247		
	.0293		
	.0288		
	.0232		
	.0307		
	.0301		
	.0228		
	.0276		
	.0296		
	.0286		
	.0368		
	.0356		
	.0346		
	.0337		
	.0328		
	.0247		
	.0293		
	.0288		
	.0232		
	.0307		
	.0301		
	.0228		
	.0276		
	.0296		
	.0286		
	.0368		
	.0356		
	.0346		
	.0337		
	.0328		
	.0247		
	.0293		
	.0288		
	.0232		
	.0307		
	.0301		
	.0228		
	.0276		
	.0296		
	.0286		
	.0368		
	.0356		
	.0346		
	.0337		
	.0328		
	.0247		
	.0293		
	.0288		
	.0232		
	.0307		
	.0301		
	.0228		
	.0276		
	.0296		
	.0286		
	.0368		
	.0356		
	.0346		
	.0337		
	.0328		
	.0247		
	.0293		
	.0288		
	.0232		
	.0307		
	.0301		
	.0228		
	.0276		
	.0296		
	.0286		
	.0368		
	.0356		
	.0346		
	.0337		
	.0328		
	.0247		
	.0293		
	.0288		
	.0232		
	.0307		
	.0301		
	.0228		
	.0276		
	.0296		
	.0286		
	.0368		
	.0356		
	.0346		
	.0337		
	.0328		
	.0247		
	.0293		
	.0288		
	.0232		
	.0307		
	.0301		
	.0228		
	.0276		
	.0296		
	.0286		
	.0368		
	.0356		
	.0346		
	.0337		
	.0328		
	.0247		
	.0293		
	.0288		
	.0232		
	.0307		
	.0301		
	.0228		
	.0276	</	

VOLUMETRIC BOILING POOL DATA



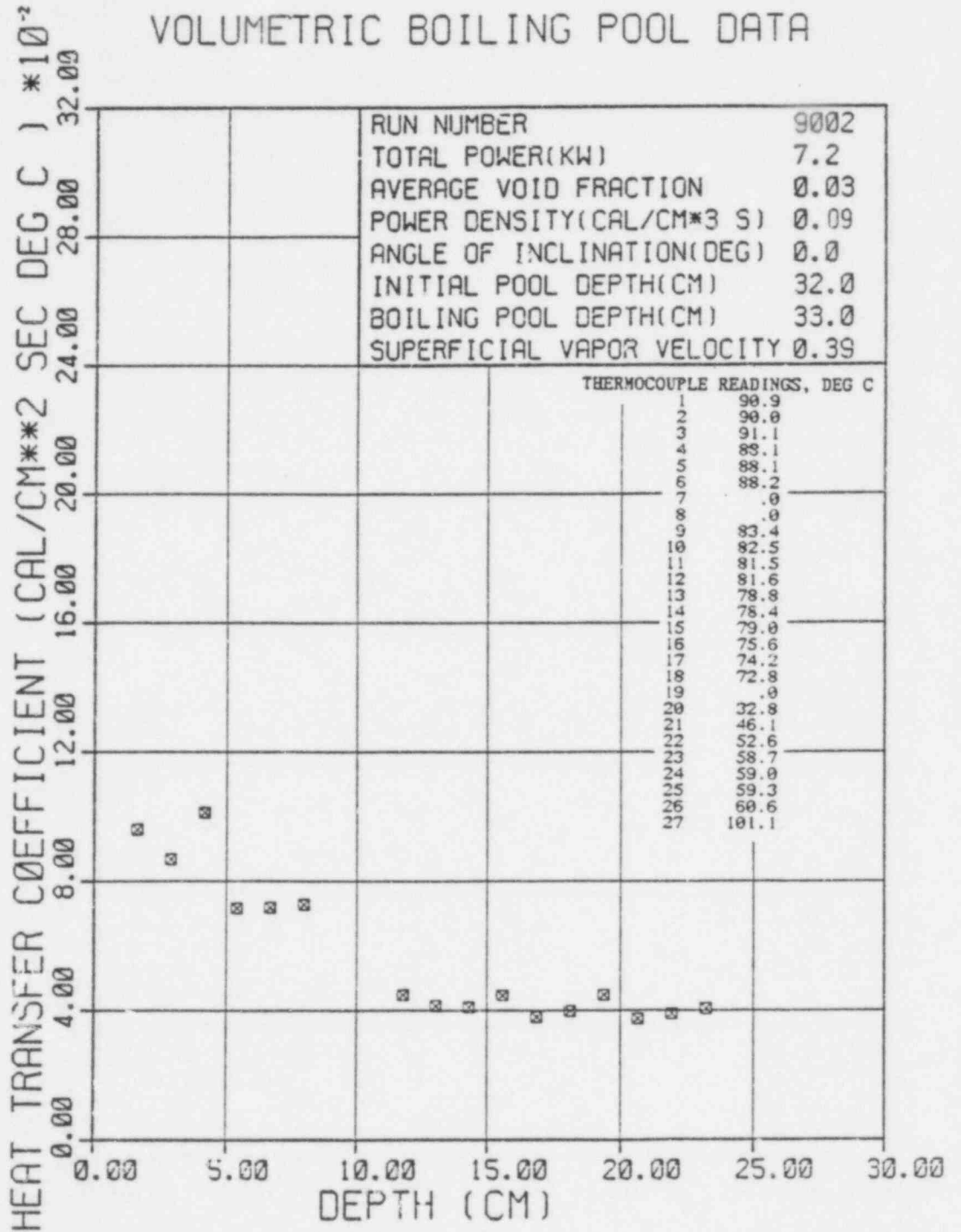
494 127

RUN NUMBER... 9002

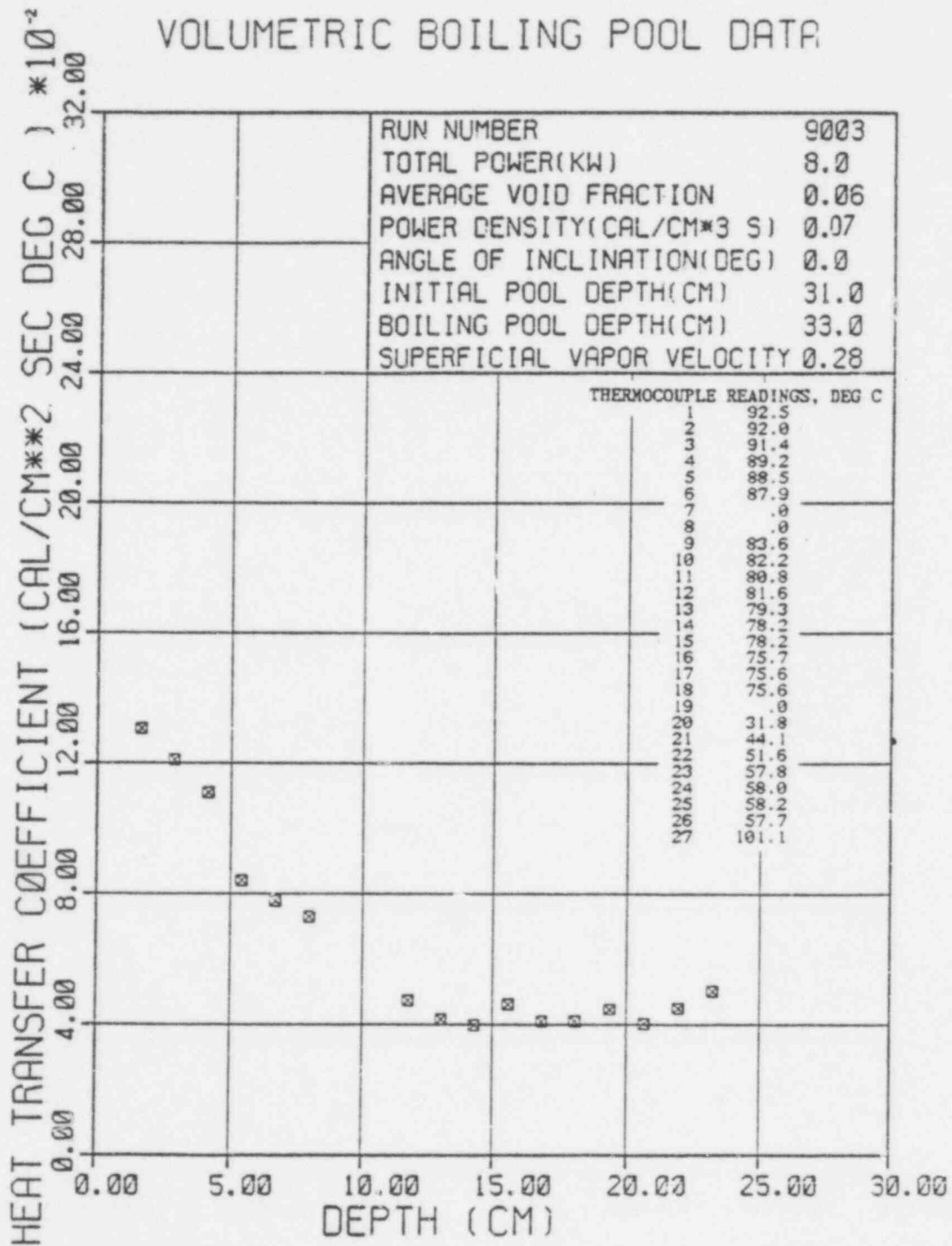
AVERAGE VOID FRACTION..... .03
 INITIAL POOL DEPTH(CM)..... 32.0
 BOILING POOL DEPTH(CM)..... 33.0
 VOL. POWER DENS.(CAL/CM3 SEC). .09
 SUPERFICIAL VAPOR VELOCITY..... .39
 ANGLE OF INCLINATION(DEGREES). .00
 POOL VOLUME(CM*3)..... 19238.
 PRANDTL NUMBER..... 1.93
 TOTAL POWER(KW)..... 7.2
 AVERAGE SURFACE TEMP.(DEG C)... 83.1

DEPTH (CM)	LOCAL HEAT TRANSFER COEFF (CAL/CM2 SEC DEG C)		NUSSELT NUMBER	MODIFIED RAYLEIGH NUMBER
	EXPT	EQ 14a		
1.600	.0959	.0546	94.5	.2403E+08
2.870	.0860	.0472	152.3	.1387E+09
4.140	.1013	.0431	238.1	.4163E+09
5.410	.0715	.0403	238.2	.9290E+09
6.680	.0718	.0382	295.2	.1749E+10
7.950	.0728	.0366	356.4	.2948E+10
9.220		.0353		
10.49		.0341		
11.76	.0449	.0332	324.9	.9542E+10
13.03	.0413	.0323	331.4	.1298E+11
14.30	.0409	.0316	360.1	.1716E+11
15.57	.0446	.0309	428.0	.2214E+11
16.84	.0379	.0303	393.2	.2302E+11
18.11	.0398	.0298	443.5	.3485E+11
19.38	.0409	.0293	535.7	.4270E+11
20.65	.0373	.0288	474.8	.5166E+11
21.92	.0390	.0284	526.9	.6179E+11
23.19	.0406	.0280	579.3	.7317E+11
24.46		.0276		

VOLUMETRIC BOILING POOL DATA



VOLUMETRIC BOILING POOL DATA



494 131

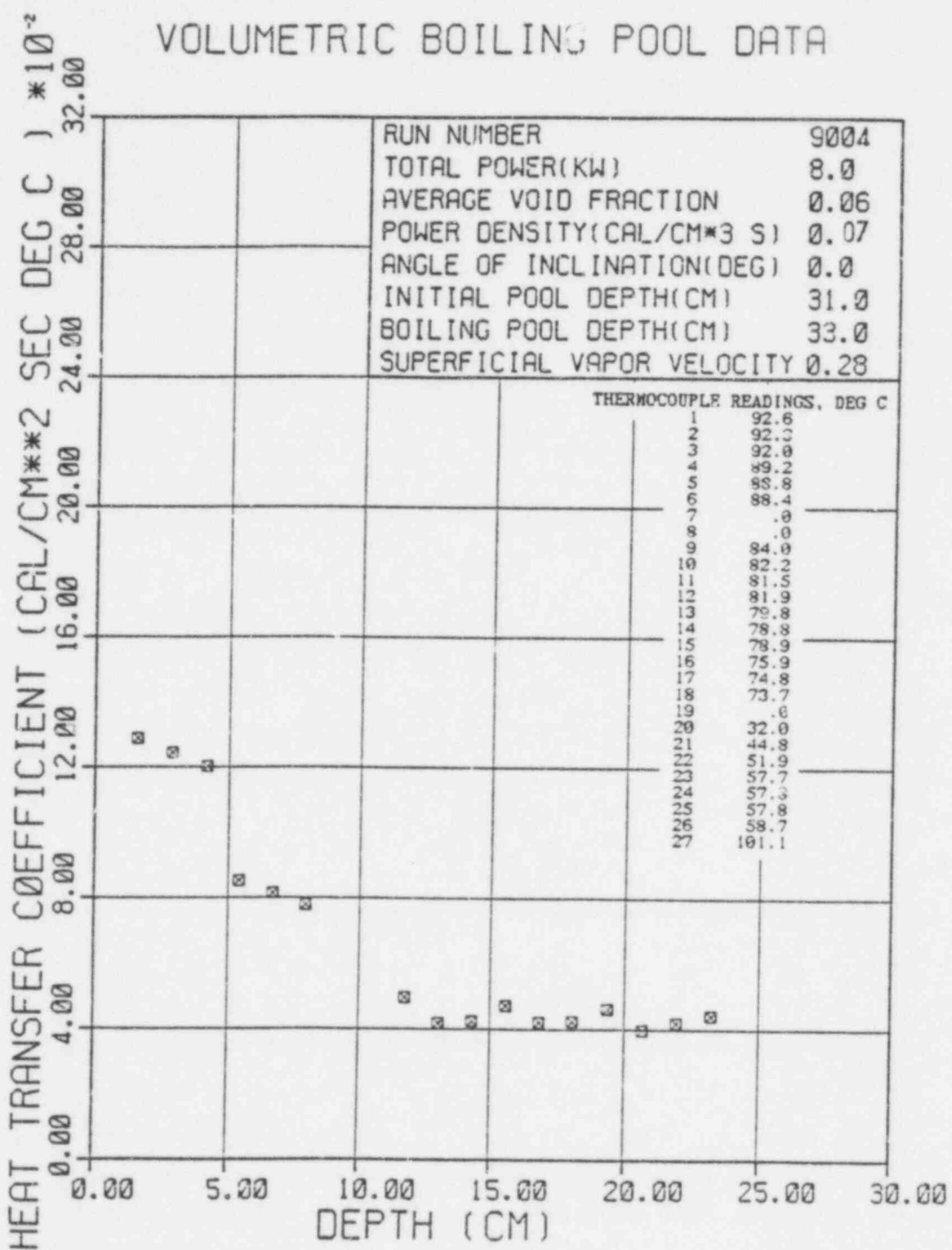
 RUN NUMBER... 9004

AVERAGE VOID FRACTION..... .96
 INITIAL POOL DEPTH(CM)..... 31.0
 BOILING POOL DEPTH(CM)..... 33.0
 VOL. POWER DENS.(CAL/CM3 SEC). .07
 SUPERFICIAL VAPOR VELOCITY.... .28
 ANGLE OF INCLINATION(DEGREES). .00
 POOL VOLUME(CM**3)..... 18637.
 PRANDTL NUMBER..... 1.92
 TOTAL POWER(KW)..... 8.0
 AVERAGE SURFACE TEMP(DEG C) ... 83.8

DEPTH (CM)	LOCAL HEAT TRANSFER COEFF (CAL/CM2 SEC. DEG C) EXPT EQ 14a EQ 10 EQ 10 N=1.0 N=0.7	NUSSLETT NUMBER	MODIFIED RAYLEIGH NUMBER			
1.600	.1288	.0650	.0598	.0891	126.8	.4822E+09
2.870	.1244	.0562	.0487	.0650	219.7	.2783E+09
4.140	.1203	.0513	.0431	.0572	306.5	.8354E+09
5.410	.0852	.0480	.0394	.0521	283.7	.1864E+10
6.680	.0814	.0455	.0367	.0485	334.6	.3599E+10
7.950	.0778	.0436	.0347	.0457	380.6	.5916E+10
9.220		.0420	.0330	.0434		
10.49		.0406	.0317	.0416		
11.76	.0496	.0395	.0305	.0400	359.0	.1915E+11
13.03	.0418	.0385	.0295	.0386	335.6	.2695E+11
14.30	.0424	.0376	.0287	.0374	373.1	.3443E+11
15.57	.0472	.0368	.0279	.0364	452.3	.4444E+11
16.81	.0423	.0361	.0272	.0354	438.3	.5623E+11
18.11	.0424	.0355	.0266	.0346	472.3	.6903E+11
19.38	.0461	.0349	.0260	.0338	550.5	.8570E+11
20.65	.0708	.0343	.0255	.0331	506.4	.1037E+12
21.92	.0421	.0338	.0250	.0325	567.5	.1240E+12
23.19	.0441	.0333	.0246	.0319	629.6	.1468E+12
24.46		.0329	.0242	.0313		

494 132

VOLUMETRIC BOILING POOL DATA



494 133

RUN NUMBER... 9065

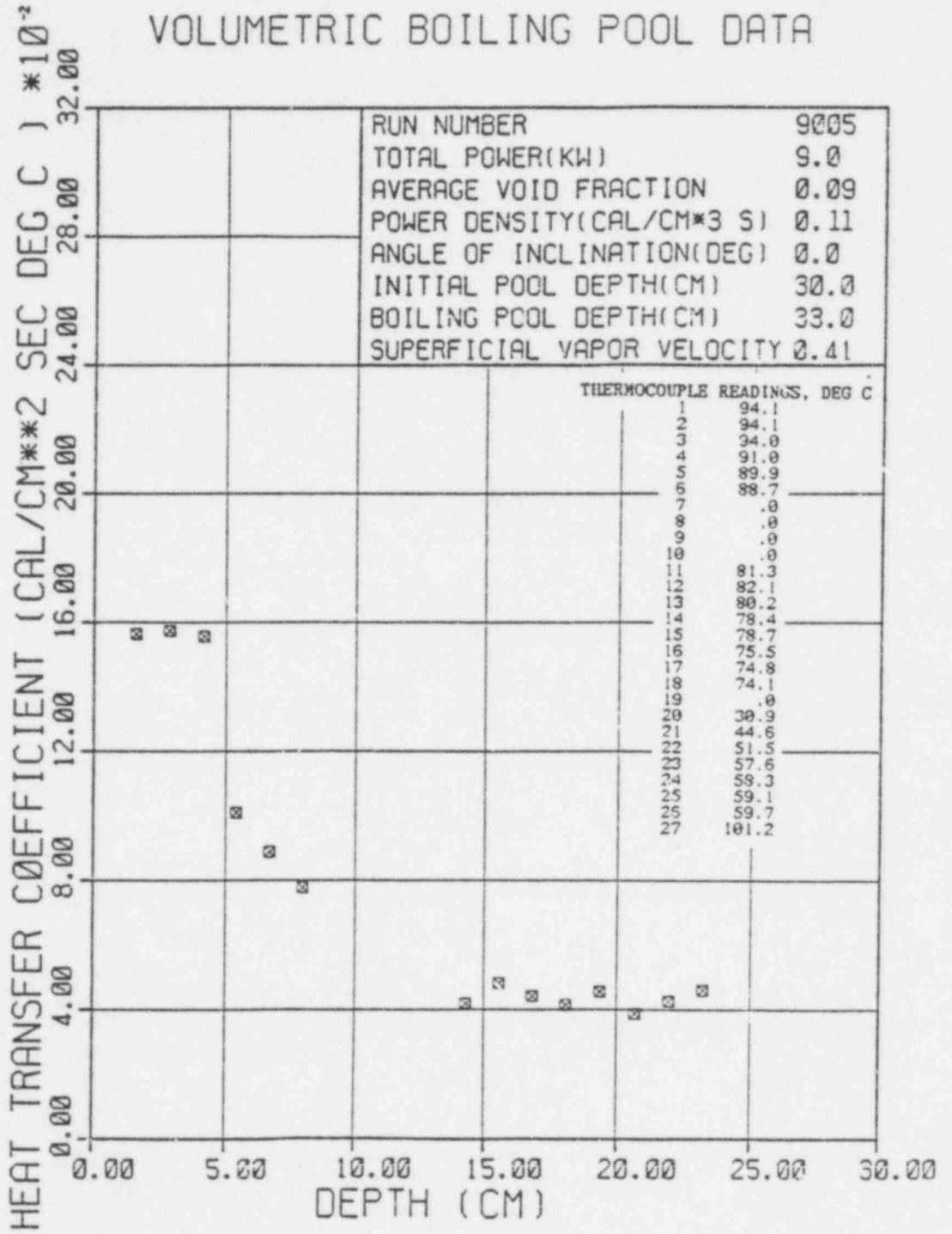
AVERAGE VOID FRACTION..... .09
 INITIAL POOL DEPTH(CM)..... 30.0
 BOILING POOL DEPTH(CM)..... 33.0
 VOL. POWER DENS. (CAL/CM3 SEC) . .11
 SUPERFICIAL VAPOR VELOCITY..... .41
 ANGLE OF INCLINATION(DEGREES) . .60
 POOL VOLUME(CM*3)..... 18036.
 PRANDTL NUMBER..... 1.91
 TOTAL POWER(KW)..... 9.0
 AVERAGE SURFACE TEMP (DEG C) ... 84.3

DEPTH (CM)	LOCAL HEAT TRANSFER COEFF (CAL/CM2 SEC DEG C)		NUSSELT NUMBER	MODIFIED RAYLEIGH NUMBER
	EXPT EQ 14a	EQ 10 N=0.7		
1.600	.1564	.0720	.0687	.0922
2.870	.1573	.0623	.0559	.0748
4.140	.1556	.0568	.0493	.0657
5.410	.1010	.0531	.0450	.0598
6.680	.0888	.0504	.0419	.0556
7.950	.0778	.0483	.0395	.0523
9.220		.0465	.0376	.0497
10.49		.0450	.0361	.0476
11.76		.0438	.0347	.0457
13.03		.0426	.0336	.0442
14.30	.0417	.0417	.0326	.0428
15.57	.0483	.0408	.0317	.0416
16.84	.0441	.0400	.0309	.0405
18.11	.0413	.0393	.0302	.0395
19.38	.0456	.0386	.0295	.0386
20.65	.0388	.0380	.0289	.0378
21.92	.0425	.0374	.0284	.0370
23.19	.0460	.0369	.0279	.0364
24.46		.0364	.0274	.0357

154.0
 277.9
 396.4
 336.2
 364.9
 380.8
 367.4
 462.7
 457.3
 460.8
 544.2
 493.3
 573.6
 656.8
 .7255E+08
 .4187E+09
 .1257E+10
 .2804E+10
 .5279E+10
 .8899E+10
 .5179E+11
 .6685E+11
 .8458E+11
 .1052E+12
 .1289E+12
 .1560E+12
 .1865E+12
 .2209E+12

494 134

VOLUMETRIC BOILING POOL DATA



494 135

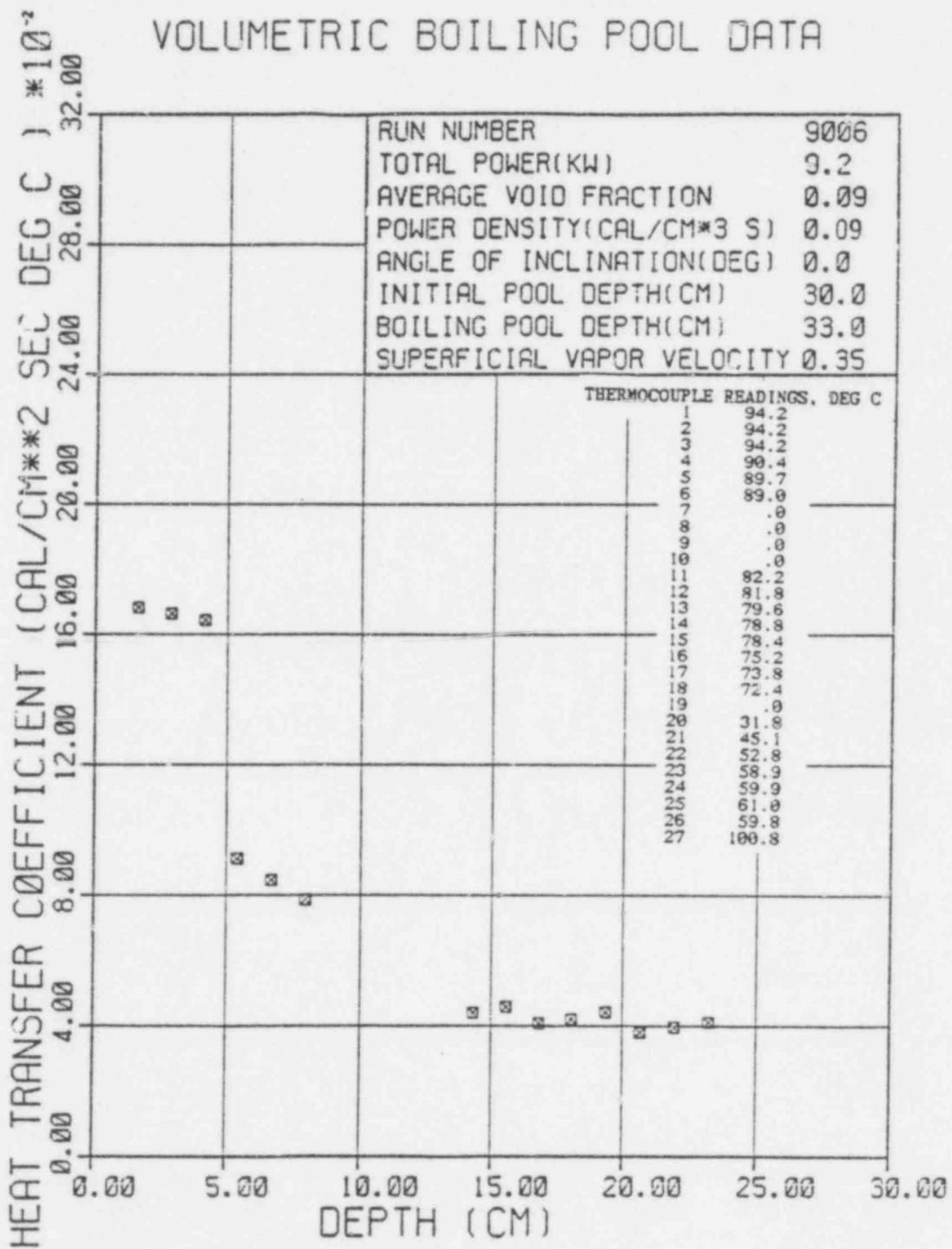
RUN NUMBER... 9006

AVERAGE VOID FRACTION..... .09
 INITIAL POOL DEPTH(CM)..... 30.0
 BOILING POOL DEPTH(CM)..... 33.0
 VOL. POWER DENS. (CAL/CM3 SEC) .09
 SUPERFICIAL VAPOR VELOCITY..... .35
 ANGLE OF INCLINATION(DEGREES) .60
 POOL VOLUME(CM**3)..... 18036.
 PRANDTL NUMBER..... 1.92
 TOTAL POWER(KW)..... 9.2
 AVERAGE SURFACE TEMP(DEG C)... 84.2

DEPTH (CM)	LOCAL HEAT TRANSFER COEFF (CAL/CM2 SEC DEG C)		NUSSELT NUMBER	MODIFIED RAYLEIGH NUMBER
	EXPT EQ 14a	EQ 10 N=1.0 M=0.7		
1.680	.1683	.0720	.0664	.0890
2.870	.1663	.0622	.0542	.0723
4.140	.1644	.0568	.0478	.0636
5.410	.0913	.0531	.0437	.0579
6.680	.0845	.0504	.0408	.0539
7.950	.0786	.0482	.0385	.0508
9.220		.0465	.0367	.0482
10.49		.0450	.0352	.0462
11.76		.0437	.0339	.0444
13.03		.0426	.0328	.0429
14.30	.0440	.0416	.0318	.0416
15.57	.0458	.0408	.0310	.0404
16.84	.0408	.0409	.0302	.0394
18.11	.0419	.0393	.0295	.0384
19.38	.0443	.0386	.0289	.0376
20.65	.0380	.0380	.0283	.0368
21.92	.0396	.0374	.0278	.0361
23.19	.0411	.0369	.0273	.0354
24.46		.0364	.0268	.0348
			165.7	.7237E+08
			293.8	.4177E+09
			418.8	.1254E+10
			303.9	.2798E+10
			347.6	.5267E+10
			384.7	.8878E+10
			387.0	.5167E+11
			439.1	.6669E+11
			423.0	.8438E+11
			467.3	.1049E+12
			528.4	.1286E+12
			482.5	.1586E+12
			534.5	.1861E+12
			586.8	.2203E+12

494 136

VOLUMETRIC BOILING POOL DATA



RUN NUMBER... 9007

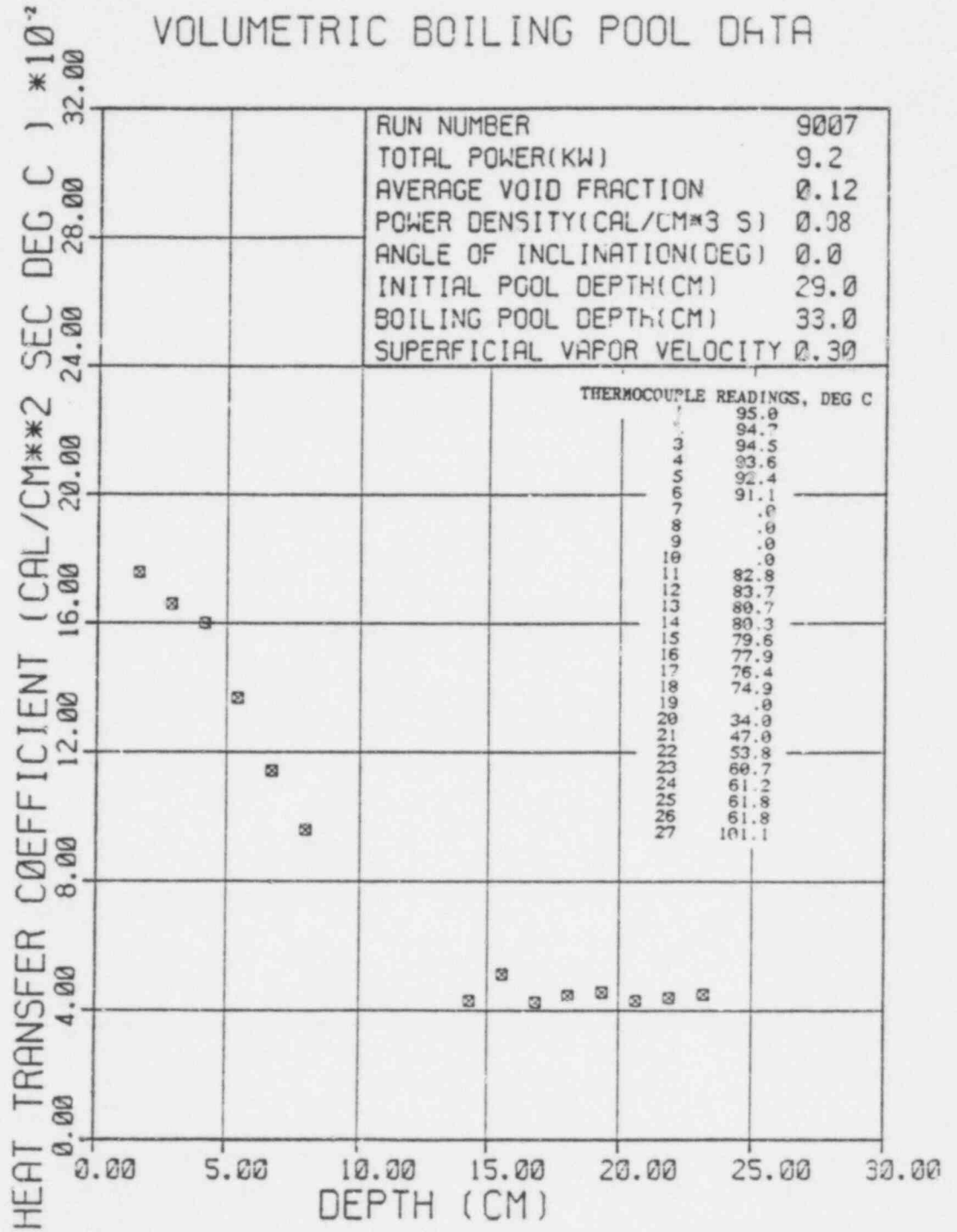
AVERAGE VOID FRACTION..... .12
 INITIAL POOL DEPTH(CM)..... 29.0
 BOILING POOL DEPTH(CM)..... 33.0
 VOL. POWER DENS. (CAL/CM3 SEC). .08
 SUPERFICIAL VAPOR VELOCITY.... .30
 ANGLE OF INCLINATION(DEGREES). .00
 POOL VOLUME(CM**3)..... 17435.
 PRANDTL NUMBER..... 1.90
 TOTAL POWER(KW)..... 9.24
 AVERAGE SURFACE TEMP(DEG C)... 85.9

-92-

49A 138

DEPTH (CM)	LOCAL HEAT TRANSFER COEFF (CAL/CM2 SEC DEG C)				NUSSELT NUMBER	MODIFIED RAYLEIGH NUMBER
	EXPT	EQ 14a	EQ 10 N=1.0	EQ 10 N=0.7		
1.600	.1757	.0776	.0675	.0900	173.0	
2.870	.1660	.0670	.0554	.0734	293.0	.9742E+08
4.140	.1599	.0612	.0490	.0647	407.4	.5623E+09
5.410	.1369	.0572	.0449	.0591	455.6	.1688E+10
6.680	.1143	.0543	.0420	.0550	469.7	.3766E+10
7.950	.0959	.0520	.0397	.0519	469.0	.7090E+10
9.220		.0501	.0378	.0493		.1195E+11
10.49		.0485	.0363	.0473		
11.76		.0471	.0350	.0455		
13.03		.0459	.0339	.0440		
14.30	.0430	.0449	.0329	.0426	378.7	
15.57	.0512	.0439	.0321	.0415	490.5	.6955E+11
16.84	.0426	.0431	.0313	.0404	441.0	.8977E+11
18.11	.0446	.0423	.0306	.0395	497.5	.1136E+12
19.38	.0455	.0416	.0299	.0386	543.1	.1413E+12
20.65	.0430	.0409	.0294	.0378	546.3	.1731E+12
21.92	.0441	.0403	.0288	.0371	594.6	.2094E+12
23.19	.0451	.0398	.0283	.0364	642.8	.2505E+12
24.46		.0392	.0279	.0358		.2966E+12

VOLUMETRIC BOILING POOL DATA



494 139

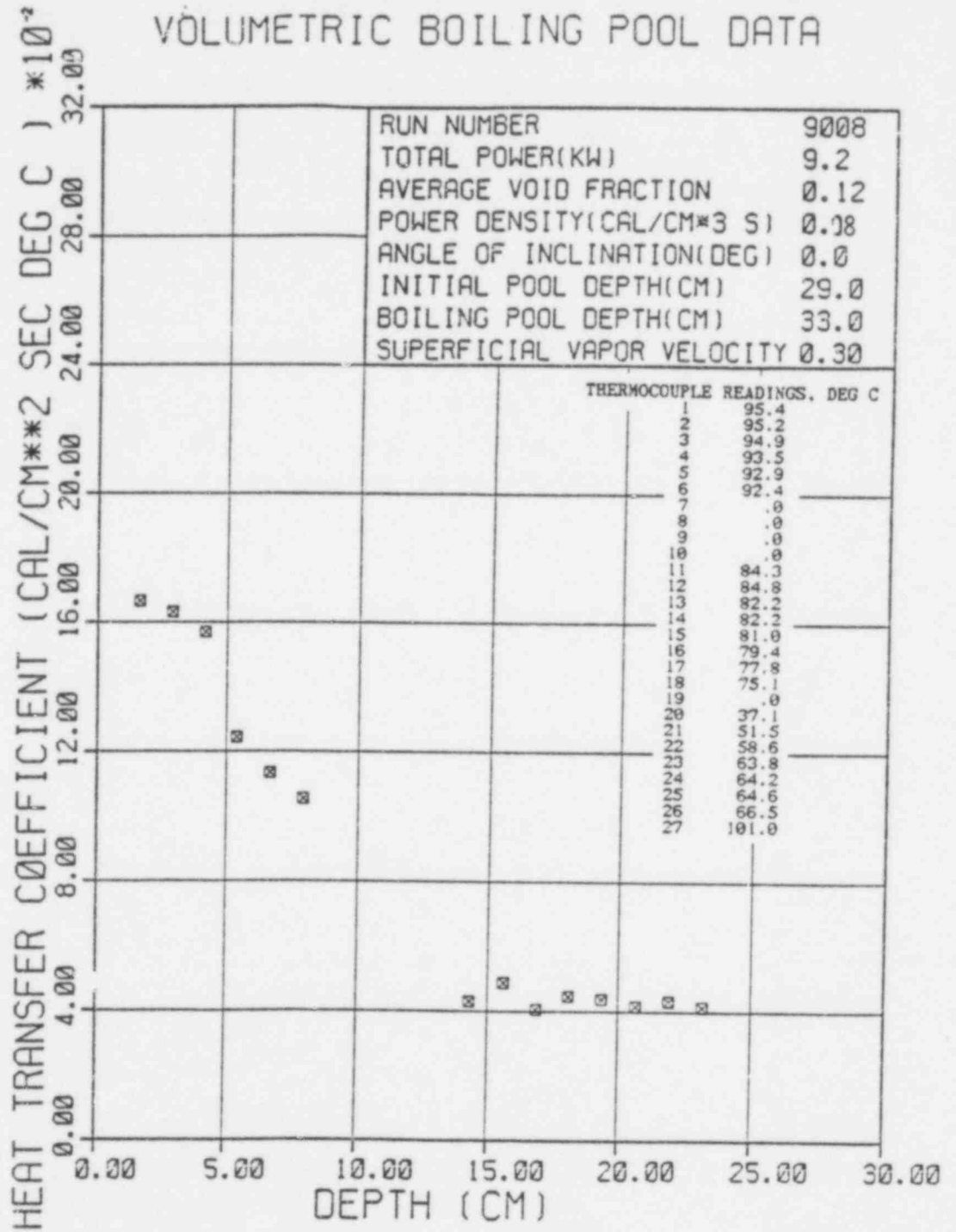
RUN NUMBER... 9608

AVERAGE VOID FRACTION..... .12
 INITIAL POOL DEPTH(CM)..... 29.0
 BOILING POOL DEPTH(CM)..... 33.0
 VOL. POWER DENS.(CAL/CM3 SEC). .08
 SUPERFICIAL VAPOR VELOCITY..... .30
 ANGLE OF INCLINATION(DEGREES). .00
 POOL VOLUME(CM**3)..... 17435.
 PRANDTL NUMBER..... 1.89
 TOTAL POWER(KW)..... 9.24
 AVERAGE SURFACE TEMP(DEG C).... 86.9

DEPTH (CM)	LOCAL HEAT TRANSFER COEFF (CAL/CM2 SEC DEG C)		MUSSELT NUMBER	MODIFIED RAYLEIGH NUMBER
	EXPT	EQ 14a		
1.600	.1666	.0777	164.0	.9782E+08
2.870	.1633	.0671	288.2	.5646E+09
4.140	.1570	.0613	399.8	.1695E+10
5.410	.1244	.0573	413.9	.3782E+10
6.680	.1133	.0543	465.6	.7119E+10
7.950	.1054	.0520	515.2	.1200E+11
9.220	.0501	.0379		
10.49	.0485	.0363		
11.76	.0472	.0351		
13.03	.0460	.0339		
14.30	.0449	.0330		
15.57	.0438	.0321	378.0	.6984E+11
16.84	.0405	.0313	466.9	.9015E+11
18.11	.0446	.0424	419.8	.1141E+12
19.38	.0438	.0416	496.7	.1419E+12
20.65	.0417	.0410	522.1	.1738E+12
21.92	.0433	.0410	529.6	.2103E+12
23.19	.0414	.0398	583.5	.2515E+12
24.46	.0393	.0279	590.3	.2978E+12

494 140

VOLUMETRIC BOILING POOL DATA



494 141

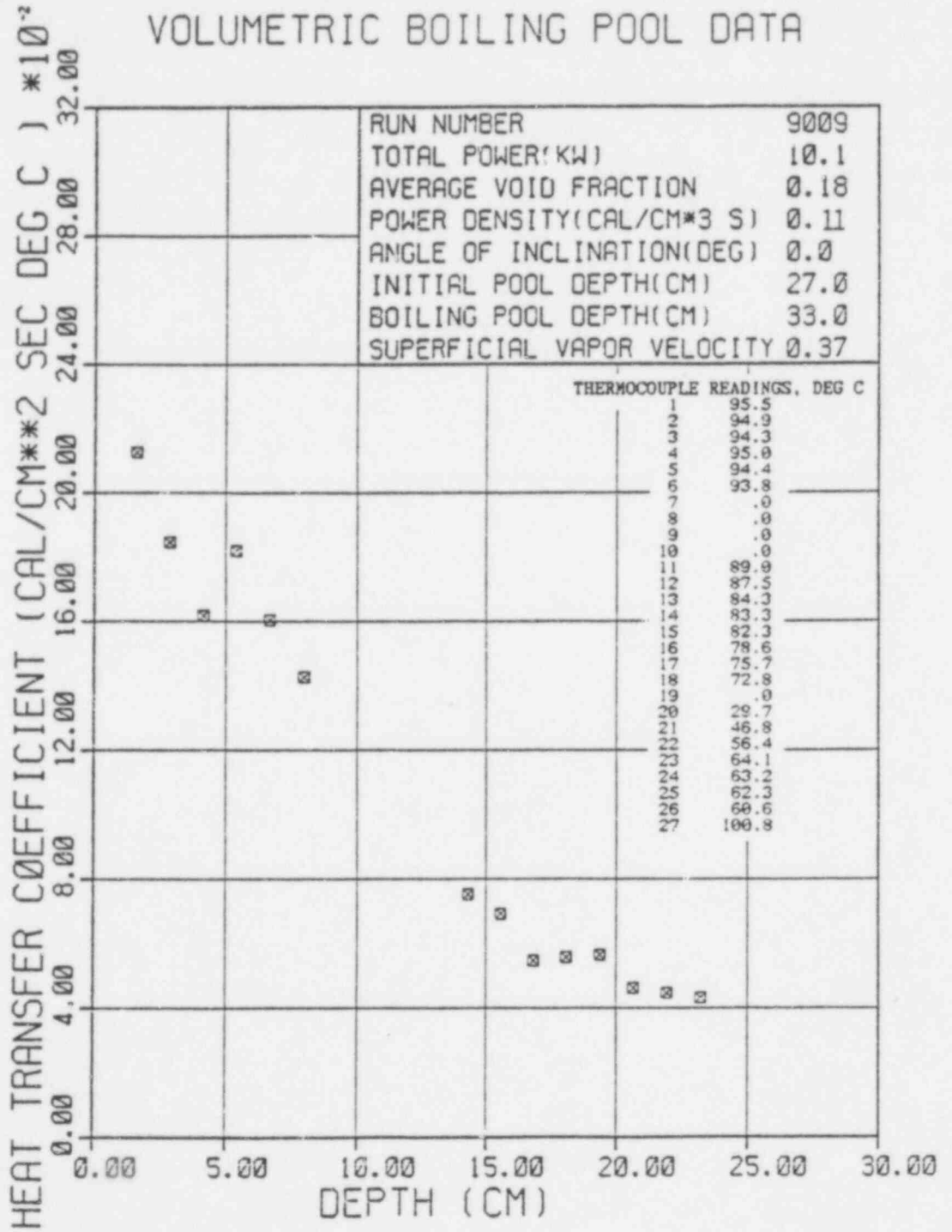
RUN NUMBER... 9009

AVERAGE VOID FRACTION..... .18
 INITIAL POOL DEPTH(CM)..... 27.0
 BOILING POOL DEPTH(CM)..... 33.0
 VOL. POWER DENS. (CAL/CM3 SEC), .11
 SUPERFICIAL VAPOR VELOCITY.... .37
 ANGLE OF INCLINATION(DEGREES), .00
 POOL VOLUME(CM**3)..... 16232.
 PRANDTL NUMBER..... 1.68
 TOTAL POWER(KW)..... 10.1
 AVERAGE SURFACE TEMP(DEG C)... 88.3

DEPTH (CM)	LOCAL HEAT TRANSFER COEFF (CAL/CM2 SEC DEG C)				NUSSELT NUMBER	MODIFIED RAYLEIGH NUMBER
	EXPT	EQ 14a	EQ 10 N=1.0	EQ 10 N=0.7		
1.600	.2126	.0861	.0750	.1000		
2.870	.1846	.0744	.0615	.0816	209.1	.1475E+09
4.140	.1617	.0679	.0545	.0719	325.7	.8515E+09
5.410	.1820	.0635	.0499	.0656	411.8	.2556E+10
6.680	.1604	.0602	.0466	.0611	605.5	.5704E+10
7.950	.1425	.0577	.0441	.0576	658.9	.1074E+11
9.220		.0556	.0420	.0548	696.6	.1810E+11
10.49		.0538	.0403	.0525		
11.76		.0523	.0389	.0505		
13.03		.0510	.0376	.0488		
14.30	.0751	.0498	.0366	.0474		
15.57	.0693	.0488	.0356	.0461	660.8	.1053E+12
16.84	.0546	.0478	.0347	.0449	663.1	.1360E+12
18.11	.0555	.0469	.0340	.0438	565.3	.1720E+12
19.38	.0564	.0462	.0333	.0429	618.3	.2140E+12
20.65	.0462	.0454	.0326	.0420	671.7	.2622E+12
21.92	.0445	.0448	.0320	.0412	587.2	.3172E+12
23.19	.0431	.0441	.0315	.0404	599.8	.3794E+12
24.46		.0436	.0309	.0397	614.9	.4492E+12

49A
142

VOLUMETRIC BOILING POOL DATA



494 143

RUN NUMBER... 9010

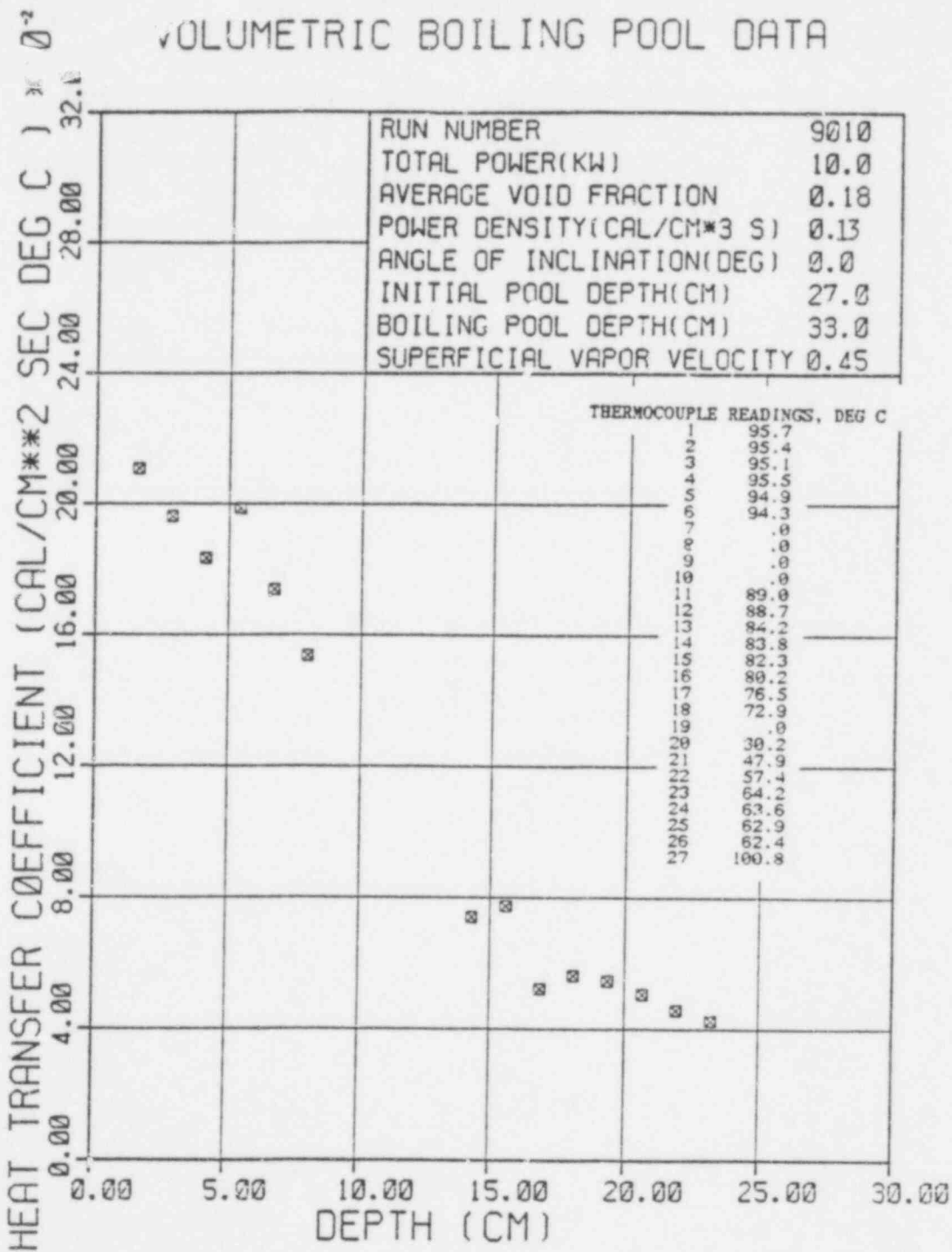
AVERAGE VOID FRACTION..... .18
 INITIAL POOL DEPTH(CM)..... 27.0
 BOILING POOL DEPTH(CM)..... 33.0
 VOL. POWER DEN. (CAL/CM3 SEC). .13
 SUPERFICIAL VAPOR VELOCITY.... .45
 ANGLE OF INCLINATION(DEGREES). .00
 POOL VOLUME(CM**3)..... 16232.
 PRANDTL NUMBER..... 1.87
 TOTAL POWER(KW)..... 10.0
 AVERAGE SURFACE TEMP(DEG C)... 88.8

DEPTH (CM)	LOCAL HEAT TRANSFER COEFF (CAL/CM2 SEC DEG C)				NUSSELT NUMBER	MODIFIED RAYLEIGH NUMBER
	EXPT	EQ 14a	EQ 10 N=1.0	EQ 10 N=0.7		
1.600	.2108	.0862	.0779	.1043	207.4	.1479E+09
2.870	.1963	.0745	.0637	.0848	346.4	.8535E+09
4.140	.1833	.0679	.0563	.0746	466.6	.2562E+10
5.410	.1986	.0635	.0515	.0681	660.5	.5717E+10
6.680	.1738	.0603	.0480	.0633	713.9	.1076E+11
7.950	.1536	.0577	.0454	.0597	751.0	.1814E+11
9.220		.0556	.0432	.0567		
10.49		.0539	.0415	.0543		
11.76		.0523	.0400	.0523		
13.03		.0510	.0387	.0505		
14.30	.0741	.0498	.0375	.0489	651.1	.1056E+12
15.57	.0775	.0488	.0365	.0476	741.5	.1363E+12
16.84	.0521	.0478	.0356	.0464	539.6	.1724E+12
18.11	.0561	.0470	.0348	.0452	625.2	.2144E+12
19.38	.0545	.0462	.0341	.0442	649.4	.2628E+12
20.65	.0506	.0455	.0334	.0433	642.7	.3179E+12
21.92	.0458	.0448	.0328	.0425	617.7	.3803E+12
23.19	.0426	.0442	.0322	.0417	607.1	.4503E+12
24.46		.0436	.0317	.0410		

-98-

49A
144

VOLUMETRIC BOILING POOL DATA



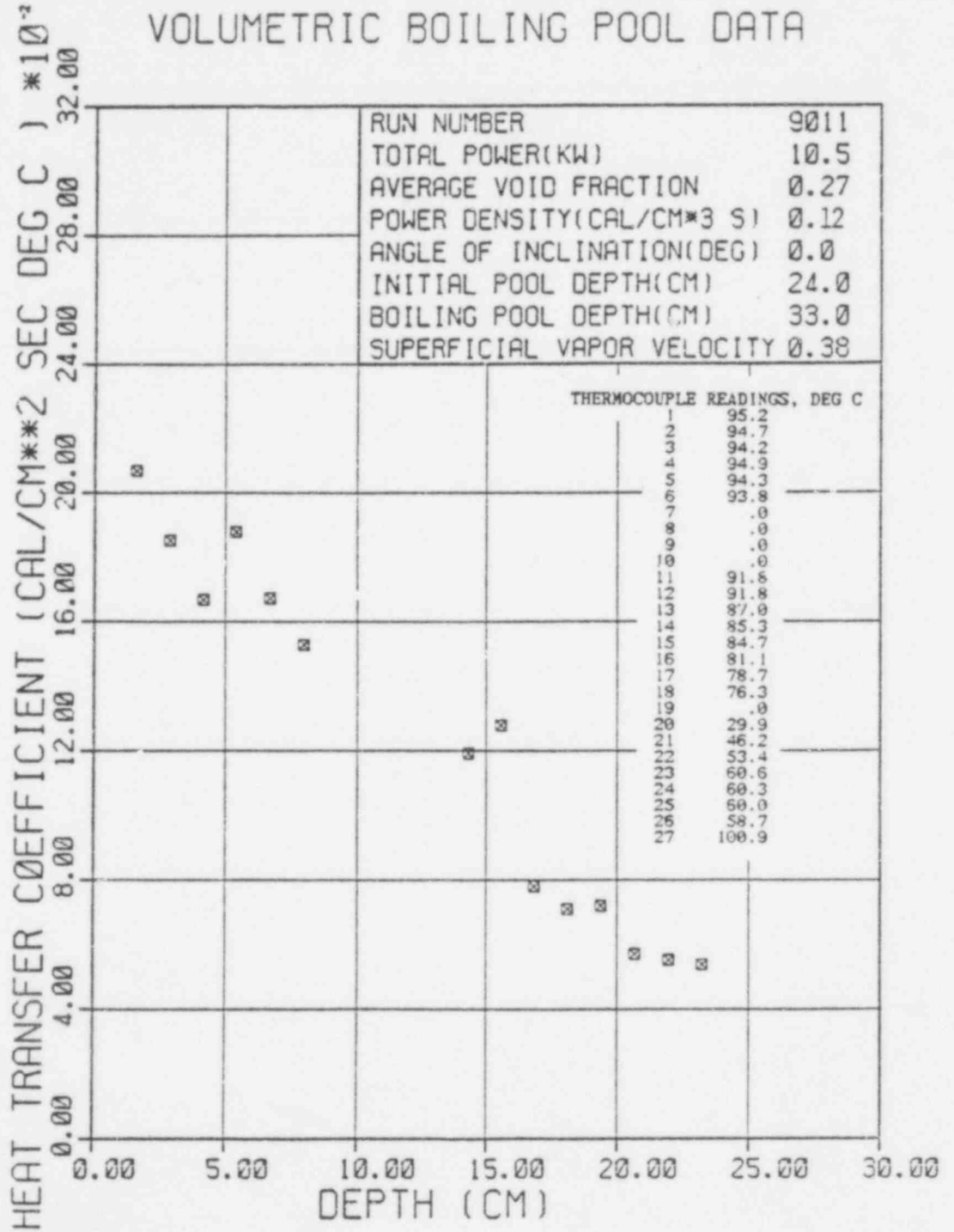
494 145

RUN NUMBER... 9011

AVERAGE VOID FRACTION..... .27
 INITIAL POOL DEPTH(C.)..... 24.0
 BOILING POOL DEPTH(CM)..... 33.0
 VOL. POWER DENS. (CAL/CM3 SEC) .12
 SUPERFICIAL VAPOR VELOCITY..... .38
 ANGLE OF INCLINATION(DEGREES) .00
 POOL VOLUME(CM**3)..... 14429.
 PRANDTL NUMBER..... 1.86
 TOTAL POWER(KW)..... 10.5
 AVERAGE SURFACE TEMP(DEG C).... 89.8

DEPTH (CM)	LOCAL HEAT TRANSFER COEFF (CAL/CM2 SEC DEG C)			RUSSELL NUMBER	MODIFIED RAYLEIGH NUMBER
	EXPT EQ 14a	EQ 10 N=1.0	EQ 10 N=0.7		
1.600	.2067	.0955	.0806	203.3	.2229E+09
2.870	.1852	.0825	.0663	326.7	.1287E+10
4.140	.1669	.0753	.0588	424.7	.3862E+10
5.410	.1878	.0704	.0539	624.4	.8618E+10
6.680	.1673	.0668	.0504	686.9	.1622E+11
7.950	.1528	.0640	.0477	746.6	.2735E+11
9.220		.0616	.0455		
10.49		.0597	.0437		
11.76		.0580	.0422		
13.03		.0565	.0408		
14.30	.1192	.0552	.0397	1047.7	.1592E+12
15.57	.1277	.0541	.0386	1222.3	.2054E+12
16.84	.0780	.0530	.0377	807.8	.2599E+12
18.11	.0710	.0521	.0369	790.1	.3233E+12
19.38	.0719	.0512	.0361	857.0	.3962E+12
20.65	.0569	.0504	.0354	722.3	.4793E+12
21.92	.0552	.0496	.0348	743.2	.5732E+12
23.19	.0538	.0490	.0342	766.3	.6788E+12
24.46		.0483	.0336		

VOLUMETRIC BOILING POOL DATA



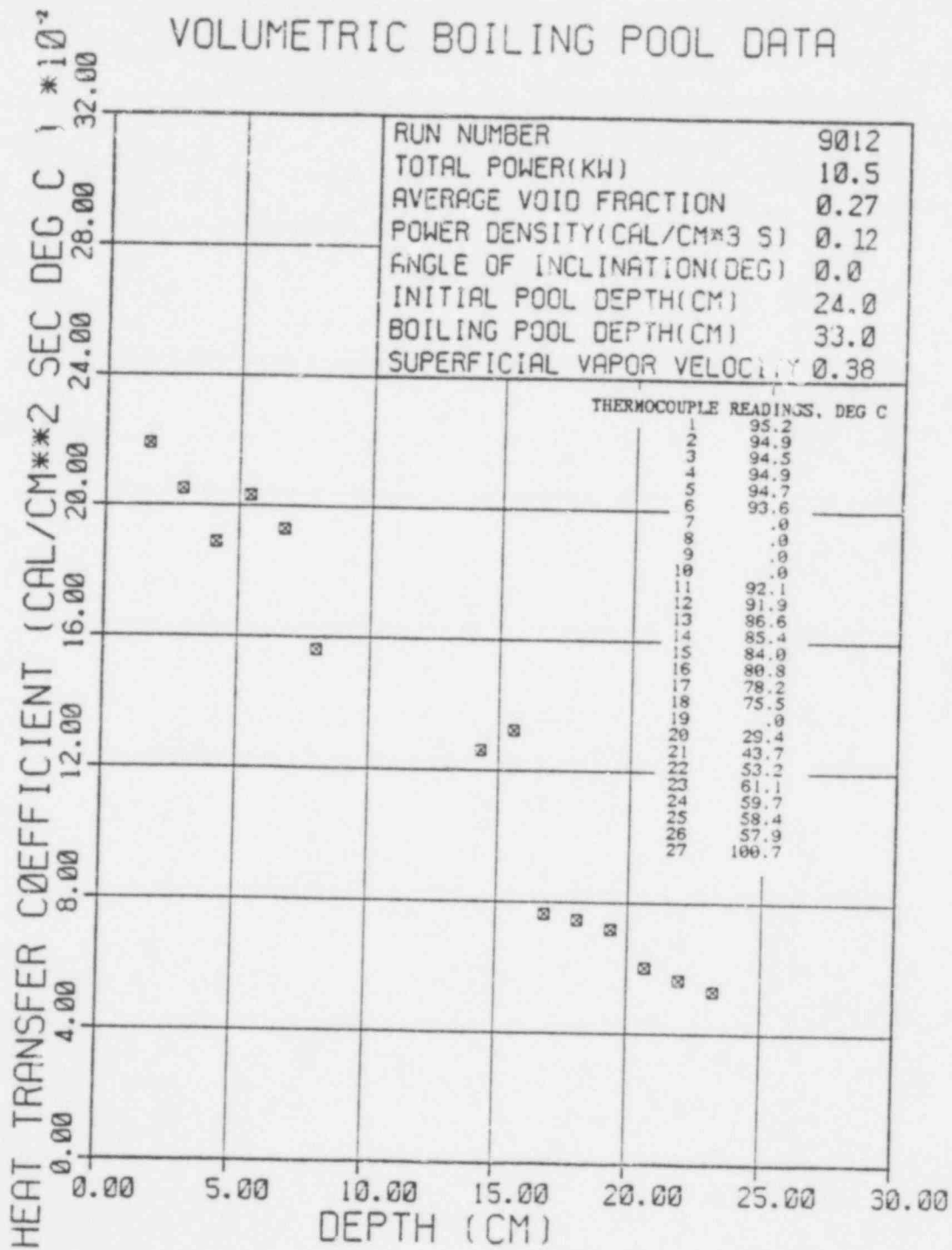
494 147

 RUN NUMBER ... 9012

AVERAGE VOID FRACTION..... .27
 INITIAL POOL DEPTH(CM)..... 24.0
 BOILING POOL DEPTH(CM)..... 33.0
 VOL. POWER DENS. (CAL/CM3 SEC) .12
 SUPERFICIAL VAPOR VELOCITY.... .38
 ANGLE OF INCLINATION(DEGREES) .00
 POOL VOLUME(CM**3)..... 14429.
 PRANDTL NUMBER..... 1.86
 TOTAL POWER(KW)..... 10.5
 AVERAGE SURFACE TEMP(DEG C) ... 89.8

DEPTH (CM)	LOCAL HEAT TRANSFER COEFF (CAL/CM2 SEC DEG C) EXPT EQ 14a EQ 10 EQ 10 N=1.0 N=0.7	MUSSELT NUMBER	MODIFIED RAYLEIGH NUMBER			
1.600	.2189	.0955	.0805	.1070	215.3	.2227E+09
2.870	.2050	.0825	.0663	.0874	361.7	.1285E+10
4.140	.1888	.0753	.0588	.0772	480.6	.3859E+10
5.410	.2032	.0704	.0529	.0705	675.6	.8610E+10
6.680	.1930	.0668	.0504	.0657	732.4	.1621E+11
7.950	.1561	.0640	.0477	.0620	762.9	.2732E+11
9.220		.0616	.0455	.0590		
10.49		.0597	.0437	.0565		
11.76		.0580	.0421	.0545		
13.03		.0565	.0408	.0527		
14.30	.1263	.0552	.0397	.0511	1109.8	.1500E+12
15.57	.0765	.0541	.0386	.0497	1266.3	.2053E+12
16.84	.0746	.0530	.0377	.0484	791.6	.2597E+12
18.11	.0718	.0521	.0369	.0473	830.7	.3230E+12
19.38	.0602	.0512	.0361	.0463	855.1	.3958E+12
20.65	.0563	.0504	.0354	.0453	764.0	.4788E+12
21.92	.0530	.0496	.0348	.0445	759.1	.5727E+12
23.19		.0489	.0342	.0437	754.8	.6781E+12
24.46		.0483	.0336	.0429		

VOLUMETRIC BOILING POOL DATA



494 149

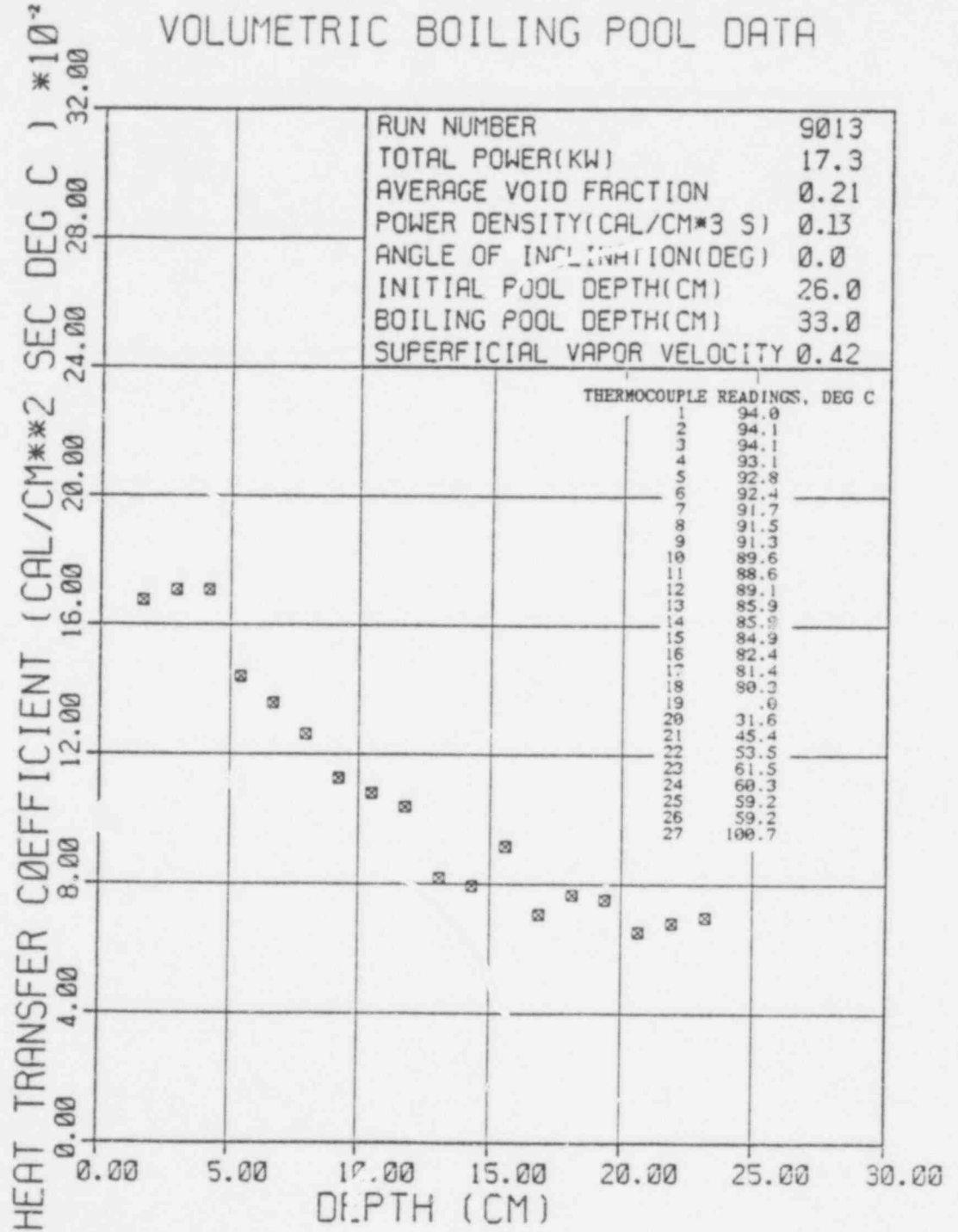
RUN NUMBER... 9013

AVERAGE VOID FRACTION..... .21
 INITIAL POOL DEPTH(CM)..... 26.0
 BOILING POOL DEPTH(CM)..... 33.0
 VOL. POWER DENS.(CAL/CM3 SEC). .13
 SUPERFICIAL VAPOR VELOCITY42
 ANGLE OF INCLINATION(DEGREES). .00
 POOL VOLUME(CM**3)..... 15631.
 PRANDTL NUMBER..... 1.87
 TOTAL POWER(KW)..... 17.3
 AVERAGE SURFACE TEMP(DEG C).... 89.1

DEPTH (CM)	LOCAL HEAT TRANSFER COEFF (CAL/CM2 SEC DEG C)		RUSSELL NUMBER	MODIFIED RAYLEIGH NUMBER
	EXPT EQ 14a	EQ 10 N=1.0 N=0.7		
1.600	.1677	.9896	.0788	.1051
2.870	.1707	.0774	.0645	.0856
4.140	.1707	.0706	.0571	.0755
5.410	.1440	.0661	.0523	.0689
6.680	.1358	.0627	.0488	.0641
7.950	.1263	.0600	.0462	.0604
9.220	.1136	.0578	.0440	.0575
10.49	.1081	.0560	.0422	.0551
11.76	.1037	.0544	.0407	.0530
13.03	.0817	.0530	.0394	.0512
14.30	.0794	.0518	.0383	.0497
15.57	.0917	.0507	.0373	.0483
16.84	.0707	.0497	.0364	.0471
18.11	.0766	.0488	.0355	.0459
19.38	.0752	.0480	.0348	.0449
20.65	.0653	.0473	.0341	.0440
21.92	.0679	.0466	.0335	.0432
23.19	.0698	.0459	.0329	.0424
24.46		.0453	.0324	.0416

494 150

VOLUMETRIC BOILING POOL DATA



RUN NUMBER... 7501

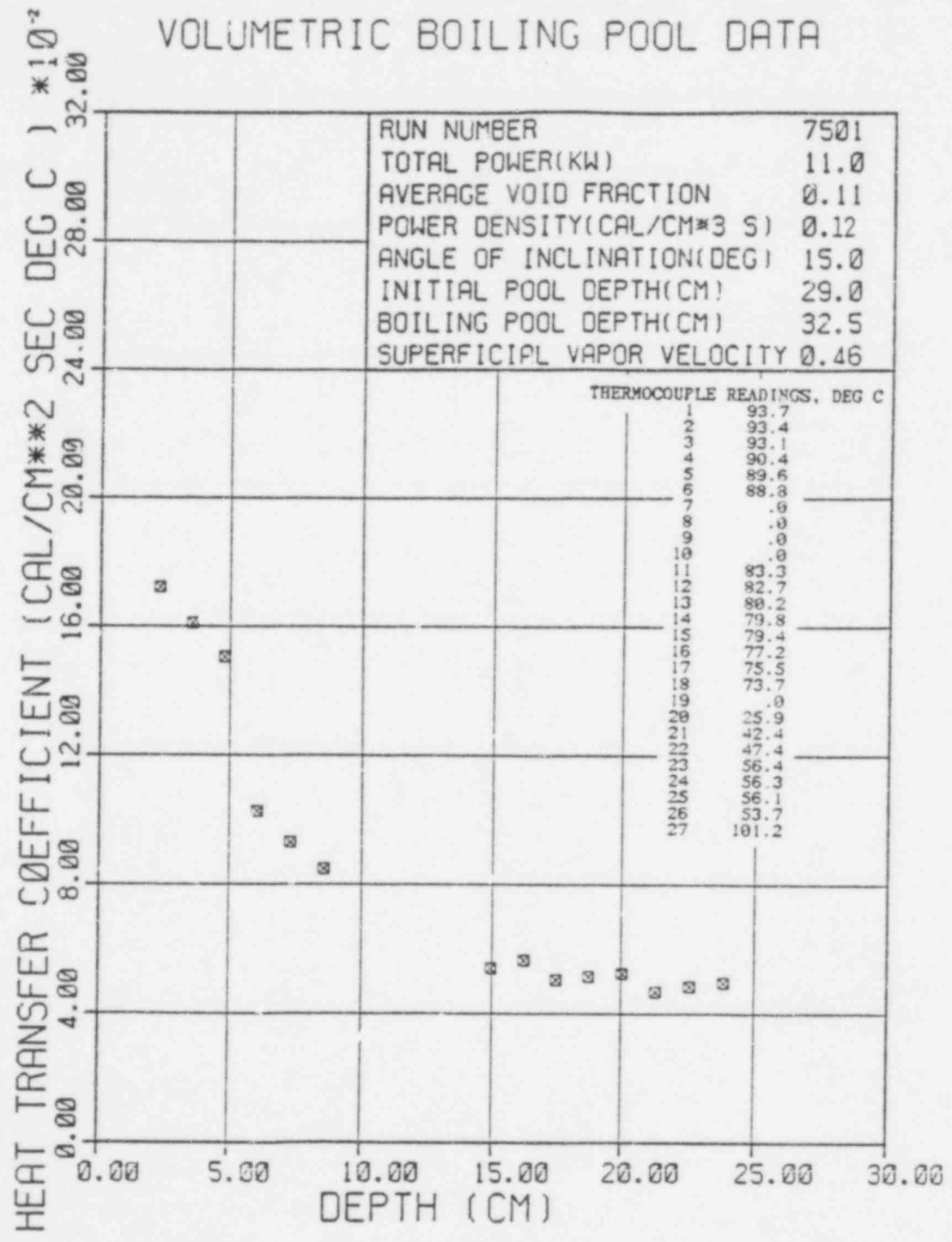
AVERAGE VOID FRACTION..... .11
 INITIAL POOL DEPTH(CM)..... 29.0
 BOILING POOL DEPTH(CM)..... 32.5
 VOL. POWER DENS. (CAL/CM3 SEC). .12
 SUPERFICIAL VAPOR VELOCITY.... .46
 ANGLE OF INCLINATION(DEGREES). 15.00
 POOL VOLUME(CM**3)..... 19463.
 PRANDTL NUMBER..... 1.91
 TOTAL POWER(KW)..... 11.0
 AVERAGE SURFACE TEMP(DEG C)... 84.7

-106-

494
152

DEPTH (CM)	LOCAL HEAT TRANSFER COEFF (CAL/CM2 SEC DEG C)				NUSSLETT NUMBER	MODIFIED RAYLEIGH NUMBER
	EXPT	EQ 14a	EQ 10 N=1.0	EQ 10 N=0.7		
2.246	.1722	.0691	.0636	.0853	238.0	.2302E+09
3.516	.1610	.0618	.0544	.0727	348.4	.8829E+09
4.786	.1507	.0572	.0489	.0652	443.8	.2227E+10
6.056	.1025	.0539	.0452	.0600	382.1	.4511E+10
7.326	.0930	.0514	.0424	.0562	419.5	.7985E+10
8.596	.0848	.0494	.0402	.0532	448.5	.1290E+11
9.866		.0477	.0384	.0507		
11.14		.0463	.0369	.0486		
12.41		.0451	.0356	.0469		
13.68		.0440	.0345	.0453		
14.95	.0539	.0430	.0335	.0440	496.0	.6780E+11
16.22	.0564	.0421	.0326	.0428	562.5	.8659E+11
17.49	.0504	.0414	.0318	.0417	542.6	.1086E+12
18.76	.0514	.0406	.0311	.0407	593.2	.340E+12
20.03	.0523	.0400	.0304	.0398	644.9	.1631E+12
21.30	.0468	.0394	.0298	.0390	613.5	.1961E+12
22.57	.0485	.0388	.0293	.0383	673.4	.2333E+12
23.84	.0497	.0383	.0288	.0376	728.4	.2750E+12
25.11		.0378	.0283	.0369		

VOLUMETRIC BOILING POOL DATA



494 153

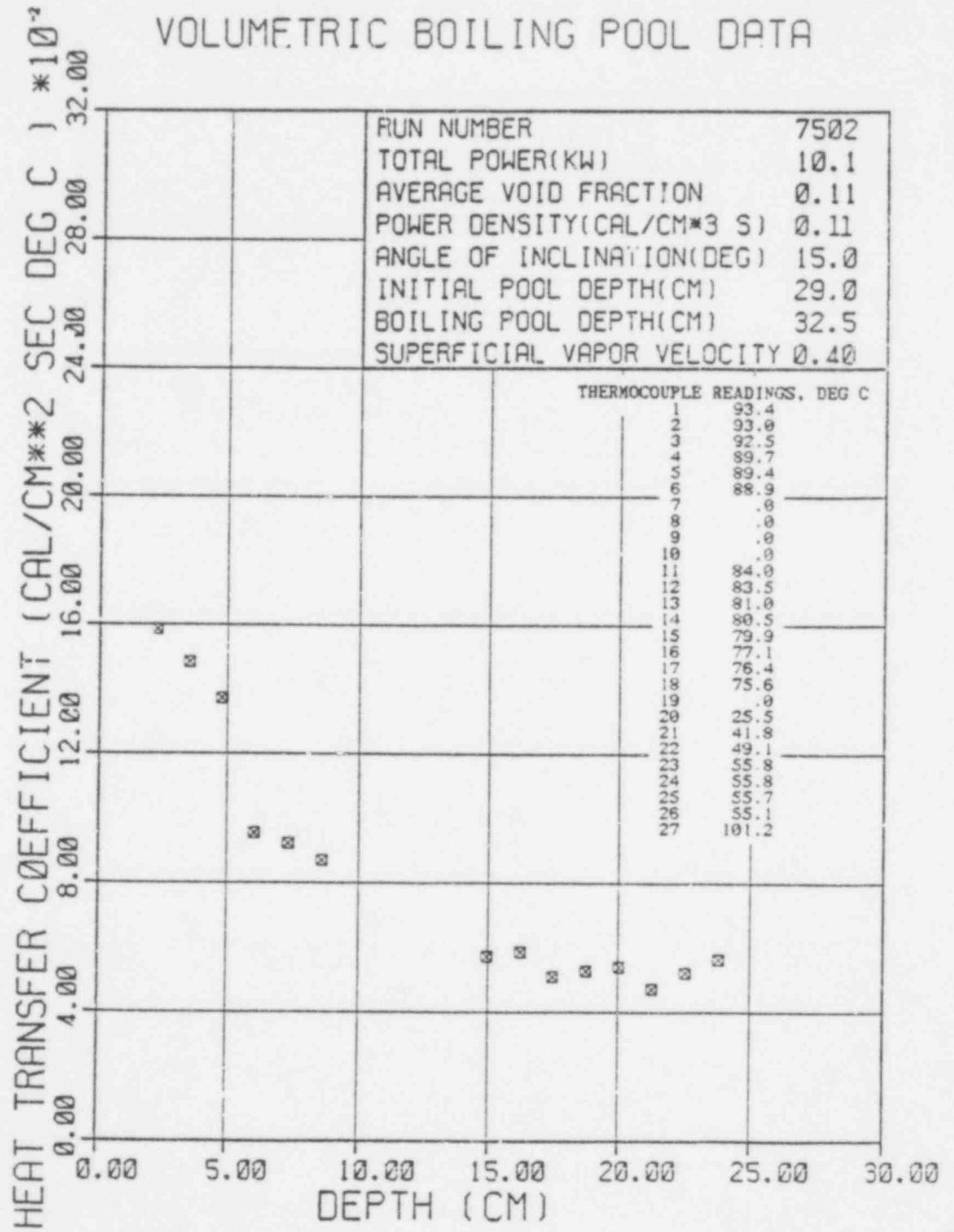
 RUN NUMBER... 7562

AVERAGE VOID FRACTION..... .11
 INITIAL POOL DEPTH(CM)..... 29.0
 BOILING POOL DEPTH(CM)..... 32.5
 VOL. FOWER DENS. (CAL/CM3 SEC) . .11
 SUPERFICIAL VAPOR VELOCITY..... .40
 ANGLE OF INCLINATION(DEGREES) . 15.00
 POOL VOLUME(CM**3)..... 19463.
 PRANDTL NUMBER..... 1.91
 TOTAL POWER(KW)..... 10.1
 AVERAGE SURFACE TEMPP(BEL C).... 85.0

DEPTH (CM)	LOCAL HEAT TRANSFER COEFF (CAL/CM2 SEC DEG C)		NUSSELT NUMBER	MODIFIED RAYLEIGH NUMBER
	EXPT	EQ 14a		
2.246	.1585	.0619	219.1	.2305E+09
3.516	.1484	.0530	321.2	.8842E+09
4.786	.1373	.0572	404.4	.2230E+10
6.056	.0954	.0539	355.7	.4517E+10
7.326	.0921	.0514	415.2	.7997E+10
8.596	.0876	.0494	460.0	.1292E+11
9.866		.0477		
11.14		.0463		
12.41		.0451		
13.68		.0440		
14.95	.0571	.0430		
16.22	.0587	.0422		
17.49	.0510	.0414	525.4	.6790E+11
18.76	.0528	.0407	585.4	.8672E+11
20.03	.0541	.0400	548.6	.1087E+12
21.30	.0473	.0394	609.0	.1342E+12
22.57	.0521	.0388	666.2	.1633E+12
23.84	.0563	.0383	619.7	.1964E+12
25.11		.0378	723.6	.2337E+12
			826.2	.2754E+12

494 154

VOLUMETRIC BOILING POOL DATA



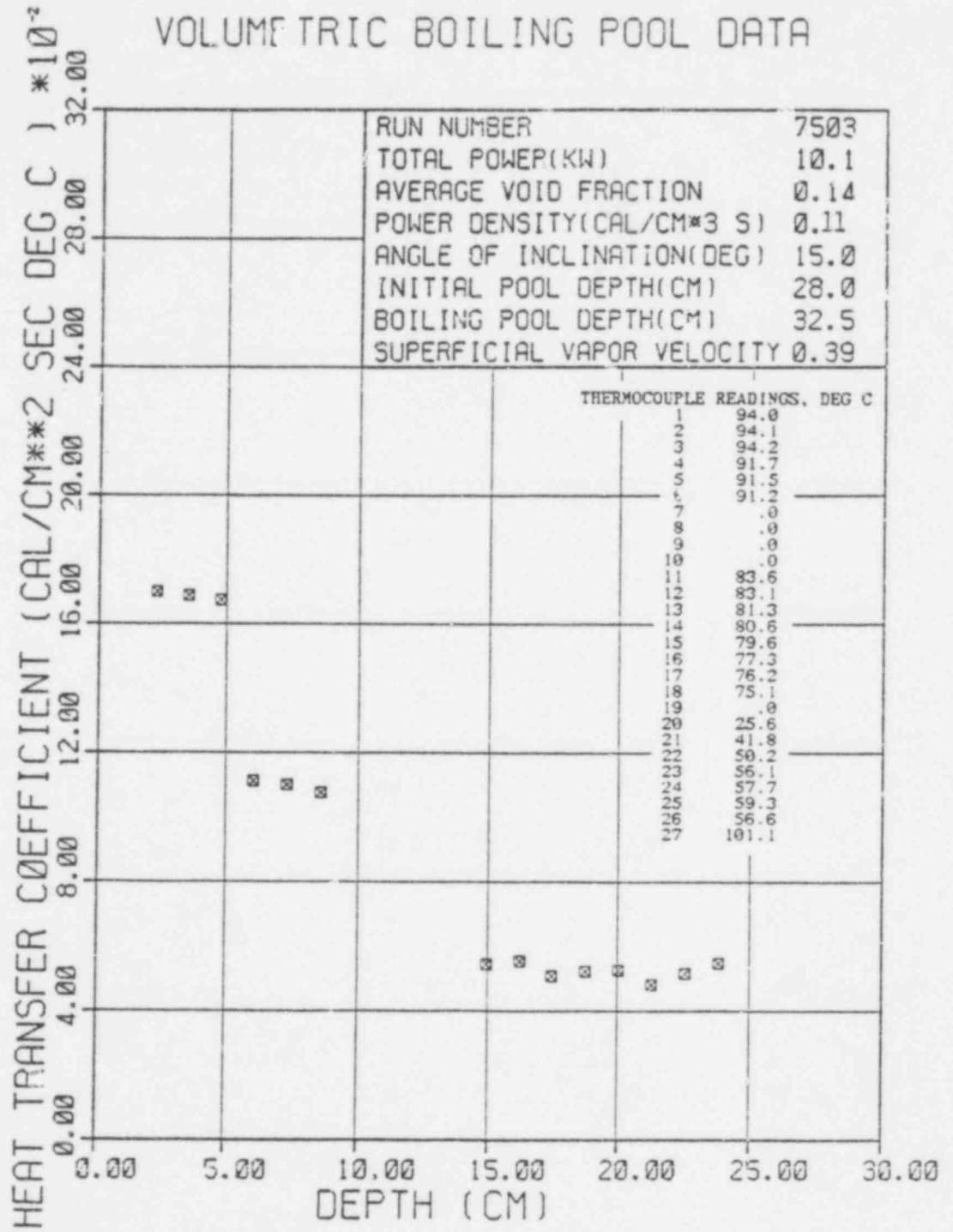
RUN NUMBER... 7503

AVERAGE VOID FRACTION..... .14
 INITIAL POOL DEPTH(CM)..... 28.0
 BOILING POOL DEPTH(CM)..... 32.5
 VOL. POWER DENS.(CAL/CM3 SEC) .11
 SUPERFICIAL VAPOR VELOCITY.... .39
 ANGLE OF INCLINATION(DEGREES). 15.00
 POOL VOLUME(CM*3)..... 18724.
 PRANDTL NUMBER..... 1.90
 TOTAL POWER(KW)..... 10.1
 AVERAGE SURFACE TEMP(DEG C)... 85.7

DEPTH (CM)	LOCAL HEAT TRANSFER COEFF (CAL/CM2 SEC DEG C)		NUSSELT NUMBER	MODIFIED RAYLEIGH NUMBER
	EXPT	EQ 14a		
2.246	.1701	.0737	.0641	.0855
3.516	.1688	.0659	.0550	.0731
4.786	.1675	.0610	.0496	.0656
6.056	.1113	.0575	.0459	.0605
7.326	.1101	.0548	.0431	.0567
8.596	.1075	.0527	.0409	.0537
9.866		.0509	.0391	.0513
11.14		.0494	.0376	.0492
12.41		.0481	.0363	.0475
13.68		.0469	.0352	.0459
14.95		.0459	.0342	.0446
16.22	.0555	.0449	.0333	.0434
17.49	.0507	.0441	.0326	.0423
18.76	.0523	.0431	.0318	.0413
20.03	.0526	.0426	.0312	.0405
21.30	.0482	.0420	.0306	.0396
22.57	.0516	.0414	.0300	.0389
23.84	.0548	.0408	.0295	.0382
25.11		.0403	.0291	.0375

494 156

VOLUMETRIC BOILING POOL DATA



494 157

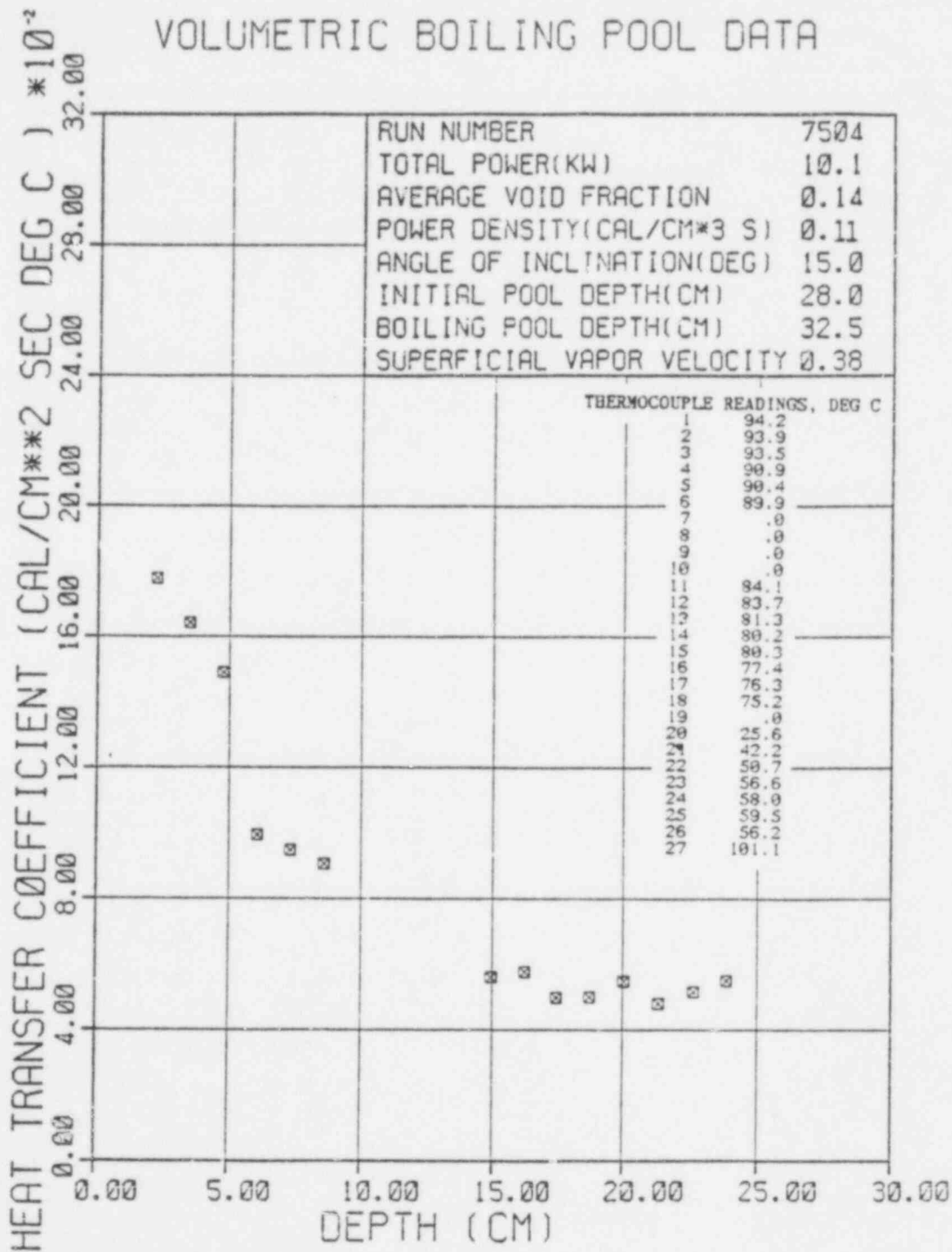
 RUN NUMBER... 7504

AVERAGE VOID FRACTION..... .14
 INITIAL POOL DEPTH(CM)..... 23.0
 BOILING POOL DEPTH(CM)..... 32.5
 VOL. POWER DENS. (CAL/CM3 SEC) .11
 SUPERFICIAL VAPOR VELOCITY.... .38
 ANGLE OF INCLINATION(DEGREES) . 15.00
 POOL VOLUME(CM**3)..... 18724.
 PRANDTL NUMBER..... 1.90
 TOTAL POWER(KW)..... 10.1
 AVERAGE SURFACE TEMP(DEG C).... 85.5

DEPTH (CM)	LOCAL HEAT TRANSFER COEFF (CAL/CM2 SEC DEG C)	NUSSELT NUMBER	MODIFIED RAYLEIGH NUMBER
2.246	.1778	245.7	.2970E+09
3.516	.1641	355.1	.1139E+10
4.786	.1491	439.1	.2872E+10
6.056	.0994	370.3	.5819E+10
7.326	.6947	427.1	.1030E+11
8.596	.0905	478.7	.1664E+11
9.866			
11.14			
12.41			
13.68			
14.95			
16.22	.0560	514.6	.8746E+11
17.49	.0576	574.5	.1117E+12
18.76	.0499	536.8	.1401E+12
20.03	.0499	576.4	.1728E+12
21.30	.0547	674.5	.2104E+12
22.57	.0479	628.3	.2530E+12
23.84	.0516	716.3	.3010E+12
25.11	.0549	805.6	.3548E+12

494 158

VOLUMETRIC BOILING POOL DATA



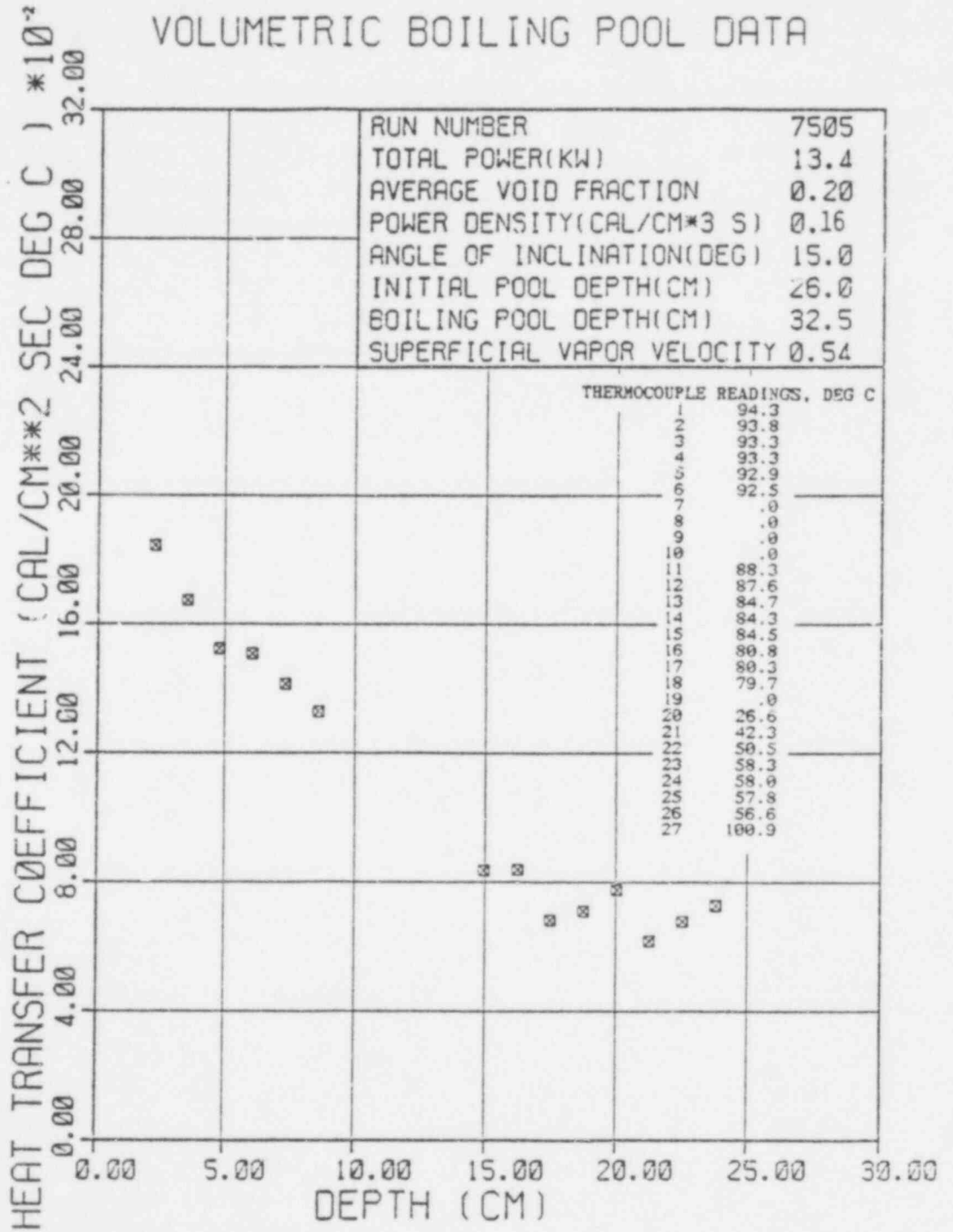
RUN NUMBER... 7505

AVERAGE VOID FRACTION..... .20
 INITIAL POOL DEPTH(CM)..... 26.0
 BOILING POOL DEPTH(CM)..... 32.5
 VOL. POWER DENS. (CAL/CM³ SEC) .16
 SUPERFICIAL VAPOE VELOCITY.... .54
 ANGLE OF INCLINATION(DEGREES). 15.00
 POOL VOLUME(CM**3)..... 17261.
 FRANDTL NUMBER..... 1.87
 TOTAL POWER(KW)..... 13.44
 AVERAGE SURFACE TEMP(DEG C)... 88.5

DEPTH (CM)	LOCAL HEAT TRANSFER COEFF (CAL/CM ² SEC DEG C)		NUSSELT NUMBER	MODIFIED RAYLEIGH NUMBER
	EXPT	EQ 14a N=1.0		
2.246	.1844	.0811	.0724	.0969
3.516	.1673	.0725	.0620	.0827
4.786	.1525	.0671	.0559	.0742
6.056	.1508	.0633	.0516	.0684
7.326	.1414	.0603	.0485	.0640
8.596	.1328	.0579	.0460	.0606
9.866		.0566	.0439	.0578
11.14		.0543	.0422	.0555
12.41		.0529	.0408	.0535
13.68		.0516	.0395	.0518
14.95	.0835	.0505	.0384	.0502
16.22	.0837	.0494	.0374	.0489
17.49	.0682	.0485	.0365	.0477
18.76	.0710	.0477	.0357	.0466
20.03	.0777	.0469	.0350	.0455
21.30	.0618	.0462	.0343	.0446
22.57	.0678	.0455	.0337	.0438
23.84	.0729	.0449	.0331	.0430
25.11		.0443	.0325	.0422
			254.7	.4345E+09
			361.8	.1667E+10
			448.8	.4203E+10
			561.6	.8514E+10
			636.9	.1507E+11
			702.2	.2435E+11
			767.6	.1280E+12
			835.0	.1634E+12
			732.8	.2049E+12
			819.4	.2579E+12
			956.6	.3078E+12
			809.7	.3702E+12
			940.1	.4404E+12
			1068.3	.5191E+12

494 160

VOLUMETRIC BOILING POOL DATA



494 161

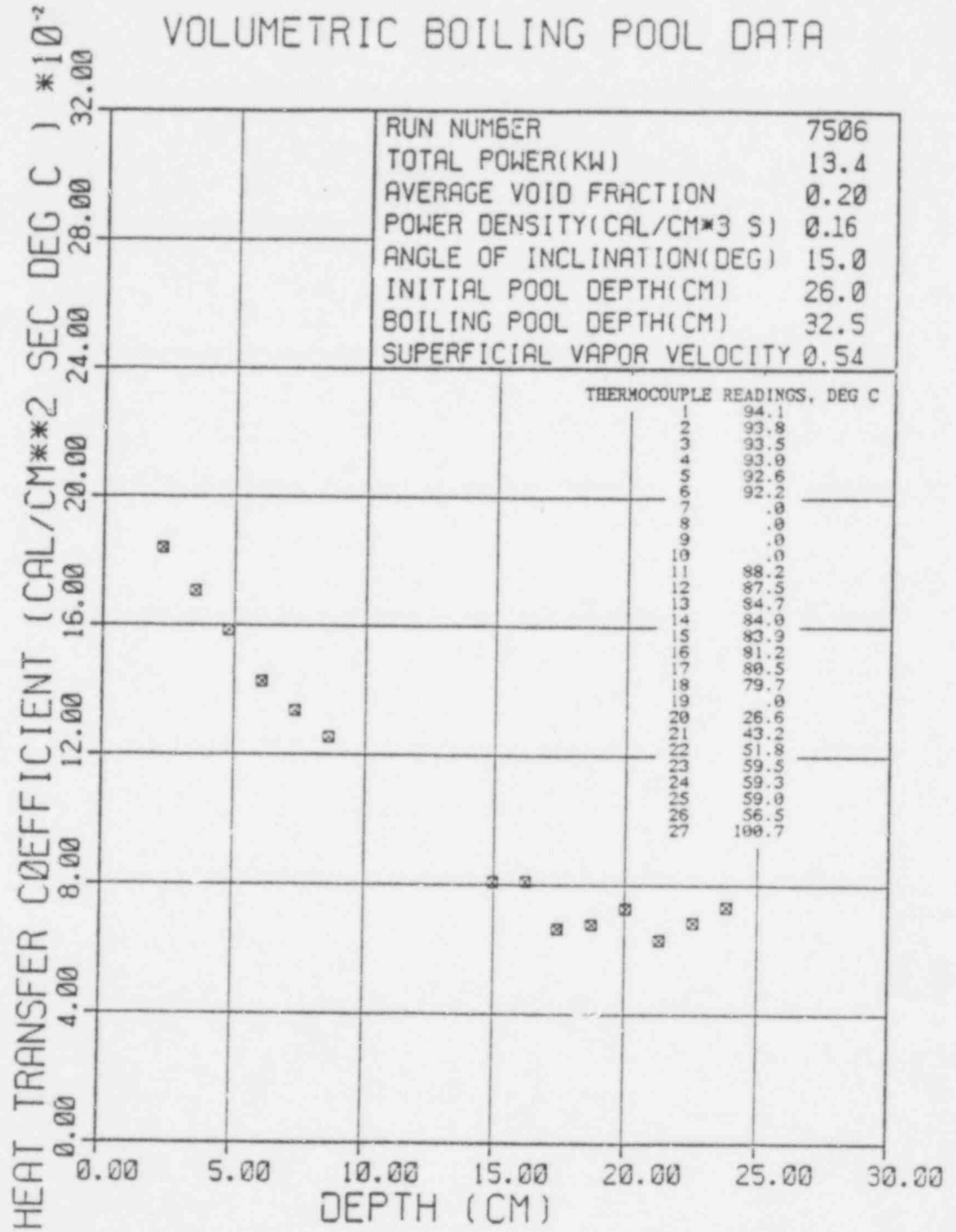
RUN NUMBER... 7506

AVERAGE VOID FRACTION..... .20
 INITIAL POOL DEPTH(CM)..... 26.0
 BOILING POOL DEPTH(CM)..... 32.5
 VOL. POWER DENS. (CAL/CM3 SEC) .16
 SUPERFICIAL VAPOR VELOCITY..... .54
 ANGLE OF INCLINATION(DEGREES) . 15.00
 COOL VOLUME(CM**3)..... 17261.
 PRANDTL NUMBER..... 1.88
 TOTAL POWER(KW)..... 13.44
 AVERAGE SURFACE TEMP(DEG C).... 88.4

DEPTH (CM)	LOCAL HEAT TRANSFER COEFF (CAL/CM2 SEC DEG C)	MUSSELT NUMBER	MODIFIED RAYLEIGH NUMBER			
2-246	.1839	.0810	.0724	.0968	254.1	.4339E+09
3-516	.1766	.0724	.0629	.0826	368.9	.1664E+10
4-786	.1584	.0671	.0558	.0742	466.3	.4197E+10
6-056	.1426	.0632	.0516	.0684	530.9	.8503E+10
7-326	.1335	.0603	.0484	.0640	601.5	.1505E+11
8-596	.1253	.0579	.0459	.0606	652.5	.2431E+11
9-866		.0560	.0439	.0578		
11-14		.0543	.0422	.0555		
12-41		.0528	.0408	.0535		
13-68		.0516	.0395	.0517		
14-95	.0808	.0504	.0384	.0502		
16-22	.0810	.0494	.0374	.0489	742.2	.1278E+12
17-49	.0674	.0485	.0365	.0476	808.0	.1632E+12
18-76	.0678	.0477	.0357	.0465	713.8	.2046E+12
20-03	.0727	.0469	.0349	.0455	781.8	.2526E+12
21-30	.0629	.0462	.0343	.0446	895.3	.3074E+12
22-57	.0685	.0455	.0336	.0438	823.8	.3697E+12
23-84	.0731	.0449	.0331	.0430	949.9	.4398E+12
25-11		.0443	.0325	.0422	1071.8	.5184E+12

494 162

VOLUMETRIC BOILING POOL DATA



494 163

RUN NUMBER... 7507

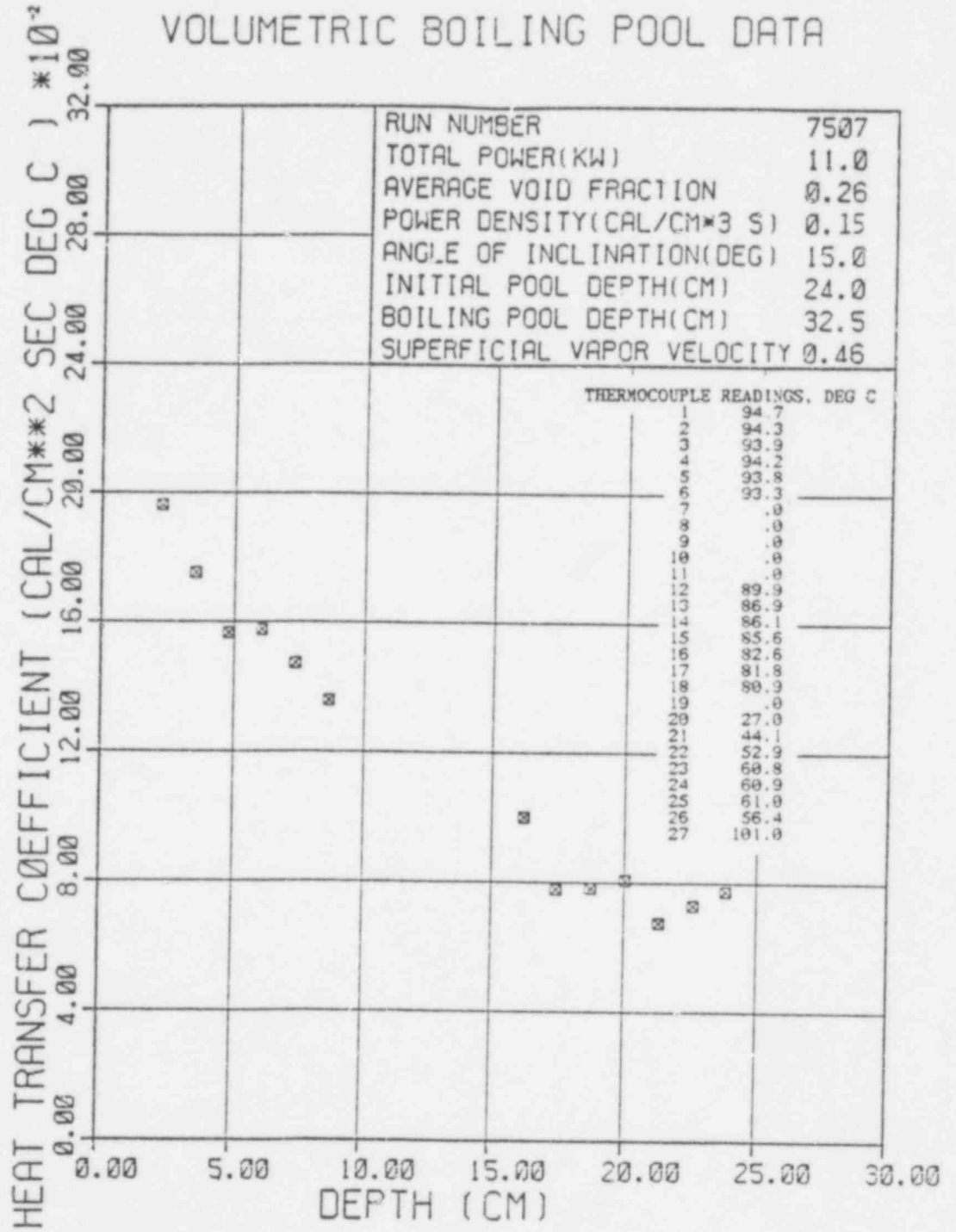
AVERAGE VOID FRACTION..... .26
 INITIAL POOL DEPTH(CM)..... 24.0
 BOILING POOL DEPTH(CM)..... 32.5
 VOL. POWER DENS. (CAL/CM3 SEC). .15
 SUPERFICIAL VAPOR VELOCITY.... .46
 ANGLE OF INCLINATION(DEGREES). 15.00
 POOL VOLUME(CM**3)..... 15818.
 PRANDTL NUMBER..... 1.86
 TOTAL POWER(KW)..... 11.0
 AVERAGE SURFACE TEMP(DEG C)... 89.8

DEPTH (CM)	LOCAL HEAT TRANSFER COEFF (CAL/CM2 SEC DEG C)				NUSSLETT NUMBER	MODIFIED RAYLEIGH NUMBER
	EXPT	EQ 14a	EQ 10 N=1.0	EQ 10 N=0.7		
2.246	.1963	.0868	.0734	.0976	271.0	.5718E+09
3.516	.1752	.0776	.0631	.0836	378.7	.2193E+10
4.786	.1566	.0719	.0570	.0751	460.6	.5531E+10
6.056	.1576	.0678	.0528	.0694	586.8	.1121E+11
7.326	.1472	.0646	.0496	.0650	663.0	.1984E+11
8.596	.1357	.0621	.0471	.0616	717.0	.3204E+11
9.866		.0600	.0451	.0588		
11.14		.0582	.0434	.0565		
12.41		.0566	.0419	.0545		
13.68		.0553	.0406	.0528		
14.95		.0541	.0395	.0512		
16.22	.1000	.0530	.0385	.0499	996.3	
17.49	.0778	.0520	.0376	.0486	836.7	.2697E+12
18.76	.0783	.0511	.0368	.0475	902.6	.3328E+12
20.03	.0808	.0503	.0360	.0465	995.2	.4051E+12
21.30	.0675	.0495	.0354	.0456	884.2	.4872E+12
22.57	.0730	.0488	.0347	.0447	1012.2	.5796E+12
23.84	.0774	.0481	.0342	.0439	1134.2	.6831E+12
25.11		.0475	.0336	.0432		

-118-

494 164

VOLUMETRIC BOILING POOL DATA



494 165

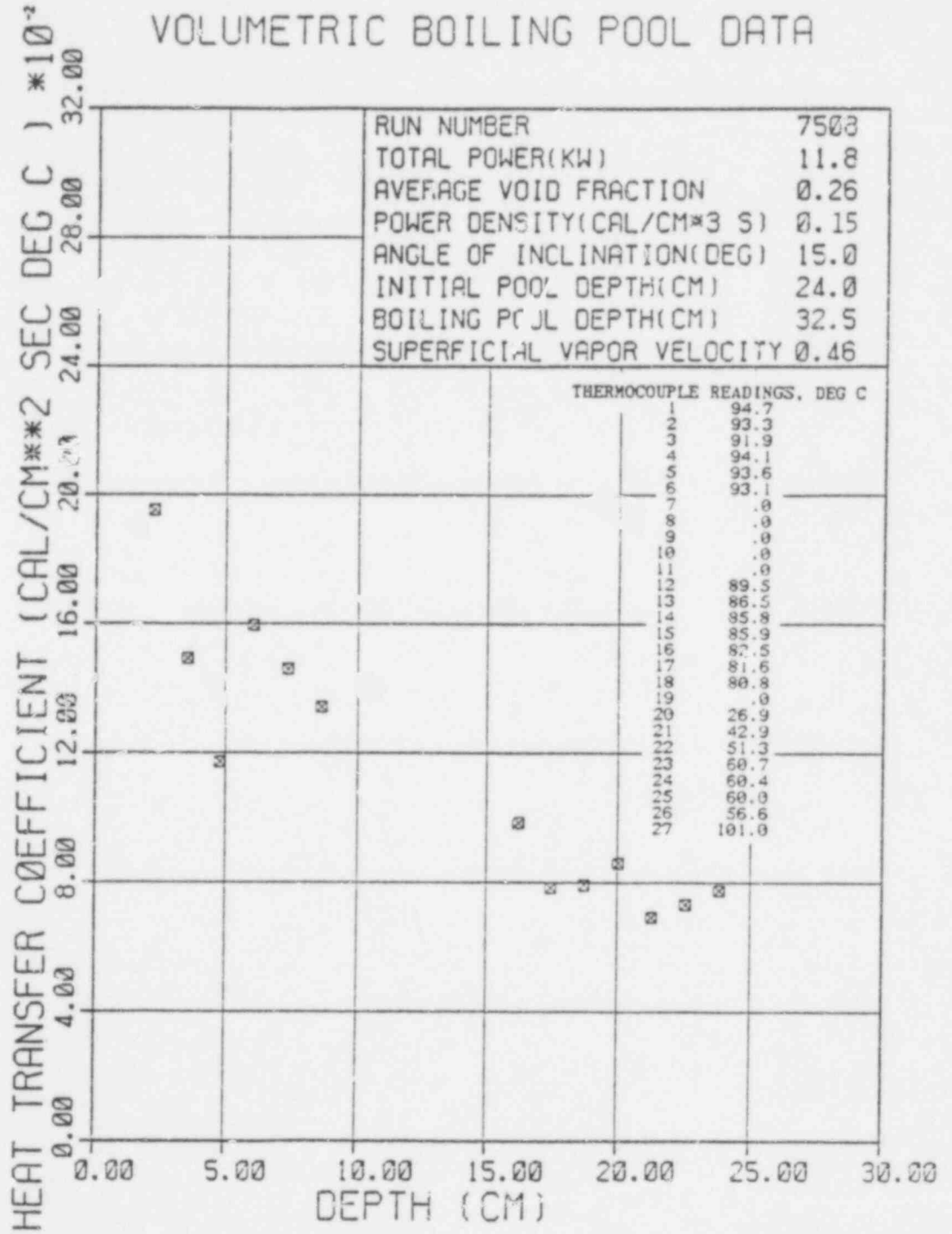
RUN NUMBER... 7508

AVERAGE VOID FRACTION..... .26
 INITIAL POOL DEPTH(CM)..... 24.0
 BOILING POOL DEPTH(CM)..... 32.5
 VOL. POWER DENS.(CAL/CM3 SEC). .15
 SUPERFICIAL VAPOR VELOCITY..... .46
 ANGLE OF INCLINATION(DEGREES). 15.00
 POOL VOLUME(CM**3)..... 15818.
 PRANDTL NUMBER..... 1.87
 TOTAL POWER(KW)..... 7.8
 AVERAGE SURFACE TEMP(DEG C).... 89.4

DEPTH (CM)	LOCAL HEAT TRANSFER COEFF (CAL/CM2 SFC DEG C)	EXPT EQ 14a	EQ 10	EQ 10	NUSSELT NUMBER	MODIFIED RAYLEIGH NUMBER
		N=1.0	N=0.7			
2.246	.0868	.0733	.0976	269.6	.5708E+09	
3.516	.0776	.0631	.0835	322.3	.2189E+10	
4.786	.0718	.0570	.0751	344.8	.5521E+10	
6.056	.0595	.0677	.0693	594.0	.1118E+11	
7.326	.0646	.0496	.0650	657.5	.1980E+11	
8.596	.0621	.0471	.0616	709.0	.3198E+11	
9.866	.0600	.0450	.0588			
11.14	.0582	.0433	.0565			
12.41	.0566	.0419	.0545			
13.68	.0553	.0406	.0527			
14.95	.0540	.0395	.0512			
16.22	.0530	.0385	.0498	981.3		
17.49	.0520	.0376	.0486	842.4		
18.76	.0792	.0511	.0368	913.4		
20.03	.0859	.0502	.0360	1058.0		
21.30	.0691	.0495	.0353	904.7		
22.57	.0733	.0488	.0347	1016.5		
23.84	.0776	.0481	.0341	1137.3		
25.11	.0475	.0336	.0432			

494 166

VOLUMETRIC BOILING POOL DATA



494 107

RUN NUMBER... 7509

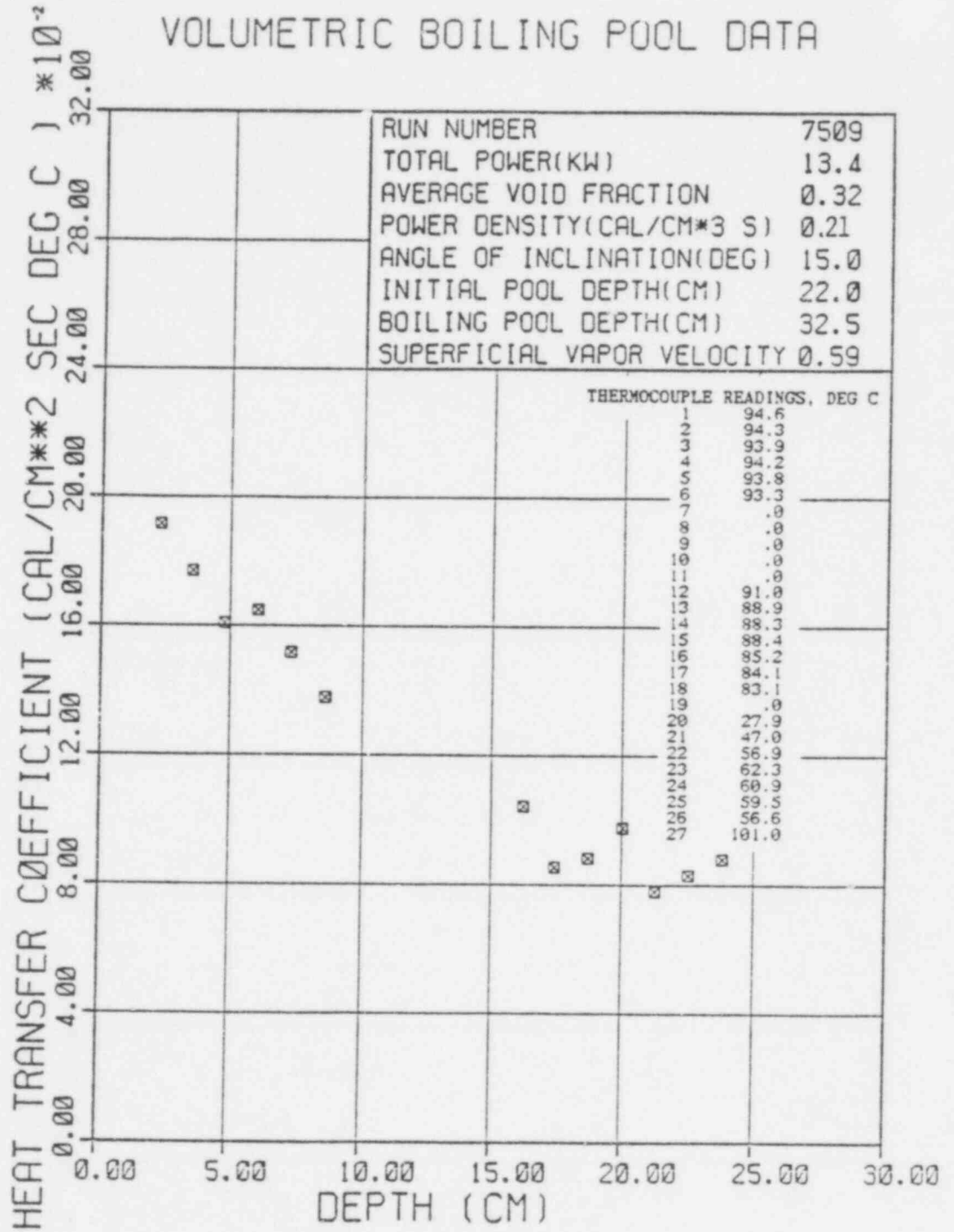
AVERAGE VOID FRACTION..... .32
 INITIAL POOL DEPTH(CM)..... 22.0
 BOILING POOL DEPTH(CM)..... 32.5
 VOL. POWER DENS. (CAL/CM3 SEC). .21
 SUPERFICIAL VAPOR VELOCITY.... .59
 ANGLE OF INCLINATION(DEGREES). 15.00
 POOL VOLUME(CM**3)..... 14394.
 PRANDTL NUMBER..... 1.85
 TOTAL POWER(KW)..... 13.44
 AVERAGE SURFACE TEMP(DEG C)... 90.8

(CM)	LOCAL HEAT TRANSFER COEFF (CAL/CM2 SEC DEG C)				NUSSELT NUMBER	MODIFIED RAYLEIGH NUMBER
	EXPT	EQ 14a	EQ 10 N=1.0	EQ 10 N=0.7		
2.246	.1917	.0917	.0795	.1061	264.6	.7096E+09
3.516	.1770	.0820	.0683	.0907	382.5	.2722E+10
4.756	.1608	.0759	.0616	.0815	473.0	.6863E+10
6.056	.1647	.0715	.0569	.0751	613.1	.1390E+11
7.326	.1517	.0682	.0535	.0704	683.0	.2461E+11
8.596	.1378	.0655	.0508	.0667	727.9	.3976E+11
9.866		.0633	.0486	.0636		
11.14		.0614	.0467	.0611		
12.41		.0598	.0451	.0589		
13.68		.0584	.0437	.0570		
14.95		.0571	.0425	.0554		
16.22	.1043	.0559	.0414	.0539	1039.1	.2669E+12
17.49	.0854	.0549	.0404	.0525	917.4	.3347E+12
18.76	.0882	.0539	.0395	.0513	1016.7	.4130E+12
20.03	.0976	.0531	.0387	.0502	1201.3	.5027E+12
21.30	.0781	.0522	.0380	.0492	1021.5	.6045E+12
22.57	.0830	.0515	.0373	.0483	1151.4	.7193E+12
23.84	.0881	.0508	.0367	.0474	1290.1	.8477E+12
25.11		.0501	.0361	.0466		

-122-

494
168

VOLUMETRIC BOILING POOL DATA



494 169

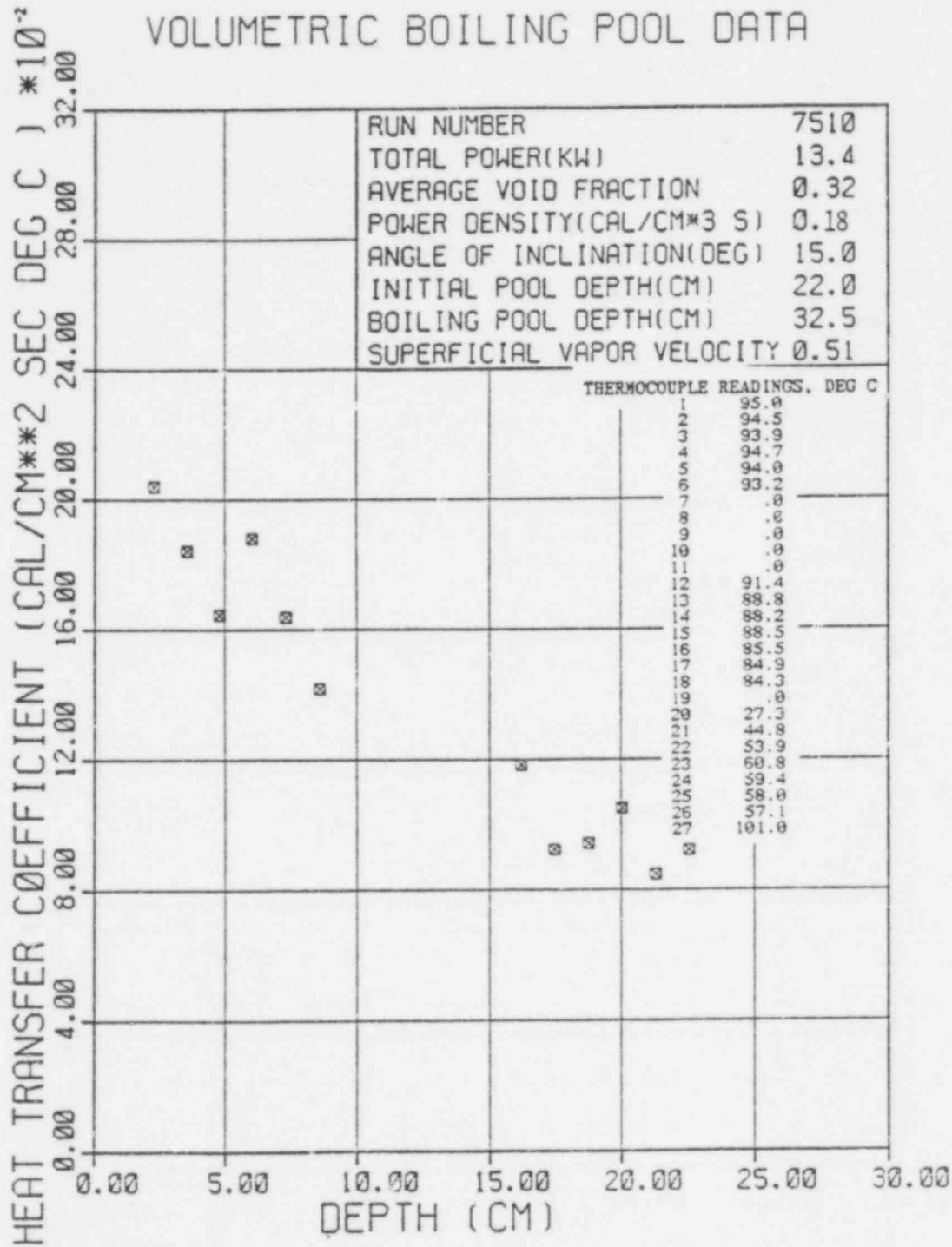
RUN NUMBER... 7510

AVERAGE VOID FRACTION..... .32
 INITIAL POOL DEPTH(CM)..... 22.0
 BOILING POOL DEPTH(CM)..... 32.5
 VOL. POWER DENS.(CAL/CM3 SEC). .18
 SUPERFICIAL VAPOR VELOCITY.... .51
 ANGLE OF INCLINATION(DEGREES). 15.00
 POOL VOLUME(CM*3)..... 14394.
 PRANDTL NUMBER..... 1.85
 TOTAL POWER(KW)..... 13.44
 AVERAGE SURFACE TEMP(DEG C) ... 91.1

DEPTH (CM)	LOCAL HEAT TRANSFER COEFF (CAL/CM2 SEC DEG C) EQ 10 EQ 10 EQ 10 EXPT EQ 10a N=1.0 N=0.7	NUSSLETT NUMBER	MODIFIED RAYLEIGH NUMBER
2.246	.2039 .0917 .0775 .1030	281.5	.7105E+09
3.516	.1843 .0820 .0666 .0882	398.2	.2725E+10
4.786	.1646 .0759 .0601 .0793	484.1	.6873E+10
6.056	.1881 .0716 .0557 .0732	699.9	.1392E+11
7.326	.1639 .0682 .0523 .0686	737.8	.2465E+11
8.596	.1418 .0656 .0497 .0650	749.2	.3981E+11
9.866	.0634 .0476 .0621		
11.14	.0615 .0458 .0596		
12.41	.0598 .0442 .0575		
13.68	.0584 .0429 .0557		
14.95	.0571 .0417 .0541		
16.22	.1184 .0560 .0406 .0526	1179.5	.2673E+12
17.49	.0924 .0549 .0397 .0513	992.3	.3351E+12
18.76	.0942 .0540 .0388 .0502	1085.2	.4136E+12
20.03	.1050 .0531 .0381 .0491	1292.4	.5034E+12
21.30	.0848 .0523 .0373 .0481	1109.3	.6054E+12
22.57	.0921 .0515 .0367 .0472	1277.2	.7202E+12
23.84	.0989 .0508 .0361 .0464	1448.7	.8488E+12
25.11	.0502 .0355		

494 170

VOLUMETRIC BOILING POOL DATA



494 171

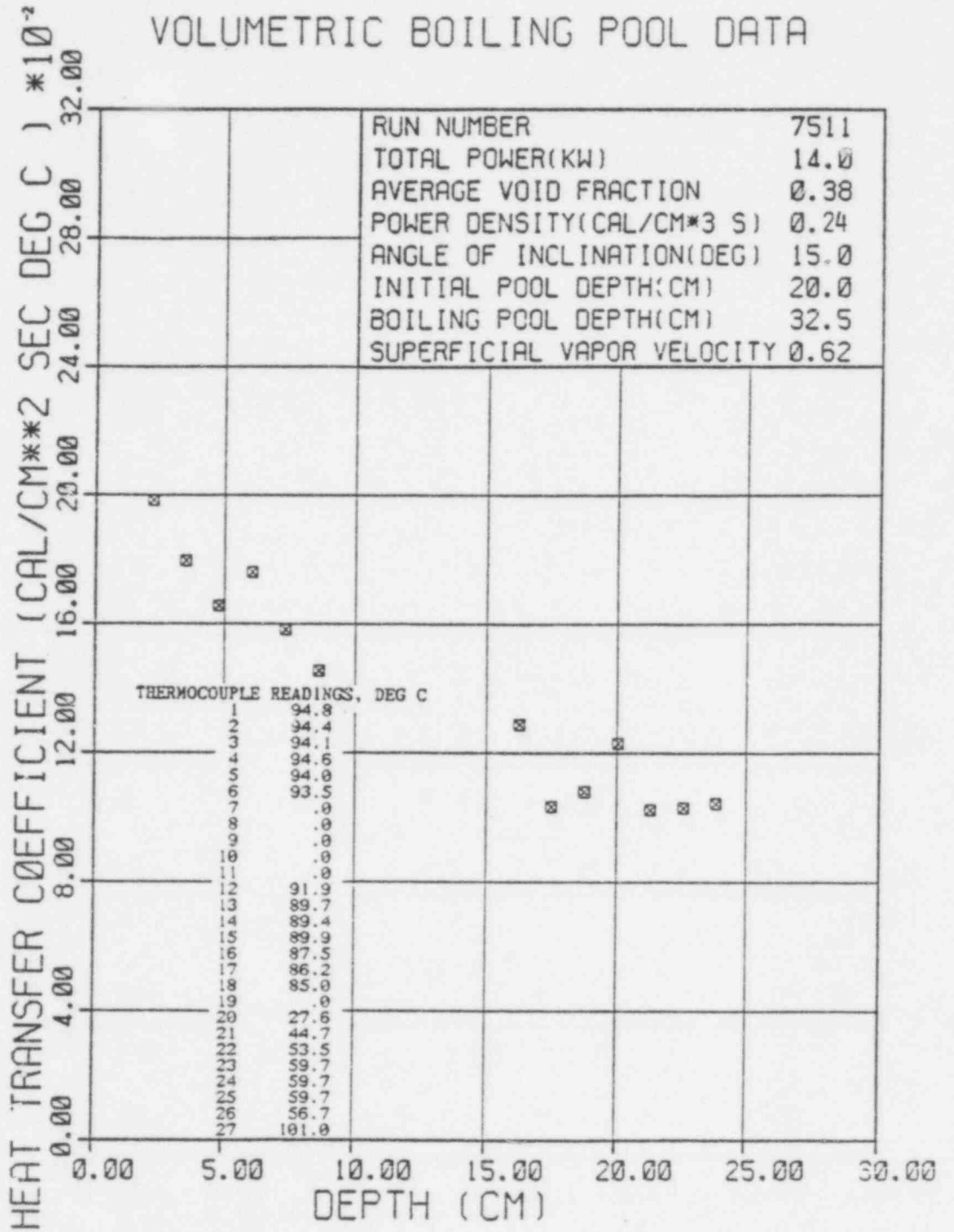
 RUN NUMBER... 7511

AVERAGE VOID FRACTION..... .38
 INITIAL POOL DEPTH(CM)..... 20.0
 BOILING POOL DEPTH(CM)..... 32.5
 VOL. POWER DENS. (CAL/CM3 SEC) .24
 SUPERFICIAL VAPOR VELOCITY..... .62
 ANGLE OF INCLINATION (DEGREES) . 15.00
 POOL VOLUME(CM**3)..... 12989.
 PRANDTL NUMBER..... 1.84
 TOTAL POWER(KW)..... 14.0
 AVERAGE SURFACE TEMP(DEG C)... 91.7

DEPTH (CM)	LOCAL HEAT TRANSFER COEFF (CAL/CM2 SEC DEG C)		NUSSELT NUMBER	MODIFIED RAYLEIGH NUMBER
	EXPT EQ 14a	EQ 10 N=1.0		
2.246	.1984	.0959	273.8	.8482E+09
3.516	.1795	.0857	387.8	.3253E+10
4.786	.1656	.0794	487.1	.8204E+10
6.056	.1760	.0748	655.1	.1662E+11
7.326	.1582	.0713	712.1	.2942E+11
8.596	.1455	.0685	768.4	.4753E+11
9.866		.0662		
11.14		.0643		
12.41		.0625		
13.68		.0610		
14.95		.0597		
16.22	.1289	.1585	1284.2	.3190E+12
17.49	.1034	.0574	1111.1	.4000E+12
18.76	.1081	.0564	1245.4	.4937E+12
20.03	.1229	.0555	1512.5	.6009E+12
21.30	.1024	.0546	1339.2	.7226E+12
22.57	.1030	.0539	1427.5	.8597E+12
23.84	.1043	.0531	1527.7	.1013E+13
25.11		.0524		

494 172

VOLUMETRIC BOILING POOL DATA



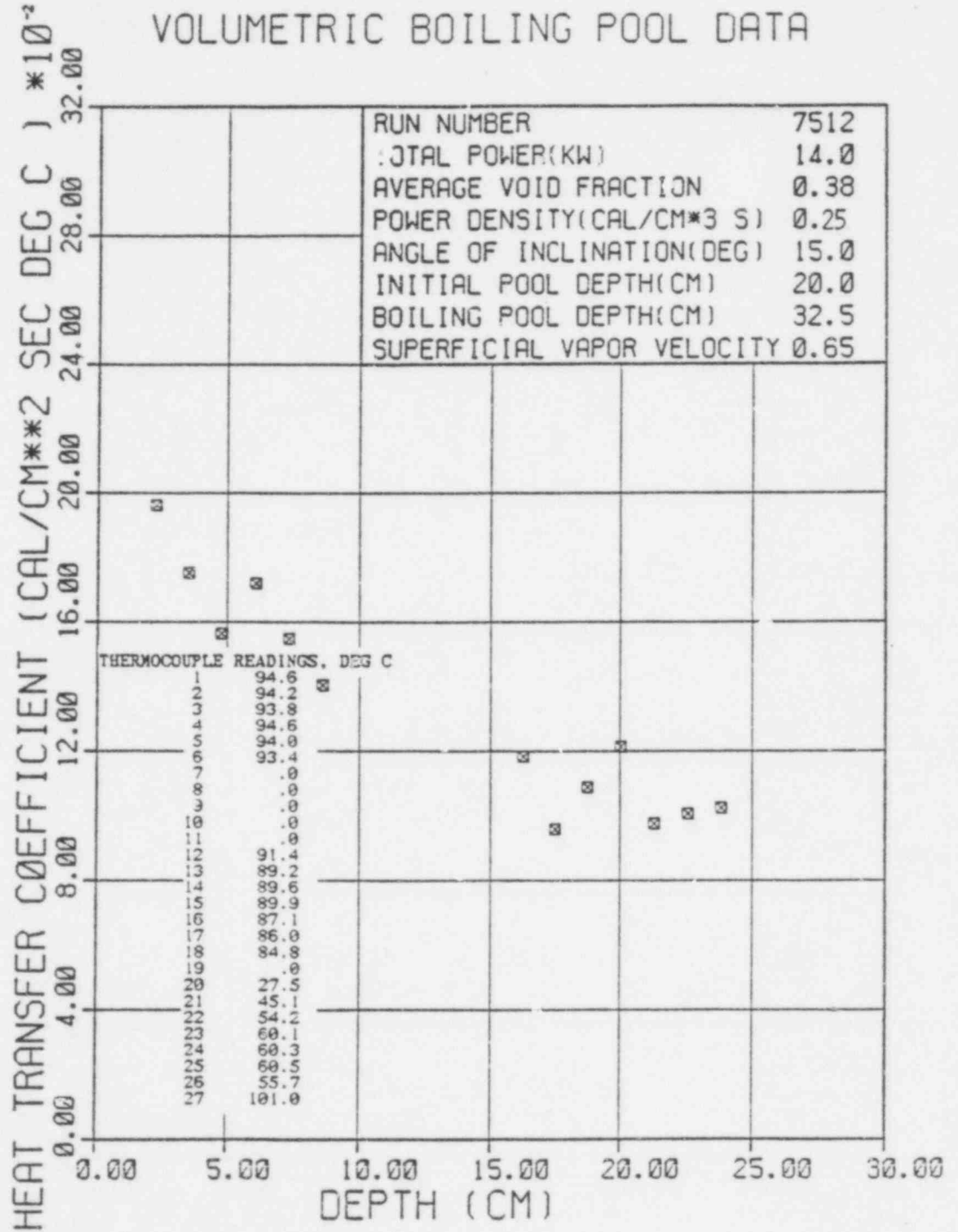
RUN NUMBER... 7512

AVERAGE VOID FRACTION..... .38
 INITIAL POOL DEPTH(CM)..... 20.0
 BOILING POOL DEPTH(CM)..... 32.5
 VOL. POWER DENS. (CAL/CM3 SEC). .25
 SUPERFICIAL VAPOR VELOCITY.... .65
 ANGLE OF INCLINATION(DEGREES). 15.00
 POOL VOLUME(CM**3)..... 12989.
 PRANDTL NUMBER..... 1.84
 TOTAL POWER(KW)..... 14.0
 AVERAGE SURFACE TEMP(DEG C)... 91.5

DEPTH (CM)	LOCAL HEAT TRANSFER COEFF (CAL/CM2 SEC DEG C)				NUSSELT NUMBER	MODIFIED RAYLEIGH NUMBER
	EXPT	EQ 14a	EQ 10 N=1.0	EQ 10 N=0.7		
2.246	.1962	.0959	.0833	.1111	270.8	.8474E+09
3.516	.1752	.0857	.0715	.0950	378.5	.3250E+10
4.786	.1565	.0793	.0645	.0853	460.2	.8197E+10
6.056	.1720	.0748	.0596	.0787	640.1	.661E+11
7.326	.1548	.0715	.0560	.0737	696.9	.939E+11
8.596	.1403	.0685	.0532	.0698	741.1	.4748E+11
9.866		.0662	.0508	.0667		
11.14		.0642	.0489	.0640		
12.41		.0625	.0472	.0617		
13.68		.0610	.0458	.0597		
14.95		.0597	.0445	.0580		
16.22	.1185	.0585	.0433	.0564	1180.5	.3188E+12
17.49	.0958	.0574	.0423	.0550	1028.8	.3997E+12
18.76	.1088	.0564	.0414	.0538	1254.3	.4932E+12
20.03	.1215	.0555	.0406	.0526	1494.7	.6003E+12
21.30	.0975	.0546	.0398	.0515	1276.4	.7220E+12
22.57	.1007	.0538	.0391	.0506	1395.6	.8590E+12
23.84	.1025	.0531	.0384	.0497	1501.1	.1012E+13
25.11		.0524	.0378	.0488		

494 174

VOLUMETRIC BOILING POOL DATA



494 175

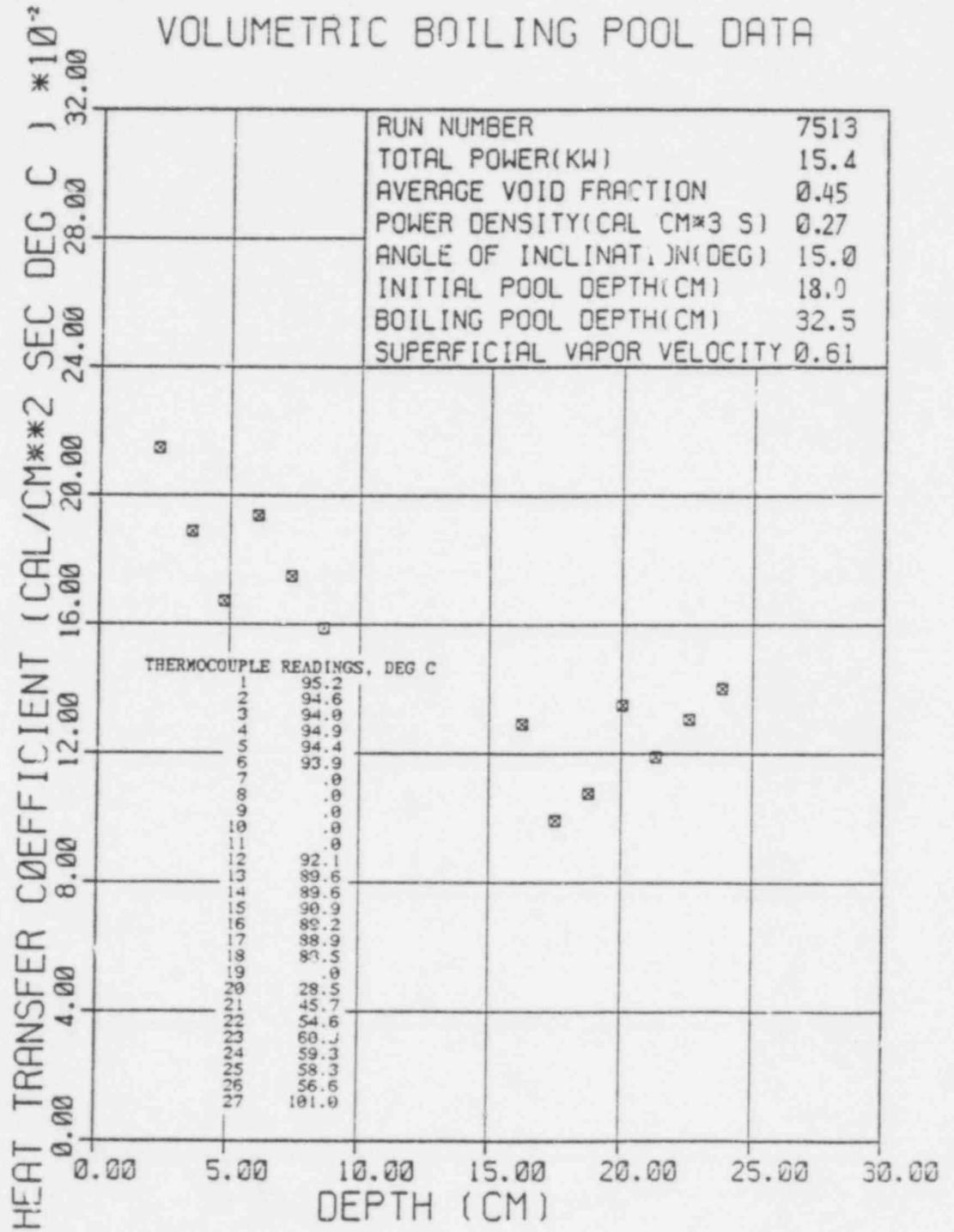
RUN NUMBER... 7513

AVERAGE VOID FRACTION..... .45
 INITIAL POOL DEPTH(CM)..... 18.0
 BOILING POOL DEPTH(CM)..... 32.5
 VOL. FOWER DENS. (CAL/CM3 SEC) . .27
 SUPERFICIAL VAPOR VELOCITY..... .61
 ANGLE OF INCLINATION(DEGREES) . 15.00
 POOL VOLUME(CM*3)..... 11603.
 PRANDTL NUMBER..... 1.84
 TOTAL POWER(KW)..... 15.4
 AVERAGE SURFACE TEMP(DEG C) ... 92.3

DEPTH (CM)	LOCAL HEAT TRANSFER COEFF (CAL/CM2 SEC DEG C) EXPT EQ 14a N=1.0 N=0.7	NUSSELT NUMBER	MODIFIED RAYLEIGH NUMBER
2.46	.1209	.0959	.126
3.516	.088	.0829	.1086
4.786	.1673	.1001	.0979
6.056	.1937	.0943	.0696
7.326	.1750	.0900	.0850
8.596	.1588	.0864	.0806
9.866	.0835	.0597	.0770
11.14	.0810	.0575	.0741
12.41	.0789	.0557	.0715
13.68	.0770	.0540	.0693
14.95	.0753	.0526	.0673
16.22	.0738	.0513	.0655
17.49	.0991	.0501	.0640
18.76	.1075	.0711	.0490
20.03	.1350	.0700	.0481
21.30	.1190	.0689	.0472
22.57	.1306	.0579	.0464
23.84	.1402	.0670	.0456
25.11	.0661	.0449	.0570
		296.5	.2143E+10
		407.9	.8220E+10
		491.8	.2073E+11
		720.7	.2000E+11
		787.4	.7434E+11
		838.8	.1201E+12
		1286.4	.8062E+12
		1664.7	.1011E+13
		1238.8	.1247E+13
		1660.7	.1518E+13
		1557.0	.1826E+13
		1809.9	.2172E+13
		2052.2	.2560E+13

494 176

VOLUMETRIC BOILING POOL DATA



494 177

RUN NUMBER... 7514

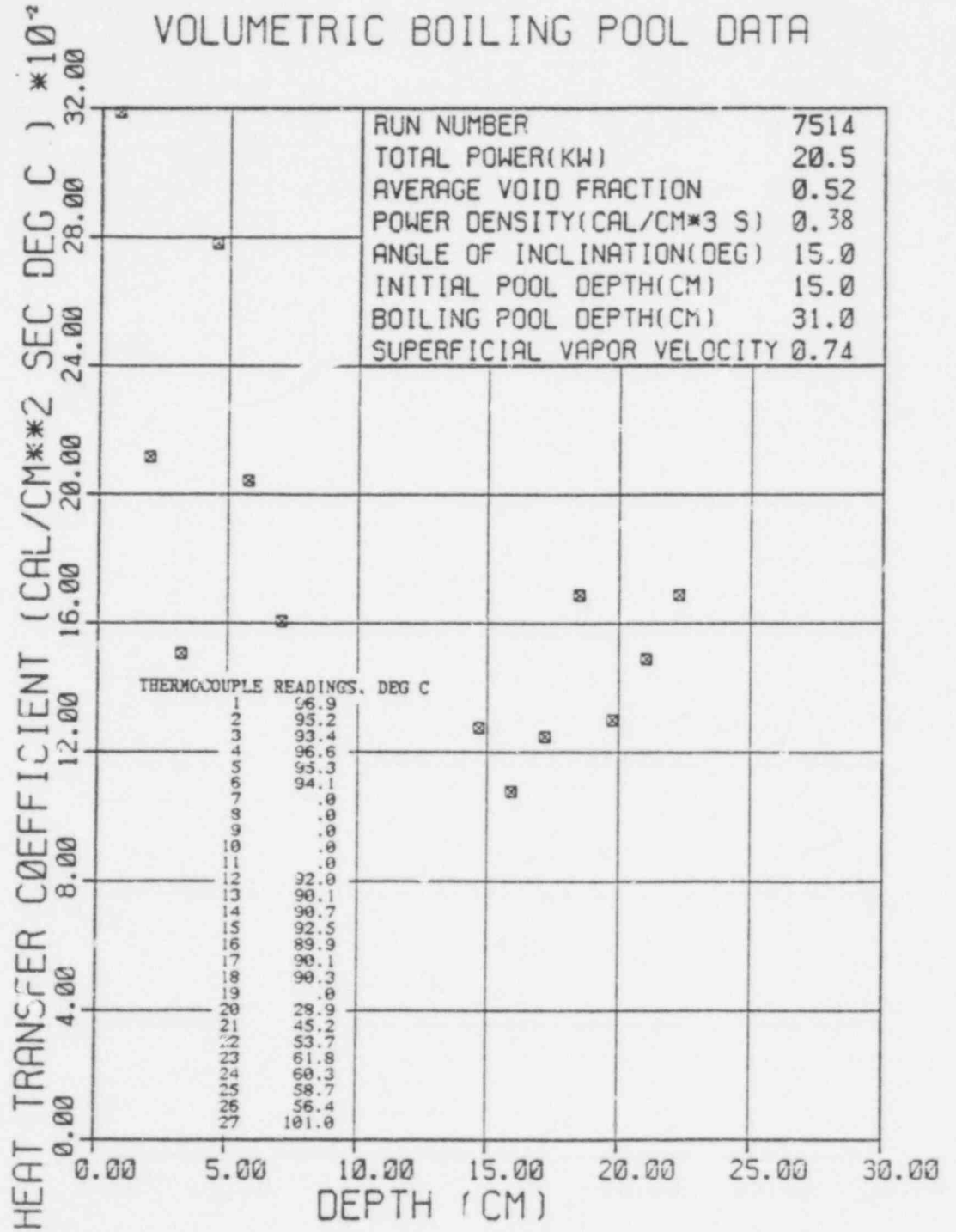
AVERAGE VOID FRACTION..... .52
 INITIAL POOL DEPTH(CM)..... 15.0
 BOILING POOL DEPTH(CM)..... 31.0
 VOL. POWER DENS. (CAL/CM3 SEC).. .38
 SUPERFICIAL VAPOR VELOCITY.... .74
 ANGLE OF INCLINATION(DEGREES).. 15.00
 POOL VOLUME(CM**3)..... 9560.6
 PRANDTL NUMBER..... 1.83
 TOTAL POWER(KW)..... 20.5
 AVERAGE SURFACE TEMP(DEG C)... 93.2

DEPTH (CM)	LOCAL HEAT TRANSFER COEFF (CAL/CM2 SEC DEG C)				NUSSELT NUMBER	MODIFIED RAYLEIGH NUMBER
	EXPT	EQ 14a	EQ 10 N=1.0	EQ 10 N=0.7		
.694	.3189	.1387	.1355	.1822	135.8	.3372E+08
1.964	.2117	.1069	.0938	.1253	255.3	.7652E+09
3.234	.1507	.0944	.0791	.1051	299.2	.3417E+10
4.504	.2781	.0863	.0767	.0937	769.2	.9232E+10
5.774	.2043	.0817	.0651	.0860	724.4	.1945E+11
7.044	.1606	.0777	.0610	.0803	694.9	.3532E+11
8.314		.0746	.0578	.0759		
9.584		.0719	.0552	.0724		
10.85		.0697	.0530	.0694		
12.12		.0678	.0512	.0669		
13.39		.0662	.0496	.0647		
14.66	.1277	.0647	.0482	.0627	115.1	.3187E+12
15.93	.1078	.0634	.0469	.0610	105.0	.4089E+12
17.20	.1249	.0622	.0458	.0595	1319.2	.5146E+12
18.47	.1689	.0611	.0448	.0581	1916.2	.6372E+12
19.74	.1300	.0601	.0438	.0568	1576.5	.7779E+12
21.01	.1491	.0591	.0430	.0557	1924.0	.9378E+12
22.28	.1689	.0583	.0422	.0546	2311.0	.1118E+13
23.55		.0575	.0415	.0536		

-132-

A9A 178

VOLUMETRIC BOILING POOL DATA



494 179

 RUN NUMBER... 7515

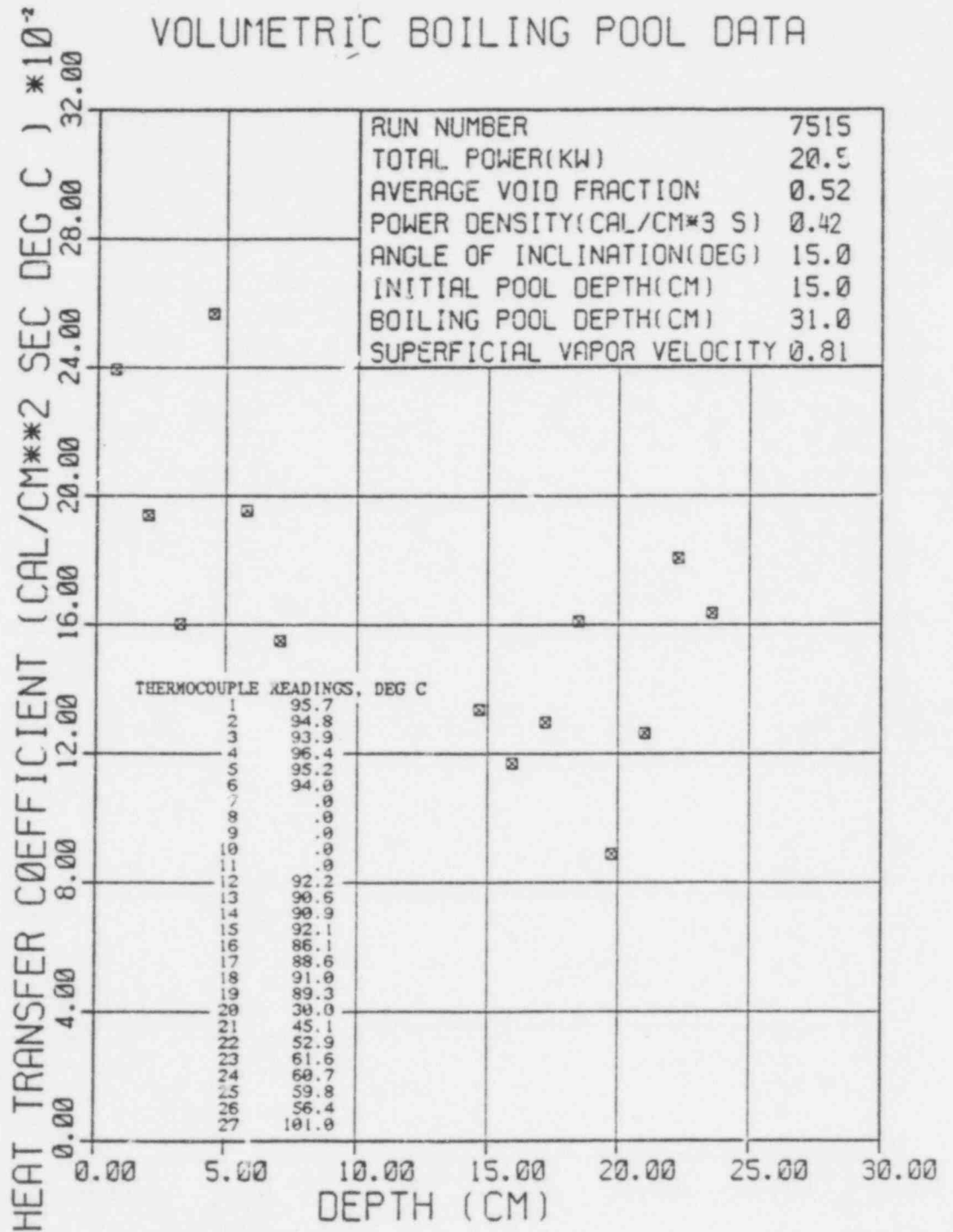
AVERAGE VOID FRACTION..... .52
 INITIAL POOL DEPTH(CM)..... 15.0
 BOILING POOL DEPTH(CM)..... 31.0
 VOL. POWER DENS.(CAL/CM3 SEC). .42
 SUPERFICIAL VAPOR VELOCITY.... .81
 ANGLE OF INCLINATION(DEGREES). 15.00
 POOL VOLUME(CM**3)..... 9560.6
 PRANDTL NUMBER..... 1.83
 TOTAL POWER(KW)..... 20.5
 AVERAGE SURFACE TEMP(DEG C)... 92.7

DEPTH (CM)	LOCAL HEAT TRANSFER COEFF (CAL/CM2 SEC DEG C)				NUSSELT NUMBER	MODIFIED RAYLEIGH NUMBER
	EXPT	EQ 14a	EQ 10 N=1.0	EQ 10 N=0.7		
.694	.2394	.1386	.1382	.1859	102.0	.3364E+08
1.964	.1940	.1069	.0954	.1276	234.0	.7635E+09
3.234	.1602	.0943	.0803	.1070	318.2	.3410E+10
4.504	.2569	.0868	.0718	.0953	710.6	.9211E+10
5.774	.1954	.0816	.0661	.0874	692.9	.1941E+11
7.044	.1550	.0777	.0619	.0816	670.4	.3524E+11
8.314		.0745	.0586	.0771		
9.584		.0719	.0559	.0735		
10.85		.0697	.0537	.0705		
12.12		.0678	.0518	.0679		
13.39		.0661	.0502	.0656		
14.66	.1335	.0646	.0487	.0637	1202.8	.3180E+12
15.93	.1170	.0633	.0475	.0619	1145.4	.4079E+12
17.20	.1298	.0621	.0463	.0604	1371.3	.5135E+12
18.47	.1611	.0610	.0453	.0589	1827.5	.6358E+12
19.74	.0888	.0600	.0443	.0576	1077.3	.7761E+12
21.01	.1264	.0591	.0435	.0565	1631.0	.9357E+12
22.28	.1907	.0582	.0427	.0554	2473.1	.1116E+13
23.55	.1636	.0574	.0419	.0544	2757.3	.1318E+13

-134-

494 180

VOLUMETRIC BOILING POOL DATA

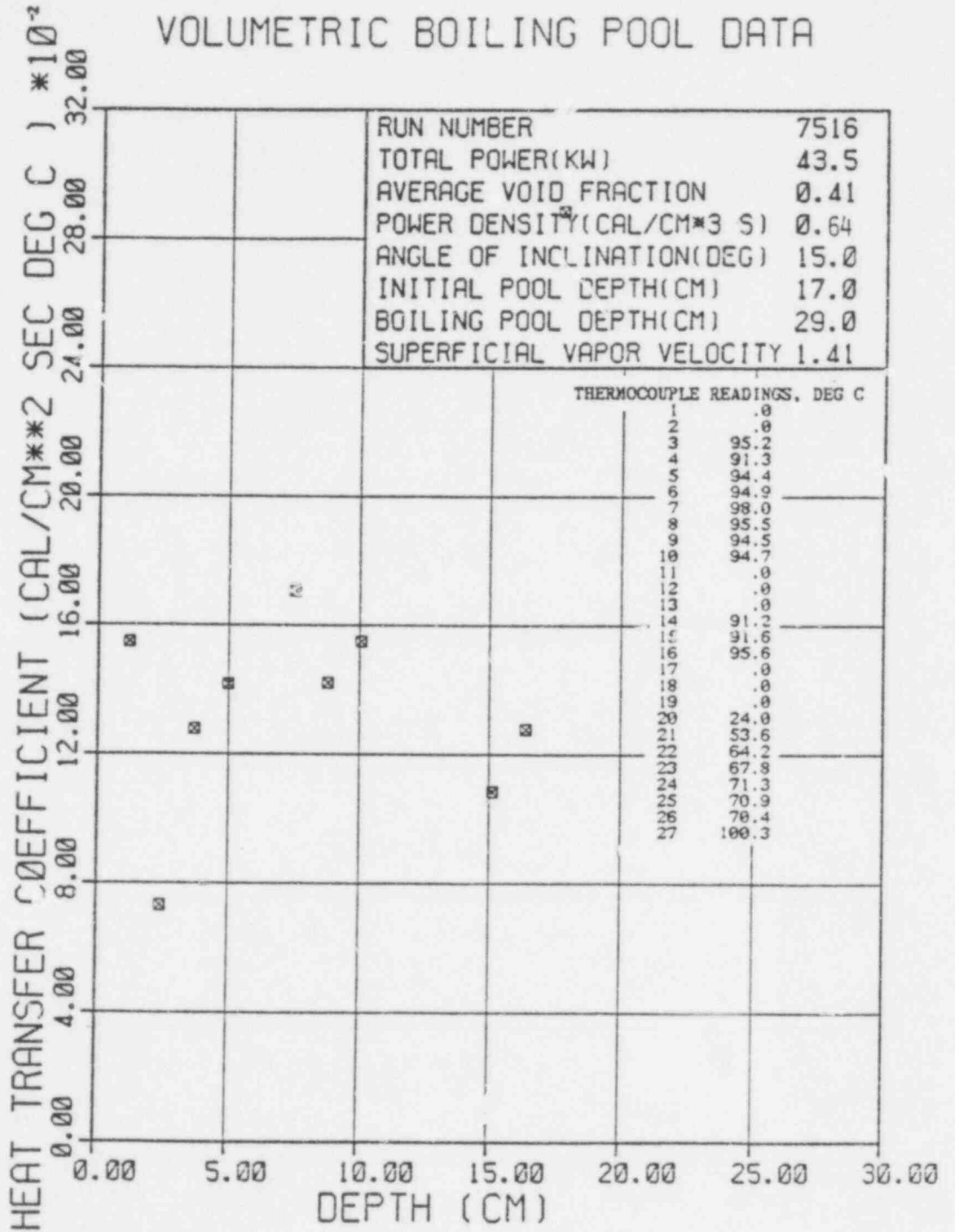


 RUN NUMBER... 7516

AVERAGE VOID FRACTION..... .41
 INITIAL POOL DEPTH(CM)..... 17.0
 BOILING POOL DEPTH(CM)..... 29.0
 VOL. POWER DENS.(CAL/CM3 SEC). .64
 SUPERFICIAL VAPOR VELOCITY..... 1.41
 ANGLE OF INCLINATION(DEGREES). 15.00
 POOL VOLUME(CM*3)..... 10917.
 PRANDTL NUMBER..... 1.83
 TOTAL POWER(KW)..... 43.45
 AVERAGE SURFACE TEMP(DEG C) ... 93.4

DEPTH (CM)	LOCAL HEAT TRANSFER COEFF (CAL/CM2 SEC DEG C) EXPT EQ 14a EQ 10 EQ 10	NUSSLETT NUMBER	MODIFIED RAYLEIGH NUMBER			
1.163	.1549	.1153	.1267	.1707	110.6	.1272E+09
2.433	.0732	.0958	.0964	.1297	109.4	.1164E+10
3.703	.1279	.0863	.0828	.1112	290.8	.4105E+10
4.973	.1419	.0802	.0745	.0999	433.4	.9944E+10
6.243	.3748	.0757	.0688	.0921	1437.1	.1967E+11
7.513	.1706	.0723	.0645	.0862	787.3	.3429E+11
8.783	.1421	.0695	.0611	.0816	766.7	.5478E+11
10.05	.1551	.0672	.0583	.0778	957.6	.8214E+11
11.32		.0653	.0559	.0746		
12.59		.0635	.0540	.0718		
13.86		.0620	.0522	.0695		
15.13	.1083	.0607	.0507	.0674	1006.9	.2802E+12
16.40	.1279	.0595	.0493	.0655	1288.6	.3568E+12
17.67	.2885	.0584	.0481	.0638	3131.7	.4463E+12
18.94		.0574	.0470	.0623		
20.21		.0565	.0460	.0609		
21.48		.0556	.0451	.0596		

VOLUMETRIC BOILING POOL DATA



494 183

 RUN NUMBER... 7517

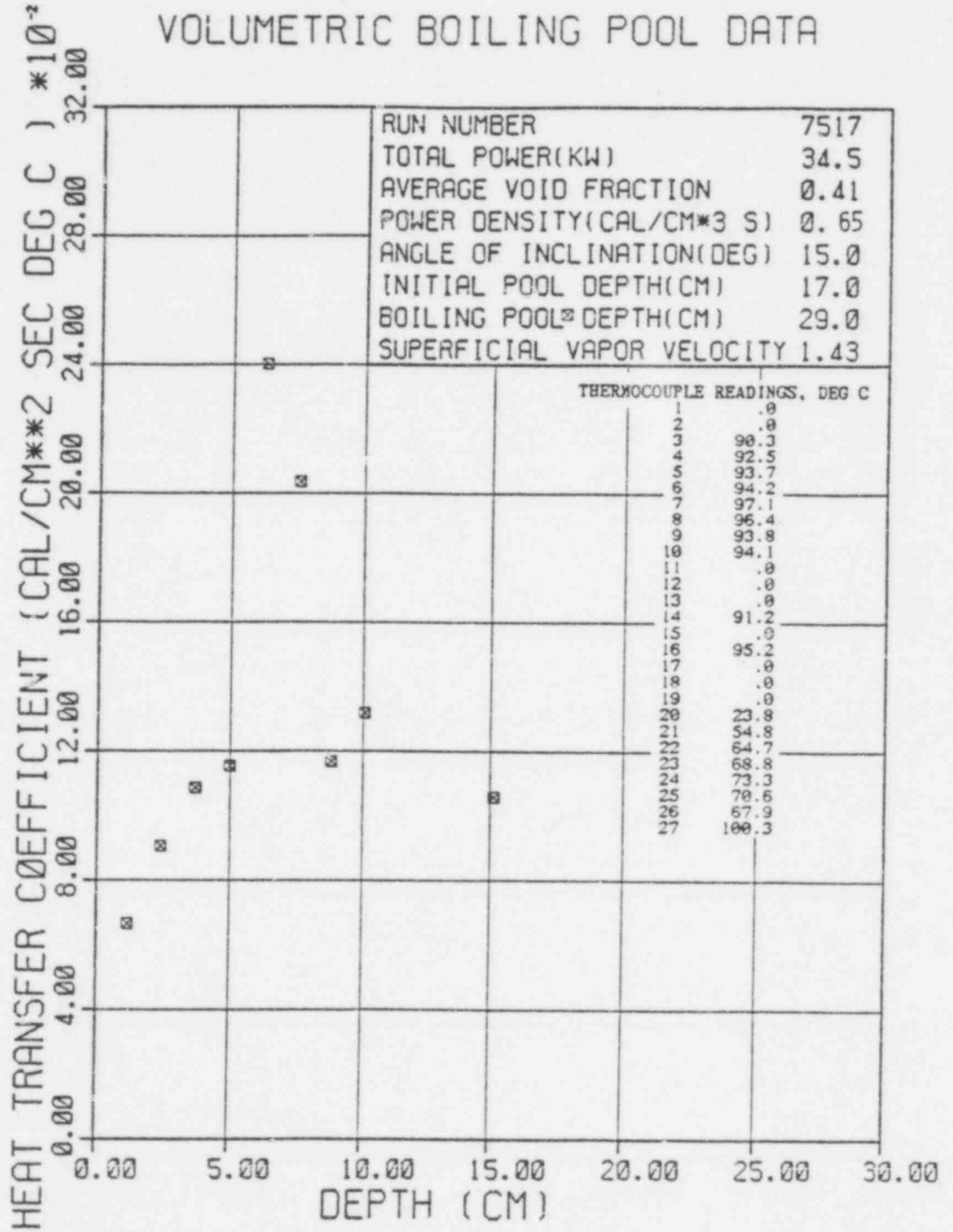
AVERAGE VOID FRACTION..... .41
 INITIAL POOL DEPTH(CM)..... 17.0
 BOILING POOL DEPTH(CM)..... 29.0
 VOL. POWER DENS.(CAL/CM3 SEC). .65
 SUPERFICIAL VAPOR VELOCITY..... 1.43
 ANGLE OF INCLINATION(DEGREES). 15.00
 POOL VOLUME(CM*3)..... 10917.
 PRANDTL NUMBER..... 1.84
 TOTAL POWER(KW)..... 34.5
 AVERAGE SURFACE TEMP(DEG C).... 93.1

 DEPTH (CM) LOCAL HEAT TRANSFER COEFF (CAL/CM2 SEC DEG C) NUSSELT NUMBER MODIFIED RAYLEIGH NUMBER
 EQ 14 EQ 10 EQ 10 EQ 10
 N=1.0 N=0.7

DEPTH (CM)	LOCAL HEAT TRANSFER COEFF (CAL/CM2 SEC DEG C) EQ 10	NUSSELT NUMBER	MODIFIED RAYLEIGH NUMBER
1.163	.0665	47.5	.1270E+09
2.433	.0906	135.5	.1163E+10
3.703	.1086	247.0	.4100E+10
4.973	.1154	352.4	.9930E+10
6.243	.2401	920.8	.1965E+11
7.513	.2036	939.8	.3424E+11
8.783	.1167	629.7	.5471E+11
10.05	.1317	813.5	.8203E+11
11.32	.0652		
12.59	.0635		
13.86	.0620		
15.13	.1057	982.8	.2798E+12
16.40	.2557	2776.3	.4457E+12
17.67			
18.94			
20.21			
21.48	.0556		

494 184

VOLUMETRIC BOILING POOL DATA



494 185

RUN NUMBER... 7518

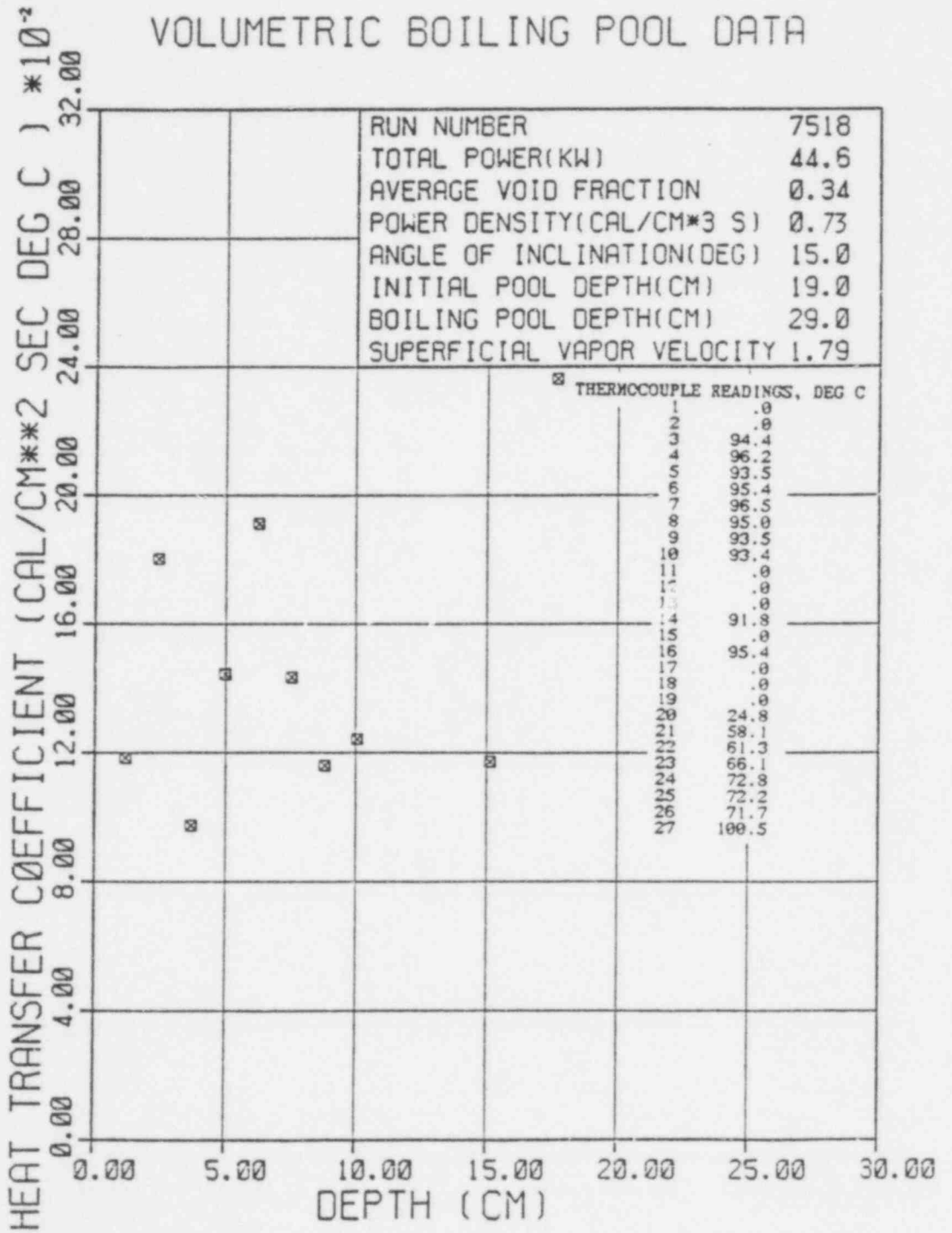
AVERAGE VOID FRACTION..... .34
 INITIAL POOL DEPTH(CM)..... 10.0
 BOILING POOL DEPTH(CM)..... 29.0
 VOL. POWER DENS. (CAL/CM3 SEC) . .73
 SUPERFICIAL VAPOR VELOCITY.... 1.79
 ANGLE OF INCLINATION (DEGREES). 15.00
 POOL VOLUME(CM**3)..... 12293.
 PRANDTL NUMBER..... 1.82
 TOTAL POWER(KW)..... 44.6
 AVERAGE SURFACE TEMP(DEG C)... 94.5

DEPTH (CM)	LOCAL HEAT TRANSFER COEFF (CAL/CM2 SEC DEG C)				NUSSELT NUMBER	MODIFIED RAYLEIGH NUMBER
	EXPT	EQ 14a	EQ 10 N=1.0	EQ 10 N=0.7		
1.163	.1184	.1103	.1323	.1780	84.5	.1066E+09
2.433	.1802	.0917	.0998	.1345	269.2	.9760E+09
3.703	.0973	.0	.0854	.1150	221.3	.3441E+10
4.973	.1443	.0	.0766	.1031	440.7	.8334E+10
6.243	.1913	.0725	.0706	.0949	733.3	.1649E+11
7.513	.1434	.0692	.0660	.0887	661.7	.2874E+11
8.783	.1161	.0666	.0624	.0838	626.0	.4591E+11
10.05	.1241	.0643	.0595	.0798	766.3	.6885E+11
11.32		.0625	.0571	.0765		
12.59		.0608	.0550	.0736		
13.86		.0594	.0532	.0711		
15.13	.1171	.0531	.0516	.0639	1088.5	.2349E+12
16.40		.0569	.0501	.0670		
17.67	.2361	.0559	.0489	.0653	2562.4	.3741E+12
18.94		.0549	.0477	.0637		
20.21		.0540	.0467	.0622		
21.48		.0532	.0457	.0609		

-140-

494
186

VOLUMETRIC BOILING POOL DATA



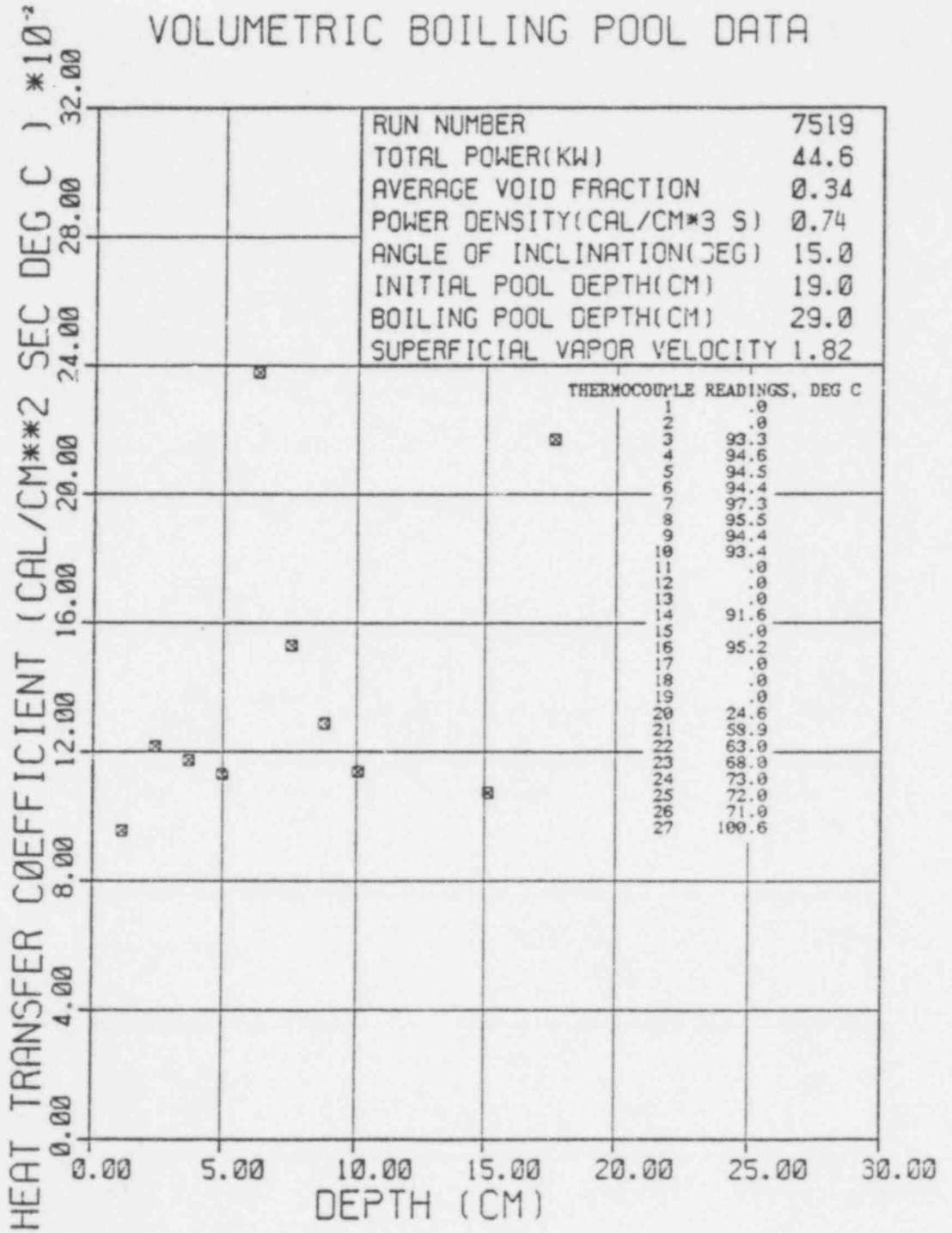
494 187

RUN NUMBER... 7519

AVERAGE VOID FRACTION..... .34
 INITIAL POOL DEPTH(CM)..... .9.0
 BOILING POOL DEPTH(CM)..... 29.0
 % OF POWER DENS. (CAL/CM3 SEC) . .74
 SUPERFICIAL VAPOR VELOCITY..... 1.82
 ANGLE OF INCLINATION(DEGREES) . 15.00
 POOL VOLUME(CM*3)..... 1229J.
 PRANDTL NUMBER..... 1.82
 TOTAL POWER(KW)..... 44.6
 AVERAGE SURFACE TEMP(DEG C) ... 94.0

DEPTH (CM)	LOCAL HEAT TRANSFER COEFF (CAL/CM2 SEC DEG C) EXPT EQ 14a N=1.0 N=0.7	EQ 10	EQ 10	EQ 10	NUSSELY NUMBER	MODIFIED RAYLEIGH NUMBER
1.163	.0957	.1103	.1328	.1787	68.3	.1064E+09
2.433	.1216	.0917	.1002	.1350	181.7	.9743E+09
3.703	.1173	.0825	.0857	.1154	266.8	.3435E+10
4.973	.1132	.0767	.0769	.1035	345.6	.8320E+10
6.243	.2377	.0724	.0708	.0952	911.4	.1646E+11
7.513	.1530	.0692	.0662	.0890	705.8	.2869E+11
8.783	.1288	.0665	.0626	.0841	694.7	.4583E+11
10.05	.1139	.0643	.0597	.0801	703.1	.6873E+11
11.32		.0624	.0572	.0767		
12.59		.0608	.0551	.0738		
13.86		.0593	.0533	.0714		
15.13	.1075	.0581	.0517	.0692	999.0	.2344E+12
16.40		.0569	.0503	.0672		
17.67	.2170	.0558	.0490	.0655	2355.4	.3734E+12
18.94		.0549	.0478	.0639		
20.21		.0540	.0468	.0624		
21.48		.0532	.0458	.0611		

VOLUMETRIC BOILING POOL DATA

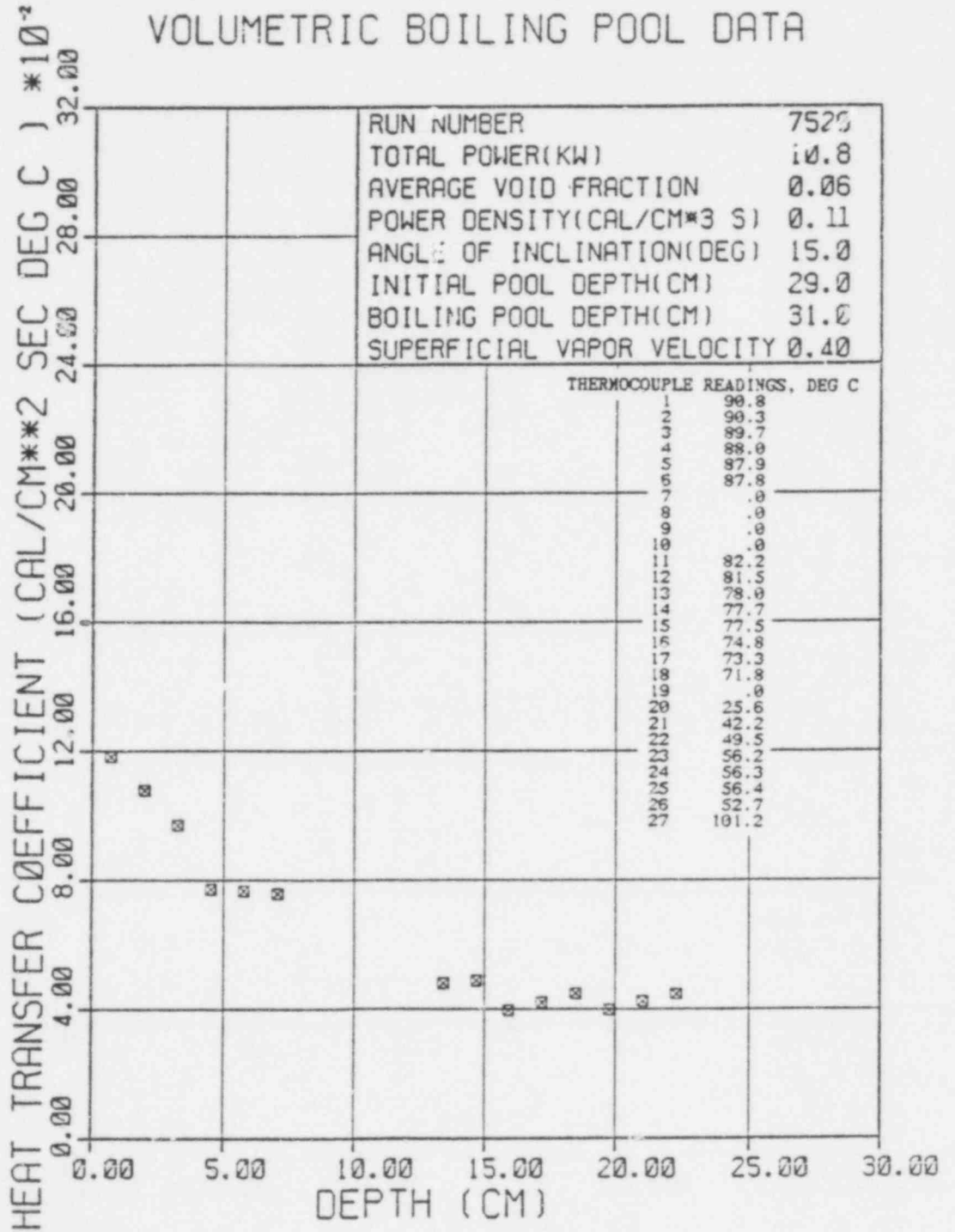


RUN NUMBER... 7520

AVERAGE VOID FRACTION..... .06
 INITIAL POOL DEPTH(CM)..... 29.0
 BOILING POOL DEPTH(CM)..... 31.0
 VOL. POWER DENS.(CAL/CM3 SEC). .11
 SUPERFICIAL VAPOR VELOCITY..... .40
 ANGLE OF INCLINATION(DEGREES). 15.00
 POOL VOLUME(CM**3)..... 19463.
 PRANDTL NUMBER..... 1.93
 TOTAL POWER(KW)..... 10.8
 AVERAGE SURFACE TEMP(DEG C).... 82.9

DEPTH (CM)	LOCAL HEAT TRANSFER COEFF (CAL/CM2 SEC DEG C) EQ 14a N=1.0 N=0.7	MUSSELT NUMBER	MODIFIED RAYLEIGH NUMBER	
.694	.1183	.0813	.0880	.1185
1.964	.1077	.0627	.0601	.0807
3.234	.0969	.0553	.0503	.0674
4.504	.0773	.0509	.0448	.0599
5.774	.0765	.0479	.0412	.0549
7.044	.0758	.0456	.0385	.0512
8.314		.0437	.0364	.0483
9.584		.0422	.0347	.0460
10.85		.0409	.0333	.0440
12.12		.0398	.0321	.0424
13.39	.0480	.0388	.0310	.0410
14.66	.0488	.0379	.0301	.0397
15.93	.0397	.0371	.0293	.0386
17.20	.0421	.0364	.0286	.0376
18.47	.0448	.0358	.0279	.0367
19.74	.0399	.0352	.0273	.0359
21.01	.0424	.0347	.0268	.0351
22.28	.0447	.0342	.0263	.0344
23.55		.0337	.0258	.0338
				50.5
				130.2
				193.0
				214.3
				272.1
				328.7
				395.6
				440.4
				389.0
				445.7
				509.2
				484.6
				548.4
				612.6
				.4023E+07
				.9130E+08
				.4077E+09
				.1102E+10
				.2321E+10
				.4214E+10
				.2897E+11
				.3802E+11
				.4878E+11
				.6140E+11
				.7603E+11
				.9281E+11
				.1119E+12
				.1334E+12

VOLUMETRIC BOILING POOL DATA

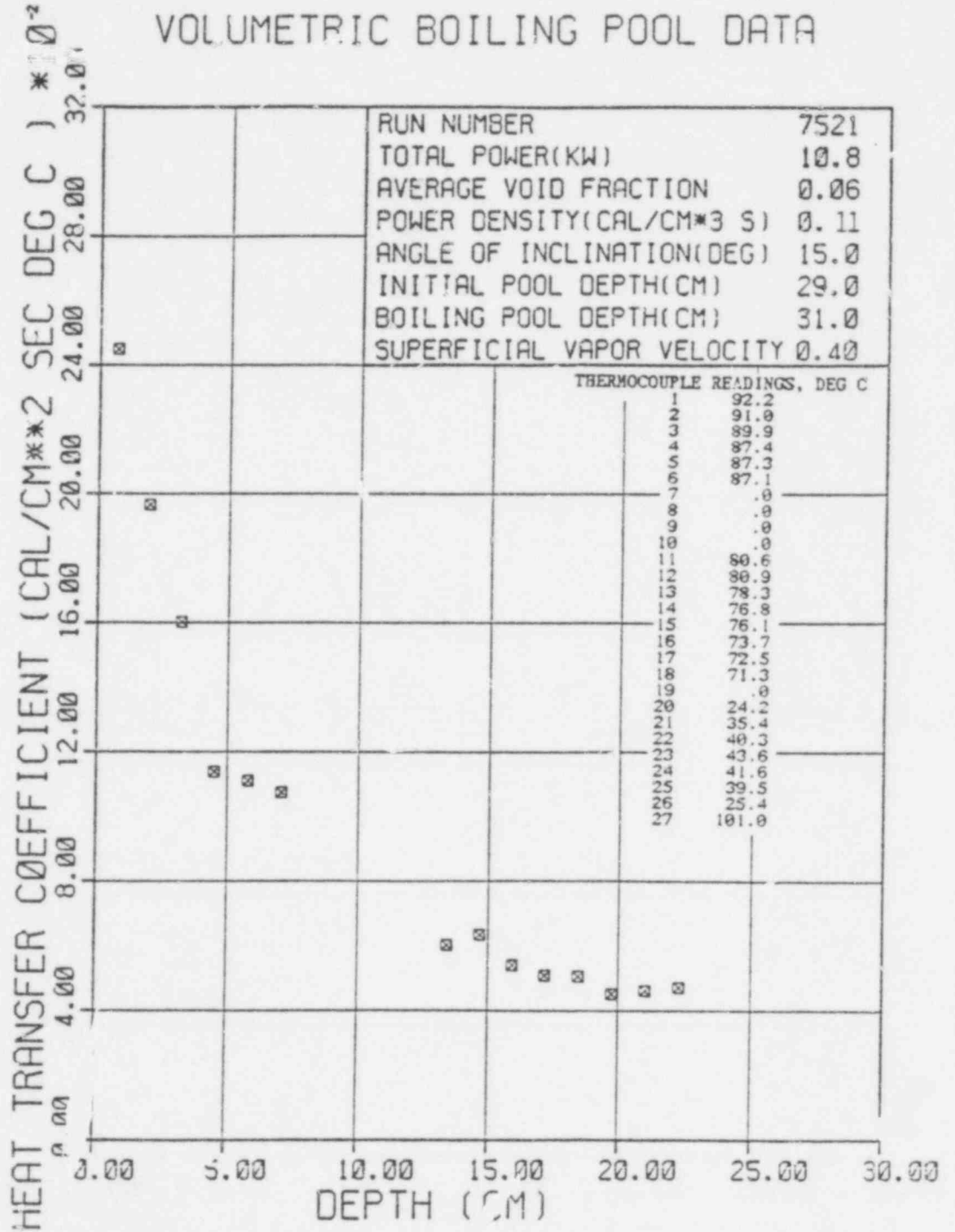


RUN NUMBER... 7521

AVERAGE VOID FRACTION..... .06
 INITIAL POOL DEPTH(CM)..... 29.0
 BOILING POOL DEPTH(CM)..... 31.0
 VOL. POWER DENS. (CAL/CM3 SEC) .11
 SUPERFICIAL VAPOR VELOCITY..... .40
 ANGLE OF INCLINATION(DEGREES) .15.00
 POOL VOLUME(CM**3)..... 19463.
 PRANDTL NUMBER..... 1.94
 TOTAL POWER(KW)..... 10.8
 AVERAGE SURFACE TEMP(DEG C) ... 82.3

DEPTH (CM)	LOCAL HEAT TRANSFER COEFF (CAL/CM2 SEC DEG C)	RUSSELL NUMBER	MODIFIED RAYLEIGH NUMBER
.694	.2451	104.7	.4008E+07
1.964	.1965	237.7	.9694E+08
3.234	.1603	319.1	.4061E+09
4.504	.1137	315.3	.1697E+10
5.774	.1110	394.6	.2312E+10
7.044	.1073	465.4	.4198E+10
8.314			
9.584			
10.85			
12.12			
13.39	.0603	527.3	.2885E+11
14.66	.0634	572.9	.3788E+11
15.93	.0540	539.3	.4859E+11
17.20	.0509	538.9	.6116E+11
18.47	.0507	576.2	.7573E+11
19.74	.0453	550.7	.9245E+11
21.01	.0463	598.5	.1115E+12
22.28	.0471	646.8	.1329E+12
23.55			

VOLUMETRIC BOILING POOL DATA



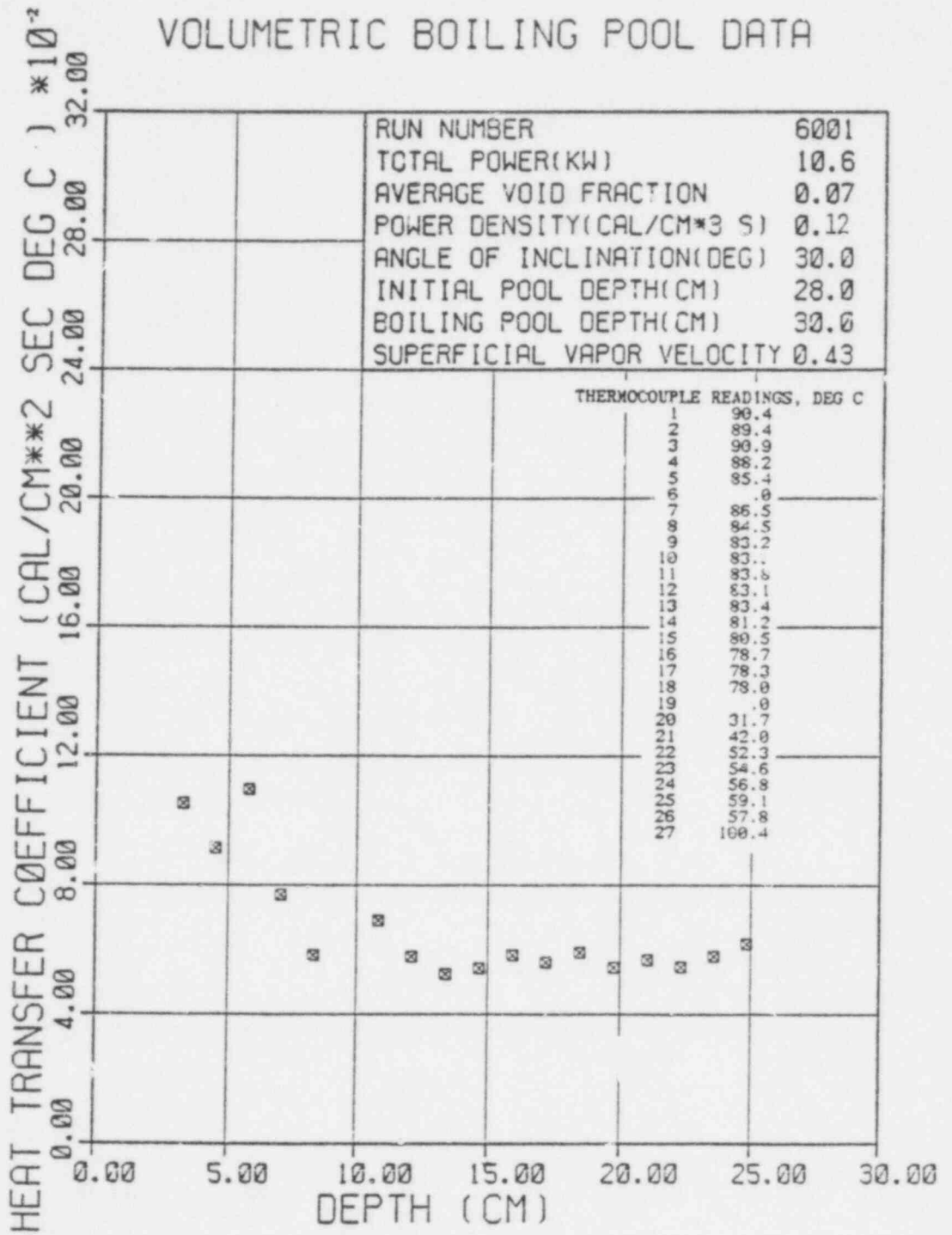
494 193

RUN NUMBER... 6001

AVERAGE VOID FRACTION..... .07
 INITIAL POOL DEPTH(CM)..... 78.0
 BOILING POOL DEPTH(CM)..... 30.0
 VOL. POWER DENS.(CAL/CM3 SEC). .12
 SUPERFICIAL VAPOR VELOCITY..... .43
 ANGLE OF INCLINATION(DEGREES). 30.00
 POOL VOLUME(CM**3)..... 20907.
 PRANDTL NUMBER..... 1.93
 TOTAL POWER(KW)..... 10.6
 AVERAGE SURFACE TEMP(DEG C)... 83.3

DEPTH (CM)	LOCAL HEAT TRANSFER COEFF (CAL/CM2 SEC DEG C)			MUSSELT NUMBER	MODIFIED RAYLEIGH NUMBER
	EXPT	EQ 14a	N=1.0		
3.241	.1052	.0557	.0504	210.0	.3796E+09
4.511	.0915	.0513	.0449	254.1	.1024E+10
5.781	.1095	.0482	.0412	389.9	.2154E+10
7.051	.0770	.0459	.0385	334.3	.3909E+10
8.321	.0583	.0440	.0364	298.5	.6424E+10
9.591		.0425	.0346		
10.86	.0690	.0412	.0332	451.3	.1429E+11
12.13	.0577	.0401	.0320	431.2	.1991E+11
13.40	.0523	.0391	.0310	431.6	.2684E+11
14.67	.0542	.0382	.0300	489.5	.3521E+11
15.94	.0583	.0374	.0292	572.0	.4517E+11
17.21	.0560	.0367	.0285	593.9	.5685E+11
18.48	.0591	.0361	.0278	672.1	.7039E+11
19.75	.0544	.0355	.0272	661.2	.8592E+11
21.02	.0569	.0349	.0267	736.3	.1036E+12
22.29	.0516	.0344	.0262	749.4	.1235E+12
23.56	.0580	.0339	.0257	842.0	.1458E+12
24.83	.0618	.0335	.0253	944.6	.1707E+12
26.10		.0331	.0249		

VOLUMETRIC BOILING POOL DATA



494 195

RUN NUMBER... 6002

AVERAGE VOID FRACTION..... .17

INITIAL POOL DEPTH(CM)..... 25.0

BOILING POOL DEPTH(CM)..... 30.0

VOL. POWER DENS.(CAL/CM3 SEC) . .15

SUPERFICIAL VAPOR VELOCITY.... .48

ANGLE OF INCLINATION(DEGREES) . 30.00

POOL VOLUME(CM**3)..... 18278.

PRANDTL NUMBER..... 1.88

TOTAL POWER(KW)..... 14.6

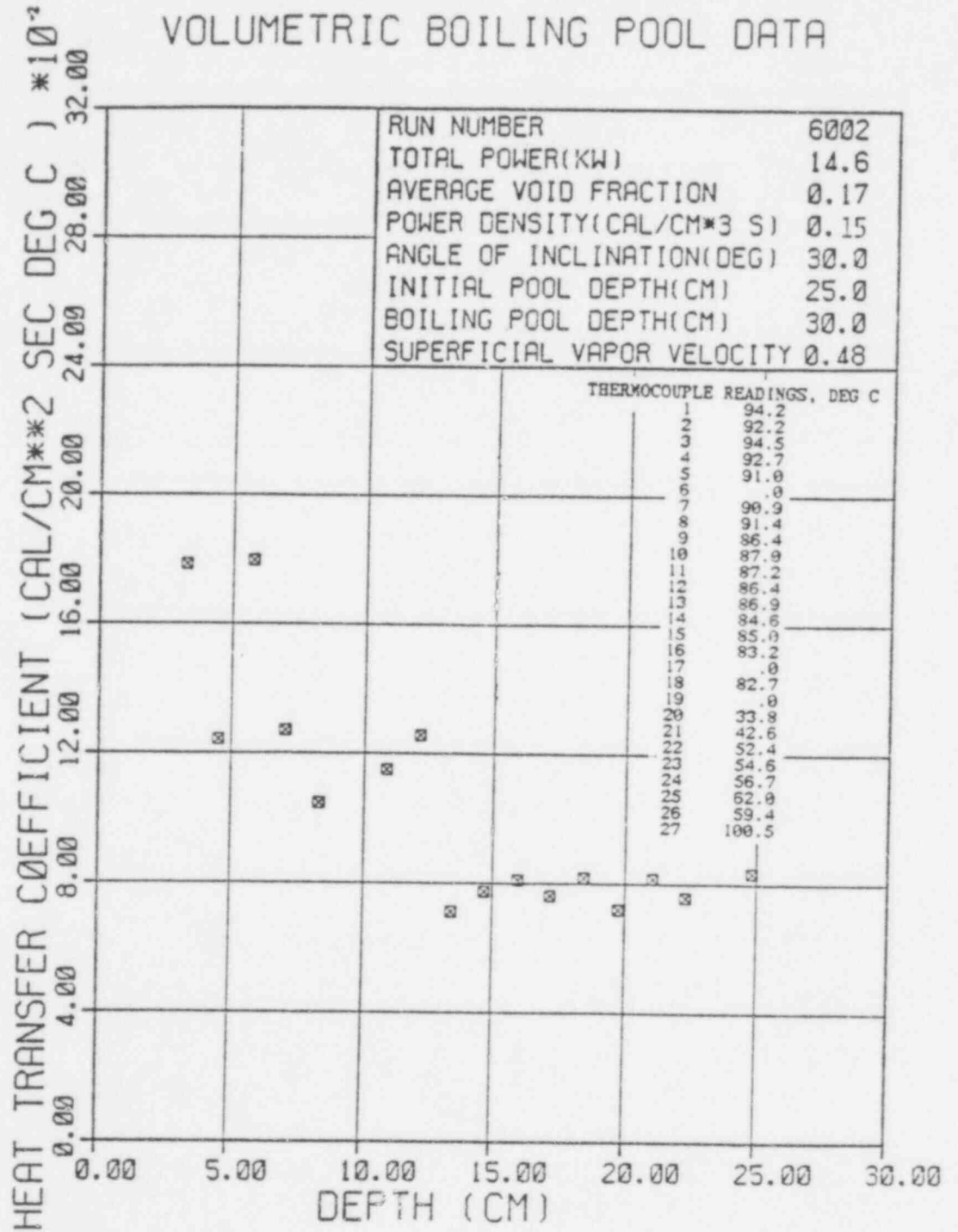
AVERAGE SURFACE TEMP(DEG C)... 88.5

DEPTH (CM)	LOCAL HEAT TRANSFER COEFF (CAL/CM2 SEC DEG C)				NUSSLETT NUMBER	MODIFIED RAYLEIGH NUMBER
	EXPT	EQ 14a	EQ 10 N=1.0	EQ10 N=0.7		
3.241	.1783	.0706	.0596	.0795	355.4	.9731E+10
4.511	.1242	.0650	.0532	.0708	344.5	.2624E+10
5.781	.1795	.0611	.0490	.0649	636.2	.5522E+10
7.051	.1271	.0581	.0458	.0606	550.9	.1002E+11
8.321	.1046	.0558	.0434	.0573	535.0	.1647E+11
9.591		.0538	.0414	.0545		
10.86	.1150	.0522	.0397	.0523	768.1	.3662E+11
12.13	.1256	.0508	.0383	.0503	915.8	.5103E+11
13.40	.0712	.0495	.0371	.0487	586.8	.6879E+11
14.67	.0775	.0484	.0360	.0472	699.0	.9026E+11
15.94	.0809	.0474	.0351	.0459	793.1	.1158E+12
17.21	.0762	.0465	.0342	.0447	806.1	.1457E+12
18.48	.0819	.0457	.0335	.0437	930.7	.1804E+12
19.75	.0720	.0449	.0328	.0427	874.6	.2202E+12
21.02	.0815	.0443	.0321	.0418	1053.6	.2655E+12
22.29	.0758	.0436	.0315	.0410	1038.5	.3156E+12
23.56		.0430	.0310	.0403		
24.83	.0834	.0424	.0305	.0396	1273.0	.4376E+12
26.10		.0419	.0300	.0389		

-150-

49A 196

VOLUMETRIC BOILING POOL DATA



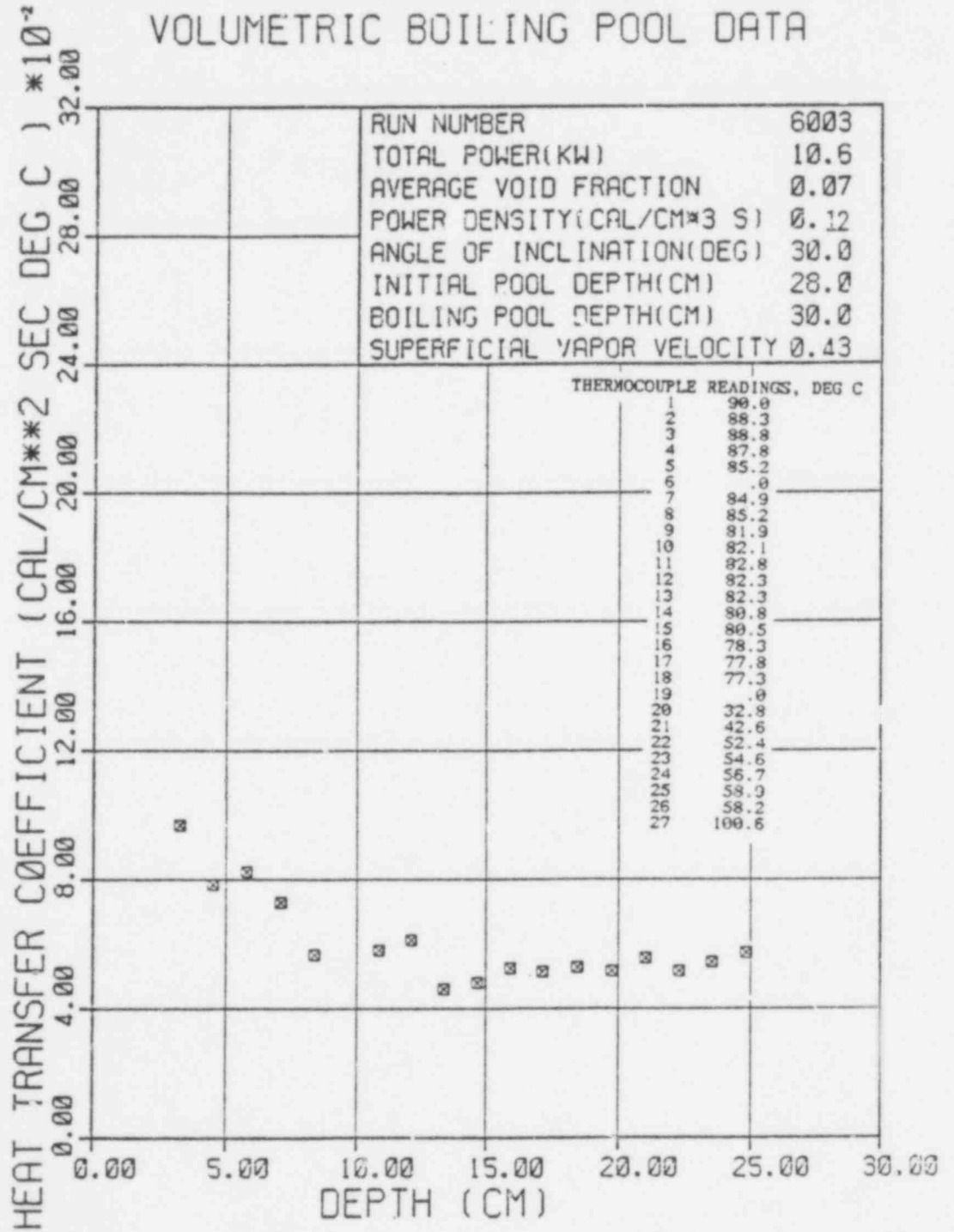
RUN NUMBER... 6003

AVERAGE VOID FRACTION..... .87
 INITIAL POOL DEPTH(CM)..... 28.0
 BOILING POOL DEPTH(CM)..... 30.6
 VOL. POWER DENS. (CAL/CM3 SEC). .12
 SUPERFICIAL VAPOR VELOCITY.... .43
 ANGLE OF INCLINATION(DEGREES). 30.60
 POOL VOLUME(CM**3)..... 20907.
 PRANDTL NUMBER..... 1.93
 TOTAL POWER(KW)..... 10.6
 AVERAGE SURFACE TEMP(NEG C)... 83.7

DEPTH (CM)	LOCAL HEAT TRANSFER COEFF (CAL/CM2 SEC DEG C) EXPT EQ 14a	EQ 10	EQ 10	MUSSELT NUMBER	MODIFIED RAYLEIGH NUMBER
		N=1.0	N=0.7		
3.241	.0969	.0558	.0505	193.2	.3807E+09
4.511	.0784	.0514	.0449	217.7	.1027E+10
5.781	.0824	.0483	.0412	293.4	.2161E+10
7.051	.0729	.0459	.0385	316.4	.3920E+10
8.321	.0567	.0441	.0364	290.3	.6443E+10
9.591		.0425	.0347		
10.86	.0580	.0472	.0332	387.7	.1433E+11
12.13	.0612	.0401	.0320	457.2	.1936E+11
13.40	.0489	.0391	.0310	378.9	.2691E+11
14.67	.0489	.0382	.0301	433.4	.3531E+11
15.94	.0525	.0375	.0292	515.0	.4530E+11
17.21	.0515	.0367	.0285	545.2	.5702E+11
18.48	.0527	.0361	.0279	600.1	.7059E+11
19.75	.0516	.0355	.0273	627.8	.8617E+11
21.02	.0556	.0350	.0267	719.9	.1039E+12
22.29	.0517	.0344	.0262	709.2	.1239E+12
23.56	.0545	.0340	.0257	790.0	.1463E+12
24.83	.0571	.0335	.0253	873.4	.1712E+12
26.10		.0331	.0249		

494 198

VOLUMETRIC BOILING POOL DATA



494 199

RUN NUMBER... 6004

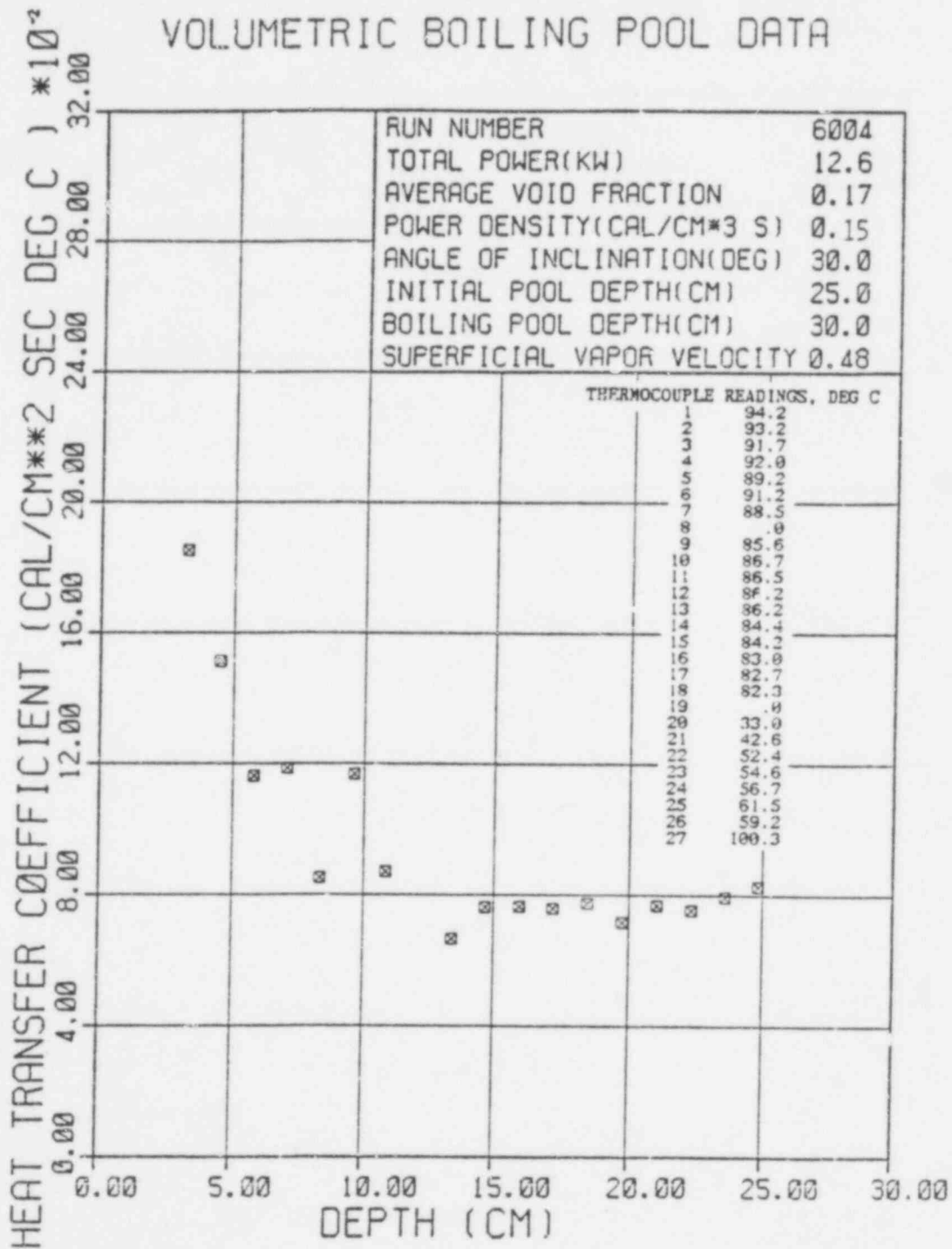
AVERAGE VOID FRACTION..... .17
 INITIAL POOL DEPTH(CM)..... 25.0
 BOILING POOL DEPTH(CM)..... 30.0
 VOL. POWER DENS. (CAL/CM3 SEC). .15
 SUPERFICIAL VAPOR VELOCITY.... .48
 ANGLE OF INCLINATION(DEGREES). 30.00
 POOL VOLUME(CM**3)..... 18278.
 PRANDTL NUMBER..... 1.89
 TOTAL POWER(KW)..... 12.6
 AVERAGE SURFACE TEMP(DEG C)... 87.8

DEPTH (CM)	LOCAL HEAT TRANSFER COEFF (CAL/CM2 SEC DEG C)				NUSSULT NUMBER	MODIFIED RAYLEIGH NUMBER
	EXPT	EQ 14a	EQ 10 N=1.0	EQ 10 N=0.7		
3.241	.1852	.0705	.0595	.0794	269.2	.9691E+09
4.511	.1511	.0649	.0532	.0707	419.3	.2613E+10
5.781	.1162	.0610	.0489	.0649	413.3	.5500E+10
7.051	.1166	.0581	.0458	.0606	514.5	.9979E+10
8.321	.6852	.0557	.0433	.0572	436.1	.1640E+11
9.591	.1167	.0538	.0413	.0545	688.5	.2511E+11
10.86	.0870	.0521	.0397	.0527	581.2	.3647E+11
12.13		.0507	.0383	.0503		
13.40	.0565	.0495	.0371	.0486	548.5	.6851E+11
14.67	.0762	.0484	.0360	.0472	687.6	.8989E+11
15.94	.0763	.0474	.0350	.0459	748.5	.1153E+12
17.21	.0757	.0465	.0342	.0447	801.4	.1451E+12
18.48	.0774	.0456	.0334	.0436	879.7	.1797E+12
19.75	.0716	.0449	.0327	.0427	869.9	.2193E+12
21.02	.0769	.0442	.0321	.0418	993.8	.2644E+12
22.29	.0754	.0436	.0315	.0410	1033.6	.3153E+12
23.56	.0794	.0430	.0309	.0402	1151.0	.3723E+12
24.83	.0827	.0424	.0304	.0395	1262.7	.4356E+12
26.10		.0419	.0299	.0389		

-154-

49A 200

VOLUMETRIC BOILING POOL DATA



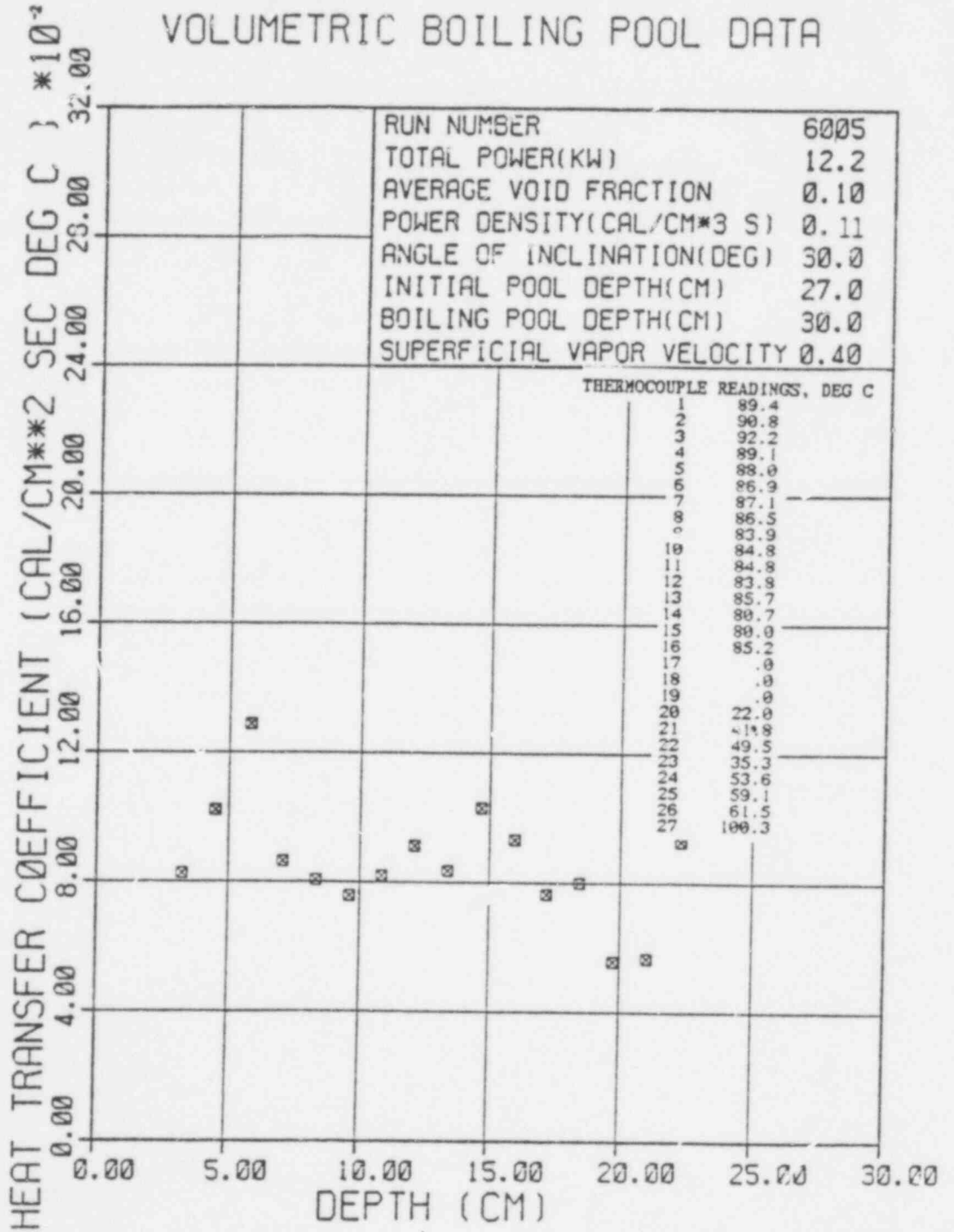
RUN NUMBER... 6005

AVERAGE VOID FRACTION..... .10
 INITIAL POOL DEPTH(CM)..... 27.0
 BOILING POOL DEPTH(CM)..... 30.0
 VOL. POWER DENS.(CAL/CM3 SEC). .11
 SUPERFICIAL VAPOR VELOCITY..... .40
 ANGLE OF INCLINATION(DEGREES). 30.00
 POOL VOLUME(CM**3)..... 20020.
 PRANDTL NUMBER..... 1.90
 TOTAL POWER(KW)..... 12.24
 AVERAGE SURFACE TEMP(DEG C).... 86.2

DEPTH (CM)	LOCAL HEAT TRANSFER COEFF (CAL/CM2 SEC DEG C) EXPT EQ 14a EQ 10 EQ 10 N=1.0 N=0.7	NUSSLETT NUMBER	MODIFIED RAYLEIGH NUMBER			
3.241	.0826	.0619	.0530	.0708	164.6	.5772E+09
4.511	.1023	.0570	.0473	.0630	283.9	.1556E+10
5.781	.1287	.0536	.0435	.0578	457.9	.3275E+10
7.051	.0865	.0510	.0407	.0539	375.2	.5943E+10
8.321	.0807	.0489	.0385	.0509	413.0	.9768E+10
9.591	.0758	.0472	.0367	.0485	447.4	.1496E+11
10.86	.0819	.0458	.0353	.0465	547.5	.2172E+11
12.14	.0912	.0445	.0340	.0448	681.0	.3027E+11
13.40	.0837	.0434	.0329	.0433	689.8	.4080E+11
14.67	.1031	.0425	.0320	.0420	930.7	.5354E+11
15.94	.0932	.0416	.0311	.0408	914.5	.6868E+11
17.21	.0764	.0408	.0303	.0398	808.8	.8643E+11
18.48	.0800	.0401	.0297	.0388	910.2	.1070E+12
19.75	.0556	.0394	.0290	.0380	677.9	.1306E+12
21.02	.0567	.0388	.0285	.0372	733.0	.1575E+12
22.29	.0928	.0382	.0279	.0364	1272.6	.1878E+12
23.56		.0377	.0274	.0358		
24.83		.0372	.0270	.0352		
26.10		.0368	.0266	.0346		

494 202

VOLUMETRIC BOILING POOL DATA



494 203

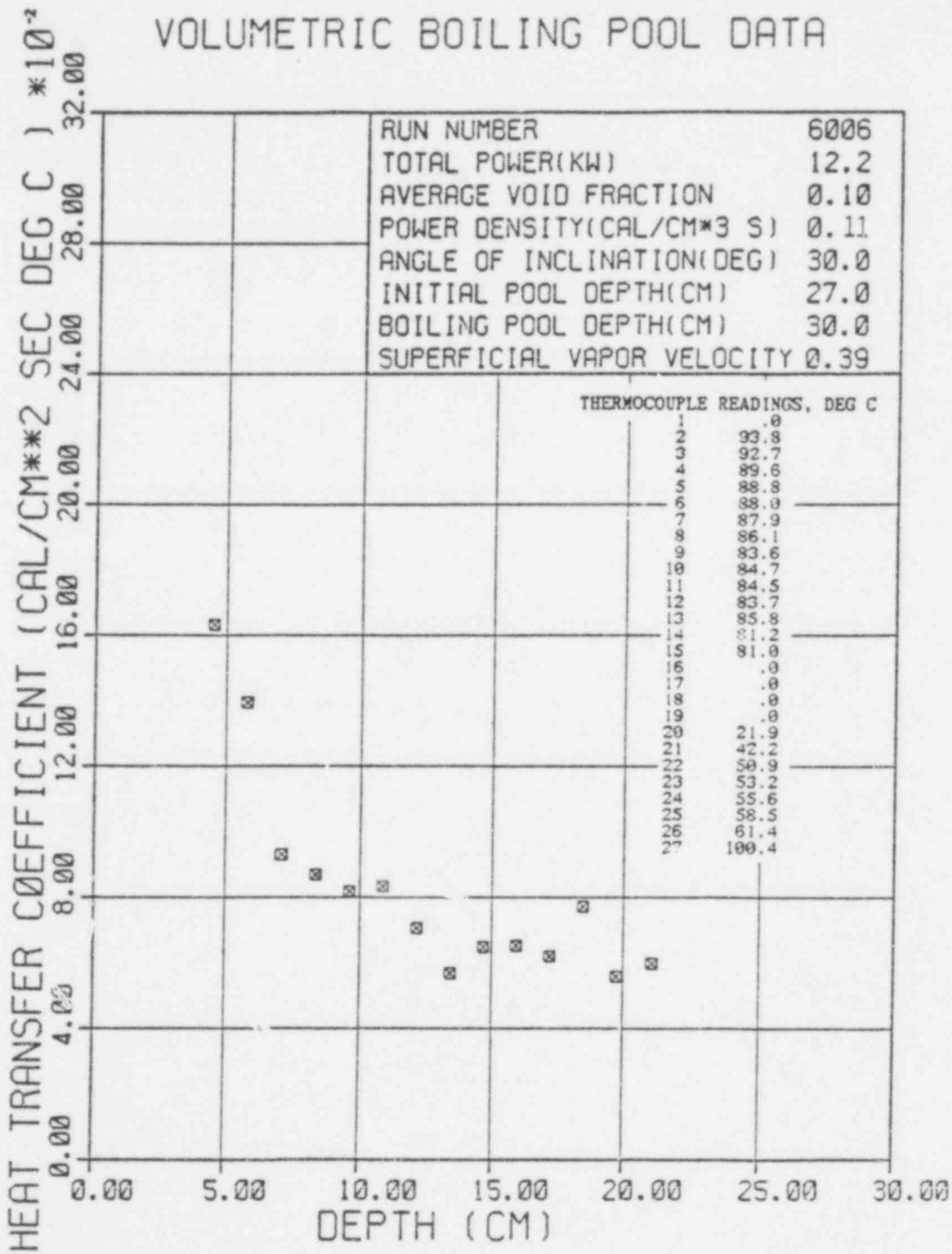
AUN NUMBER... 6006

AVERAGE VOID FRACTION..... .10
 INITIAL POOL DEPTH(CM)..... 27.0
 BOILING POOL DEPTH(CM)..... 30.0
 VOL. FOWER DENS. (CAL/CM3 SEC) . .11
 SURFICIAL VAPOR VELOCITY.... .39
 ANGLE OF INCLINATION(DEGREES) . 30.00
 POOL VOLUME(CM**3)..... 20020.
 PRANDTL NUMBER..... 1.90
 TOTAL POWER(KW)..... 12.24
 AVERAGE SURFACE TEMP(DEG C).... 87.0

DEPTH (CM)	LOCAL HEAT TRANSFER COEFF (CAL/CM2 SEC DEG C)	MUSSELT NUMBER	MODIFIED RAYLV TM NUMBER
EXPT	EQ 14a	EQ 10	EQ 10
	N=1.0	N=0.7	
3.241	.0620	.0528	.0705
4.511	.0571	.0472	.0628
5.781	.0537	.0434	.0576
7.051	.0511	.0406	.0537
8.321	.0490	.0384	.0507
9.591	.0473	.0366	.0483
10.86	.0458	.0352	.0463
12.13	.0446	.0339	.0446
13.40	.0435	.0328	.0431
14.67	.0425	.0319	.0418
15.94	.0416	.0310	.0407
17.21	.0409	.0303	.0396
18.48	.0401	.0296	.0387
19.75	.0395	.0290	.0378
21.02	.0389	.0284	.0370
22.29	.0383	.0279	.0363
23.56	.0378	.0274	.0357
24.85	.0373	.0269	.0350
26.10	.0368	.0265	.0345

.1563E+10
 .3289E+10
 .5968E+10
 .9808E+10
 .1502E+11
 .2181E+11
 .3039E+11
 .4097E+11
 .5376E+11
 .6896E+11
 .8679E+11
 .1075E+12
 .1312E+12
 .1581E+12

VOLUMETRIC BOILING POOL DATA



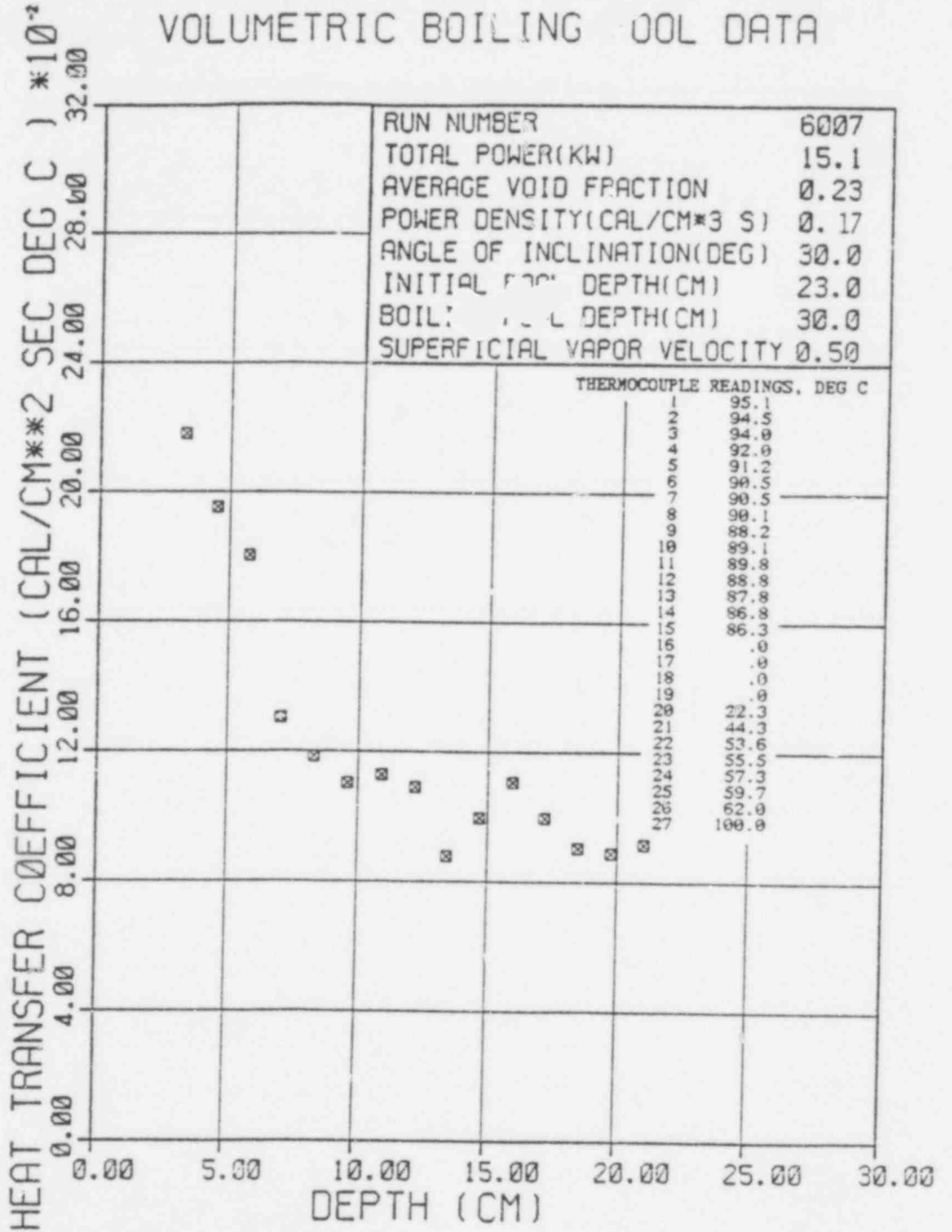
494 205

 RUN NUMBER ... 6607

AVERAGE VOID FRACTION23
 INITIAL POOL DEPTH(CM) 23.0
 BOILING POOL DEPTH(CM) 30.0
 VOL. POWER DENS. (CAL/CM3 SEC) . .17
 SUPERFICIAL VAPOR VELOCITY50
 ANGLE OF INCLINATION(DEGREES) . 30.00
 POOL VOLUME (CM**3) 16576.
 PRANDTL NUMBER 1.86
 TOTAL POWER(KW) 15.12
 AVERAGE SURFACE TEMP (DEG C) ... 90.5

DEPTH (CM)	LOCAL HEAT TRANSFER COEFF (CAL/CM2 SEC DEG C)			RUSSELL NUMBER	MODIFIED RAYLEIGH NUMBER
	EXPT	EQ 1 _{6a}	EQ 10 N=1.0 N=0.7		
3.241	.2181	.0770	.0634	434.5	.1372E+10
4.511	.1953	.0709	.0567	541.5	.3698E+10
5.781	.1804	.0666	.0522	641.2	.7784E+10
7.051	.1303	.0634	.0489	564.9	.1412E+11
8.321	.1185	.0608	.0463	606.1	.2321E+11
9.591	.1101	.0587	.0442	649.1	.3555E+11
10.86	.1128	.0569	.0425	753.2	.5162E+11
12.13	.1089	.0553	.0410	812.2	.7193E+11
13.40	.0878	.0540	.0397	723.4	.9696E+11
14.67	.0995	.0528	.0386	897.5	.1272E+12
15.94	.1106	.0517	.0376	1083.4	.1632E+12
17.21	.0996	.0507	.0366	897.5	.2054E+12
18.48	.0905	.0498	.0358	1054.1	.2543E+12
19.75	.0888	.0490	.0351	1028.1	.3104E+12
21.02	.0917	.0482	.0344	1077.9	.3743E+12
22.29		.0475	.0338	1184.5	
23.56		.0469	.0332		
24.83		.0463	.0326		
26.10		.0457	.0321		

VOLUMETRIC BOILING POOL DATA

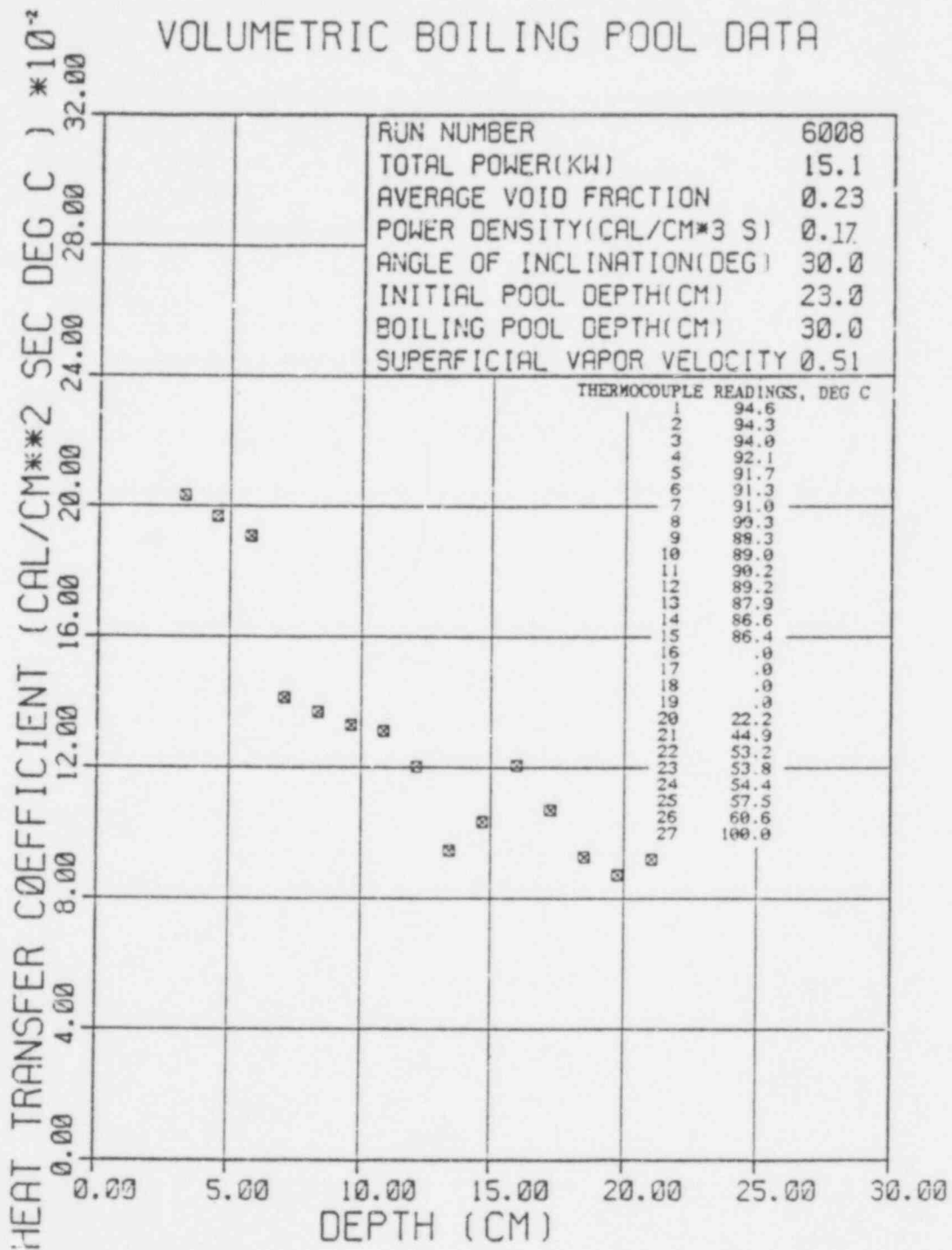


RUN NUMBER... 6009

AVERAGE VOID FRACTION..... .23
 INITIAL POOL DEPTH(CM)..... 23.0
 BOILING POOL DEPTH(CM)..... 36.0
 VOL. POWER DENS. (CAL/CM3 SEC) .17
 SUPERFICIAL VAPOR VELOCITY.... .51
 ANGLE OF INCLINATION(DEGREES) . 30.00
 POOL VOLUME(CM**3)..... 16576.
 PRANDTL NUMBER..... 1.86
 TOTAL POWER(KW)..... 15.12
 AVERAGE SURFACE TEMP (DEG C) ... 90.7

DEPTH (CM)	LOCAL HEAT TRANSFER COEFF (CAL/CM2 SEC. DEG C)		NUSSLETT NUMBER	MODIFIED RAYLEIGH NUMBER
	EXPT EQ 14a	EQ 10 N=1.0 N=0.7		
3.241	.2933	.0770	.0637	.0848
4.511	.1967	.0709	.0569	.0755
5.781	.1908	.0666	.0524	.0693
7.051	.1414	.0634	.0491	.0648
8.321	.1370	.0608	.0465	.0612
9.591	.1331	.0587	.0444	.0583
10.86	.1313	.0569	.0426	.0559
12.13	.1201	.0554	.0411	.0538
13.40	.0946	.0540	.0398	.0521
14.67	.1633	.0528	.0387	.0505
15.94	.1206	.0517	.0377	.0491
17.21	.1070	.0507	.0368	.0479
18.48	.0926	.0498	.0359	.0468
19.75	.0871	.0490	.0352	.0457
21.02	.0919	.0482	.0345	.0448
22.29		.0475	.0339	.0439
23.56		.0469	.0333	.0431
24.83		.0463	.0327	.0424
26.10		.0457	.0322	.0417
			404.9	.1373E+10
			545.5	.3702E+10
			678.1	.7791E+10
			612.8	.1414E+11
			700.9	.2323E+11
			784.6	.3558E+11
			876.5	.5167E+11
			895.9	.7199E+11
			779.6	.9705E+11
			931.6	.1273E+12
			1181.4	.1634E+12
			1132.1	.2056E+12
			1051.7	.2546E+12
			1057.8	.3107E+12
			1188.0	.3746E+12

VOLUMETRIC BOILING POOL DATA



RUN NUMBER... 6009

AVERAGE VOID FRACTION..... .37

INITIAL POOL DEPTH(CM)..... 19.0

BOILING POOL DEPTH(CM)..... 30.0

VOL. POWER DENS. (CAL/CM3 SEC). .37

SUPERFICIAL VAPOR VELOCITY.... .92

ANGLE OF INCLINATION(DEGREES). 30.00

POOL VOLUME(CM**3)..... 13299.

PRANDTL NUMBER..... 1.85

TOTAL POWER(KW)..... 24.0

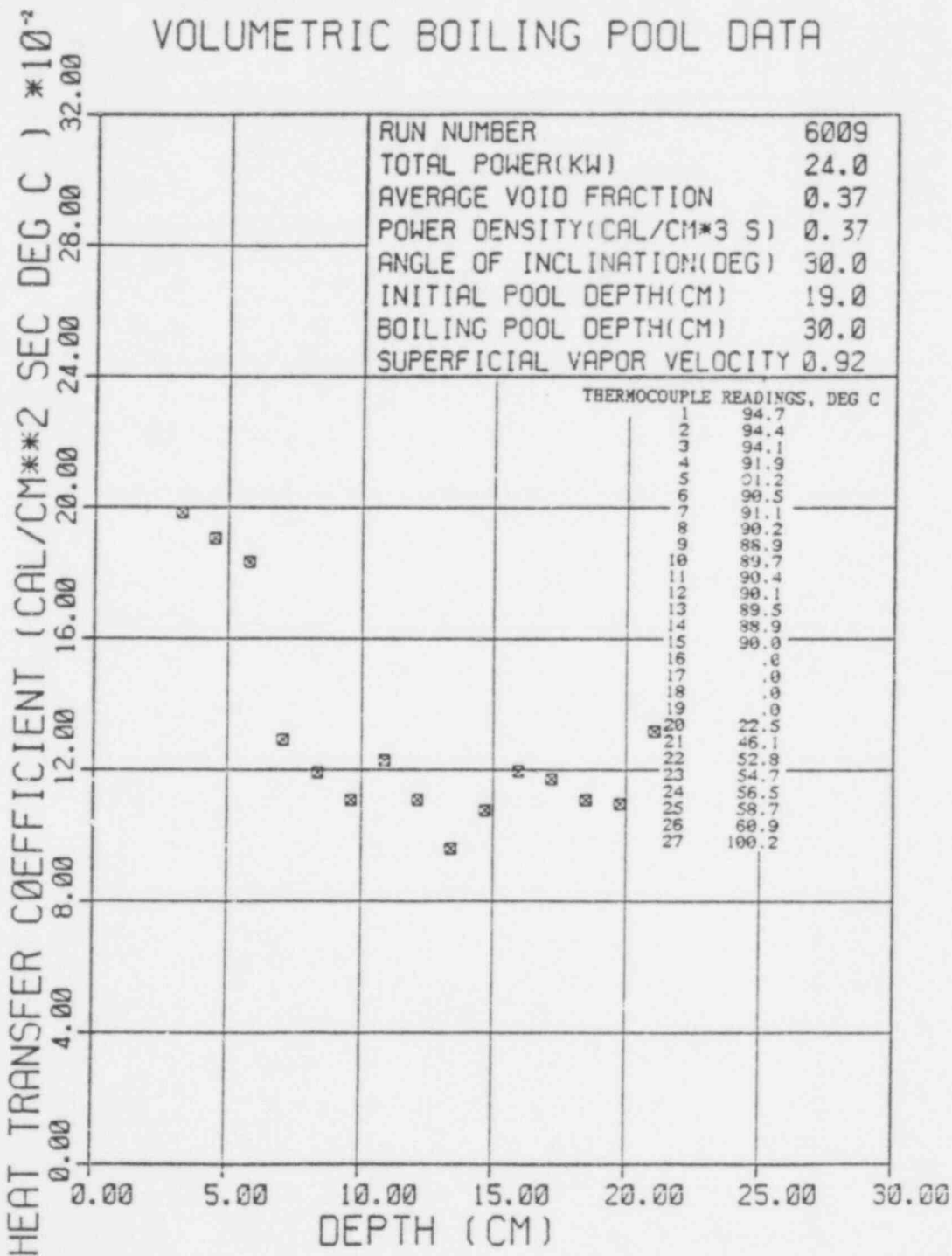
AVERAGE SURFACE TEMP(DEG C)... 91.4

DEPTH (CM)	LOCAL HEAT TRANSFER COEFF (CAL/CM2 SEC DEG C)				NUSSELT NUMBER	MODIFIED RAYLEIGH NUMBER
	EXPT	EQ 14a	EQ 10 N=1.0	EQ 10 N=0.7		
3.241	.1984	.0863	.0765	.1025	395.2	.2166E+10
4.511	.1905	.0795	.0682	.0911	528.2	.5841E+10
5.781	.1835	.0747	.0626	.0835	651.8	.1229E+11
7.051	.1291	.0711	.0585	.0779	559.6	.2231E+11
8.321	.1192	.0682	.0553	.0735	609.6	.3666E+11
9.591	.1107	.0658	.0527	.0699	652.6	.5614E+11
10.86	.1227	.0638	.0506	.0670	819.3	.8152E+11
12.13	.1107	.0621	.0488	.0645	825.5	.1136E+12
13.40	.0960	.0605	.0472	.0623	790.5	.1531E+12
14.67	.1076	.0592	.0458	.0604	979.2	.2009E+12
15.94	.1197	.0580	.0445	.0587	1172.5	.2578E+12
17.21	.1172	.0569	.0434	.0572	1239.6	.3244E+12
18.48	.1107	.0559	.0424	.0558	1257.6	.4016E+12
19.75	.1095	.0549	.0415	.0546	1329.3	.4903E+12
21.02	.1319	.0541	.0407	.0534	1703.6	.5910E+12
22.29		.0533	.0399	.0524		
23.56		.0526	.0392	.0514		
24.83		.0519	.0386	.0505		
26.10		.0512	.0379	.0497		

-164-

494 210

VOLUMETRIC BOILING POOL DATA



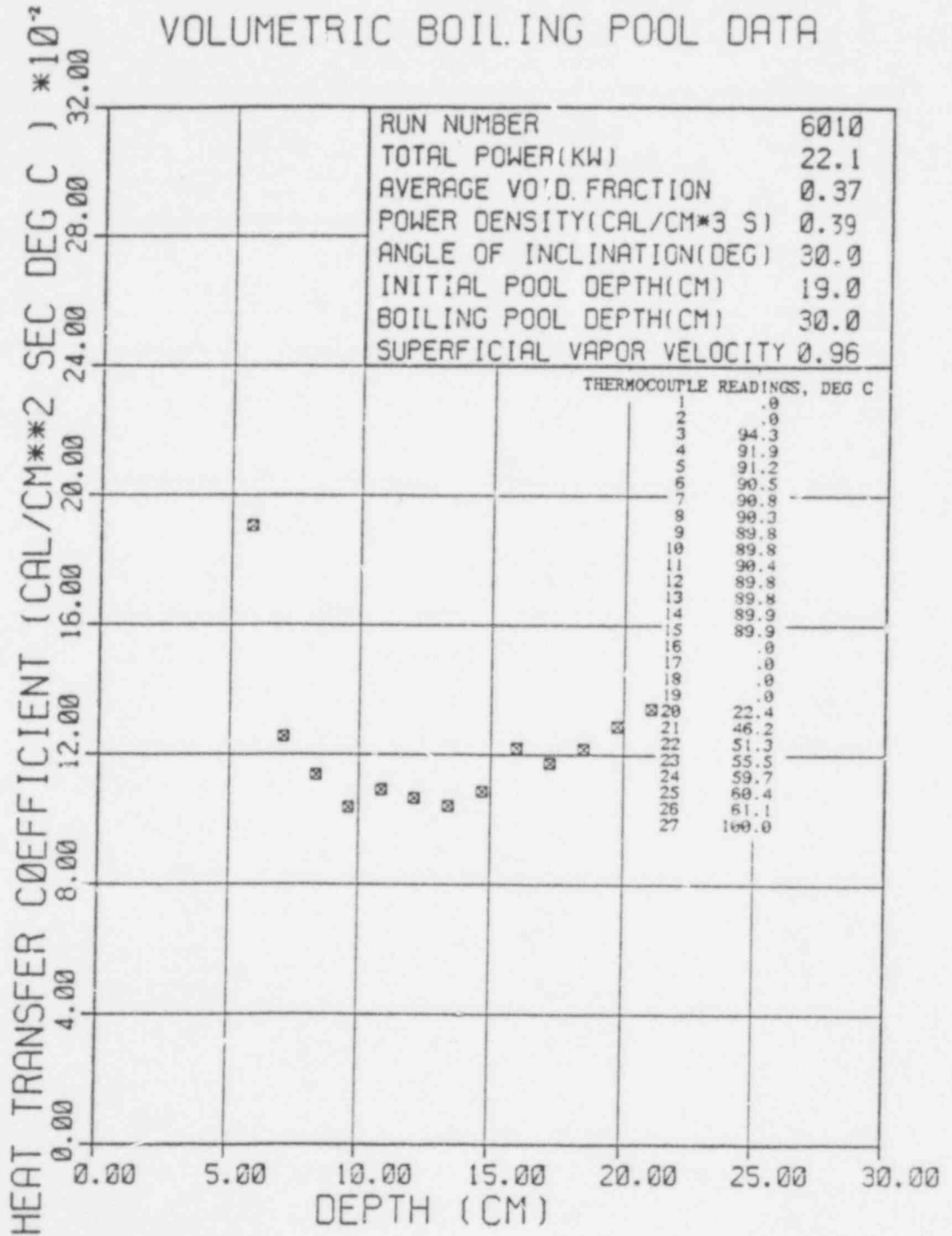
RUN NUMBER... 6010

AVERAGE VOID FRACTION..... .37
 INITIAL POOL DEPTH(CM)..... 19.0
 BOILING POOL DEPTH(CM)..... 30.0
 VOL. POWER DENS. (CAL/CM3 SEC), .39
 SUPERFICIAL VAPOR VELOCITY.... .56
 ANGLE OF INCLINATION(DEGREES), 30.00
 POOL VOLUME(CM**3)..... 13299.
 PRANDTL NUMBER..... 1.85
 TOTAL POWER(KW)..... 22.08
 AVERAGE SURFACE TEMP (DEG C)... 91.9

DEPTH (CM)	LOCAL HEAT TRANSFER COEFF (CAL/CM2 SEC DEG C)	EXPT EQ 1a EQ J: E010 N=1.0 N=0.7	NUSSLETT NUMBER	MODIFIED RAYLEIGH NUMBER
3.24	.0863	.0772	.1035	
4.511	.0795	.0688	.0920	
5.781	.0747	.0631	.0842	
7.051	.0711	.0590	.0786	677.4
8.321	.0682	.0558	.0741	544.0
9.591	.0658	.0531	.0705	582.1
10.86	.0638	.0510	.0676	612.2
12.13	.0621	.0491	.0650	728.4
13.40	.0606	.0475	.0628	793.9
14.67	.0592	.0461	.0609	857.5
15.94	.0580	.0449	.0592	978.7
17.21	.0569	.0437	.0577	1195.8
18.48	.0559	.0427	.0563	1241.9
19.75	.0550	.0418	.0550	1383.8
21.02	.0541	.0410	.0539	1563.4
22.29	.0533	.0402	.0528	1734.1
23.56	.0526	.0395	.0518	
24.83	.0519	.0388	.0509	
26.10	.0513	.0382	.0501	

494 212

VOLUMETRIC BOILING POOL DATA



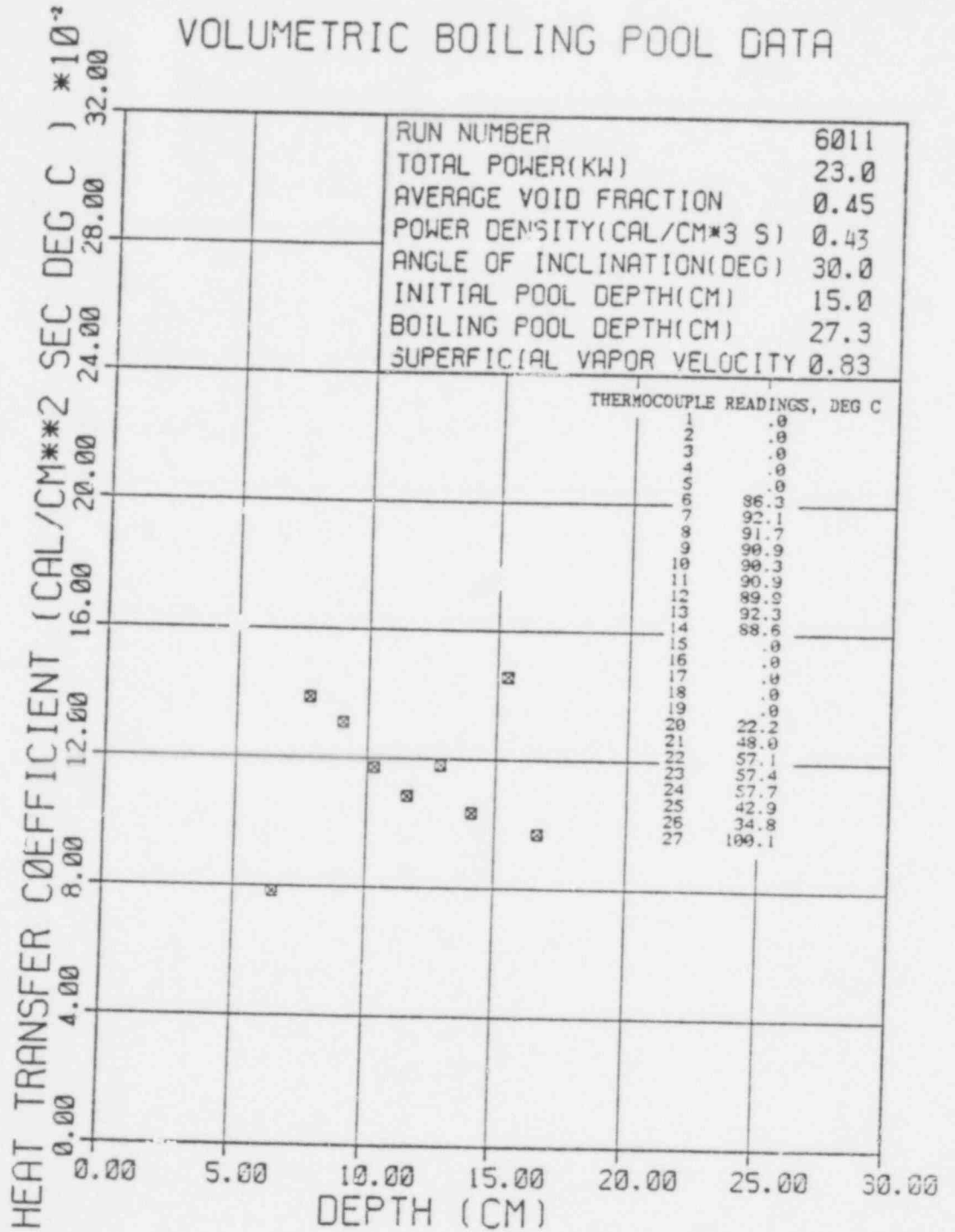
494 213

RUN NUMBER... 6011

AVERAGE VOID FRACTION..... .45
 INITIAL POOL DEPTH(CM)..... 15.0
 BOILING POOL DEPTH(CM)..... 27.3
 VOL. POWER DENS. (CAL./CM3 SEC). .43
 SUPERFICIAL VAPOR VELOCITY..... .63
 ANGLE OF INCLINATION(DEGREES) . 30.60
 POOL VOLUME(CM**3)..... 10187.
 PRANDTL NUMBER..... 1.86
 TOTAL POWER(KW)..... 23.0
 AVERAGE SURFACE TEMP (DEG C) ... 90.7

DEPTH (CM)	LOCAL HEAT TRANSFER COEFF (CAL./CM2 SEC DEG C) EXPT EQ 14a N=1.0	EQ 10 N=6.7	NUSSLETT NUMBER	MODIFIED RAYLEIGH NUMBER
.123	.2055	.2594	.3481	
1.393	.1121	.1040	.1397	
2.663	.0953	.0828	.1107	
3.933	.0865	.0723	.0964	
5.203	.0806	.0658	.0874	
6.473	.0764	.0611	.0810	
7.743	.0730	.0575	.0761	
9.013	.0703	.0547	.0723	
10.28	.0680	.0524	.0691	
11.55	.0661	.0504	.0664	
12.82	.0644	.0487	.0641	
14.09	.0629	.0473	.0620	
15.36	.0615	.0460	.0603	
16.63	.0603	.0448	.0587	
17.90	.0592	.0437	.0572	
19.17	.0582	.0428	.0559	
20.44	.0573	.0419	.0547	
21.71	.0564	.0411	.0536	
22.93	.0556	.0404	.0526	
			312.1	.2113E+11
			660.7	.3617E+11
			726.1	.5704E+11
			749.8	.8471E+11
			769.6	.1201E+12
			929.3	.1643E+12
			896.5	.2181E+12
			1375.8	.2825E+12
			991.1	.3585E+12

VOLUMETRIC BOILING POOL DATA



RUN NUMBER... 6012

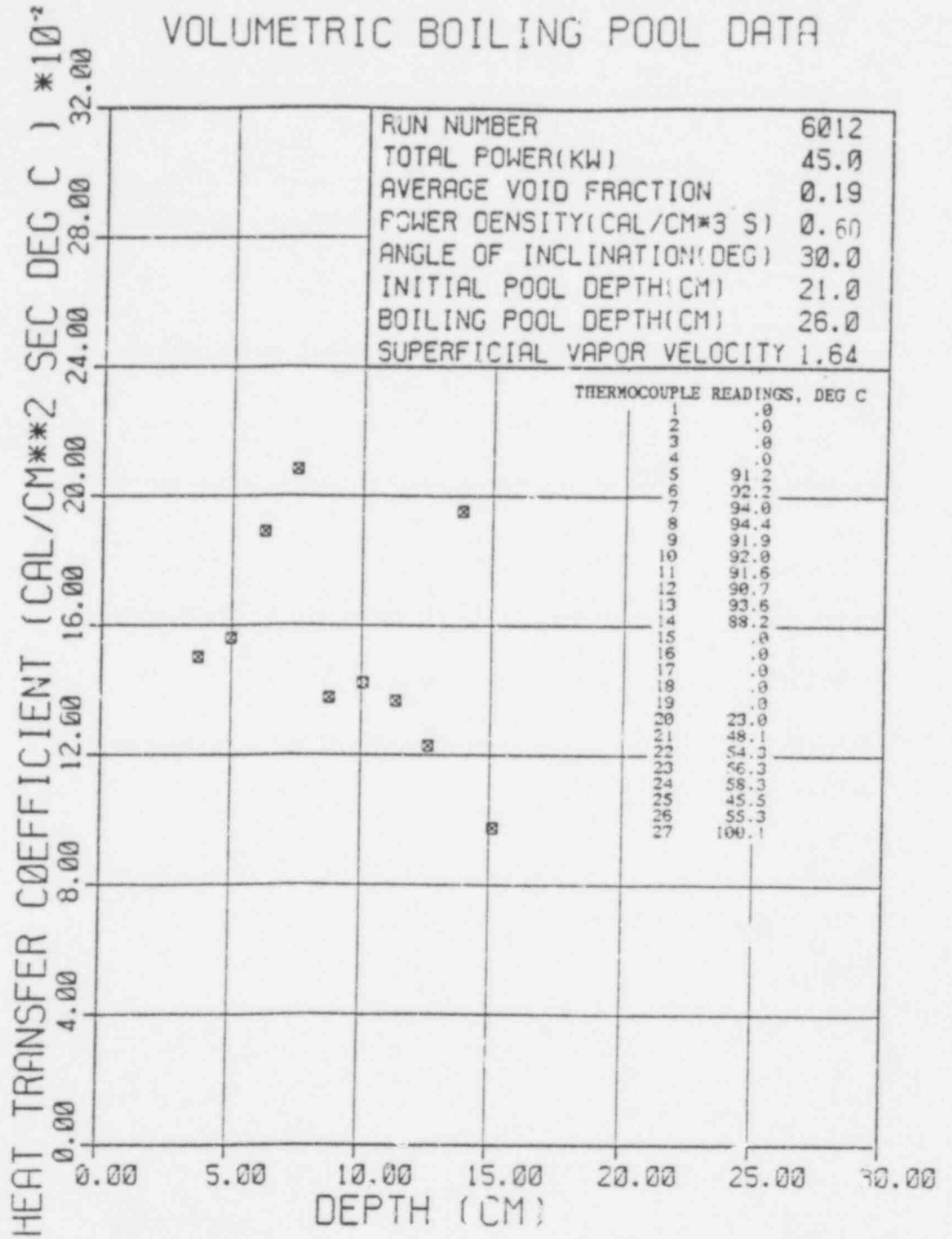
AVERAGE VOID FRACTION..... .19
 INITIAL POOL DEPTH(CM)..... 21.0
 BOILING POOL DEPTH(CM)..... 26.0
 VOL. POWER DENS.(CAL/CM3 SEC). .60
 SUPERFICIAL VAPOR VELOCITY.... 1.64
 ANGLE OF INCLINATION(DEGREES). 30.00
 POOL VOLUME(CM**3)..... 14917.
 PRANDTL NUMBER..... 1.85
 TOTAL POWER(KW)..... 45.0
 AVERAGE SURFACE TEMP(DEG C)... 92.2

-170-

DEPTH (CM)	LOCAL HEAT TRANSFER COEFF (CAL/CM2 SEC DEG C)			NUSSELT NUMBER	MODIFIED RAYLEIGH NUMBER
	EXPT	EQ 14a	EQ 10 N=1.0		
1.162		.0950	.1195	.1602	
2.432		.0790	.0895	.1205	
3.702	.1503	.0711	.0763	.1028	341.9
4.972	.1560	.0661	.0683	.0920	476.5
6.242	.1889	.0624	.0628	.0845	724.7
7.512	.2082	.0596	.0587	.0790	961.2
8.782	.1375	.0573	.0554	.0745	742.1
10.05	.1423	.0554	.0528	.0709	878.8
11.32	.1366	.0538	.0505	.0679	950.3
12.59	.1227	.0524	.0486	.0653	949.5
13.86	.1952	.0511	.0470	.0631	1662.5
15.13	.0976	.0500	.0456	.0611	907.2
16.40		.0490	.0443	.0594	
17.67		.0481	.0431	.0578	
18.94		.0473	.0421	.0564	
20.21		.0455	.0411	.0551	
21.48		.0458	.0403	.0539	

494
216

VOLUMETRIC BOILING POOL DATA



494 217

APPENDIX D

Algebraic Development of Equations 28 and 29.

In single phase natural convection heat transfer along a vertical flat plate, it has been determined that for Pr equal 2.0, the local free convection heat transfer correlations for laminar and turbulent flow are

$$\text{Nu}(x) = 0.42 [\text{Gr} \cdot \text{Pr}]^{1/4} \quad (\text{D-1})$$

and

$$\text{Nu}(x) = 0.0295 \text{Gr}^{2/5} \text{Pr}^{7/15} [1 + .494 \text{Pr}^{2/3}]^{-2/5} \quad (\text{D-2a})$$

respectively. Equation D-2 may be reduced to the following approximate form by grouping $(\text{Gr} \cdot \text{Pr})^{2/5}$ and letting $\text{Pr} = 2.0$;

$$\text{Nu}(x) \approx 0.0245 [\text{Gr} \cdot \text{Pr}]^{2/5} \quad (\text{D-2b})$$

In order to compare these results to average experimental heat transfer data, it has been necessary to convert these local heat transfer coefficients into the corresponding average values along the surface. By introducing the expression for the Grashof number into the above equations, it can be seen that the local heat transfer coefficient is proportional to the distance from the leading edge along the laminar boundary layer to the $-1/4$ power⁽²⁵⁾, i.e.,

$$h(x) \sim x^{-1/4} \quad (\text{D-3a})$$

and for the turbulent case, proportional to the distance from the leading edge along the boundary layer to the power 0.2 ⁽²⁶⁾, i.e.,

$$h(x) \sim x^{0.2} \quad (\text{D-3b})$$

It may be readily shown by integrating equations D-1 and D-2 a,b that the average heat transfer coefficient over the length of the plate, L, is related to the local coefficient at $x = L$ as follows: for the laminar boundary layer (Eq. D-1),

$$\bar{h} = \frac{1}{L} \int_0^L h(x) dx = \frac{4}{3} h(x) \Big|_{x=L} \quad (D-4a)$$

and for the turbulent boundary layer (Eqs D-2 a,b),

$$\bar{h} = \frac{1}{L} \int_0^L h(x) dx = \frac{h(x)}{1.2} \Big|_{x=L} \quad (D-4b)$$

Thus, the local Nusselt relations (Eqs. D-1 and D-2 a,b,) may be modified to represent the average heat transfer behavior by substituting \bar{h} for $h(x)$, L for x , and multiplying the correlation coefficient, K, by the factor 1.33 (for laminar case) or .83 (for turbulent case). When this is done, Eqs. D-1, D-2a, and D-2b are transformed into the average correlations below, respectively,

$$\bar{Nu} = 0.56[Gr \cdot Pr]^{1/4} \quad (D-5)$$

$$\bar{Nu} = 0.0246 Gr^{2/5} Pr^{7/15} [1 + .494 Pr^{2/3}]^{-2/5} \quad (D-6a)$$

$$\bar{Nu} = 0.0210[Gr \cdot Pr]^{2/5} \quad (D-6b)$$

These correlations are in excellent agreement with empirically derived relations in the literature.

The above conversion procedure is valid only in the case that the free stream properties are constant. In the case of boundary layer heat transfer

from volume-heated boiling pools, it has been shown that there exists a vertical distribution of vapor fraction which is defined by the solution to Eq. 20. Thus, the integration demonstrated in Eqs. D-4 a,b will depend not only on the explicit spatial dependence in the Grashof number, but upon the implicit spatial variation in the void fraction distribution as well.

The forms of the local void distribution that will be considered are listed below:

a. $\alpha(x) = \bar{\alpha}$

b. $\alpha(x) = 2 \bar{\alpha}(x/L)$

c. $\alpha(x) = 1.5 \bar{\alpha}(x/L)^{1/2}$

d. $\alpha(x) = 3 \bar{\alpha}(x/L)^2$

The procedure for determining the ratio of the average heat transfer correlation based upon $\bar{\alpha}$ to the local heat transfer correlation based upon $\alpha(x)$ is identical to that previously described. The results of the integration are presented in Table D-1 for both the laminar case ($Nu \sim Ra^{1/4}$) and the turbulent case ($Nu \sim Ra^{2/5}$).

The local heat transfer data from Ref. 12 has been correlated by both local and average void fraction with little observed sensitivity in the result, as demonstrated by Eqs. 14 a,b. On this justification, the local heat transfer data from this work was correlated on the basis of the average void fraction. As yet, only preliminary correlations of the data have been performed for laminar bubbly flow heat transfer. The results indicate quite close agreement with case d. Final results for local correlation of both laminar and turbulent bubbly flow data will be reported in the future.

TABLE D-1

SUMMARY OF LOCAL-TO-AVERAGE HEAT TRANSFER CORRELATION
CONVERSION UPON FREE STREAM VOID DISTRIBUTION

VOID DISTRIBUTION FUNCTION	K_{ave}/K_{local}^*	
	LAMINAR	TURBULENT
$\alpha(x) = \bar{\alpha}$	1.33	.83
$\alpha(x) = 2 \bar{\alpha}(x/L)$	1.19	.82
$\alpha(x) = 1.5 \bar{\alpha} (x/L)^{1/2}$	1.26	.84
$\alpha(x) = 3 \bar{\alpha}(x/L)^2$	1.05	.78

* K_{ave} is the average heat transfer correlation coefficient,

$\overline{Nu} = K_{ave} (Gr^* \cdot Pr)^n$ where $n = 1/4$ for laminar flow, $n = 2/3$ for turbulent flow.

* K_{local} is the local heat transfer correlation coefficient, $Nu(x) = K_{local} (Gr^* \cdot Pr)^n$ where $n = 1/4$ for laminar flow, $n = 2.5$ for turbulent flow.

DISTRIBUTION

BNL RSP Division Heads
BNL RSP Group Leaders
BNL RSE Person: 1

P. Abramson, ANL
A. Alter, DOE
L. Baker, ANL
S. G. Bankoff, Northwestern Uni.
D. Basdekas, NRC
J. Boudreau, LASL
I. Catton, Uni. of California
J. C. Chen, Lehigh Uni.
R. Coates, Sandia Laboratory
R. T. Curtis, NRC
A. Dukler, Uni. of Houston
D. T. Eggen, Northwestern Uni.
E. Epstein, ANL
J. Gabor, ANL
W. Gammill, NRC
R. Henry, ANL
H. H. Hummel, ANL
W. Y. Kato, BNL
M. S. Kazimi, MIT
C. N. Kelber, NRC
H. J. Kouts, BNL
T. Kress, ORNL
F. Kulacki, Ohio State Uni.
J. T. Larkins, NRC
J. Martin, HEDL
R. Ostensen, Sandia Laboratory
A. Reynolds, Uni. of Virginia
M. Silberberg, NRC
R. Stein, ANL
M. Stevenson, LASL
H. Todosow, BNL
T. G. Theofanus, Purdue Uni.
J. C. Walker, Sandia Laboratory
R. W. Wright, NRC

U.S. NRC Division of Technical Information and Control